Final Technical Summary Report

on

Vapor Filled Thermionic Converter Materials and Joining Problems
Plasma Research Pertinent to Thermionic Converter Operation

15 November 1961 - 15 December 1962

Contract No. NObs-86220
ARPA Order No. 219-61
Project Serial No. S R007 12 01

BUREAU OF SHIPS
DEPARTMENT OF THE NAVY
WASHINGTON 25, D.C.

GENERAL ELECTRIC

Electronic
TUBES

FINAL TECHNICAL SUMMARY REPORT
on
Vapor Filled Thermionic Converter Materials & Joining Problems;
Plasma Research Pertinent to Thermionic Converter Operation

15 November 1961 - 15 December 1962

Prepared for:

Bureau of Ships
Department of the Navy
Washington 25, D. C.

Prepared by:

Power Tube Department
General Electric Company
Schenectady, New York

Project Engineers:
M. J. Slivka, Tel. FR 4-2211, Ext. 5-4608
R. H. Bristow, Tel. FR 4-2211, Ext. 5-3621
M. D. Gibbons, Tel. FR 4-2211, Ext. 99-6156

Contract No. NObs-86220
Project Serial No. SR007 1201
ARPA Order No. 219-61
Date of Contract: 15 December 1961
Contract Expiration Date: 15 December 1962
Amount of Contract: $146, 508.00
G-E File No. SD-109
Report No. R-572F
February 21, 1963

This contract is sponsored by the Advanced Research Project Agency.

CONTENTS

FOREWORD

From experience to date with cesium vapor thermionic converters, it is evident that a number of material problems of varying degrees of severity must be overcome before reliable vapor converters capable of long life performance (such as 10,000 hours and longer) will be realizable. The major known problem areas include cesium attack on converter materials and structures, mechanical and physical stability of envelope materials, metal-ceramic seal integrity, and joining problems. Of considerable importance also is attainment of a more complete understanding of discharge phenomena in cesium and emission from cesiated surfaces.

This contract was originated to conduct two research programs on thermionic converters. The first program was concerned with vapor filled thermionic converter materials and joining problems, and the second with plasma and emission research pertinent to thermionic converter operation. Specifically, the research effort was to be divided into the following areas, as outlined in the contract:

"1. Cesium Attack

"a. Mechanisms, and rate of attack as a function of time, temperature, and cesium pressure for various types of ceramic bodies, especially Lucalox,* 97% Al_2O_3 and 99% Al_2O_3 ceramics.

"b. Envelope Material (1300-1800°C)
Attack resistance, cladding, coating.

"c. Brazing alloys (1300-1800°C) and ceramic-metal seals (800-900°C)
Attack resistance, coating, diffusion bonding.
(Elimination of brazing alloys.)

*Lucalox is a General Electric trade name for a high-purity alumina ceramic.

"2. Envelope Material (Metals, Ceramics, Cermets)

"a. Mechanical stability.

"(1) Grain growth.
Stabilized materials, SAP materials, single crystals.

"(2) High temperature strength.
Creep, thermal fatigue, embrittlement.

"b. Thermal and physical stability.
Outgassing, thermal and electrical conductivity, oxidation resistance, sublimination, cesium attack.

"3. Metal-Ceramic Seals

"a. High temperature tolerance (800-900°C).
Thermal cycling, thermal shock, life.

"b. Environmental effects.

"4. Joining (Metal-to-Metal)

"a. Brazing.
High temperature (1200-2000°C) brazing process and alloys, diffusion or sublimation altered solidus.

"b. Grain growth, high temperature strength, ductility, expansion properties of selected brazing alloys.

"c. Diffusion bonding as a substitute for brazing.

"d. Environmental effects on brazing alloys.

"5. Saturated Emission Data from Cesiated Surfaces

"The measurements shall be taken over a range of substrate materials, temperatures, and cesium arrival rates of interest to a valid scientific interpretation of the emission problem and to the practical vapor thermionic converter problem.

These measurements shall be made in very carefully designed vehicles to reduce to a minimum such problems as fringe area emission and poor substrate temperature distributions, which can yield misleading data.

"6. Arc Initiation and Maintenance Potential Investigations

"Detailed measurements of arc initiation and maintenance potential shall be made over cesium pressures, cathode temperatures, and spacing conditions for geometries and conditions of interest to the vapor thermionic problems.

"7. Positive Column Data

"Measure the positive column drop with a variable spacing research vehicle.

"8. Theoretical Calculations

"The results of 5, 6 and 7 shall be used as numerical inputs to calculate as precisely as possible the behavior of the vapor thermionic converter.

"9. Surface Ionization Studies

"Sufficient additional work should be done in this area, if necessary, to allow a definitive interpretation of the probable ionization processes."

The effective dates of the contract were November 15, 1961 through December 15, 1962 and program progress for this period is detailed in this report. During the contract period, efforts were concentrated on four phases of the project: i.e. Item 1, Cesium Attack; Item 3, Metal-Ceramic Seals; Items 5 and 6, Plasma Research and Emission from Cesiated Surfaces. These areas were chosen as those warranting the most immediate investigation. Assignments of responsibility for the individual areas of research in process were as follows: Cesium Attack - Mr. M. J. Slivka, Metal-Ceramic Seals - Mr. R. H. Bristow, and Plasma Research and Emission from Cesiated Surfaces - Mr. M. D. Gibbons.

A section including an abstract for each phase of the program is presented in the following pages. Then each phase of the work program is detailed in individual sections.

ABSTRACT

VAPOR FILLED THERMIONIC CONVERTER MATERIALS AND JOINING PROBLEMS

I. Cesium Attack

This report describes a study of the compatibility of specific materials used in thermionic converters with cesium vapor at elevated temperatures. The materials investigated included ceramics, metal-ceramic seals, and metals.

Only high-purity alumina ceramic bodies exhibited resistance to attack by cesium vapor at temperatures up to 900°C. Commercial high alumina ceramics which were tested were found to exhibit unpredictable degrees of susceptibility to attack by cesium vapor.

Active alloy metal-ceramic seals employing a high-purity alumina ceramic brazed to tantalum with either titanium-nickel or zirconium nickel alloy were shown to resist attack by cesium vapor at 1 Torr pressure up to 900°C. However, extensive attack on the seals was found to occur when the cesium pressure was increased to 100 Torr.

Data were obtained for a number of metallic materials of interest. In certain cases an unusual variation was exhibited in weight gain and weight loss as a function of temperature as a result of reaction with cesium vapor. The significance of possible material transport being the result of attack by cesium vapor on certain metallic materials is discussed.

II. Metal-Ceramic Seals

The reported work comprised an evaluation of the high-temperature capability of titanium-nickel bonded ceramic-to-metal seals, a study of the effect of sealing alloy composition on the physical and mechanical properties of the joint, and an investigation of new ceramic-to-metal sealing systems and techniques.

Ceramic-to-ceramic and ceramic-to-metal seals were prepared using two types of ceramics (pure sintered alumina and a 97 percent alumina) and six metals (titanium, tantalum Kovar, nickel, Type 304 stainless steel, and Type 430 stainless steel). Foil washers of titanium and/or nickel formed a liquid phase at the sealing temperature and effected the bond to the ceramic. Sealing was performed in vacuum.

Life testing of seals was performed at temperatures of 700°C and 900°C, in a vacuum environment, with cycling to room temperature every 240 hours. Seals were examined with respect to vacuum tightness, flexural strength, microstructure, and hardness of the sealing alloy as well as changes in these properties which occurred as a result of long time heat treatment.

Seals or sealing alloys containing a titanium phase (alpha or beta solid solution) exhibited very short lives at 900°C due to continued reaction with the ceramic, resulting in hardening and embrittlement of the alloy. At 700°C, the same mechanism of seal degradation is operative but at a reduced rate. At this temperature the best lives were recorded for seals of alumina-to-titanium and alumina-to-tantalum. At 900°C, the only seals which had lives in excess of several hundred hours were titanium-shim seals of alumina-to-nickel sealed so as to form $TiNi_3$ at the interface.

PLASMA RESEARCH PERTINENT TO THERMIONIC CONVERTER OPERATION

I. Experimental Studies of the Emission and Discharge Characteristics of the Ta-Cs System

This report describes emission and discharge measurements made on a Cs-Ta emitter in a tube with parallel electrode geometry and with an adjustable emitter-collector spacing. Some discharge and spectrographic measurements on a Cs-W emitter are also described. Emission results indicated that this particular Ta-Cs emitter surface has an emission capability greater than that reported by Taylor and Langmuir for Cs-W, while the emission maxima are shifted to lower temperatures. This increase in emission over that usually reported for Cs-Ta is believed due to a preferred orientation of the tantalum surface. The large enhancement of the emission during the discharge is believed due to the lowering of the work function by the effective increase in the adsorption of cesium which is due to the increased arrival rate caused by the retarding field for ions. This mechanism is probable in the region where the surface ionization is expected

The discharge studies involved the measurement of the breakdown and maintenance potentials of the hot cathode arc discharge for various emitter-collector spacings, emitter temperatures, and cesium pressures. Corrections for the contact potential and sheath potentials are applied to the experimental data. For a pressure the order of one millimeter, and high emitter temperatures, the results indicate that the magnitude of the emitter sheath potential is close to the first resonance level of cesium. This strongly suggest a multi-step process.

Ion densities determined by line broadening and the discharge parameters were measured on a tungsten-emitter tube. These tungsten data are similar to the tantalum data. However, these results manifest the need for having the emission, discharge parameters, and plasma properties measured simultaneously in the same experimental vehicle.

VAPOR FILLED THERMIONIC CONVERTER MATERIALS AND JOINING PROBLEMS

SECTION I

Cesium Alone

by

[illegible]

SECTION II

Metal-Ceramic Seals

by

[illegible]

SECTION I

Cesium Attack

by
M. J. Slivka
Power Tube Department
General Electric Company

TABLE OF CONTENTS

LIST OF ILLUSTRATIONS

CESIUM ATTACK

by
M. J. Slivka

INTRODUCTION

The use of cesium vapor in thermionic converters for space charge neutralization and work function adjustment introduced the problem of compatibility of converter construction materials with this reactive element. Limited information in the literature[1, 2, 3, 4, 5] describes the specific corrosion characteristics of cesium on various materials, whereas considerable published information is available on corrosion or attack phenomena involving other elements of the alkali metal group, namely sodium, potassium, lithium and rubidium.[1, 6, 7, 8 9, 10, 11]

In early work with cesium vapor converters, conducted within the General Electric Company, the first signs of a cesium attack problem were observed in the ceramic/metal-ceramic seal area. An example of this problem is shown in Figure 1* which depicts a cross-section of an active-alloy metal-ceramic seal, taken from an early cesium vapor converter. The seal had operated for 320 hours in a temperature range of 600 - 700°C and in approximately 1 Torr of cesium vapor, before seal and subsequent converter failure occurred. The effects of attack by the cesium vapor are apparent in the photomicrograph. Evidence was also discernable in early converters, on the attack by cesium vapor on other elements of the devices, in particular on brazed joints operating at elevated temperatures.

The program to be described was conducted in order to achieve an understanding of the phenomenon of cesium attack on materials and to evolve a series of materials that are resistant to cesium which could be used in the construction of reliable, long-lived vapor thermionic converters. Materials that were studied included ceramic materials, active-alloy metal-ceramic seals and metallic materials. The order just given is that

*See APPENDIX for illustrations

in which they were studied, in general, as well as that of indicated susceptibility to attack by cesium vapor.

Samples of material under study were contained in one of two types of vessel that were used. One was constructed of stainless steel and the other of a high purity alumina ceramic. Most of the tests were conducted in 1 Torr of cesium vapor. Tests were also performed in 10 Torr and 100 Torr. The range of temperature over which materials were studied was from about 400°C to 1200°C, depending on the material. The time of exposure of samples to the cesium vapor was in most cases 24 hours but extended tests were also performed in excess of 1000 hours in certain cases. After exposure of a sample to cesium vapor the extent of attack by the cesium on the material was determined by the change in weight produced in the sample or through visual and metallographic examination.

SUMMARY

Results of the study on ceramic materials indicated that the high alumina (97 percent Al_2O_3) type of ceramic being employed initially in converter fabrication was indeed subject to attack by cesium vapor at elevated temperatures. The results demonstrated further that high-purity alumina ceramic bodies such as sapphire, Lucalox* alumina, and bodies basically comparable to Lucalox alumina were resistant to attack by cesium vapor up to a temperature of 900°C.

Results of high-temperature operation in cesium vapor of Lucalox alumina and bodies basically comparable to Lucalox alumina have shown that such bodies are resistant to attack by cesium vapor up to a temperature of 1500°C. [12]

An additional finding on ceramic materials was that heat treatment (prior thermal history) can have an appreciable effect on the extent to which a ceramic body is attacked by cesium vapor.

In the study of active-alloy metal-ceramic seals it was demonstrated that seals containing an attack-resistant (high-purity alumina)

*General Electric tradename for sintered transparent to translucent high-purity alumina ceramic containing 99.7 percent Al_2O_3, nominal, balance MgO.

ceramic brazed with either titanium-nickel or zirconium-nickel alloy to tantalum are resistant to attack by cesium vapor at a pressure of 1 Torr, in accelerated tests performed at 900°C. Only in a considerably higher cesium pressure of 100 Torr were indications observed of reaction by the cesium with seal components.

A variety of metallic materials of po ential interest in thermionic converter construction were evaluated. First, a number of metals and alloys were tested, together, in approximately 1 Torr of cesium at a temperature of 900°C for 280 hours in a screening test. Then selected metallic materials were tested individually and in considerable detail.

Results of the screening test indicated that molybdenum and possibly the stainless steel which was included in the test (Type 430) alone showed resistance to cesium attack. All other materials tested showed signs of reaction. This test is now considered to have been very crude, in light of knowledge gained in later studies on metallic materials, and the results are viewed with reservation.

Time available in the present program permitted detailed reaction experiments to be performed only on copper, a 65 w/o copper-35 w/o gold alloy, and platinum. Results of these tests showed that for copper and platinum, an unpredictable and unusual variation of the extent of reaction with cesium vapor occurred as a function of temperature. Possible significance of these unusual results are discussed.

EXPERIMENTAL PROCEDURE AND EQUIPMENT

I. Test Vessel

Two types of test vessel were used to hold samples of material during testing, one being constructed of stainless steel and the other of high-purity alumina ceramic. In general, the study program on ceramic materials the initial survey of metal-ceramic seals, and the screening test on metallic materials were conducted using the stainless steel type of test vessel, while all other test programs exclusive of those listed above were conducted using the ceramic vessel.

The vessel used first (shown schematically in Figure 2) was constructed of Type 304 stainless steel, this being one of the best materials known at the start of the program for resisting attack by alkali metals.[1, 6, 7, 8, 9, 10] Type 304 stainless steel is also, of course, a

material which can be operated at a elevated temperatures in air. Operation or testing of the vessels in an air furnace was planned in order to keep the testing procedure as simple as possible. The container proper consisted of a six-inch length of two-inch diameter stainless steel tubing with a stainless steel header heliarc welded, under helium purging, to each end. A four-inch length of 1/4-inch diameter stainless steel tubing was inserted into a hole in the center of one of the headers and welded in place. This tubing, in turn, was copper-gold brazed to a length of 5/16-inch diameter OFHC copper tubing. A cesium-filled metallic pellet was positioned between two nickel mesh spacers at the container end of the copper tubing, while a threaded male connector suitable for connecting to an exhaust system manifold was brazed to the other end of the tubing (dotted line in Figure 2).

When it was ascertained that Lucalox ceramic and ceramic bodies comparable to it, such as the A-976* body, were resistant to attack by cesium vapor, the test vessel proper was constructed using the Type A-976 ceramic. A line drawing of this ceramic test vessel is shown in Figure 3. An exploded view showing the component parts of this test vessel is presented in Figure 4 while a photograph of a processed vessel is shown in Figure 5. After some experience in the use of the ceramic vessel, the molybdenum springs, shown in Figures 3 and 4, were omitted as being unnecessary.

Use of the high-purity alumina ceramic in the vessel proper (in place of stainless steel) offered two important advantages. First, it was believed that sublimation and outgassing of extraneous elements and impurities into the interior of the vessel during operation would be minimized. Second, testing in an air furnace could be accomplished at higher temperatures ($>1000^{\circ}C$) than is possible with stainless steel.

Other modifications in this improved test container included the use of:

(1) A modified Lucalox ceramic (A-976) platform or pallet for supporting samples under test.

(2) A radiation baffle made of the same ceramic material to minimize (a) thermal radiation from the hot zone of the vessel toward the appendage end,

---

*General Electric Power Tube Department designation

and (b) sublimation of extraneous material from the metallic portion of the vessel in the direction of the test samples.

As can be seen in Figures 2 and 3, both types of test vessel employed a similar type of appendage section which served two purposes: (1) it was the means by which the vessel was exhausted, and (2) it served as the cesium reservoir section of the final processed unit. Copper was selected for the outer section of the appendage for two reasons: (1) to insure reliable pinching off of the assembly after exhaust, and (2) to provide a cesium reservoir section having uniform temperature distribution (which the high conductivity of copper provided).

Before copper was finally adopted, two potential problems in its use were investigated and found to be of minor concern. One possible problem was oxidation of the copper during test operation, which was in air, when the copper would attain a temperature of 278°C while testing materials in 1 Torr of cesium, or up to a temperature of 515°C when testing materials up to 100 Torr of cesium. To minimize this oxidation problem, the final copper section of the appendage was nickel plated using a sulfamate bath which produces a dense coat. The effectiveness of this procedure in minimizing oxidation of the underlying copper was proven when a number of nickel-plated copper tubing samples, pinched off on both ends, were operated in an air furnace at 600°C for 48 hours. The pinch-offs remained leak tight and no appreciable oxidation of the underlying copper was observed in cross-sections of the samples. The other potential problem was cesium attack of the copper during test operation. Metallographic examination of the copper from the first few test vehicles indicated no appreciable reaction with the copper at the temperatures to which the copper was subjected. From results obtained during the study of copper at a later date, however, it was learned that copper does begin to react with cesium vapor at about 400°C. This reaction will be discussed under RESULTS. III. Metallic Materials.

A metallic pellet, filled with liquid cesium, was positioned between two nickel mesh spacers in the appendage section of the vessel. Prior to operating a test vessel containing material samples (more specifically, after pinch-off of the vessel from the exhaust system and before nickel plating), the pellet was crushed, releasing cesium to the interior of the vessel. In this manner, approximately 40 mg of cesium was inserted into each vessel. A final step in the preparation of the vessel assembly consisted of squeezing the crushed section of the appendage

in a vise at a 90-degree angle to the original squeezing. This step reopened the crushed section of the appendage allowing for free flow of cesium vapor along the full length of the reservoir section.

II. Processing

Before assembly of the test containers, all container materials as well as samples of materials to be tested were chemically cleaned according to accepted electronic tube fabrication practice consistent with the type of material involved. After chemical cleaning, the metallic material samples were fired in dry hydrogen, when this was compatible with the material, for five minutes at a temperature of from 850°C to 1000°C, the actual temperature depending on the specific material being processed. The metallic materials which were tested in the screening experiment were also vacuum fired at 850°C. Thereafter, the vacuum firing operation of material samples prior to incorporation into a test vessel was omitted since the samples received a vacuum firing at an appropriately high temperature during exhaust of the test vessel. The final operation for all ceramic materials entering into the test vessels, including ceramic parts of the vessels as well as ceramic samples, consisted of an air firing at 1000°C for one hour.

After a test vessel was constructed, the unit was connected to a vacuum system by means of the threaded connector. After suitable pumping, the temperature was raised to a selected value by induction heating (in the case of the stainless steel vessel) or in a globar furnace (in the case of the ceramic vessel), where it was held for one hour. The temperature selected for outgassing was, in general, kept constant for a given material and was, with few exceptions, at least as high as the highest planned testing temperature. The heating rate was so controlled that vacuum pressure was maintained below 1×10^{-5} Torr throughout the exhaust process, and the final pressure was between 1 and 5×10^{-6} Torr. After this, the container was pinched off from the vacuum system in the manner shown in Figure 2; the cesium pellet was crushed to release cesium to the interior of the vessel, and the copper was nickel plated to provide oxidation resistance. A photograph of a ceramic type test vessel while still contained in the bake-out oven and after exhaust and pinch off is presented in Figure 6.

III. Test Procedure

Figure 7 shows a schematic of a stainless steel type test vessel in place in an air furnace during test. The location of thermocouples (chromel-alumel) for measuring sample temperature and cesium reservoir temperature is shown, the former being spot welded to the stainless steel container and the latter being tightly bound to the end of the reservoir with nickel wire. In this case, the cesium reservoir temperature was adjusted to the desired value by moving the entire test container longitudinally in or out of the furnace, as required, after the desired sample temperature had been reached and became stabilized, while keeping the main portion of the container in the hot zone of the furnace, thereby adjusting the temperature gradient along the appendage. In this method of obtaining the desired cesium source temperature, the measured temperature at the cesium reservoir section of the appendage was the desired minimum of the system. A hood of aluminum foil which was formed around the protruding appendage, served to minimize extraneous effects from drafts and other room air currents. The cesium source temperature could be controlled to about $\pm 5^{\circ}C$ using this technique, but the process of adjusting for equilibrium conditions proved to be cumbersome and time consuming.

With the adoption of the ceramic test vessel, a change was required in the method of controlling cesium reservoir temperature during test. In this type of vessel, the required amount of heat conduction between the ceramic portion of the vessel and the appendage section could not be relied upon to heat the reservoir section to the required temperature. Also, it was necessary to take measures to avoid overheating the metal-to-ceramic seal in the assembly. Accordingly a heating tape was used for independently heating the reservoir section of the vessel. The tape was wound around the appendage and operated from a separate temperature controller receiving its sensing from a thermocouple bound to the end of the nickel-plated copper section. Comparable reservoir temperature control could be obtained, as with the passive method used with the steel vessel, with a minimum of manual adjustments required to bring all temperatures to equilibrium. A photograph of a ceramic vessel, in place in a furnace ready for test, is shown in Figure 8. The aluminum foil has been removed to show the arrangement of the heating tape.

Standard procedure for thermocouple placement around the ceramic type of vessel consisted of one thermocouple bound firmly to

the vessel proper, at the position of the sample inside, for measuring sample temperature, and two thermocouples bound firmly to the end of the reservoir section. Of the latter two, the controller thermocouple was placed on top of the reservoir temperature measuring thermocouple, which was in direct contact with the nickel-plated copper. The thermocouples consisted of chromel-alumel except in a limited number of tests performed above 1100°C, where the sample temperature measuring thermocouple consisted of platinum-platinum 10 percent rhodium.

Before this system employing the ceramic vessel could be used with assurance, it was necessary to establish the fact that the temperature of the copper section of the appendage was the minimum of the system during test operation. Otherwise, of course, the true cesium pressure during testing would be unknown. This was accomplished by attaching additional thermocouples on the flat portion of the vessel header and another thermocouple near the seal, and operating one of the vessels over the expected range of sample test temperatures and cesium reservoir temperatures. The results showed that the reservoir temperature remained the minimum of the system under all planned test conditions.

When the stainless steel test container was used, it was removed from the furnace while at test temperature and allowed to cool in the room air after completion of an experiment. After cooling, the end of the cesium reservoir section was cut off and examined to assure the presence of excess cesium in the vessel. (This portion of the assembly would be the first to cool and invariably it was here that all observable excess cesium would be found.) Then, the arc weld on the appendage end of the container was machined off, without using a coolant, and the samples were removed for examination.

Several procedures for terminating a test utilizing the ceramic test vessel were evaluated before an optimum method was adopted. This vessel, being made of ceramic, could not be removed directly from the furnace while at test temperature, lest it crack from thermal shock. This meant that a gradual cooling was required. At the same time, with excess cesium remaining in the vessel, the cesium could not be allowed to condense on the sample during the cooling period, thereby obliterating changes in weight and in surface condition produced in the sample during test. This required preferential condensation of the excess cesium in the appendage section of the assembly during the cooling process. Additionally, it was required that the sample not be subject to cesium pressure conditions different from those experienced during testing, particularly

in cooling from the more elevated test temperatures. This might likewise alter changes in weight and in surface condition produced during the test proper.

The test termination procedure adopted as standard with the ceramic vessel was as follows. At the end of the testing period, the furnace controller setting was adjusted to a temperature about 70°C higher than the existing cesium reservoir temperature, and the furnace and vessel were allowed to cool to this value while the reservoir heater was left in operation, maintaining the set reservoir temperature. When the vessel temperature reached the new setting, both furnace and reservoir heater were turned off simultaneously and the entire assembly was allowed to furnace cool to room temperature. Data taken on a number of vessels during this last step showed that the reservoir section cooled quickly (in about 20 minutes) to about 100°C, while the vessel proper took several hours to cool. As with the steel vessel, the excess cesium contained in the vessel was found condensed in the appendage section of the assembly, with no cesium being observed in the opposite end of the vessel where the sample was located.

After a vessel had cooled to room temperature, the weld between the appendage header and the vessel cup was cut off, and the sample was removed and immediately weighed. Subsequently, the appendage obtained from the vessel was cut open and examined to: (a) assure the presence of excess cesium in each case, and (b) to note the appearance of the copper inside, which, if bright, was an additional check that the vessel had remained leak tight during test.

IV. Samples and Measurements

A list of the various materials tested during this program is given in Table I.

The extent of attack on samples of materials being tested was measured principally by measuring change in weight produced under given test conditions. Metallographic and visual examination were also used to observe microstructural and other changes produced as a result of attack by cesium vapor especially in the case of gross attack on materials, in the work on metal-ceramic seals, and as a general check on exposed materials. It was concluded, in the course of the work, that a change in weight of a material sample was a more sensitive measure of

Table I - List of Material Samples Tested

A. Ceramics

1. Commercial 90% Beryllia
2. Commercial 85% Alumina
3. Commercial 99.5% Alumina
4. Commercial 94% Alumina
5. G-E Forsterite (F-202)*
6. G-E 97% Alumina (A-917)*
7. G-E 97% Alumina (A-923)*
8. G-E 97% Alumina (A-922)*
9. Sapphire
10. G-E Lucalox Alumina
11. Modified Lucalox (Type A-974)*
12. Modified Lucalox (Type A-976)*

B. Metal-Ceramic Seals

1. Tantalum - (Zirconium-Nickel) - 97% Alumina (A-923)*
2. Tantalum - (Titanium-Nickel) - G-E 96% Alumina (2548)**
3. Tantalum - (Zirconium-Nickel) - G-E Lucalox (A-976)*
4. Tantalum - (Titanium-Nickel) - G-E Lucalox (A-976)*

C. Metallic Materials

1. Molybdenum - 0.011-inch strip
2. Tantalum - 0.005-inch strip
3. Platinum - 1/8-inch wide x 0.002-inch ribbon
4. Columbium Alloy (FS-82) - 0.010-inch strip
5. Type 430 Stainless Steel - 0.010-inch strip
6. High purity Nickel (1001) - 0.006-inch strip
7. OFHC Copper - 0.010-inch strip
8. Copper-Gold (50%-50%) - 0.060-inch diameter wire
9. Gold - 0.001-inch foil
10. Fe-Cr-Al-Y Alloy - 0.011-inch strip
11. Carboloy (WC + 6% Co) - 0.053-inch diameter rod

*Power Tube Department designation

**Research Laboratory designation

the initiation or extent of attack by cesium vapor than was the result of metallographic or visual examination. For example, conclusive evidence of attack was not observed by metallographic examination in certain metallic materials, such as in the case of copper-gold alloy samples after 24-hour exposures, in spite of the fact that a substantial change in weight was observed.

A Sartorius (Semi-Mikro) Selecta balance readable to 0.01 mg with a precision of 0.02 mg according to the manufacturer's specification, was used for weighing. The total random error inherent in the weighing process was determined to be $\pm$ 0.03 mg by repeated weighing at random time intervals over a period of a week, of a cleaned and fired stainless steel sample selected for the purpose. A minimum of three weighings was made on each sample, before and after a test, and the average of these weights was taken as the measured value. Samples of metallic materials were weighed to the nearest 0.01 mg, while ceramic material samples were weighed to the nearest 0.1 mg.

In most of the experiments, exposure time of a sample to cesium vapor under specific temperature and cesium pressure conditions was held constant at 24 hours. This time period was selected as being sufficient to allow measurable reaction to take place between cesium vapor and a sample under test, and yet was not so long that an inordinately long test time would be required to completely investigate the rate of reaction versus temperature relationship for a given material. This was particularly significant when it became evident that tests conducted at temperatures spaced at short intervals were required to encompass unusual variations in degree of reaction versus temperature.

RESULTS

I. Ceramics

The results obtained on the various types of ceramic materials tested in the first part of the program, i.e., with the use of the stainless steel vessel, are summarized in Table II and plotted in Figure 9 in terms of gain in weight per unit area versus temperature after a 24-hour exposure in approximately 1 Torr of cesium. It should be noted that the values ($\Delta W/cm^2$) plotted along the ordinate in Figure 9 differ from those reported previously for the same set of curves.

Table II - Results Obtained on Ceramic Materials Tested for 24 Hours in One Torr of Cesium Pressure*

Test Temperature (°C)	Weight**	Commercial Beryllia (Frenchtown 787)	Commercial 85% Alumina (Coors AD85)	Commercial 99.5% Alumina (Wesgo AL995)	Commercial 94% Alumina (Coors AD94)	G-E Forsterite (F-202)	G-E 97% Alumina No. 1 (A-917)	G-E 97% Alumina No. 2 (A-922)	G-E 97% Alumina No. 3 (A-923)
620	(a)	0.0283	0.3240	0.9357	0.5759	0.8019	1.9088	1.6233	1.7043
	(b)	0.0	+0.1	+0.1	0.0	0.0	0.0	0.0	+0.1
	(c)	0.0	+0.048	+0.026	0.0	0.0	0.0	0.0	+0.017
650	(a)	0.0455	0.3117	0.9154	0.5771	-	-	1.6349	-
	(b)	+0.6	+0.2	+0.3	+0.5	-	-	+0.4	-
	(c)	+0.94	+0.099	+0.079	+0.17	-	-	+0.07	-
700	(a)	0.0282	0.3241	0.9358	0.5811	-	-	1.7511	-
	(b)	+0.5	+0.6	+0.2	+0.2	-	-	+0.1	-
	(c)	+1.07	+0.29	+0.052	+0.068	-	-	+0.016	-
740	(a)	0.0432	0.2971	0.9034	0.5793	0.8123	2.0176	-	1.6313
	(b)	+0.9	+1.2	+0.7	+0.3	+7.1	+10.0	-	+6.6
	(c)	+1.45	+0.61	+0.19	+0.102	+1.63	+1.50	-	+1.14
800	(a)	0.0430	0.2814	0.8176	0.5800	0.8049	0.7661	1.7974	1.6527
	(b)	+1.5	+2.2	+1.8	+0.5	+6.5	+6.2	+0.4	+4.4
	(c)	+2.42	+1.16	+0.51	+0.170	+1.50	+1.02	+0.065	+0.756
830	(a)	-	-	0.6909	-	-	1.8288	-	1.8061
	(b)	-	-	+4.0	-	-	+6.2	-	+3.8
	(c)	-	-	+1.38	-	-	+0.99	-	+0.615
900	(a)	-	-	-	0.5773	0.8094	1.7720	1.7581	1.6729
	(b)	-	-	-	+1.6	+5.6	+3.1	+0.2	+2.2
	(c)	-	-	-	+0.545	+1.29	+0.51	+0.033	+0.374

*T_{Cs} = 300°C
Bakeout = 900°C - 950°C for one hour

**(a) Original weight in grams, weighed to nearest 0.1 mg
(b) Change in mg
(c) Change in mg/cm^2 (estimated)

A commercial beryllia ceramic, containing 90 percent BeO, exhibited severe attack in 24 hours starting at a temperature of about 650°C (Figure 9, Curve1), and the rate of attack increased rapidly with temperature. The composition of this ceramic body was not determined during the course of this study program except that it contained a nominal 90 percent of BeO, as reported by the manufacturer. Also, it was noted that the ceramic body was quite porous when it was examined metallographically after having been exposed to cesium vapor at the various elevated temperatures. For these reasons it is believed that the results reflect the properties of a specific commercial beryllia ceramic only and not of BeO per se.

Three commercial alumina bodies of varying Al_2O_3 content (85 percent, 99.5 percent and 94 percent, as published by the manufacturers) were tested with the results shown in Figure 9, Curves 2, 3, and 4, respectively. All were attacked severely by the cesium but the extent of the attack as a function of temperature had no consistent relationship to the Al_2O_3 content. It should be noted particularly that the 99.5 percent Al_2O_3 body (Figure 9, Curve 3) was attacked more extensively as a function of temperature than was a body containing 94 percent Al_2O_3 (Curve 4).

Results of an anomalous nature were obtained on three General Electric Power Tube Department bodies, a Forsterite ceramic, F-202, and two 97 percent Al_2O_3 bodies, A-917 and A-923. The results are shown in Figure 9, Curves 5, 6, and 7, respectively. These ceramic bodies exhibited decreasing cesium attack with increasing temperature between 740°C and 900°C. The effect was shown to be real and not due to a possible unaccounted loss in weight that occurred during the high temperatures experienced during exhaust and test. The depth of reaction as determined metallographically also decreased with increasing temperature for the two alumina bodies in question, as shown in Figure 10. One of these ceramic bodies (A-923) was subsequently studied in greater detail, as described later, to ascertain the nature of the indicated anomalous behavior.

A somewhat surprising result was obtained with the third 97 percent Al_2O_3 body produced internally (A-922) as shown in Figure 9, Curve 8. Here, the anomalous effect was not obtained as in the case of the other 97 percent alumina ceramics (A-917 and A-923) and the level of attack by cesium vapor at temperatures up to 900°C for 24-hour periods was definitely lower, as measured by weight change and as noted in

metallographic examination. The unusual feature in these results stems from the fact that all three 97 percent alumina bodies experienced the same sintering schedule; in fact, they were fired at the same time (the significance of which will be referred to later). Also, the A-922 body contains the same fluxing agents as A-923, except in different proportions. It is believed that the difference observed in behavior in cesium vapor is a function of the latter condition, that is, the difference in composition of the fluxing agents. This will be discussed in greater detail in the DISCUSSION.

Four ceramic bodies showed no evidence of attack (either by change in weight or as evidenced in metallographic examination) after the 24-hour exposures at temperatures up to 900°C in the cesium of approximately 1 Torr pressure. These ceramic bodies, which are listed but not plotted in Figure 9, were sapphire, Lucalox alumina, and two modified versions of Lucalox alumina, designated A-974 and A-976. The two modified Lucalox alumina bodies are fundamentally the same as true Lucalox alumina, except that a less expensive alumina powder is used in the starting material of the former, and time-temperature sintering conditions are reduced during manufacture.

In a subsequent test, samples of these four bodies, a sample of A-922 (the promising 97 percent Al_2O_3 body), and a sample of the 94 percent Al_2O_3 body used as a control were tested in the same cesium pressure as before and in the same vessel at 800°C for 1076 hours. No evidence of attack was observed in the case of sapphire and the three types of Lucalox alumina either in terms of change in weight or as a result of metallographic examination, the A-922 body showed moderate attack, and the 94 percent Al_2O_3 body was corroded throughout.

For illustrative purposes, Figure 11 shows a photomicrograph of a ceramic body, 85 percent Al_2O_3, after attack by cesium vapor, while Figure 12 shows a photomicrograph of the modified Lucalox Type A-976 ceramic sample which was not attacked in the test of 24 hours at 800°C and a cesium temperature of 500°C.

These tests described on ceramic materials were conducted in the stainless steel type of vessel. Subsequently, the ceramic type of vessel was used when the A-923 ceramic, which had exhibited the anomalous behavior described previously, was selected for additional study of this effect. Here, individual samples of A-923 ceramic, disks 1.030 inches in diameter by 0.094 inch thick, were each operated in 1 Torr of

cesium vapor at various temperatures between 650°C and 1100°C for a period of 24 hours. The results obtained, in terms of gain in weight per unit area (mg/cm^2) versus temperature, are shown plotted in Curve A of Figure 13. It was clear that a discrepancy existed between these results and those obtained previously on the same ceramic body. The variation of weight change versus temperature followed a "normal" course, i.e., it increased exponentially with temperature with no indication of the anomalous effect observed previously.

Various parameters in the testing procedure were varied in an effort to repeat the results obtained previously with no success. Perhaps the most significant change made in the intervening period was in the type of vessel used. Therefore, using the same type of ceramic samples (A-923), several tests were repeated in a stainless steel vessel, following the exact same test procedure used in the tests which yielded the anomalous results. Also, other variables such as condensing out (by placing a water cooled copper plate in contact with the tip of the appendage during the cooling period) versus not condensing out of the excess cesium in the ceramic vessel at the completion of the test period were investigated in repeat tests. Investigation of the variables accounts for the group of points shown plotted around 780°C on Curve A of Figure 13. None of the variations investigated affected the results; all data obtained could be plotted on Curve A.

Further study at this point revealed a significant fact. It was ascertained that the latter samples of the A-923 ceramic body were from a different firing lot than the former (anomalous) group. A different sintering schedule had been used for the second group of ceramics which included a normal, slow cool from maturing temperature, whereas the group exhibiting the anomalous behavior came from an experimental lot which had received a fast cool. (Further details are given under DISCUSSION.)

Accordingly, a new batch of A-923 samples was prepared from the older (fast cool) lot of material and the series of experiments were repeated. The results are shown as Curve B of Figure 13. It was concluded that the unusual behavior thus exhibited stemmed from the particular prior thermal history of the ceramic samples. (See DISCUSSION.) The data shown plotted in Figure 13 are summarized in Table III.

Table III - Results Obtained for Two Lots of the A-923 Ceramic Body (G-E 97 Percent Alumina No. 3) Having Different Thermal Histories after 24 Hours in One Torr of Cesium Pressure*

Vessel** No	Order of Test	Bakeout Temperature (°C)	Test Temperature (°C)	Initial Weight (Grams)	Final Weight (Grams)	Change In Weight (mg)	Sample Area (cm^2)	Change In Sample Area (mg/cm^2)
1. Firing No. 335, "Normal" Cool								
M-12	1	850	690	4.76944	4.76964	+0.20	12.7	+0.0079
M-18	2	850	690	4.69914	4.69918	+0.04	12.7	+0.0016
11A	10	900-950	762	4.76351	4.76377	+0.26	12.7	+0.0204
3XA	8	900-950	780	4.82560	4.82551	-0.09	12.7	-0.0071
5A	7	900-950	785	4.69204	4.69250	+0.46	12.7	+0.0362
10A	4	900-950	785	4.34040	4.34043	+0.03	12.7	+0.0024
M-19	3	1250	790	4.81504	4.81543	+0.39	12.7	+0.0154
6A	9	900-950	885	4.84467	4.84608	+1.41	12.7	+0.1110
7A	5	900-950	885	4.78157	4.78203	+0.46	12.7	+0.0362
M-23	11	900	990	4.76070	4.76322	+2.52	12.7	+0.1980
12A	6	900-950	1045	4.69632	4.70196	+5.64	12.7	+0.4450
2. Firing No. 227, "Fast" Cool								
M-30	3	900	665	1.83465	1.83468	+0.03	4.17	+0.0072
M-29	2	900	690	1.84816	1.84836	+0.20	4.17	+0.048
M-31	4	900	730	1.76543	1.76556	+0.13	4.17	+0.0312
M-33	6	900	760	1.87070	1.87315	+2.45	4.17	+0.587
M-26	1	900	790	1.99127	1.99724	+5.97	4.17	+1.43
M-34	7	900	845	1.88059	1.88325	+2.66	4.17	+0.638
M-32	5	900	890	1.69764	1.69877	+1.13	4.17	+0.271
M-41	10	950	960	1.87061	1.87246	+1.85	4.17	+0.444
M-37	8	1000	1000	1.71830	1.72093	+2.63	4.17	+0.630
M-38	9	1100	1095	1.88913	1.89264	+3.51	4.17	+0.841

*Bakeout = at indicated temperatures for one hour

**M-xx = ceramic vessel, all others = stainless steel vessel

II. Metal-Ceramic Seals

The metal-ceramic seal portion of the program was conducted in two phases. In the first phase, a broad investigation, initiated to gain knowledge on the problem, consisted of accelerated testing on samples of early, state-of-the-art vapor thermionic converter seals at a temperature of 800°C and in approximately 1 Torr of cesium vapor (300°C cesium source temperature) in the stainless steel vessel. These seals contained 96 percent and 97 percent Al_2O_3 alumina bodies. Results of this investigation indicated that severe attack by cesium was occurring on the ceramic portion of the seals and possibly on the ceramic-to-active-alloy interface region.

When it was determined that it was necessary to use a high-purity alumina type of ceramic in the seals to avoid attack on the ceramic proper, a series of test seals was made using this type of ceramic body (A-976) brazed to tantalum by titanium-nickel and zirconium-nickel alloy. As the second phase of this part of the cesium attack program, these seals were then studied in detail in the ceramic type of test vessel to determine where other attack problems, if any, existed.

The seal shown in Figure 1, which experienced attack by cesium vapor after 320 hours at temperatures between 600°C and 700°C, contained tantalum brazed to a 97 percent alumina body (A-923) with eutectic zirconium-nickel alloy. Subsequently, accelerated tests were performed on samples of similar active-alloy seals at a temperature of 800°C and a cesium reservoir temperature of 300°C for various lengths of time. Figure 14 shows cross-sections of tantalum-(zirconium-nickel)-97 percent alumina ceramic (A-923) seals tested under these conditions for 24 hours, 15 hours and 6 hours, reading from left to right. The tantalum portion of the seals is not readily apparent in the photomicrographs of the seal cross-sections. It was sealed to the right side of each ceramic.

Figure 15 shows tantalum-(titanium-nickel)-96 percent alumina ceramic seals tested under the same conditions. Here the tantalum was sealed to both sides of the ceramic. The type of ceramic employed in the seals shown in Figure 15 was not included in the previous series of tests on ceramic bodies.

It should be noted that, in both of these types of seal, the attack on the particular ceramics used could have been predicted if results

on ceramic materials reported in the previous section had been available at the time of the tests. Actually results on the ceramic materials reported in the previous section were being obtained simultaneously or were available at a later date.

Study of the active-alloy metal-ceramic seals was then pursued in greater detail, using the attack resistant Lucalox Type A-976 ceramic in the seals. Emphasis was placed on investigating the compatibility with cesium vapor of seal constituents other than the ceramic, particularly the brazing alloy and the reaction products formed between this alloy and the ceramic.

Tests were made at 900°C in cesium pressures of 1 Torr and 100 Torr on sections of sample backed-up butt seals consisting of the A-976 ceramic brazed to tantalum with titanium-nickel and zirconium-nickel brazing alloy. For the main series of tests, pairs of seal sections each containing one of the two brazing alloys were operated together. In these tests the tantalum thickness was held constant at 0.010 inch. In a parallel experiment, several groups of seals were made and tested in which the tantalum seal metal thickness was varied, including 0.010 inch, 0.020 inch, and 0.030 inch. The brazing alloy was titanium-nickel. The objective was to determine the effect of mechanical stress in seals on the rate of attack by cesium vapor, the variable stress being produced by the different thicknesses of seal metal. Originally, it was planned to make the series of stressed seals using different thicknesses of molybdenum for the seal metal. It was found, however, that satisfactory seals could not be made consistently using molybdenum greater in thickness than 0.010 inch.

A summary of test conditions which applied in experiments on the active-alloy seals is given in Table IV.

Specific cross-sections of the sample seals were made: (1) for optimum exposure of all seal constituents to the cesium atmosphere during test, and (2) for subsequent evaluation of extent of cesium attack. These are shown in Figure 16.

For the first purpose, the cylindrical seal assemblies were cut across on the diameter and the resulting faces were metallographically polished. This cross-section, termed the transverse section, is shown in Figure 16B. After being cleaned, which followed the polishing operation, the transverse sections were examined metallographically

Table IV - Cesium Compatibility Test Conditions, Active-Alloy Metal-to-Ceramic Seals

Vessel No.	Sample No.	Type of Sample	Test Temp. (°C)	Cs Temp. (°C)	Cs Pressure (Torr)	Time (hours)	Shown in Figure No.
M-1	T-1A	0.010 inch Ta-TiNi-A976 seal, transverse section	900	278	1	24	17 (Initial)
	Z-2A	0.010 inch Ta-ZrNi-A976 seal, transverse section	900	278	1	24	18 (Initial)
M-3	T-4A	0.010 inch Ta-TiNi-A976 seal, transverse section	900	515	100	24	-
	Z-3A	0.010 inch Ta-ZrNi-A976 seal, transverse section	900	515	100	24	-
M-4	T-4B	0.010 inch Ta-TiNi-A976 seal, transverse section	900	278	1	144	19
	T-4B	0.010 inch Ta-TiNi-A976 seal, longitudinal section	900	278	1	144	23
	Z-3B	0.010 inch Ta-ZrNi-A-976 seal, transverse section	900	278	1	144	20
	Z-3B	0.010 inch Ta-ZrNi-A976 seal, longitudinal section	900	278	1	144	24
M-7	T-5B	0.010 inch Ta-TiNi-A976 seal, transverse section	900	515	100	144	28
	T-5B	0.010 inch Ta-TiNi-A976 seal, longitudinal section	900	515	100	144	30
	T-5B	0.010 inch Ta-TiNi-A976 seal, longitudinal section after etching	900	515	100	144	31
	Z-9B	0.010 inch Ta-ZrNi-A976 seal, transverse section	900	515	100	144	29
	Z-9B	0.010 inch Ta-ZrNi-A976 seal, longitudinal section	900	515	100	144	-
M-8	T-3A	0.010 inch Ta-TiNi-A976 seal, transverse section	900	278	1	144	-
	T-4-20A	0.020 inch Ta-TiNi-A976 seal, transverse section	900	278	1	144	-
	T-4-30A	0.030 inch Ta-TiNi-A976 seal, transverse section	900	278	1	144	-
M-9	T-3B	0.010 inch Ta-TiNi-A976 seal, transverse section	900	515	100	144	33
	T-4-20B	0.020 inch Ta-TiNi-A976 seal, transverse section	900	515	100	144	32
	T-4-30B	0.030 inch Ta-TiNi-A976 seal, transverse section	900	515	100	144	-
M-6	T-5A	0.010 inch Ta-TiNi-A976 seal, transverse section	900	278	1	1000	21
	T-5A	0.010 inch Ta-TiNi-A976 seal, longitudinal section	900	278	1	1000	25
	Z-9A	0.010 inch Ta-ZrNi-A976 seal, transverse section	900	278	1	1000	22
	Z-9A	0.010 inch Ta-ZrNi-A976 seal, longitudinal section	900	278	1	1000	26
M-11	T-6B	0.010 inch Ta-TiNi-A976 seal, transverse section	900	515	100	1000	-
	Z-11B	0.010 inch Ta-ZrNi-A976 seal, transverse section	900	515	100	1000	-
M-10	T-6A	0.010 inch Ta-TiNi-A976 seal, transverse section	900	No cesium	-	144	-
	T-6A	0.010 inch Ta-TiNi-A976 seal, longitudinal section	900	No cesium	-	144	27
	Z-11A	0.010 inch Ta-ZrNi-A976 seal, transverse section	900	No cesium	-	144	-

and photomicrographs of typical examples were taken, before testing in cesium vapor. Examination and photomicrographing were repeated after exposure to cesium in the tests.

Then, the transverse section was mounted and a cut was made perpendicular to one of the faces, as shown in Figure 16C. The new face, called the longitudinal section, was polished, examined metallographically, and photomicrographed. This latter cross-sectioning permitted viewing the profile of all constituents in the sample seals and determining the extent of attack on specific components.

No detectable reaction between the cesium and constituents of either the titanium-nickel or the zirconium-nickel seals was observed after 24 hours, after 144 hours, or after 1000 hours at 900°C and 1 Torr of cesium. In Figures 17 and 18, the transverse sections of a titanium-nickel and a zirconium-nickel seal, respectively, are shown before testing in cesium. The transverse sections of the corresponding types of seal samples are shown in Figures 19 and 20 after 144 hours at 900°C in 1 Torr of cesium and in Figures 21 and 22 after 1000 hours under the same conditions. As can be seen in Figures 19 and 20, in particular, the ceramic in the seal is separated from the brazing alloy. This separation occurred during handling of the transverse sample after the test in cesium. It was learned through experience with this and subsequent samples that very careful handling was required to keep samples of active-alloy seals intact after test operation at a temperature of 900°C. (See SECTION II of this report on embrittlement of active-alloy seals during high-temperature operation.)

It was concluded that the discoloration or darkening of the brazing alloy seen in Figures 19 through 22 was the result of thermal etching that took place during the 900°C operation rather than the result of reaction with cesium. The first supporting evidence for this conclusion was the fact that similar active-alloy metal-ceramic seal samples being operated in vacuum at 900°C (described in SECTION II of this report) all showed similar darkening of the brazing alloy. More direct evidence was obtained when the longitudinal sections of the samples in question were examined. The longitudinal sections of the titanium-nickel and the zirconium-nickel brazed samples corresponding to those depicted in transverse section in Figures 19 through 22 are shown in Figures 23 through 26 respectively. No evidence of reaction by the cesium vapor was observed. For comparison purposes, the longitudinal section of a titanium-nickel brazed seal is shown in Figure 27 after operation at 900°C for 144 hours, with no cesium included in the test vessel.

After 24 hours at 900°C and 100 Torr of cesium, a slight surface reaction on both the titanium-nickel and zirconium-nickel brazing alloy constituents was observed. After 144 hours under the same conditions, what appears to be an alloying between the brazing alloy and the cesium occurred, forming a low melting product that flowed over the seal constituents, preferentially over the metallic constituents of the seals. This can be seen in Figures 28 and 29, the transverse sections of titanium-nickel and zirconium-nickel brazed seal samples, respectively, after 144 hours at 900°C in 100 Torr of cesium. An additional point to be noted in the last two figures is that the ceramic became etched during operation at 100 Torr of cesium. The longitudinal section of the titanium-nickel brazed seal, from the two just described, is shown in Figure 30, unetched, and in Figure 31, etched. As can be seen in these four illustrations, the ceramic became separated from the brazing alloy during handling of the samples after the test operation in cesium vapor.

A composite view of the entire transverse section of a titanium-nickel seal containing 0.020-inch thick tantalum seal metal (from one of the "stressed" seal series that was tested) is shown in Figure 32 after 144 hours at 900°C in 100 Torr of cesium vapor. This further illustrates the flowing effect, in addition to revealing the fact that the product which is formed in the test operation in the high pressure of cesium tends to originate in the brazing alloy fillet of the seal where an excess of the brazing alloy is found. Another composite view of the entire transverse section of a titanium-nickel brazed seal after 144 hours at 900°C in 100 Torr of cesium vapor is shown in Figure 33.

In the series of seals containing different thicknesses of seal metal, no evidence of attack was observed after 144 hours at 900°C in 1 Torr of cesium. At 100 Torr of cesium and the same time and temperature, all samples exhibited the alloying and flow effect. No effect attributable to the different seal metal thicknesses, and thus to the supposed different stress levels, was demonstrated in either group of seals.

III. Metallic Materials

The evaluation of the compatibility of metallic materials with cesium vapor was also conducted in two phases. In the first phase, selected materials of random size and shape were exposed, in the same stainless steel vessel, to cesium vapor of approximately 1 Torr (300°C reservoir temperature) for 281 hours at a temperature of 900°C. Then, they were examined visually and metallographically to determine extent

of reaction with the cesium vapor. This was a rather crude screening test performed in order to obtain urgently needed information as soon as possible for converter design purposes. In the second phase, selected metallic materials were studied in the ceramic test vessel, one sample at a time, varying temperature, cesium pressure, and time.

Before the group of metallic materials was selected for test in the first phase of this study, constitution diagrams of the various combinations of elements involved were examined to make sure that no combinations were present which would form a melt at the intended test temperature of 900°C. As a result, several materials under consideration, for example silver, were eliminated. Even so, after the test was completed, there was evidence of some interaction having occurred between the samples that were selected, so that the results of the test are viewed with reservations.

Figures 34 through 37 show photomicrographs of the most severely attacked of these metallic materials, namely, OFHC copper, 50 w/o copper-50 w/o gold alloy, gold, and platinum, respectively, after the operation at 900°C for 281 hours in approximately 1 Torr of cesium. The results of visual and metallographic examination of these samples are summarized in Table V.

When a quantitative study of metallic materials was undertaken in the second phase of this work, the ceramic type of test vessel was used and samples of uniform size, except for thickness of material, were used. The samples, disks 7/8 inch in diameter, were punched from sheet material. In each experiment, an individual sample of a material was used. Time and funds available permitted extensive data to be taken only on OFHC copper, a 65 w/o copper-35 w/o gold alloy, and commercially pure platinum. Data on these metallic materials are presented in Tables VI, VII, and VIII, respectively.

In Figure 38 data are plotted in terms of weight change in mg/cm^2 versus temperature for OFHC copper after being operated in 1 Torr and in 10 Torr of cesium vapor for 24 hours, while the same type of information is presented in Figures 39 and 40 for 65 w/o copper-35 w/o gold alloy, and pure platinum after operation for 24 hours in 1 Torr of cesium vapor. The results obtained for copper and platinum were quite unexpected and are discussed further under DISCUSSION.

Table V - Visual Appearance and Results of Metallographic Examination of Metallic Materials After Exposure to Cesium Vapor at 900°C for 281 hours (Phase I)

Material	Results Obtained
Molybdenum	Bright surface;[1] no visible reaction[2]
Tantalum	Mixed bright and matte surface;[3] internal pores and precipitate near surface
Platinum	Matte surface; brittle; internal pores (Shown in Figure 37)
Columbium Alloy (FS-82)	Mixed bright and matte surface; reaction zone at surface
Type 430 Stainless Steel	Bright surface; no visible reaction
Nickel	Mixed bright and matte surface; reaction zone at surface
Copper	Matte surface; "cored" structure throughout (Shown in Figure 34)
Copper-Gold (50%-50%)	Matte surface; cored as in copper; large pores throughout (Shown in Figure 35)
Gold	Matte surface; surface attack (Shown in Figure 36)
Fe-Cr-Al-Y Alloy	Matte surface; mild surface attack
Carboloy (WC + 6% CoO)	Mixed bright and matte surface; no visible reaction

1. Visual appearance
2. Metallographic examination
3. Non-uniform surface reaction

Table VI - Results Obtained for OFHC Copper after 24 Hours*

Vessel No.	Order of Test	Test Temperature (°C)	P_{Cs} (Torr)	Initial Weight (Grams)	Final Weight (Grams)	Change In Weight (mg)	Change (mg/cm^2)
M-87	13	652	1	0.25546	0.25544	-0.02	-0.0026
M-83	11	735	1	0.25169	0.25156	-0.13	-0.017
M-89	15	740	1	0.25316	0.25311	-0.05	-0.0064
M-77	8	805	1	0.26335	0.26330	-0.05	-0.0064
M-82	10	825	1	0.24528	0.24529	+0.01	+0.0013
M-80	9	862	1	0.25670	0.25679	+0.09	+0.0115
M-86	12	903	1	0.25688	0.25695	+0.07	+0.0090
M-54	2	910	1	0.24888	0.24883	-0.05	-0.0064
M-88	14	950	1	0.24976	0.24979	+0.03	+0.00385
M-53	1	975	1	0.25442	0.25441	-0.01	-0.0013
M-61	5	1022	1	0.27260	0.27255	-0.05	-0.0064
M-66	7	1030	1	0.27365	0.27375	+0.10	+0.013
M-57	4	1080	1	0.25700	0.25726	+0.26	+0.0334
M-65	6	1150	1	0.26345	0.26363	+0.18	+0.0231
M-56	3	912	100	0.24846	0.24848	+0.02	+0.0026

*Platinum material = 7/8-inch diameter x 0.002-inch thick
Total surface area = 7.8 cm^2
Bakeout = 1200°C for one hour

Table VII - Results Obtained for 65 w/o Copper-35 w/o Gold Alloy after 24 Hours*

Vessel No.	Order of Test	Test Temperature (°C)	P_{Cs} (Torr)	Initial Weight (Grams)	Final Weight (Grams)	Change In Weight (mg)	Change (mg/cm^2)
M-50	6	505	1	0.22936	0.22918	-0.18	-0.023
M-49	5	618	1	0.23010	0.22963	-0.47	-0.0605
M-48	4	690	1	0.23335	0.23242	-0.93	-0.12
M-28	1	785	1	0.23370	0.23052	-3.18	-0.41
M-35	2	910	1	0.24330	0.23305	-10.25	-1.32
M-46	3	895	No cesium	0.24757	0.24719	-0.38	-0.049

*Copper-gold alloy = 7/8-inch diameter x 0.002-inch thick
Total surface area = 7.8 cm^2
Bakeout = 900°C for one hour

Table VIII - Results Obtained for Platinum after 24 Hours*

Vessel No.	Order of Test	Test Temperature (°C)	P_{Cs} (Torr)	Initial Weight (Grams)	Final Weight (Grams)	Change In Weight (mg)	Change (mg/cm^2)
M-67	13	457	1	1.66708	1.66700	-0.08	-0.0099
M-52	7	495	1	1.67880	1.67868	-0.12	-0.015
M-51	6	590	1	1.69915	1.69900	-0.15	-0.0185
M-64	12	655	1	1.67735	1.67730	-0.05	-0.0062
M-27	2	690	1	1.68844	1.68850	+0.06	+0.0074
M-60	9	740	1	1.68410	1.68422	+0.12	+0.015
M-63	11	762	1	1.69123	1.69102	-0.21	-0.026
M-25	1	790	1	1.69341	1.69333	-0.08	-0.0099
M-62	10	830	1	1.68501	1.68484	-0.17	-0.021
M-59	8	865	1	1.68955	1.68939	-0.16	-0.02
M-36	3	885	1	1.69165	1.69139	-0.26	-0.032
M-79	21	440	10	1.67212	1.67200	-0.12	-0.015
M-72	18	490	10	1.68753	1.68733	-0.20	-0.025
M-71	17	605	10	1.69245	1.69191	-0.54	-0.067
M-78	20	648	10	1.69432	1.69410	-0.22	-0.027
M-70	16	715	10	1.69510	1.69511	+0.01	+0.001
M-74	19	755	10	1.68835	1.68821	-0.14	-0.017
M-69	15	800	10	1.69355	1.69350	-0.05	-0.006
M-81	22	852	10	1.69137	1.69113	-0.24	-0.03
M-68	14	905	10	1.68820	1.68680	-1.40	-0.173
M-43	4	910	100	1.68775	1.68605	-1.7	-0.21
M-44	5	885	No cesium	1.69336	1.69291	-0.45	-0.056
			After 900°C Bakeout only				
M-84	23	-	-	1.70006	1.69995	-0.11	-0.0136
M-85	24	-	-	1.70379	1.70351	-0.28	-0.0346
M-90	25	-	-	1.70406	1.70389	-0.17	-0.021
M-95	26	-	-	1.69201	1.69168	-0.33	-0.0407

*OFHC copper material = 7/8-inch diameter x 0.020-inch thick
Total surface area = 8.1 cm^2
Bakeout = 900°C at one hour

Data obtained for the rate of reaction in terms of weight change (loss, in this instance) per unit area versus cesium vapor pressure for copper at a temperature of 900°C for 24 hours are plotted in Figure 41.

DISCUSSION

I. Ceramic Materials

A. General

It was shown conclusively during the course of this investigation that certain high-purity alumina ceramics, such as sapphire, Lucalox alumina, and sintered ceramic bodies comparable to Lucalox alumina are resistant to attack by cesium vapor at temperatures up to 900°C. In other work, not a part of this program,[12] Lucalox alumina and modified Lucalox alumina (A-976 and A-974 bodies) were shown to be resistant to attack up to 1500°C.

On the other hand, it was shown that standard commercially available high-alumina ceramics, even those containing in excess of 99 percent Al_2O_3 may be subject to appreciable attack. It is logical to assume that in these cases cesium vapor reacts with a compound or compounds other than Al_2O_3 contained in the bodies in the amount of 100 percent minus the percent of Al_2O_3. Further, it was shown that the extent of attack was not necessarily a function of how high the alumina content is in a given ceramic body; rather, the results indicate that it is also a function of the type of extraneous material other than Al_2O_3 contained in the ceramic body. There are strong indications that SiO_2 is a main offender when it is one of the ingredients in a ceramic body.[12] The specific proportions of the additive oxides (fluxing agents) in an alumina ceramic body may be a significant factor determining susceptibility of the ceramic body to reaction with cesium vapor. This will be discussed further under C. Composition of Fluxing Material.

B. Effect of Prior Thermal History

It was shown that a high-alumina ceramic body could exhibit markedly different susceptibility to reaction with cesium vapor at elevated temperatures, depending upon the rate at which the ceramic was cooled from its maturing temperature. Thus, for the A-923 ceramic body, the degree of reaction with cesium vapor at elevated temperatures was considerably lower when the ceramic was cooled from 1300°C

to 1000°C at a "normal" 50°C per hour after the maturing firing than it was when the ceramic was cooled over the same range of temperatures in one hour. It is generally accepted that a slower cooling rate favors the formation of crystalline phases in the fluxing materials of a ceramic, versus formation of glassy phases in the course of rapid cooling. It is also generally accepted that a material of a specific composition will be more reactive thermally when it is in the glassy phase than when it is crystalline.

The reason for the peak in attack by cesium vapor versus temperature obtained for the rapidly cooled A-923 samples (Curve B of Figure 13) was not investigated. However, assuming the above reasoning is correct, it is quite probable that the peak and subsequent decline in reaction with temperature signifies the onset and progressive increase of devitrification of glassy phases which were formed during the rapid cooling.

C. Composition of Fluxing Material

Comparison of the results obtained on two of the 97 percent alumina ceramic bodies, A-922 and A-923 (Figure 9, Curves 8 and 7, respectively) lends support to the belief that specific proportions of the additive oxides in the fluxing material of an alumina ceramic influence susceptibility to reaction with cesium vapor at elevated temperatures. Both ceramics contain the same oxides in the three percent of the fluxing material present in each, namely SiO_2, MgO and CaO and both sets of ceramic samples experienced the same firing schedule, i.e., with a fast cool since both sets of samples were in the same firing lot. In the A-922 body, however, the mol fractions in the three percent total of additive oxides are 0.28, 0.42, and 0.30 for SiO_2, MgO, and CaO, respectively, whereas in the A-923 body they are 0.68, 0.185, and 0.135, respectively.

The increased susceptibility to reaction with cesium vapor of the A-923 ceramic can probably be attributed in part to the higher mol fraction of SiO_2 contained in this body. However, the quantity of SiO_2 contained in the A-922 ceramic body is still appreciable, being on the order of one percent by weight. On this basis alone, A-922 would be expected to have been much more severely attacked by the cesium vapor at the elevated temperatures than it was relative to the other alumina bodies studied. Its relatively high resistance to cesium attack is believed

to stem from the formation of a cesium resistant phase or phases (probably a crystalline phase or phases as opposed to a glassy phase) in the fluxing material of the ceramic developed on the original cooling of the ceramic during its manufacture. This is a function of composition of the fluxing material and the cooling rate.

Additional insight was gained in regard to composition of ceramic materials and how this appears to affect reaction to cesium vapor, in the results obtained on the Forsterite ceramic. The samples of the Forsterite ceramic which were tested (Figure 9, Curve 5) did not receive a fast cool during processing as did the A-917, and A-923 alumina samples. Yet the Forsterite ceramic samples exhibited the same type of anomalous behavior as the fast cooled alumina samples between temperatures of about 740°C and 900°C. A Forsterite ceramic normally contains a higher proportion of glassy material than does a high-alumina ceramic even after normal processing in the case of the former. Therefore, the anomalous behavior observed with the Forsterite samples is believed to be part of the same devitrification phenomenon discussed previously regarding the rapidly cooled alumina ceramics.

II. Metal-Ceramic Seals

It was shown during this investigation that metal-ceramic seals consisting of tantalum brazed with titanium-nickel or zirconium-nickel alloy to Type A-976 (modified Lucalox alumina) ceramic are resistant to cesium attack at 900°C in 1 Torr of cesium vapor. Seals of this composition have been tested in excess of 1000 hours under these conditions. The test temperature used here is well above the predicted maximum useful operating temperature for such seals. (See SECTION II) In a parallel work effort,[13] the predicted resistance to cesium vapor at approximately 1 Torr pressure is being verified since several cesium vapor thermionic converters, containing titanium-nickel brazed seals of the type discussed above, are operating on life test in excess of 1500 hours at a seal temperature of above 600°C.

It has also been shown that at a much higher cesium pressure of 100 Torr and at a temperature of 900°C, gross reaction occurred between both types of brazing alloy and the cesium, forming a product which melted and flowed over the seal interface region. Where this gross reaction begins to occur as a function of cesium pressure at a temperature of 900°C or as a function of temperature at 100 Torr of cesium was not investigated. Such active-alloy seals should therefore

be used with caution at elevated temperatures in cesium pressures appreciably above 1 Torr. Investigation of this phenomenon more fully remains to be done in future work.

Also remaining to be investigated in future work is the compatibility of other types of metal-ceramic seals with cesium vapor, in particular those seals containing a metallizing layer such as that produced by the conventional molybdenum-manganese process. Study of such alternative types of metal-ceramic seals was not undertaken in this program because of the lack of reliable information on the compatibility of the brazing alloys with cesium vapor. The work on copper and copper-gold alloy was initiated to obtain such data.

III. Metallic Materials

Results obtained on the 65 w/o copper-35 w/o gold alloy (Figure 39) were perhaps the most "straightforward" obtained during the study of metallic materials. Several significant conclusions can be drawn from these data. Comparing these results with those obtained on copper alone (Figure 38), it would seem that the gold component in the copper-gold alloy is attacked predominently. Further, the attack was manifested by a significant loss in weight of the copper-gold alloy samples over the entire range of temperatures at which they were tested. This agrees with results obtained in the longer time test of a copper-gold sample in cesium vapor at 900°C, which resulted in the formation of a considerable quantity of voids in the material (Figure 30).

Significance of the results obtained on the three metallic materials (copper, copper-gold, and platinum) where the effect produced by cesium attack was a net loss in weight in the material over specific intervals of temperature, warrants discussion. First, this effect implies that volatile reaction products are formed between the cesium vapor and the material being attacked under such conditions. However, little is known about the nature of such a reaction or the reaction products formed. Second, such an effect signifies transport of the material being so attacked to surrounding regions of a device in which the material is incorporated. Since such material transport and ultimate deposition can be of critical importance in devices utilizing cesium vapor (such as deposition of foreign matter on the emitter, collector, or insulator of a thermionic converter), this phenomenon should be studied in greater detail. It is of considerable importance to identify the reaction products formed under these conditions as well as to ascertain the deposition mechanism of the process.

Opportunity was not available for investigating more fully the very unusual and unexpected results obtained in the variation with temperature of the level and type of attack by cesium vapor on copper and platinum (Figures 38 and 40), resulting in apparent weight gain as well as weight loss of material as a function of temperature. Resolution of the unusual phenomenon involved must await further investigation.

Several undesirable features were recognized in the course of the experiments performed on copper and platinum. These features will require modification in future work in order to improve upon the reliability of the results obtained. First, in many of the cesium reaction experiments the net change in weight produced in the test samples was undesirably near to the estimated random error in the weighing process (± 0.03 mg). In future work, the incremental changes should be increased by increasing certain test parameters such as time or cesium pressure. In spite of this factor, however, continuous curves could be drawn through the data points (which were obtained in a random order) which lends support to the belief that the fluctuations in reaction rate with temperature for copper and platinum represent a real effect.

Second, it was realized late in the sequence of tests on copper that an excessively high bake-out temperature of $900^{\circ}C$ had been selected for this material. At this temperature, copper has an appreciable sublimation rate, on the order of 4.5×10^{-8} g/cm^2/sec,[14] and during the hour at temperature during bake-out, the samples could theoretically lose up to 1.31×10^{-3} grams by sublimation.

The actual loss thus sustained during bake-out was measured on four samples of copper which were taken through the bake-out operation and weighed. These data are tabulated at the end of Table VI, while the average of the four values obtained in terms of mg/cm^2 is shown in the form of the dotted line in Figure 38 (-0.0275 mg/cm^2). An unexpectedly large spread was measured in the change in weight engendered during bake-out in the four samples thus tested which requires further investigation.

In the experiments on the copper-gold alloy (Figure 39), a comparable correction for loss in weight due to sublimation during bake-out would also be required for the results to be fully accurate. Here, however, the ultimate error involved is negligible because of the large changes in weight which resulted during the reaction experiments.

For platinum, the error due to unaccounted sublimation during bake-out, at 1200°C, is also much less than in the experiments on copper because of the respectively lower vapor pressure of platinum. The estimated quantity thus involved, for platinum, is 0.001 mg/cm^2.[14]

It is suggested that at least over part of the range of testing temperatures, the factors of grain size and quantity of grain-boundary-material present under given temperature-time conditions, may play a part in the results obtained on copper. The temperature corresponding to the inflection obtained in the weight change data (Figure 38) at about 600°C also corresponds to the temperature of rapid grain growth for copper.[15] This possibility was suggested during microscopic examination of the surface of exposed copper samples, in which the grain boundaries were the areas predominently showing evidence of attack. This hypothesis could not, however, be definitely proved on the basis of examining grain size of samples which were operated for the 24-hour test periods at the test temperatures of 450°C to 900°C. While a slight, progressive increase in grain size was discernible in the samples with increasing test temperature, no decided increase in grain size was observed in the samples which were tested starting at about 600°C and higher.

Part of the marked loss in weight of copper samples tested at about 750°C and higher is felt to be due to sublimation of the material during the test period. Because data were not available on the rate of sublimation of copper in the various pressures of cesium vapor at these temperatures, this factor cannot be taken into account quantitatively.

Several factors regarding the testing of materials became clear, particularly during the metallic materials compatibility study. First, it is believed that a given material should not be tested solely at some single, selected temperature in cesium vapor in order to properly categorize its compatibility with cesium vapor. Rather it is necessary to study materials over a range of elevated temperatures and probably over a range of cesium pressures in order to encompass possible variation in degree and type of reaction with temperature, such as was observed for copper (Figure 38) and even more for platinum (Figure 40).

Second, visual or metallographic examination alone cannot be relied upon as a means of determining extent of reaction between cesium vapor and a material under test. Supposing the effect of the reaction is removal or loss of the material being tested, the results may

not be observable in metallographic examination of the material after test. This was found to be true for the three metallic materials which were tested in detail in the present program under the 24-hour test period conditions. Here, evidence of reaction with cesium vapor was not definitely discernible in metallographic examination of any of the samples after exposure to the cesium vapor, although positive changes in weight in the samples were measurable. The latter is believed to be a corollary of the statement made above, namely, that measurement of a change in weight of a sample of material being evaluated for compatibility with cesium vapor is a more accurate and sensitive measure of initiation and extent of reaction between cesium vapor and the material being evaluated.

IV. Purity of Cesium Employed

Two grades of metallic cesium of differing purity were used in the present investigation. The analysis is shown in Table IX. In the data presented in Figures 13 and 38 through 41, data points shown as circles were obtained with Type A, or the less pure cesium; data points shown as squares were obtained using Type B or the higher purity cesium. In all other work Type A cesium was used. There was no definite trend in the results obtained which would indicate that differing levels of impurities in the cesium in the elements listed in the analysis, had an effect on rate of attack on materials.

However, information in the literature[1, 6] regarding the corrosion behavior of cesium and of alkali metals other than cesium, indicates that extent of attack by alkali metals on various materials can be greatly influenced by the presence of certain impurity elements in the cesium, an important element being oxygen. In future work, therefore, it will be important to investigate and to take into account this effect of impurity elements or contaminants in the cesium and to learn how they influence the reactivity of cesium vapor on materials of interest.

CONCLUSIONS AND RECOMMENDATIONS

Experimental evidence has shown that high-purity alumina ceramics where no glassy fluxing material is present are resistant to attack by cesium vapor up to 900°C. Limited experiments indicated resistance to attack as high as 1500°C. Ceramic bodies such as Lucalox alumina and modified Lucalox alumina's A-974 and A-976 are recommended as materials which meet this requirement.

Table IX - Analysis of Metallic Cesium

Element	Type A (parts per million)	Type B (parts per million)
Na	1048	29
K	131	13
Rb	372	115
Li	<16	<16
Ba	101	≤8
Sr	<2	<2
Ca	194	24
Fe	1339	26
Cr	194	<2
Ni	31	<2
Co	118	-
Cu	13	5
Al	11	3
Mg	15	8
Mn	37	3
Ti	5	<2
Tl	≤2	≤2
Pb	≤2	≤2
Sn	≤8	≤8
B	<16	<16
Si	100	24

Metal ceramic seals consisting of tantalum to Lucalox alumina with an intermediate braze of nickel-titanium or nickel zirconium alloy have been found to be cesium resistant at temperature up to 900°C at cesium vapor pressures normally encountered in practical thermionic converters.

The tests on copper, copper-gold alloy and platinum indicate interactions with the cesium vapor. The nature of these results is unexpected and should be confirmed by an independent experimental approach. These interactions occur above 400°C so that these materials are satisfactory for use in the reservoir region of a converter where this temperature is not exceeded.

REFERENCES

1. R. N. Edwards and H. Kirtchik, "Research and Development of Propellent Feed System for Ion Engines," Contract No. NAS 8-1615 (November 15, 1961).

2. P. Wagner and S. R. Coriell, Rev. Sci. Inst., 30, 937 (1959).

3. L. Yang and F. D. Carpenter, J. Electr. Soc., 108, 1079 (1961).

4. F. Tepper et al., "Factors Affecting the Compatibility of Liquid Cesium with Contaminant Metals," Contract AF 33(657)-9168, MSAR Job. No. XA-720317.

5. F. G. Block et al., "The Development of a Low Temperature Vapor Filled Thermionic Converter for Nuclear Applications," Contract NObs 84823, Index No. SF 013 0624, Task 2853.

6. Liquid Metals Handbook, Sodium-Na K Supplement, TID-5277, Atomic Energy Commission - Dept. of the Navy (July 1, 1955).

7. A. d. Brasunas, Corrosion, 9, 78 (1953).

8. A A. Smith and G. C. Smith, Iron and Steel Inst. Jour., 196, 29 (1960).

9. W. D. Mauly, Corrosion, 12, 46 (1956).

10. J. W. Taylor and A. G. Ward, Nuclear Power, 3, 101 (1958).

11. M. E. Ihnat, "The Reaction of Glasses, Pyrolytic Graphite, and Selected Refractories with Sodium Vapor at Elevated Temperatures," Contract AF 49(638)-659, ARPA Order No. 6-58, Task No. 11.

12. E. Fungold, "Attack by Cesium Vapor on Silica-doped Alumina at Elevated Temperatures," Contract AF 49(648)-1092.

13. E. A. Baum, "Evaluation of a Molybdenum Emitter Low Voltage Arc Thermionic Power Converter," AF 33(657)-8323.

14. S. Dushman, "Scientific Foundations of Vacuum Technique," John Wiley and Sons, Inc., Second Edition, pp. 696-699 (1962).

15. ASM Metals Handbook, pp. 260 (1948).

APPENDIX
ILLUSTRATIONS

Figure 1 - Photomicrograph of cross-section of a thermionic converter seal (tantalum - zirconium-nickel G-E 97 percent alumina ceramic) after approximately 300 hours of operation

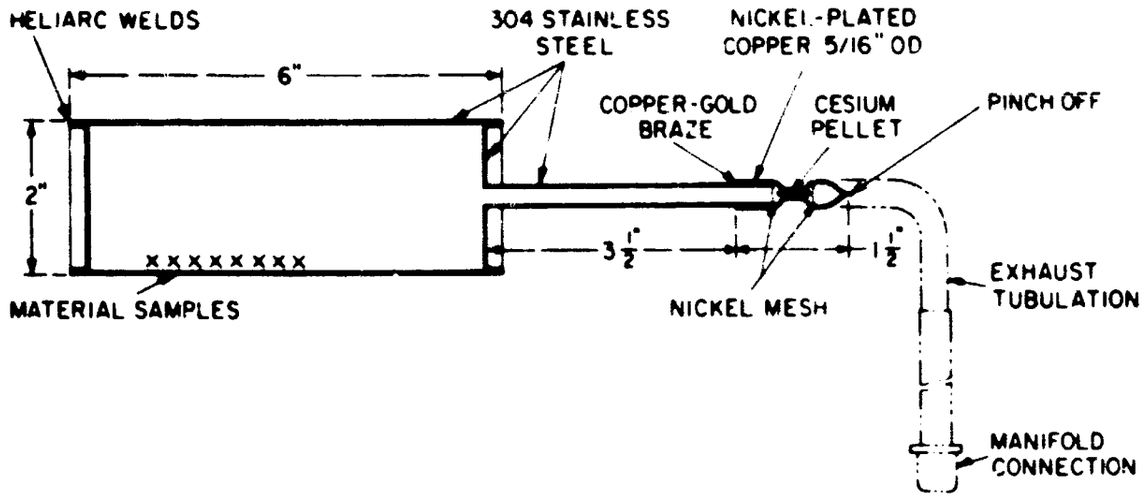

Figure 2 - Schematic cross-section of stainless steel test vessel

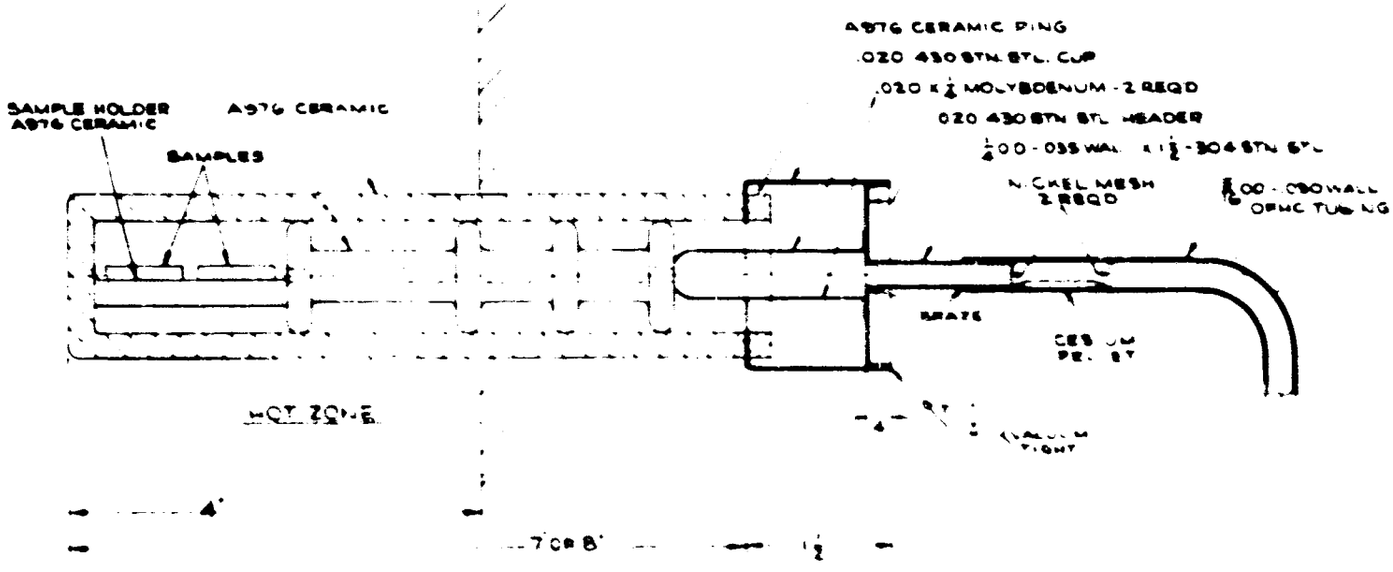

Figure 3 - Schematic cross-section of ceramic test vessel

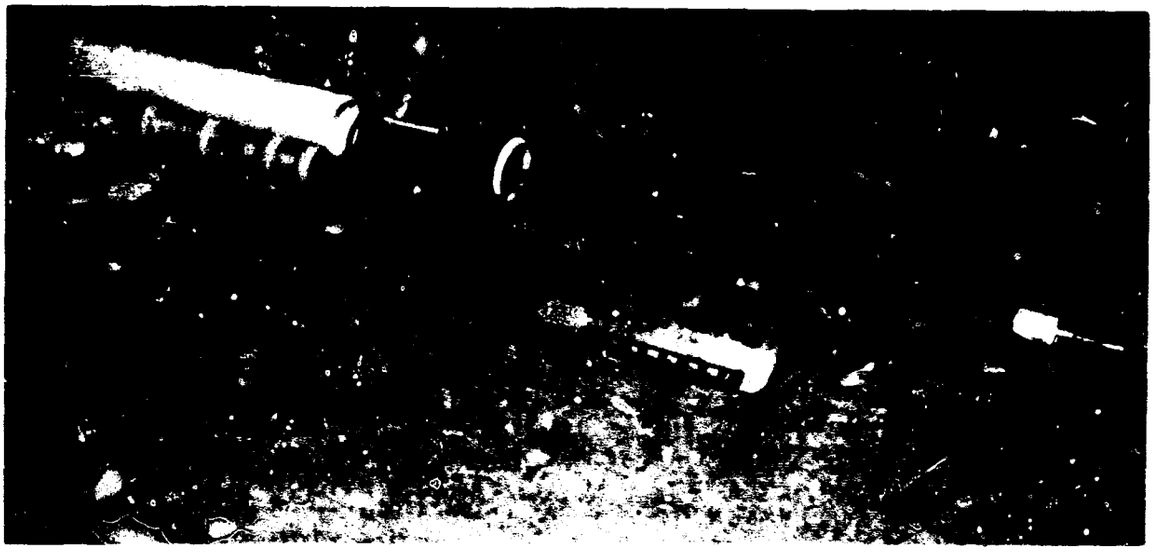

Figure 4 - Exploded view showing component parts of ceramic test vessel

Figure 5 - Processed ceramic test vessel

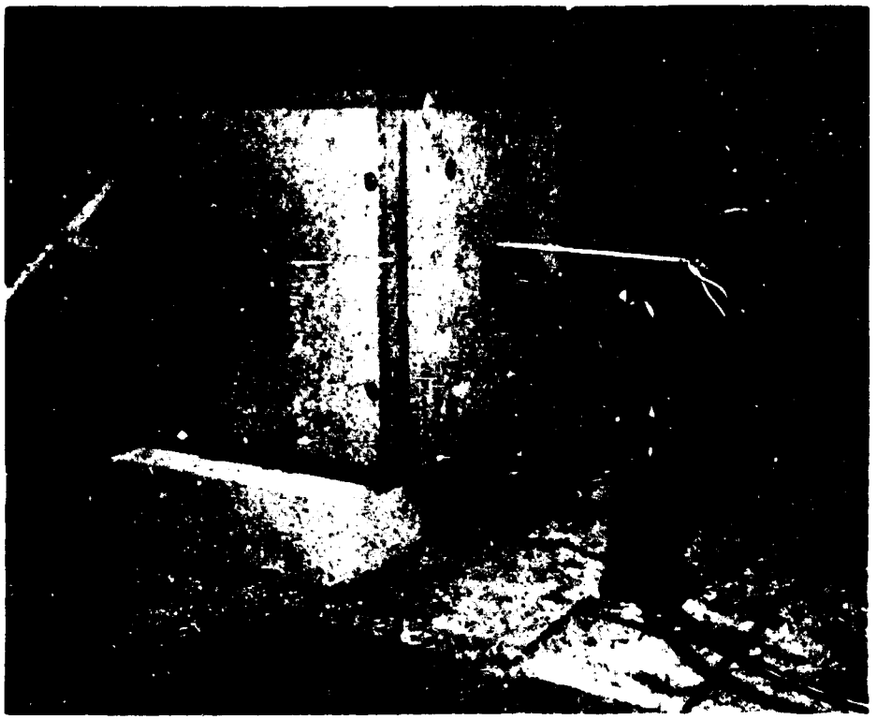

Figure 6 - Ceramic test vessel in exhaust furnace after pinch off

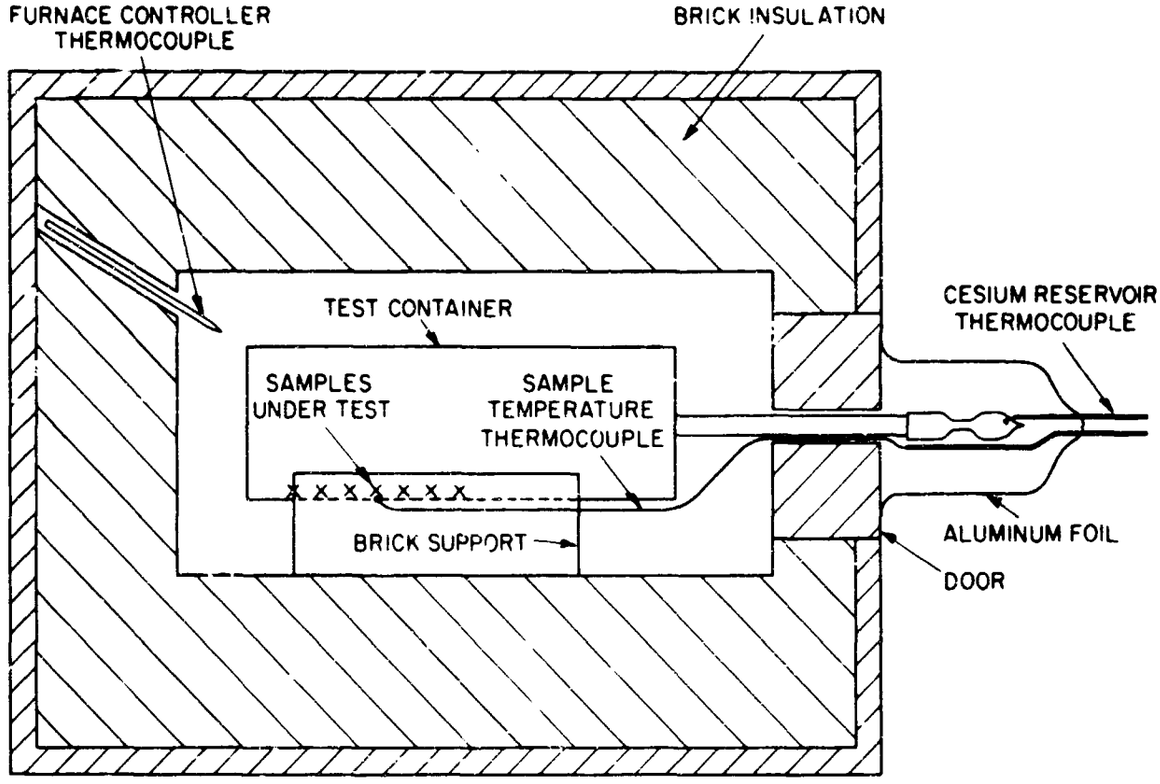

Figure 7 - Schematic of stainless steel test vessel under test in furnace

Figure 8 - Ceramic test vessel undergoing test

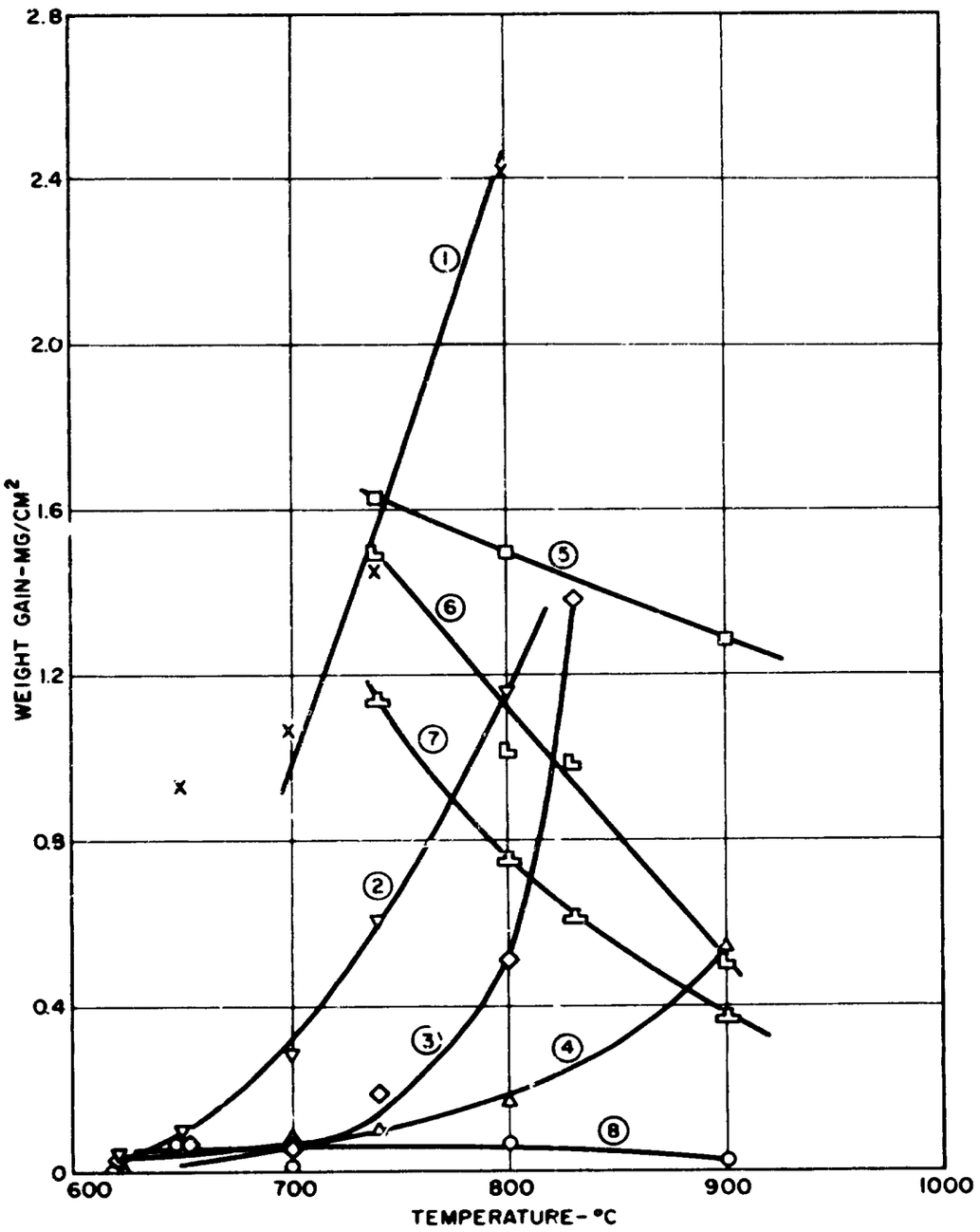

CURVE	MATERIAL
①	X COMMERCIAL BERYLLIA
②	▽ COMMERCIAL 85% ALUMINA
③	◇ COMMERCIAL 99.5% ALUMINA
④	△ COMMERCIAL 94 % ALUMINA
⑤	□ G-E FORSTERITE
⑥	G-E 97% ALUMINA NO. 1
⑦	G-E 97 % ALUMINA NO. 3
⑧	○ G-E 97 % ALUMINA NO. 2

SAPPHIRE, LUCALOX ALUMINA, A-974 (MODIFIED LUCALOX ALUMINA NO. 1), A-976 (MODIFIED LUCALOX ALUMINA, NO. 2), SHOWED NO SIGNIFICANT CHANGE IN WEIGHT UP TO 900°C.

Figure 9 - Variation of gain in weight versus temperature for selected ceramic materials (exposure time = 24 hours, cesium pressure = 1 Torr)

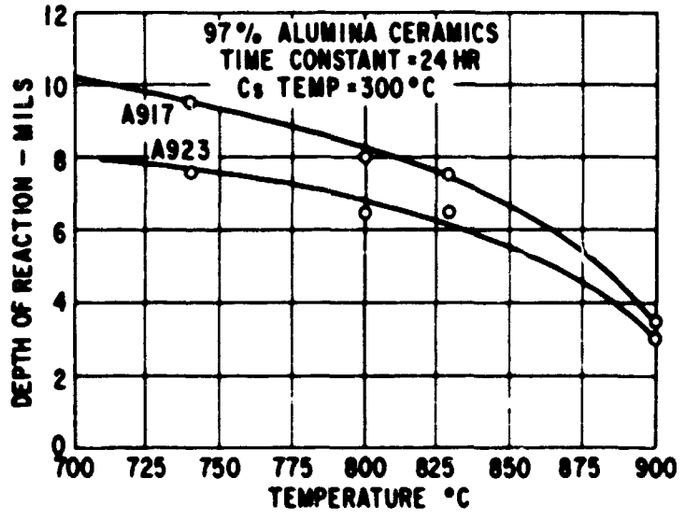

Figure 10 - Depth of reaction in 24 hours versus temperature for two 97 percent alumina ceramics

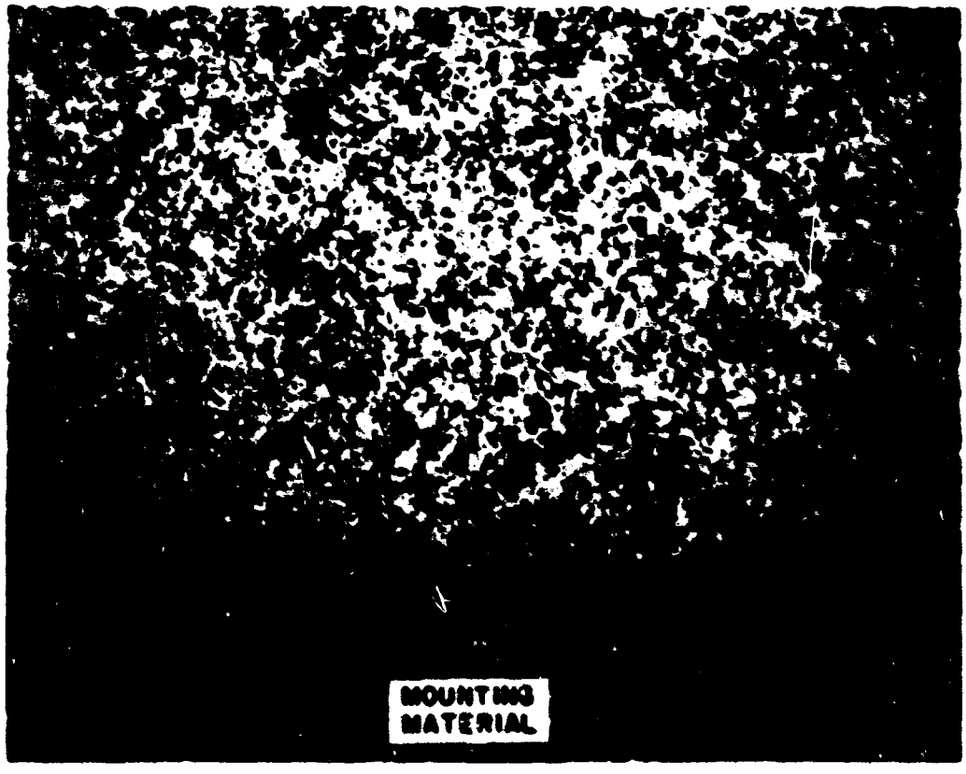

Figure 11 - Photomicrograph of 85 percent alumina ceramic after 24 hours at 800°C in 1 Torr of cesium vapor, 100 X

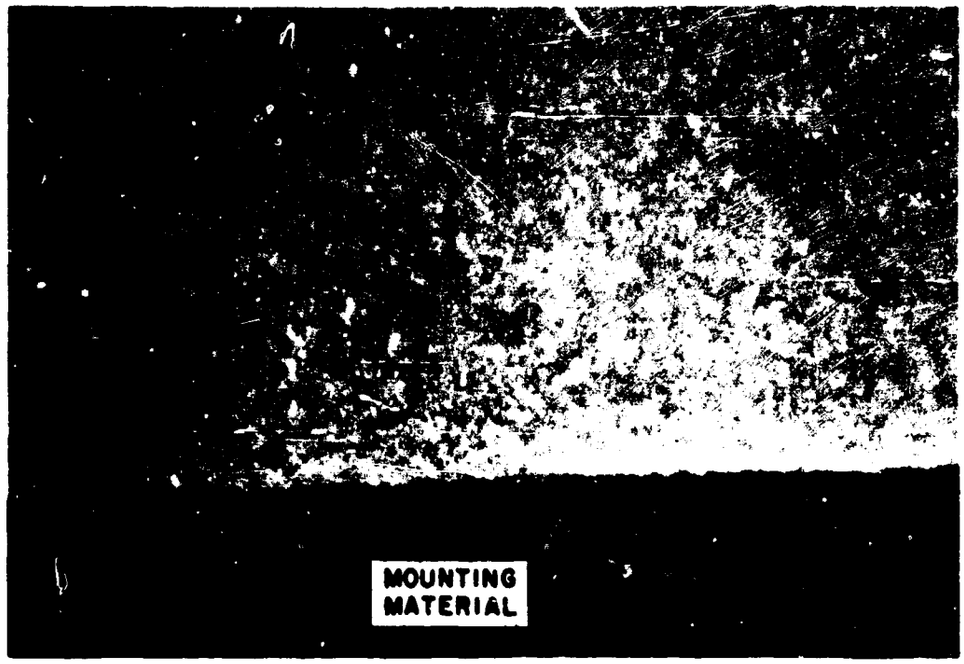

Figure 12 - Photomicrograpn of modified Lucalox alumina (A-976) after 24 hours at 800°C in 1 Torr of cesium vapor, 100 X

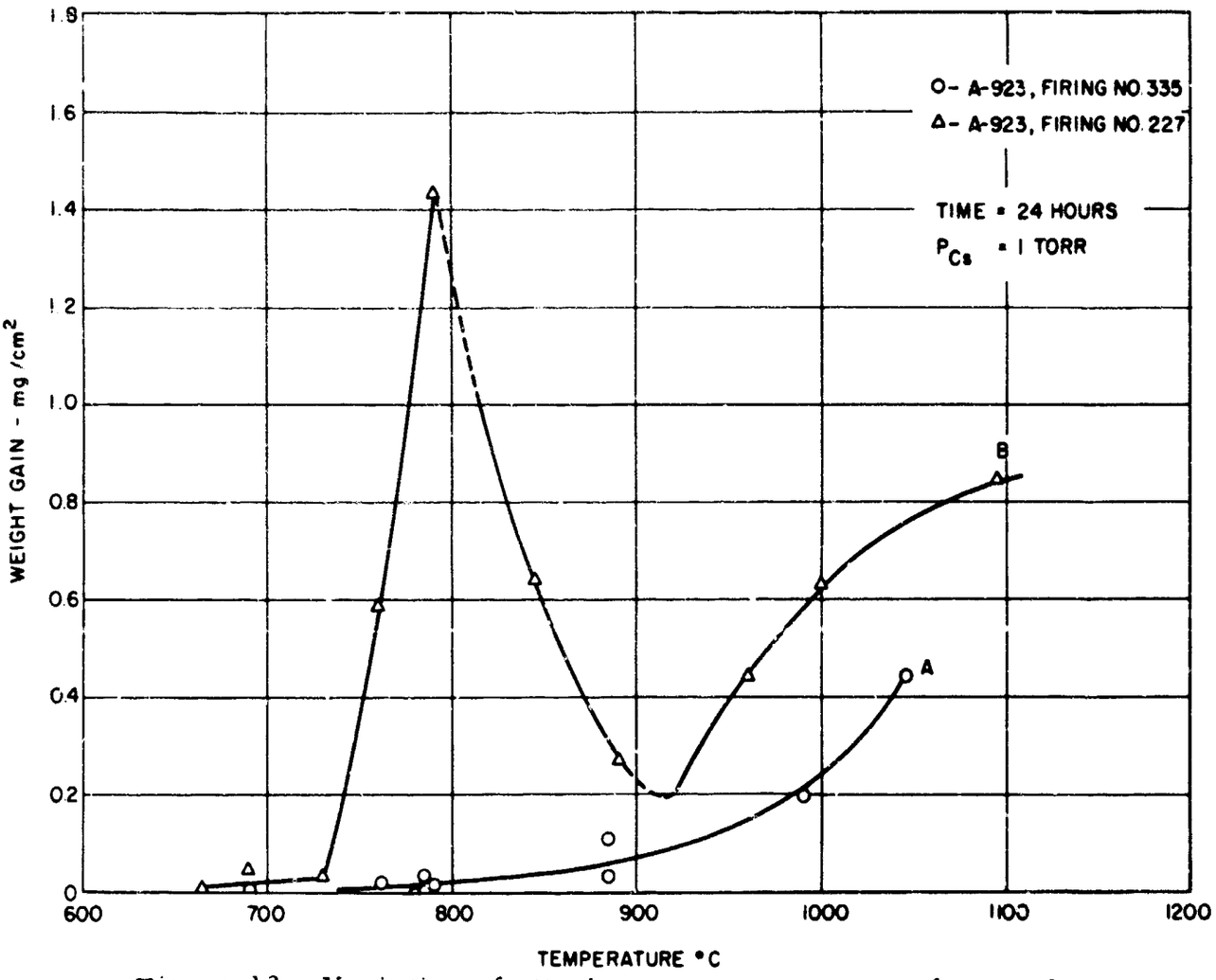

Figure 13 - Variation of attack versus temperature for two lots of the A-923 ceramic body having different thermal histories

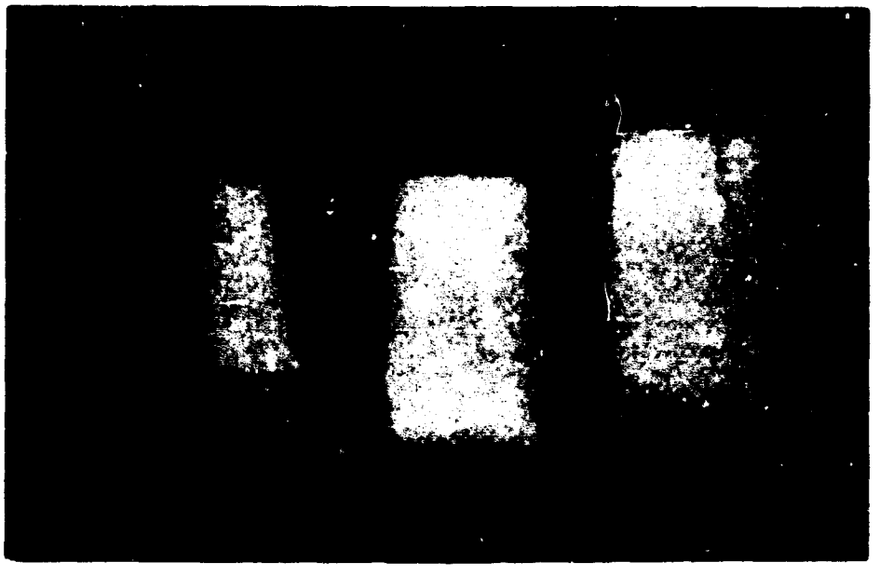

Figure 14 - Cross-sections of Ta-(ZrNi)-97 percent alumina metal-ceramic seals after 24 hours, 15 hours, and 6 hours (left to right) at 800°C in 1 Torr of cesium vapor, 16 X

Figure 15 - Cross-sections of Ta-(TiNi)-96 percent alumina metal-ceramic seals after 24 hours, 15 hours, and 6 hours (left to right) at 800°C in 1 Torr of cesium vapor, 16 X

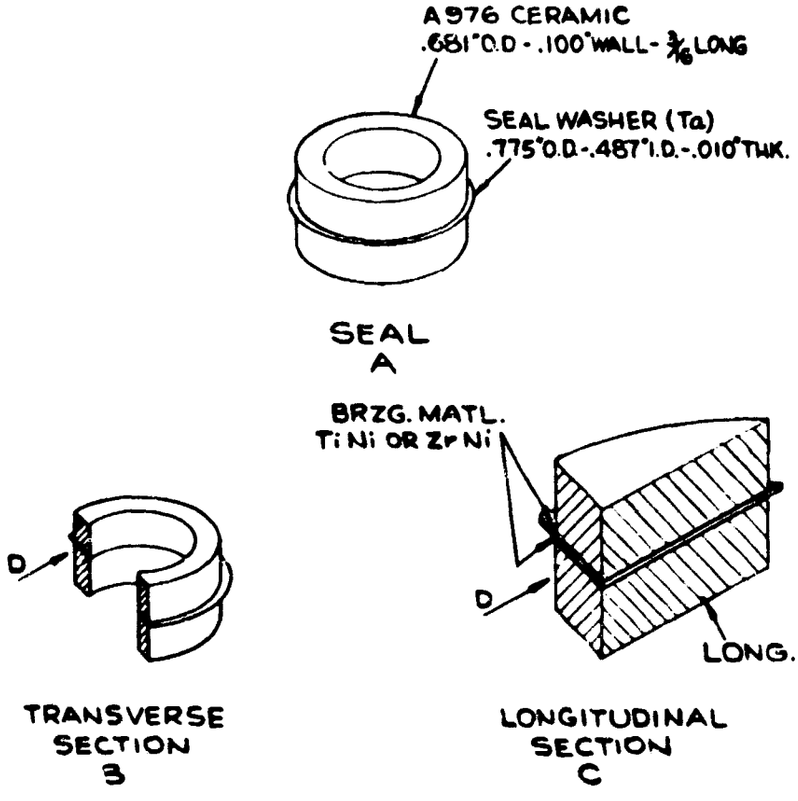

Figure 16 - Metal-to-ceramic seal test sample

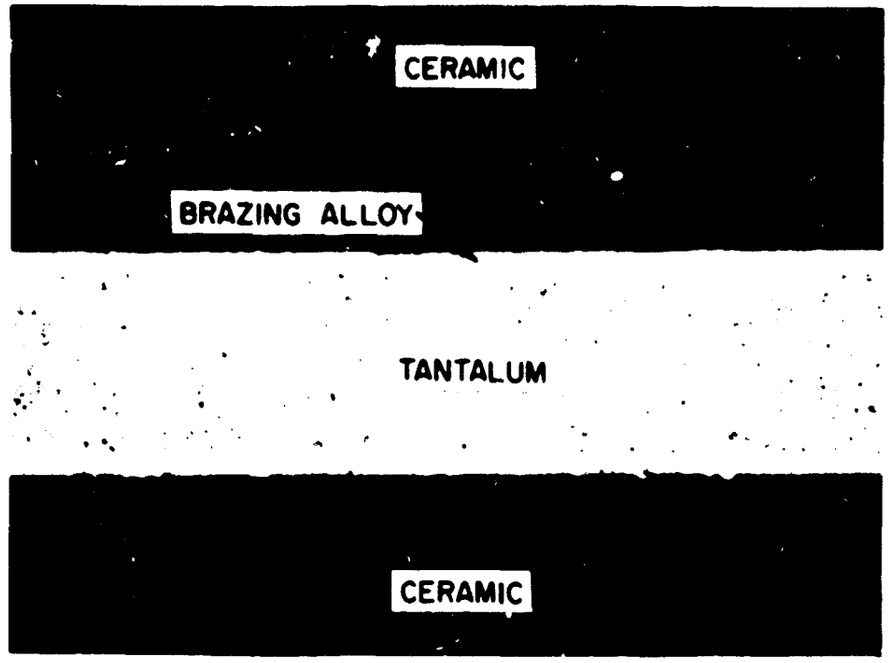

Figure 17 - Photomicrograph of seal sample T-1A, transverse section, initial test, 100 X

Figure 18 - Photomicrograph of seal sample Z-2A, transverse section, initial test 100 X

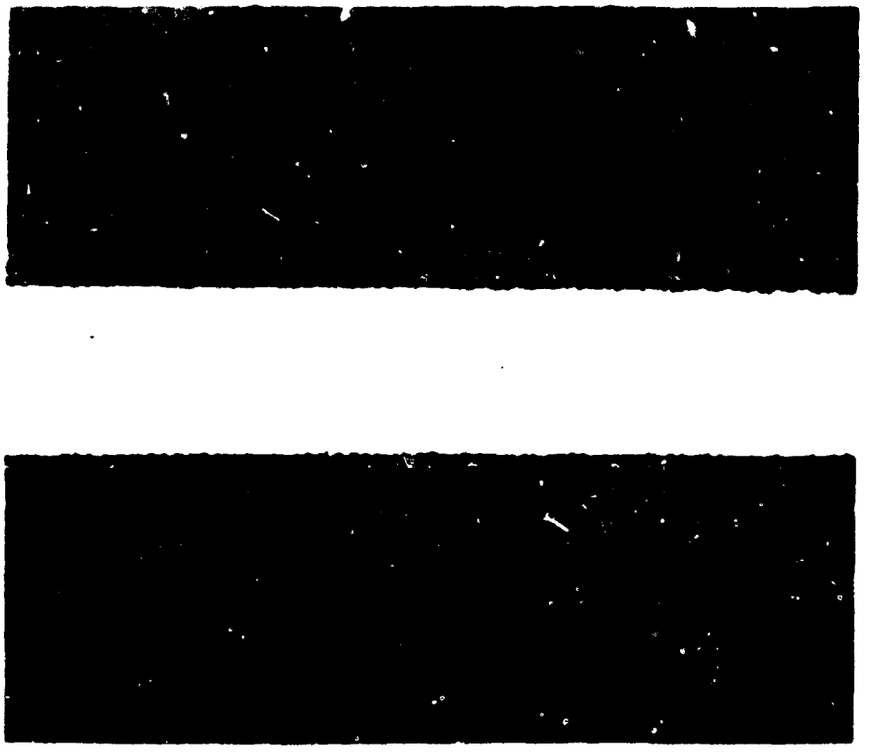

Figure 19 - Photomicrograph of seal sample T-4B, transverse section, after 144 hours at 900°C in 1 Torr of cesium vapor, 100 X

Figure 20 - Photomicrograph of seal sample Z-3B, transverse section, after 144 hours at 900°C in 1 Torr of cesium vapor, 100 X

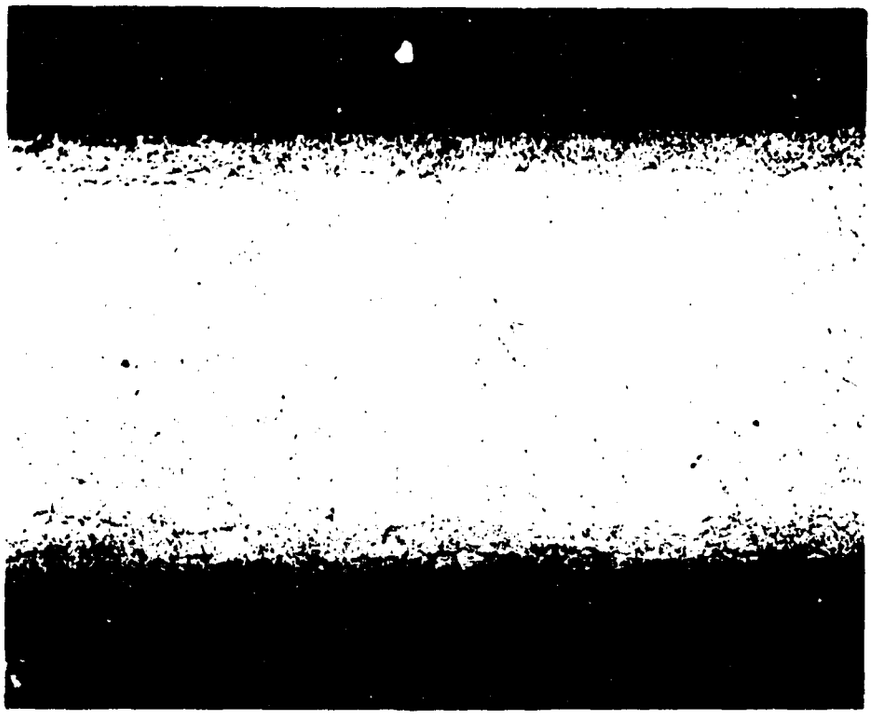

Figure 21 - Photomicrograph of seal sample T-5A, transverse section, after 1000 hours at 900° C in 1 Torr of cesium vapor, 250 X

Figure 22 - Photomicrograph of seal sample Z-9A, transverse section, after 1000 hours at 900°C in 1 Torr of cesium vapor, 250 X

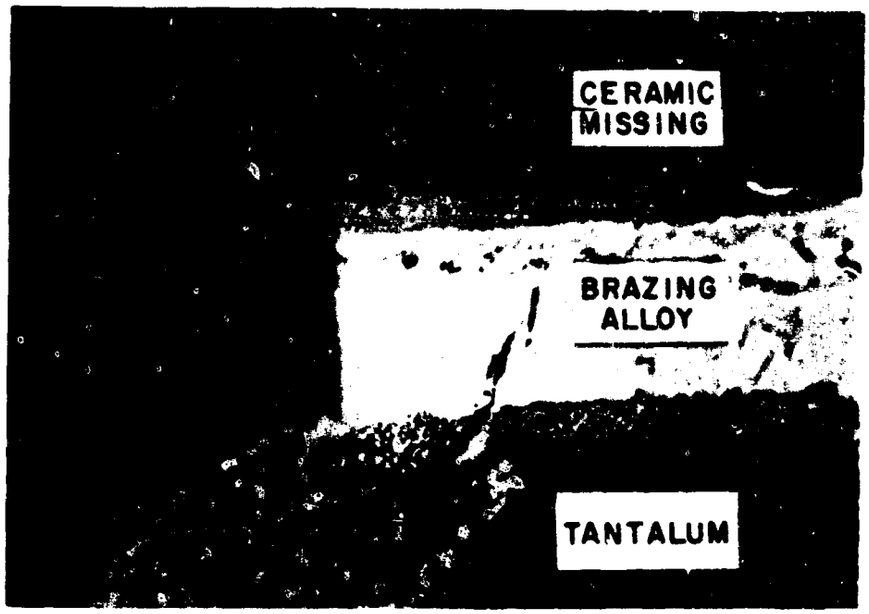

Figure 23 - Photomicrograph of seal sample T-4B, longitudinal section, after 144 hours at 900°C in 1 Torr of cesium vapor, 1000 X

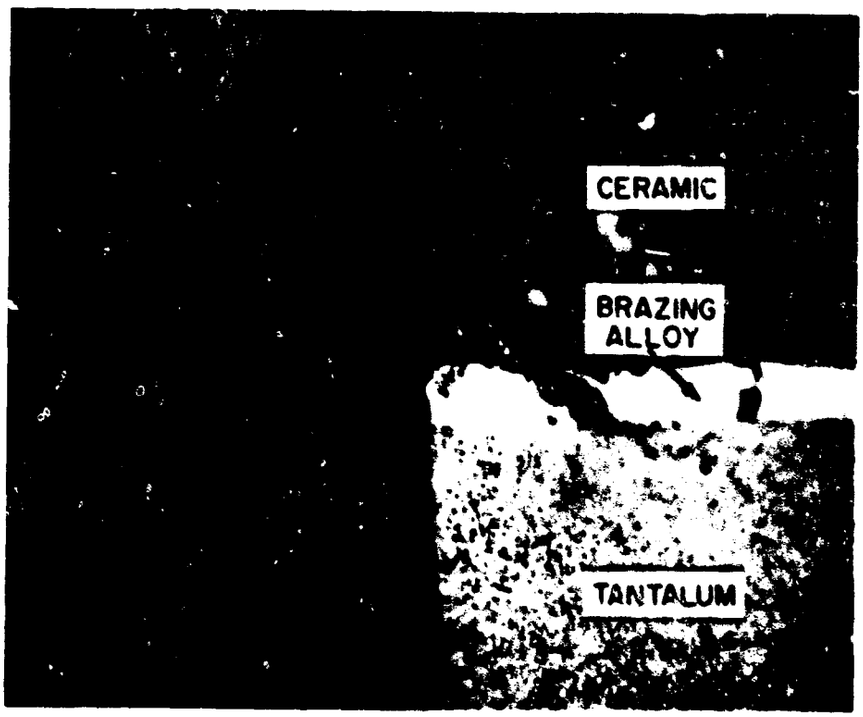

Figure 24 - Photomicrograph of seal sample Z-3B, longitudinal section, after 144 hours at 900°C in 1 Torr of cesium vapor, 250 X

Figure 25 - Photomicrograph of seal sample T-5A, longitudinal section, after 1000 hours at 900°C in 1 Torr of cesium vapor, 250 X

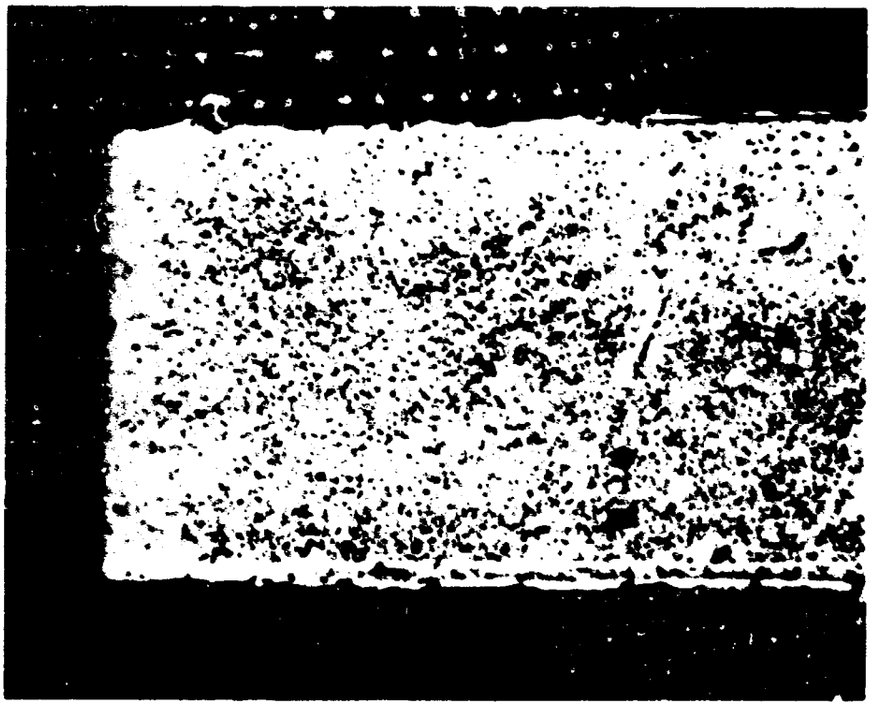

Figure 26 - Photomicrograph of seal sample Z-9A, longitudinal section, after 1000 hours at 900°C in 1 Torr of cesium vapor, 250 X

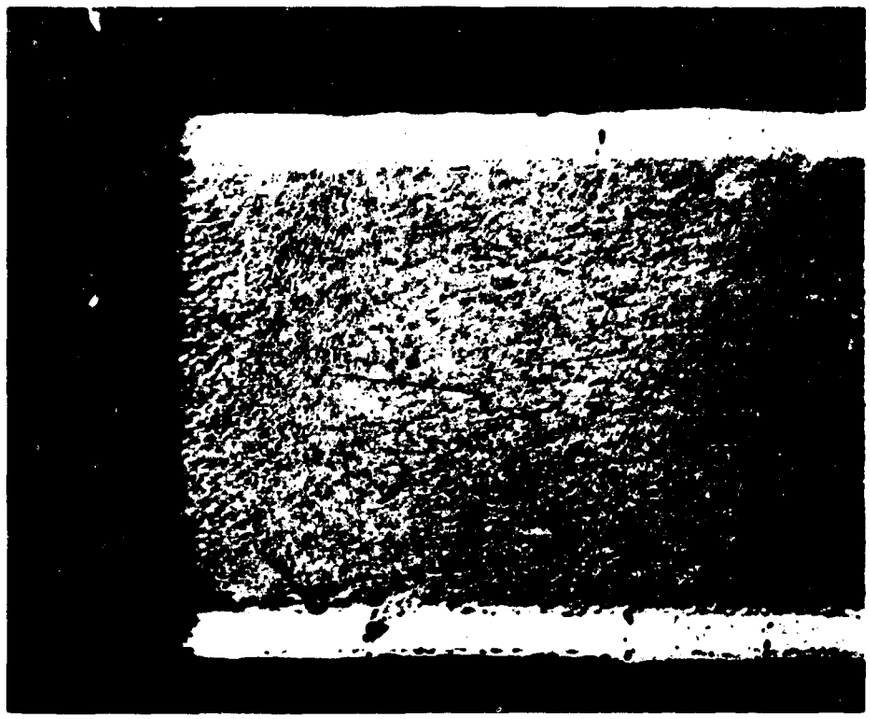

Figure 27 - Photomicrograph of seal sample T-6A, longitudinal section, after 144 hours at 900°C with no cesium, 250 X

Figure 28 - Photomicrograph of seal sample 1-5B, transverse section, after 144 hours at 900°C in 100 Torr of cesium vapor, 100 X

Figure 29 - Photomicrograph of seal sample Z-9B, transverse section, after 144 hours at 900°C in 100 Torr of cesium vapor, 100 X

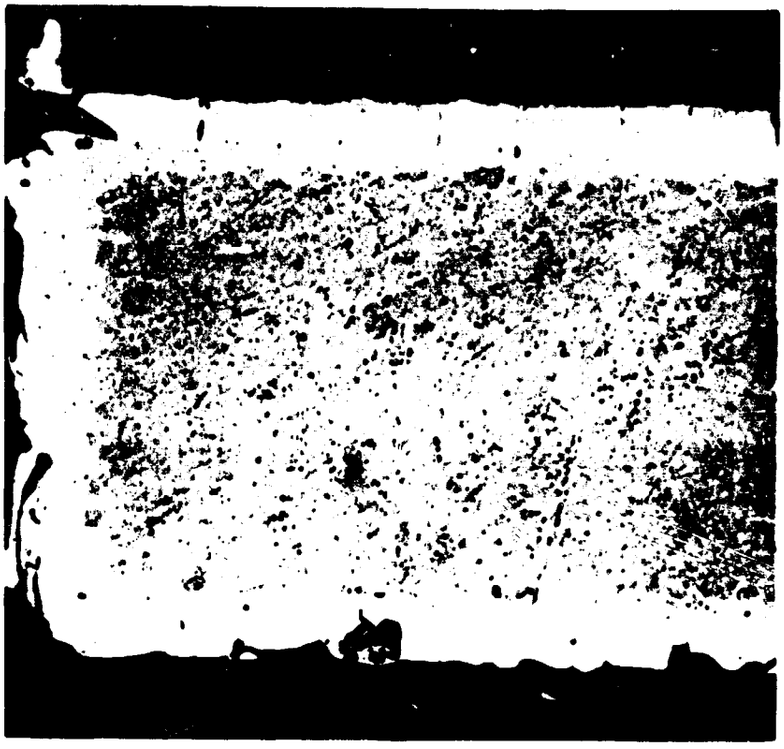

Figure 30 - Photomicrograph of seal sample T-5B longitudinal section, after 144 hours at 900°C in 100 Torr of cesium vapor, 250 X

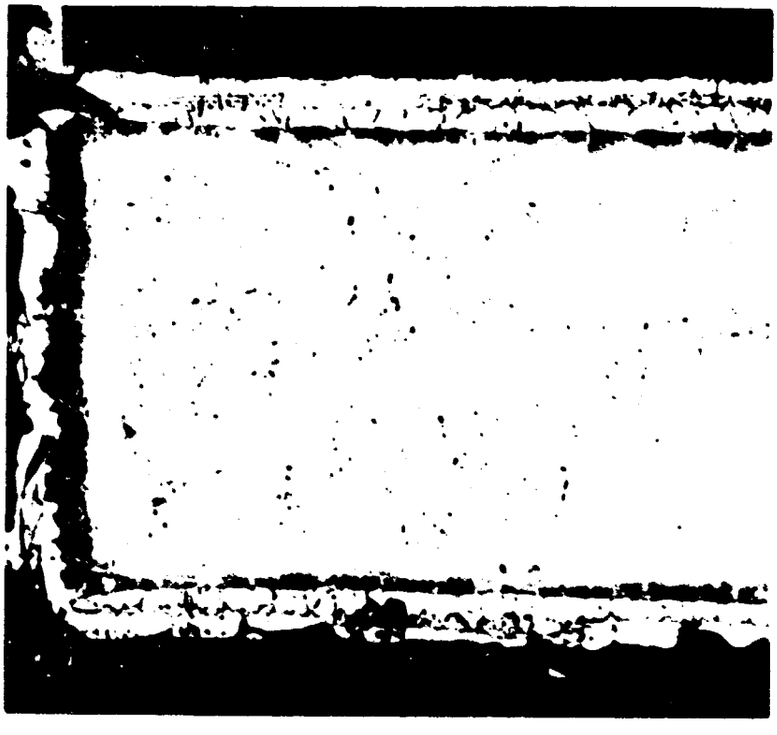

Figure 31 - Photomicrograph of seal sample T-5B, longitudinal section, after 144 hours at 900°C in 100 Torr of cesium vapor, after etching, 250 X

Figure 32 - Photomicrograph of seal sample T-4-20B, composite view of entire transverse section, after 144 hours at 900°C in 100 Torr of cesium vapor, 50 X

Figure 33 - Photomicrograph of seal sample T-3B, composite view of entire transverse section, after 144 hours at 900°C in 100 Torr of cesium vapor, 100 X

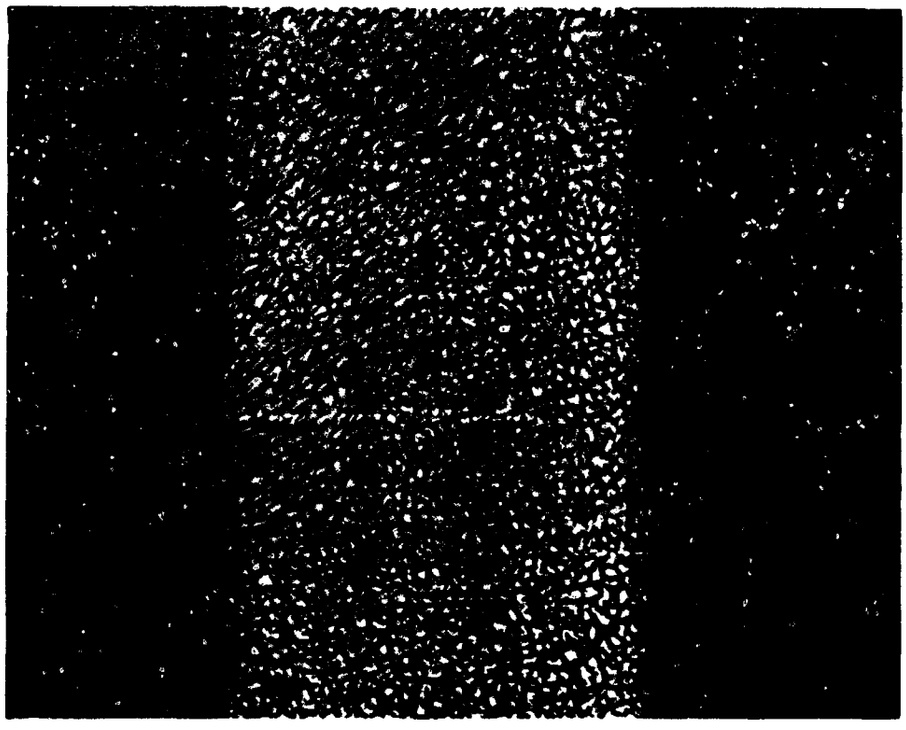

Figure 34 - Photomicrograph of OFHC copper, after 281 hours at 900°C in 1 Torr of cesium vapor, unetched, 250 X

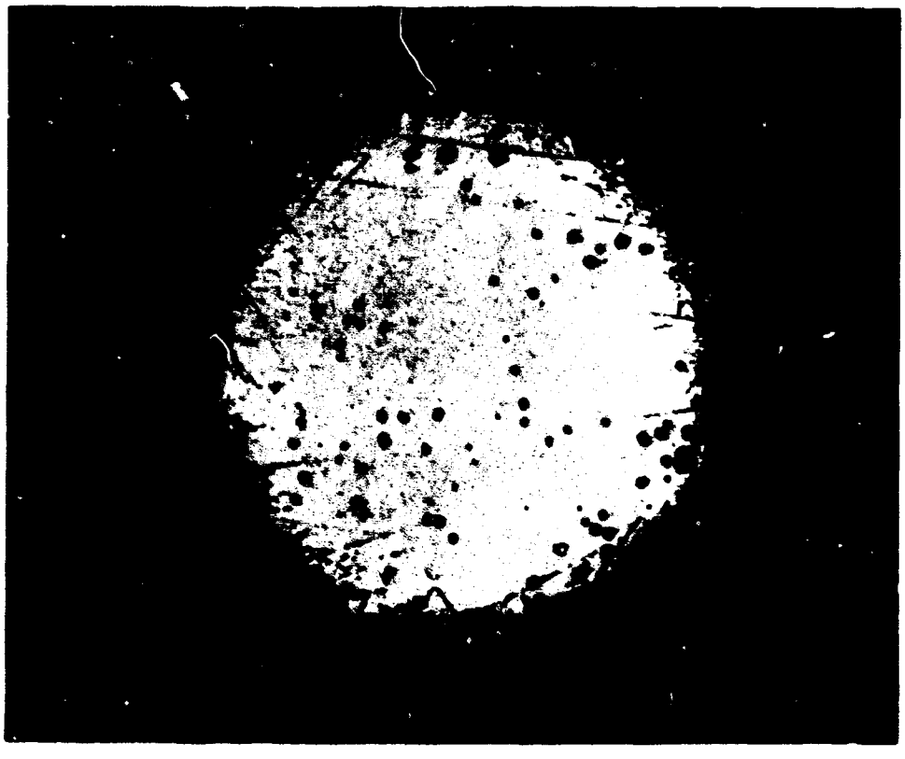

Figure 35 - Photomicrograph of 50-50 CuAu alloy wire, after 281 hours at 900°C in 1 Torr of cesium vapor, unetched, 75 X

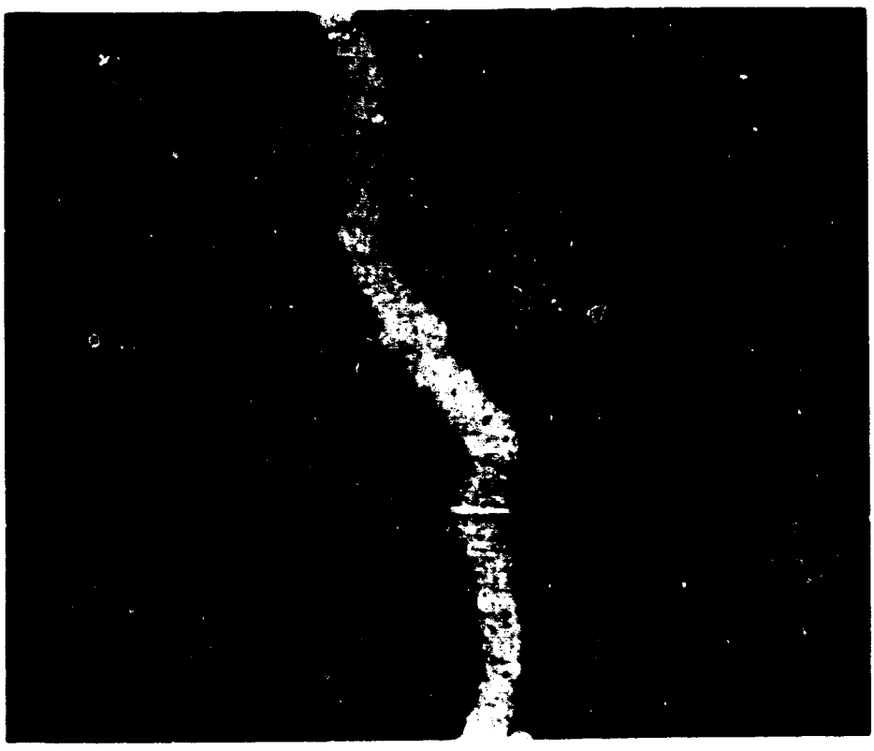

Figure 36 - Photomicrograph of gold foil, after 281 hours at 900°C in 1 Torr of cesium vapor, unetched, 250 X

Figure 37 - Photomicrograph of platinum ribbon after 281 hours at 900°C in 1 Torr of cesium vapor, unetched, 250 X

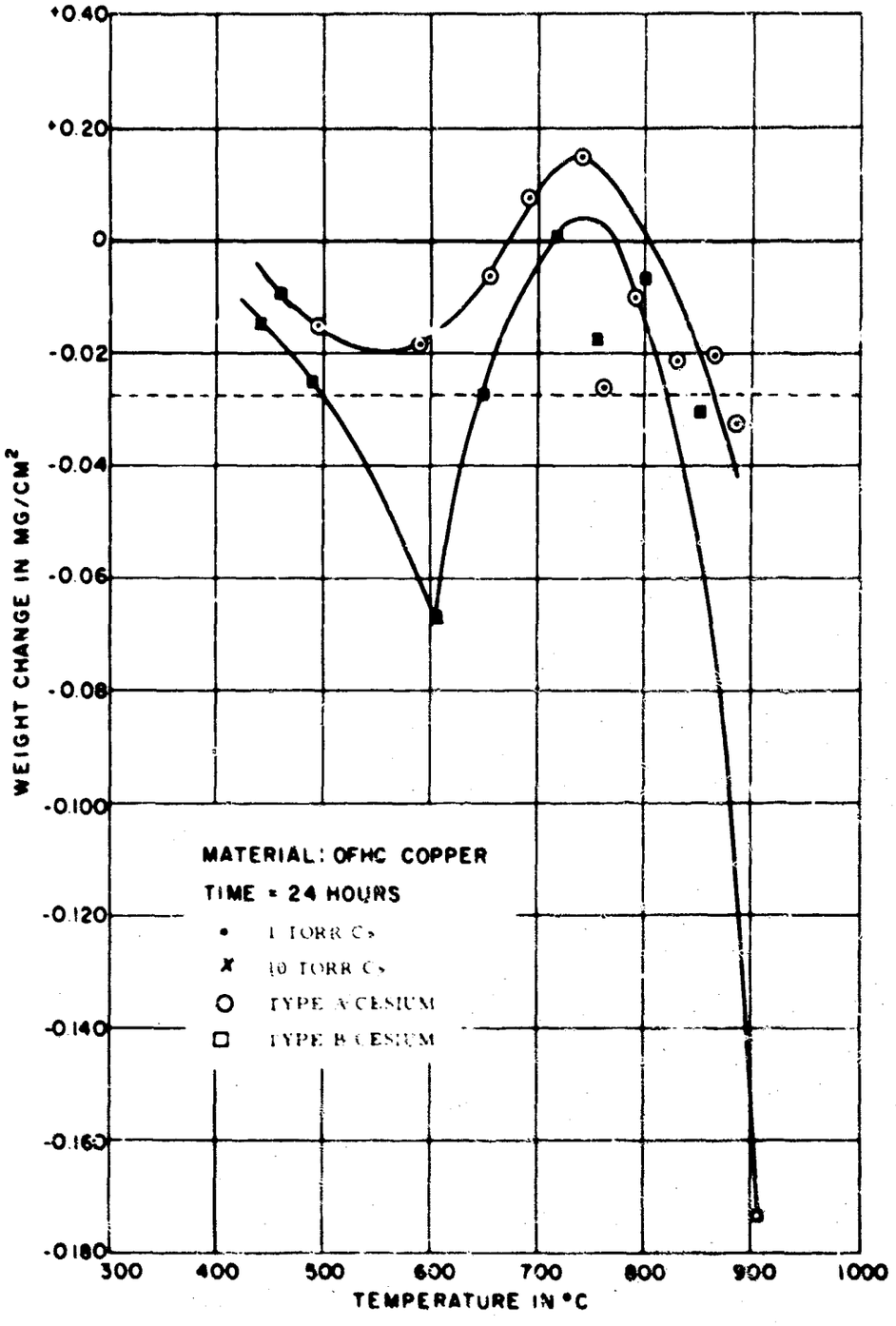

Figure 38 - Weight change in mg/cm^2 versus temperature for OFHC copper

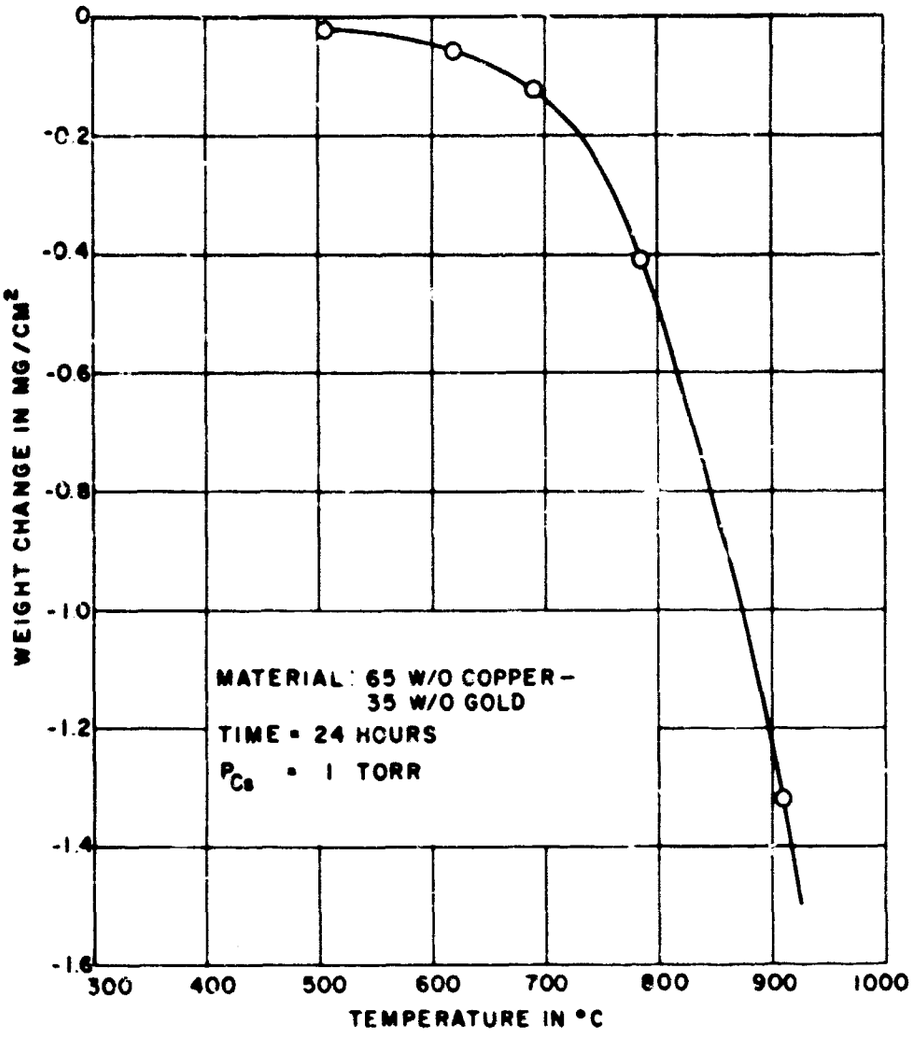

Figure 39 - Weight change in mg/cm^2 versus temperature for 65 w/o copper-35 w o gold alloy

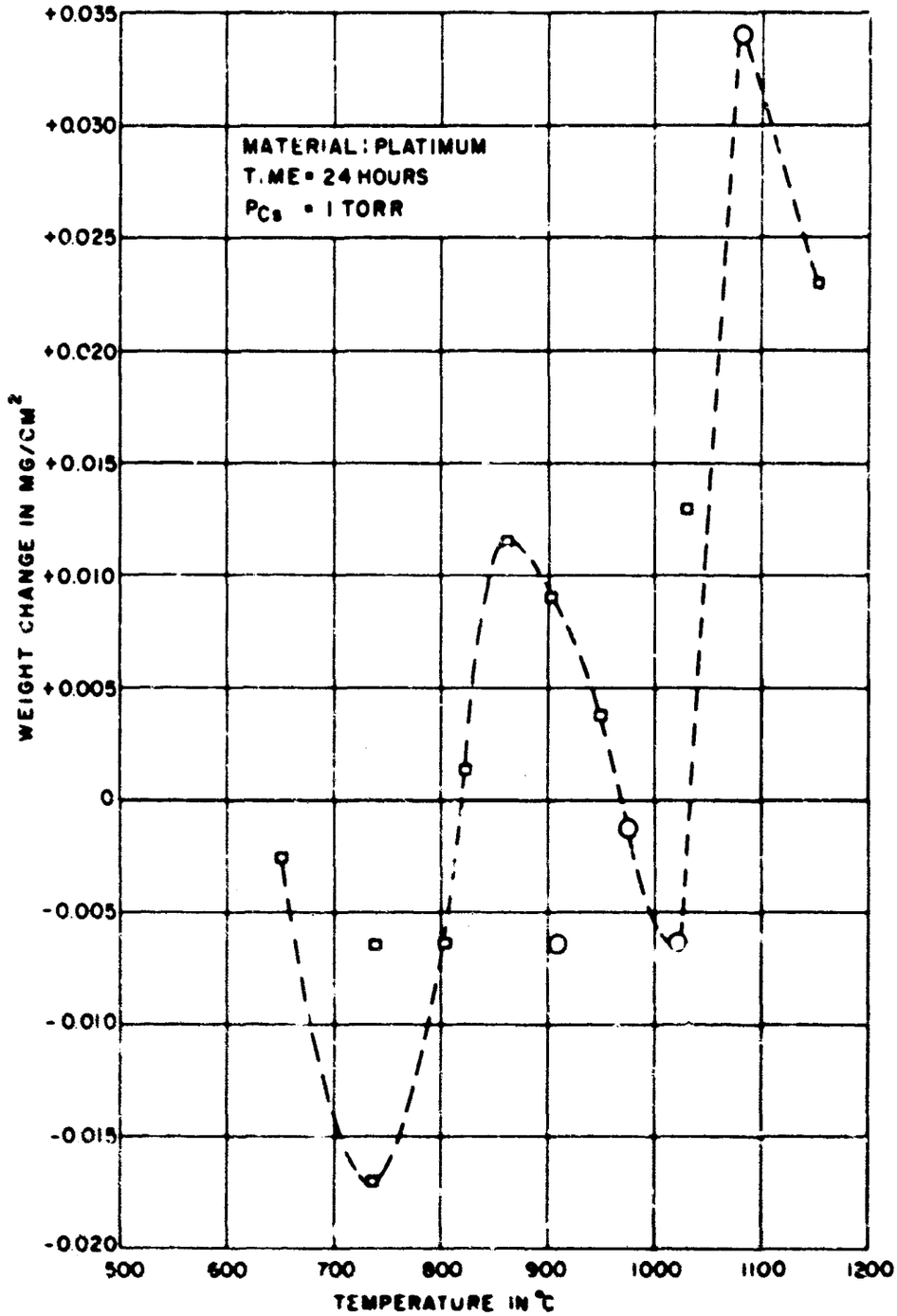

Figure 40 - Weight change in mg/cm.^{2} versus temperature for platinum

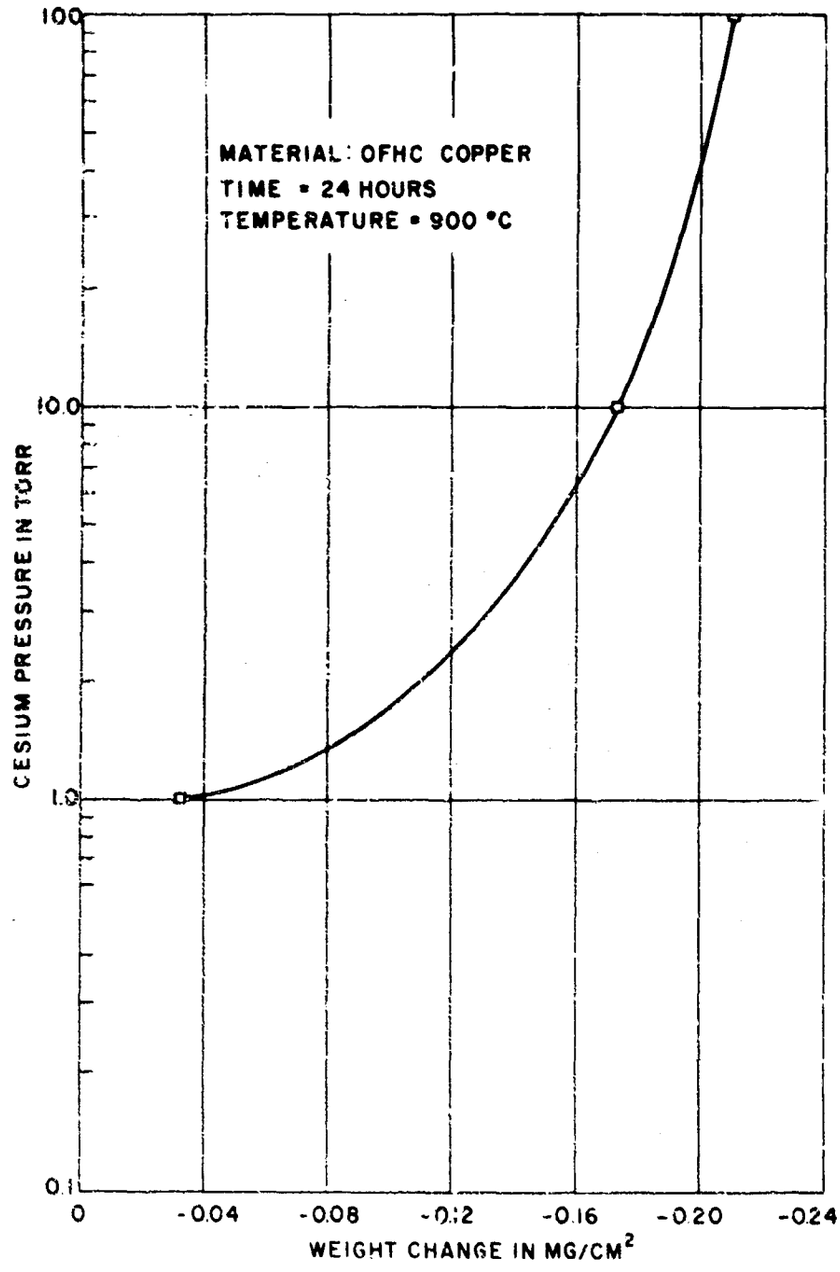

Figure 41 - Weight change in mg/cm^2 versus cesium pressure for OFHC copper

SECTION II

Metal-Ceramic Seals

by

R. H. Bristow
Power Tube Department
General Electric Company

TABLE OF CONTENTS

LIST OF ILLUSTRATIONS

METAL-CERAMIC SEALS

by
R. H. Bristow

INTRODUCTION

The need exists for high-temperature tolerant, ceramic-to-metal seals for application in cesium vapor thermionic converters. Their availability would permit improvements in operating efficiency as well as design simplification of both the converters and the associated power systems. The present interest is in sealing systems capable of sustained operation at temperatures up to approximately 900°C.

The atmospnere surrounding an operating converter may be air in some applications and a vacuum or inert gas in other applications. In either case, the materials of construction must, in addition to possessing mechanical strength, refractoriness, stability, and low vapor pressure, be resistant to cesium attack at the required operating temperature.

The following paragraphs will discuss briefly fundamental considerations which led to the selection of the specific program of seal evaluation and development which was pursued in performance of this contract. Although the subject to be treated is the method by which a conductor can be sealed hermetically to an insulator, attainment of a suitable sealing system will depend on other information, some of which is not yet available, including (1) the resistance of metals, alloys, oxides, and cermets to cesium attack at temperatures up to proposed cathode operating temperatures, (2) the stability and oxidation resistance of metals and alloys proposed for use as cathode structural members, as well as (3) the sublimation rate and consequent effect on tube life of promising oxidation resistant alloys and cermets.

Two distinctly different sealing techniques are commonly used to effect ceramic-to-metal seals for application in electronic devices: (1) active-alloy sealing and (2) refractory metal metallizing. In the former method, a molten brazing alloy is suitably doped or "activated" to impart ceramic wetting and bonding characteristics, thereby permitting direct

union of the ceramic and metal members to be joined. In the second method, a thin layer of powdered refractory metal (usually with admixed metals or oxides) is sintered to the surface of the ceramic in order to provide a metallic layer to which a conventional braze can be made.

It is apparent that the suitability of a ceramic-to-metal seal for application in high-temperature, vapor thermionic converters will be largely dependent upon the refractoriness and stability of the component parts and their resistance to cesium attack at the desired operating temperature.

Available data indicate that seals made with so-called high-alumina ceramics (94 to 99 percent alumina), which have been metallized by the now widely used molybdenum-manganese method of metallizing, are not suitable for application at the desired temperature in a cesium vapor atmosphere. Their inadequacy stems from the fact that the ceramics as well as the interfacial region, which is developed during sintering of the metallizing to the ceramic, contain silica. Amorphous or crystalline silica, as well as many silica-containing compounds, are attacked readily by cesium at elevated temperatures. Pure sintered alumina, containing no silica, has been found to be the most cesium-resistant ceramic yet tested. Since the metallizing of pure alumina with a refractory metal, without the introduction of secondary phases which may be susceptable to cesium attack, is not readily accomplished, other methods of sealing have appeared more suitable.

Even if the metallizing approach to sealing were to be pursued, a brazing alloy which was resistant to cesium attack at the desired operating temperature, i.e., up to about 900°C, would have to be selected. Brazing alloys commonly used in electron tube assembly, such as copper, gold-copper, gold-nickel, palladium-nickel, etc., are lacking in the need for low vapor pressure and resistance to cesium attack. In the latter case, it has been fairly well established that noble metals (and probably their alloys) do not possess the desired resistance to cesium attack. Thus, not only are the number of brazing alloys which meet these requirements extremely limited, but the few which might be considered possess either undesirably high melting temperatures or they have a high solubility for the refractory metal metallizing coating which could result in complete loss of adherence.

Although a number of techniques other than brazing are potentially attractive for hermetically joining an insulator to a conductor, including

electron beam welding and diffusion bonding, such techniques were not included within the scope of this investigation.

At the outset of this study, the most satisfactory seals available for use in vapor thermionic converters at high temperatures were believed to be those employing sintered alumina ceramics bonded to a near-matching metal, such as tantalum or columbium, by means of a titanium-nickel or zirconium-nickel alloy which was capable of wetting both the metal and the ceramic. Such seals could not, of course, be operated in an air atmosphere and were limited (arbitrarily) in operating temperature to about 650°C. Just how closely the operating temperature could approach the original sealing temperature (slightly above the 942°C and 961°C eutectics, respectively) had to be established and constituted a portion of the planned program.

PROGRAM OF EVALUATION AND INVESTIGATION

The specific program which was proposed and which was pursued comprised two phases. Although these two phases were often under study concurrently during this investigation, primary effort was devoted to Phase I.

I. Phase I - Evaluation of State-of-the-Art Seals

A. Evaluation of the capability of state-of-the-art titanium-nickel bonded ceramic-to-metal seals with respect to maximum temperature for sustained operation in vacuum.

1. The test specimens were to consist of two thin-walled cylindrical ceramic cylinders bonded together or to either side of a thin metal washer through the use of the 942°C titanium-nickel eutectic alloy. Two types of ceramics were to be used, a polycrystalline sintered alumina of near-theoretical density and a 97 percent alumina ceramic. Both ceramic-to-ceramic and ceramic-to-metal specimens were to be employed, since the presence of a metal member influences significantly the stress in such seals and might alter the composition of the brazing material during brazing or during subsequent heat treatment.

2. Sealed specimens were to be heat treated in vacuum at temperatures up to 900°C for times ranging from several hours to hundreds of hours.

3. Treated specimens would be examined for vacuum tightness, mechanical strength, and changes in microstructure of the brazing alloy as determined by microscopic examination of polished sections. Microhardness, x-ray diffraction, and microprobe analyses would be used, where desirable, to establish the cause and effect of observed microstructural changes in the brazing alloy or seal metal.

4. Transverse mechanical strength was to be determined using four-point loading of butt sealed tubular ceramic specimens.

B. Evaluation of the effect of sealing alloy composition on the physical and mechanical properties of the joint, before and after long time heat treatment.

When using a titanium-nickel alloy to seal a ceramic to another ceramic or to metal, it had been generally considered desirable to utilize thin foil washers of titanium and nickel in the proper proportions to yield the 942°C eutectic. When sealing to a titanium member, it was recognized that the melt would become enriched with titanium as the sealing temperature was increased. When sealing to nickel or nickel-containing alloys, the composition of the melt would be expected to drift away from that of the eutectic toward the brittle intermetallic compound Ti_2Ni. The effect on the composition and properties of titanium-nickel alloys which had been enriched with other elements through solution of the tantalum, Kovar, nickel, or stainless steel sealing washer was not known and was to be determined.

II. Phase II - Investigation and Development of New Ceramic-to-Metal Sealing Systems and Techniques

SUMMARY OF RESULTS

The ceramic-to-metal seal study portion of this thermionic converter materials research program comprised two phases.

(1) Evaluation of state-of-the-art seals

   (a) Evaluation of the effect of sealing alloy composition on the physical and mechanical properties of the joint, before and after long time heat treatment.

   (b) Evaluation of the capability of state-of-the-art titanium-nickel bonded ceramic-to-metal seals with respect to maximum temperature for sustained operation in vacuum.

(2) Investigation and development of new ceramic-to-metal sealing systems and techniques.

A total of 631 ceramic-to-ceramic and ceramic-to-metal seal specimens was prepared during this investigation. All seals were prepared using nickel-titanium alloys (but of different compositions) to effect the bond between two ceramic cylinders, or, in the case of ceramic-to-metal seals, to either side of a metal washer. The metals studied included titanium, tantalum, nickel, Kovar, Type 304 and Type 430 stainless steel. All seals were made in a vacuum bell jar using a resistance heated tantalum oven surrounding the seals which were held under spring pressure in a molybdenum fixture. The sealing time and the temperature controlled the degree of alloying which took place with the metal washer.

Seals were sectioned, diamond polished, and etched preparatory to metallographic examination. In those seals which contained only nickel and titanium, it was generally possible to identify the phases which were formed during sealing as well as changes in the quantity and distribution of these phases as a function of sealing time and temperature. Identification of the phases in the four and five component systems which resulted from sealing to Kovar and stainless steel was usually not attempted. Microhardness measurements were of considerable value in studying the sealing alloys, even though the average joint thickness was only about 20 microns wide and many of the phase layers which made up the joint were only two microns wide.

The need for the first task of Phase I resulted from an observed change in the composition and microstructure of the titanium-nickel sealing alloy due to solution of and interdiffusion with the metal member to which the seal was being made. When sealing to a titanium member, the melt becomes enriched with titanium, while when seals are made to nickel or nickel-containing alloys, the composition of the melt drifts away from that of the lowest melting eutectic toward the brittle intermetallic compound Ti_2Ni. Thus, a more complete knowledge of the metallurgy of active-alloy ceramic-to-metal sealing was a prerequisite to interpretation of the data to be accumulated during life testing of state-of-the-art seals.

Seals were prepared for high-temperature testing using sealing times, temperatures, and alloy compositions selected from the study conducted during the first task. Seal specimens were prepared using both a pure sintered alumina of 99.5 percent theoretical density and a high strength 97 w/o alumina ceramic containing CaO, MgO and SiO_2.

The test specimens were placed on molybdenum trays and inserted into impermeable, closed-end ceramic tubes which were attached to a vacuum system. A furnace surrounding each tube permitted heating the samples to the desired temperature in a vacuum which measured from 1 to 5×10^{-5} Torr.

Test temperatures of 700°C and 900°C were used. Results obtained can be summarized as follows.

(1) When a titanium-nickel alloy having the composition of the 942°C eutectic is used to effect a ceramic-to-ceramic or a ceramic-to-metal seal, the resulting alloy contains a large proportion of the brittle intermetallic compound Ti_2Ni. Small cracks through the alloy of such seals are commonly observed and result from the difference in thermal expansion between the Ti_2Ni and the other phases, predominately alpha titanium, contained therein.

(2) Use of an alloy composition which is considerably richer in titanium than the 942°C eutectic is advantageous in that it reduces the amount of Ti_2Ni which is formed and thereby minimizes the possiblity of cracking.

(3) "Overbrazing" of either the eutectic or the titanium-rich type of seal results in hardening and embrittlement of the titanium phase (due to excessive reaction with the ceramic),

leading to severe cracking of the alloy and a degradation of the alloy-to-ceramic bond.

(4) When seals are made to thick titanium members, using nickel foil to form a eutectic liquid with the surface of the titanium, the melt rapidly loses nickel due to diffusion into the "infinite" titanium source. This is the most satisfactory method for minimizing the formation of Ti_2Ni and the promotion of a bond possessing maximum ductility. Although such joints are also subject to severe hardening through overbrazing, the alloy does not contain layers of different phases to cause cracking, as is the case with alloys of near-eutectic composition.

(5) Seals in which the sealing alloy contains a titanium phase (α or β solid solution) exhibit a very short life at a temperature of 900°C. Failure occurs through loss of hermeticity or, in more severe cases, physical separation of the component parts. Continued reaction of the sealing alloy with the ceramic, resulting in severe hardening and embrittlement of the titanium phase and/or the formation of new phases at the interface, causes seal failure. Degradation of such seals occurs so rapidly that it masks any contribution to alloy embrittlement caused by gettering of residual gas in the test chamber.

(6) The life of seals containing a titanium phase, when tested at a temperature of 700°C, is related to the rate at which hardening of the sealing alloy occurs. The rate of hardening is related to the volume of material into which the hardening elements can diffuse as well as to the number of ceramic-sealing alloy interfaces from which hardening elements can be derived. At a temperature of 700°C, the life of seals is sufficiently long that gettering of residuals in the test chamber can contribute to hardening of the alloy.

(7) At a temperature of 900°C, the rate of reaction with a ceramic, of a titanium phase-containing seal, is so rapid that it masks any effect of ceramic composition. At a temperature of 700°C, however, hardness measurements suggest that the rate of reaction with a high-purity sintered

alumina (body A-976*) is less than that with a 97 percent alumina (body A-923*) possibly reflecting the presence of the more easily reducible oxide silica.

(8) Seals containing a titanium phase are suitable for short time exposure to a temperature of 700°C. Seals of alumina-to-titanium and alumina-to-tantalum are to be preferred and lives up to 2000 hours were recorded. Alumina-to-columbium seals should also be quite satisfactory but were not tested.

(9) At a temperature of 900°C, the only seals which exhibited a life of more than 240 hours were compensated butt seals of alumina-to-nickel. Many specimens of this seal type were still vacuum tight at the end of 910 hours exposure. Such seals do not appear to be sensitive to the composition of the alumina ceramic which is used (A-976 or A-923) or to the presence of residuals in the vacuum environment. A sample examined after 480 hours exposure showed evidence of loss of the $TiNi_3$ phase at the interface through solutioning by the nickel washer, a finding which necessitates further study.

(10) Seals made to nickel, using titanium foil to form a eutectic liquid with the surface of the nickel, contain Ti_2Ni, TiNi, $TiNi_3$, or a nickel solid solution at the ceramic-nickel interface, depending upon the time-temperature sealing treatment which is used.

(a) Sealing at low temperatures, less than about 1100°C, causes the formation of large amounts of Ti_2Ni and results in severe cracking of the alloy.

(b) Sealing at temperatures above 1120°C and below 1300°C promotes the formation of an alloy containing predominately TiNi and $TiNi_3$. The amount of each phase is determined by the time-temperature treatment, higher temperatures, and longer sealing times promoting the formation of $TiNi_3$.

*General Electric Power Tube Department designation

(c) Seals made at a temperature just below the 1304°C eutectic contain predominately $TiNi_3$ at the interface. Seal times of a few seconds to four minutes have been satisfactorily used. Such seals are easily and reproducibly made, show excellent strength, and are of the type which has already withstood 910 hours in the 900°C life test. Further study and testing is needed, however, since a sample examined after 480 hours exposure showed evidence of loss of the $TiNi_3$ phase at the interface through solutioning by the nickel washer.

(d) Seals made at a temperature slightly above the 1304°C eutectic contain a nickel solid solution at the ceramic-nickel interface. The vacuum tightness of such seals appears to be quite sensitive to time at sealing temperature. No."soak" at peak sealing temperature is required or is desirable.

(e) Compensated butt seals between alumina (A-923) and 0.010-inch thick nickel, sealed in such a manner as to form only the nickel solid solution at the interface, show flexural strengths approximately one-third that which is obtained if sealing is performed so as to form a thin layer of $TiNi_3$ at the interface.

EXPERIMENTAL PROCEDURE AND EQUIPMENT

I. Ceramic-to-Metal Test Specimens

The test specimens selected for this study consisted of two polycrystalline ceramic cylinders (0.690-inch outside diameter, 0.480-inch inside diameter, 0.200-inch long) which were butt sealed to each other or to either side of a metal washer forming what are hereafter referred to as ceramic-to-ceramic specimens and ceramic-to-metal specimens, respectively. The ceramic cylinders were prepared by conventional ceramic fabrication techniques, including ball milling of the constituent materials, spray drying to form pressing granules, dry pressing, and firing to maturity. The ends of the fired cylinders were ground flat and parallel on a Blanchard grinder equipped with a 220-grit, resinoid-bonded diamond wheel. The ground specimens were ultrasonically

cleaned using detergent-water solutions and acetone rinses, followed by air firing to a temperature of 1000°C for one hour.

Two types of specimens were used in the study:

(1) A polycrystalline alumina, designated body A-976, containing a small amount of MgO as a grain growth inhibitor which was sintered to a density of approximately 99.5 percent of theoretical.

(2) A 97 percent alumina, designated body A-923, containing CaO, MgO, and SiO_2 as fluxing agents.

Only the pure sintered alumina is sufficiently resistant to cesium attack to permit use at temperatures above about 600°C. The 97 percent alumina ceramic was included in the test program in order to ascertain whether the presence of the three percent of "fluxing oxides" had an observable effect on sealing characteristics and seal quality.

Two of the ceramic specimens were sealed to each other or to either side of a metal washer through the use of an "active" alloy which was liquid or partially liquid at the sealing temperature. The metal washers to which seals were made, including titanium, tantalum, nickel, Kovar, Type 304 and Type 430 stainless steel, were all nominally 0.010-inch thick and had the same outside and inside diameters as the ceramics. The active sealing alloy was derived, at the sealing temperature, by fusion of titanium and nickel foil washers of the proper thickness to yield the desired composition. The Grade 499 nickel foil which was used was 0.0003-inch thick. Titanium foil, Grade A-75, was used in three different thicknesses, 0.00025 inch, 0.0005 inch, and 0.001 inch.

Quantitative analyses for carbon and semiquantitative emission spectrographic analyses for other impurities were conducted, with the results shown in Tables I and II. All metal washers and foil were cleaned using accepted electron tube processing methods but were not given any vacuum or hydrogen firing treatment prior to sealing.

Table I

Material	Weight Percent Carbon
0.001-inch titanium foil, Grade A-75	0.0129
0.010-inch titanium washers, Grade A-40	0.0346

Table II

Contaminating Element	Weight Percent
Iron	0.001 - 0.01%, estimated to be near 0.01%
Manganese	0.001 - 0.01%, estimated to be near 0.005%
Copper	$<$ 0.001%
Silic n	$<$ 0.001%

All thicknesses of titanium foil, 0.00025 inch, 0.0005 inch, and 0.001 inch, had the same type and quantity of impurities.

II. Sealing of Test Specimens

All specimens were sealed in the vacuum bell jar shown in Figure 1.* The assembled specimens were stacked in a spring-loaded molybdenum fixture and suspended within the resistance-heated tantalum oven. The pressure in the system never exceeded 5×10^{-4} Torr during the sealing operation.

Temperature was controlled and observed using a combination of several methods: power input to the oven, observed formation of the eutectic alloy, and optical pyrometer readings. The tantalum oven and the outer heat shield each contained a narrow slit which permitted observation of the specimens during sealing. Thus, the formation of the titanium-nickel eutectic liquid could be observed readily by sighting on the joint area with a micro-optical pyrometer. Power input to the tantalum oven was controlled by a Variac on the primary of a transformer feeding the oven. Very close control over the rate of heating was thus

*See Appendix for illustrations.

possible and close duplication of a particular heating schedule was readily accomplished. With a given load and a given heating schedule, the time of formation of the eutectic liquid would not vary more than about ten seconds from test to test.

Optical pyrometer readings were made also in order to establish and monitor heating schedules. Mir o-optical pyrometer readings, made on the side of one of the ceramic specimens, were adequate even though they included a large (but reproducible) error due to reflections from the hot oven. For more precise work, readings were made using a "black body" specimen. Melting p int dete: minations were made in order to establish temperature corre tions for t.e glass bell jar.

Three basically different heating schedules were used, as shown in Figure 2. The curves represent the sample temperature during the last stage of heating only. The heating schedule was comprised of several stages, each stage con sting of a fixed amount of time at a fixed current input to the oven. The rate of heat input during the first several stages of heating was relatively slow in order to keep the pressure down during evolution of the isobutyl methacrylate binder which was used to temporarily cement the specimens and shims together, and to prevent heat shocking of the ceramic . This consumed approximately 12 minutes. During the next four minutes, all specimens were "soaked" to an equilibrium temperature slightly below the 942°C eutectic. A soak temperature of about 880°C was usually used. During the last stage of the heating schedule the specimens were heated rapidly to a temperature at which the nickel and titanium react to form the eutectic liquid. This heating stage was achieved by setting the current input to the oven at some predetermined value which caused the tantalum oven to rise immediately to some fixed temperature. The temperature of the specimens would then rise, as a function of time, and approach the temperature of the tantalum oven. It is the temperature of the specimen during this last stage of heating that is represented by the curves of Figure 2. It is clear that if power were kept on for three minutes after the melt was observed, the specimen would have reached a higher final temperature than if the power were shut off at 15 seconds.

The three heating schedules shown in Figure 2 are those which were used most often. Of course, many departures were made from these schedules in order to investigate the effect of temperature or elapsed time at a particular temperature on the metallography of a joint. Schedule A was used when sealing ceramic-to-ceramic using

titanium-nickel alloys of the eutectic or near-eutectic composition, as well as for sealing ceramic-to-titanium using nickel foil. Schedule B was used for sealing ceramic-to-ceramic using nickel-titanium alloys containing from about 30 percent to 65 percent nickel, while Schedule C was used for sealing ceramic-to-nickel, using titanium foil, and for sealing ceramic-to-ceramic using some of the very high nickel content titanium-nickel alloys.

The length of time at which the seal was held at temperature, after initial melt formation, is discussed in the applicable portion of RESULTS AND DISCUSSION of this study, but was usually from 15 seconds to four minutes. Schedules A, B, and C do not necessarily represent the optimum time-temperature heating schedule for the alloys listed but were designed primarily to achieve several basically different but easily reproducible schedules for experimental purposes.

Near the end of the program, it was found that the temperature control required to produce ceramic-to-nickel seals having the desired characteristics was beyond the capability of the system and procedure in use. In order to provide the required precision of temperature control, the brazing oven and seal fixturing were modified so as to permit placing a thermocouple either in contact with the work (and shielded from radiation) or inserted into a small ceramic cup placed adjacent to the work. Thermocouple millivoltage was plotted on an X-Y-time recorder, corrected for cold junction compensation, and converted to temperature. By manually adjusting the current through the oven, it was possible to accurately follow any desired heating (within the limits of the power supply), soak, and cooling schedule.

A cooling curve which is typical of that experienced by a specimen after the power to the oven is shut off, is plotted in Figure 3.

III. Metallographic Specimen Preparation

Specimens for metallographic examination were prepared by cutting a sealed ceramic specimen in half on a diameter, mounting the half-specimen in Bakelite, followed by metallographic polishing. The following sequence of polishing operations was performed.

(1) Thirty-micron diamond paste on a cast iron lap

(2) Thirty-micron diamond paste on airplane wing cloth

(3) Fifteen-micron diamond paste on airplane wing cloth

(4) Three-micron diamond paste on airplane wing cloth

(5) Linde A on black suede cloth

(6) Linde B on black suede cloth

The following etchant was used on most specimens and was applied with a swab for from three to 10 seconds.

(1) Forty-five parts nitric acid

(2) Forty-five parts water

(3) Ten parts hydrofluoric acid

(4) Ninety parts lactic acid (85 percent)

IV. Microhardness Measurements

Hardness measurements were made using a Kentron microhardness tester equipped with a Knoop indenter. All measurements were made with a 10-gram load.

Buehler and Wiley[1] conducted an intensive study of the TiNi phase region in the titanium-nickel system. (Their work was discussed in the Semiannual Technical Summary Report on this contract.) Some hardness measurements interpolated from several illustrations contained in their report are presented in Table III and will be useful for comparison with data obtained in this study.

Table III

Alloy Composition	Hardness, DPH
TiNi, 54.5 w/o Ni	230
TiNi, 55.1 w/o Ni	340
Ti_2Ni	625
$TiNi_3$	365

Stover and Wulff[2] also detected significant differences in hardness between the intermetallic compounds in the titanium-nickel system. They found that the hardness (all values compared at a constant indentation diagonal of 10 microns) of the Ti_2Ni phase was 700 kg per sq mm and was increased slightly by additions of carbon to 900 kg per sq mm. In the TiNi phase area, the microhardness increased from 300 to 700 kg per sq mm as the nickel content increased from 50 a/o to 57 a/o. Carbon additions had no effect on the hardness of the TiNi phase. $TiNi_3$ prepared from sponge titanium was found to have a hardness of 660 kg per sq mm, and individual plates could be plastically deformed.

V. High-Temperature Life Testing Equipment

Life testing was performed in a vacuum set having a two-port manifold, as shown in Figure 4. Closed-end, impermeable mullite tubes were sealed to each port by means of quick-clamping arrangements employing Viton gaskets. The closed-end of each ceramic tube projected through the hole in the door of a small furnace, the furnace temperature being controlled by a Brown millivoltmeter indicator-controller. A two-deck molybdenum boat, on which the samples were placed, was inserted into each tube and was followed by a four-plate molybdenum radiation baffle. Titanium sheets spot-welded to the plates of the radiation baffle served as getters and reduced the possibility of backstreaming pump oil contacting the samples under test.

A vacuum of 1×10^{-5} Torr was attained in the manifold at the start of the life testing phase of this study. Near the end of the program, the vacuum as read on an ion gauge attached to the manifold just below table level was only about 5×10^{-5} Torr. The actual vacuum within the ceramic test chamber may have been somewhat different from that read on the ion gauge. Hardness measurements made on several metals (titanium, tantalum, and columbium) capable of gettering oxygen, nitrogen, and carbon, served as monitors of the atmosphere within the heated test chambers during a life test.

RESULTS AND DISCUSSION

I. Ceramic-to-Metal Sealing

A. General

Since the discovery[3] of the unique ability of a molten metal or alloy, containing a small percentage of the active metal titanium,

to wet and bond to ceramic surfaces, many novel methods have been developed for forming the "active alloy" in situ, resulting in the now familiar "titanium hydride process,"[4] the "titanium-cored silver solder method," the "mixed powder" technique, and the "active alloy shim" process.[5] Most "active alloy" sealing, however, has been performed using such brazing alloys as copper, silver-copper, and gold-copper. Unfortunately, such alloys are not considered sufficiently resistant to cesium attack to permit their use in cesium vapor thermionic converters wherein the seals are designed to operate at temperatures above about 600°C.

Beggs[5] utilized the low melting eutectics which form in certain binary titanium-alloy systems to seal the titanium electrodes of a tube envelope to a matching ceramic. He accomplished this by interposing a thin shim of nickel or copper between the surfaces to be joined, and heating to the temperature at which the lowest melting eutectic would be formed, 942°C in the case of the titanium-nickel system and 875°C in the case of titanium-copper. This process is now commonly referred to as the "active metal shim" process.

Since the titanium-nickel alloy was predicted, and later demonstrated, to possess good resistance to cesium attack, the titanium-nickel active metal shim process appeared to be a very desirable method for fabricating thermionic converters. In converters, however, it was necessary to use such structural metals as tantalum and stainless steel, making it necessary to supply both nickel and titanium shims in the proper thickness to yield the eutectic composition. This was accomplished, for example, by using one washer of 0.0003-inch thick nickel foil, one washer of 0.001-inch titanium foil, and one washer of 0.0005-inch titanium foil, yielding an alloy having the composition 71.8 w/o titanium, 28.2 w/o nickel (calculated using the actual weights of the respective shims). The 942°C eutectic in the titanium-nickel system has the composition 71.5 w/o titanium, 28.5 w/o nickel.

In practice, it was found that seals made using this eutectic alloy appeared to be less reliable than those prepared by the method developed by Beggs, i.e., in which the molten alloy is formed from and is in contact with an essentially "infinite" supply of titanium. A look at the titanium-nickel phase diagram, Figure 5, shows that as the temperature is raised above the 942°C eutectic temperature, the composition of the melt becomes enriched with titanium. In a seal between tantalum and a ceramic, using the titanium-nickel eutectic composition as the sealing alloy, the melt could only become enriched with

tantalum or the products of reaction with the ceramic, neither of whose effect on seal properties was known. It was apparent from the phase diagram and from the voluminous literature on titanium and its alloys, that intermetallic compounds could form in titanium-nickel aloys (and would be expected in an alloy of the 942°C eutectic composition) and that most of these intermetallic phases were extremely hard and brittle. It was also known that molten titanium reacts vigorously with most metal oxides, rapidly contaminating the melt.

Consequently, the need existed for a better understanding of the titanium-nickel sealing process with respect to the effect, on physical and mechanical properties of the joint, of the sealing alloy composition and time-temperature sealing cycle, and possible compositional changes in the sealing alloy through solution of the structural metal member or by reaction with the ceramic.

During this study, seals were prepared for metallographic examination, microhardness measurement, microprobe analyses, and high-temperature life testing. The seals were of two basic types: (1) ceramic-to-ceramic, and (2) ceramic-to-metal. The first type included seals which were made using titanium and nickel foil washers of proper thickness to yield the alloy compositions given in Table IV. The compositions shown are based upon the actual weight of the titanium and nickel shims whose nominal thicknesses are given.

Seals of the second type included those wherein two ceramic cylinders were sealed to either side of a metal washer using one of the above mentioned titanium-nickel alloy compositions, usually the near-eutectic composition 71.8 w/o Ti, 28.2 w/o Ni, or the higher titanium content alloy 76.8 w/o Ti, 23.2 w/o Ni. The metal washers used included tantalum, Kovar (nickel-cobalt-iron alloy), Type 304 stainless steel (nickel-chromium-iron alloy), and Type 430 stainless steel (chromium-iron alloy). In addition, seals were made to titanium washers using a 0.0003-inch nickel shim on each side, and to nickel washers using a thin titanium shim on each side. A few seals were made to Kovar and the stainless steels using only a titanium shim on each side and relying on eutectic formation with the nickel or iron content of the metal washer.

In addition, ceramic-to-metal seals were made to tantalum, Kovar, and the stainless steels using a 0.010-inch thick titanium "buffer" washer on either side of the structural metal washer. The

Table IV

Weight Percent Composition		Number of Shims of Each Size Required to Yield the Alloy Composition Indicated			
Titanium	Nickel	Titanium (0.00025 inch)	Titanium (0.0005 inch)	Titanium (0.001 inch)	Nickel (0.0003 inch)
83.2	16.8	-	-	3	1
76.8	23.2	-	-	2	1
71.8	28.2	-	1	1	1
65.8	34.2	-	-	1	1
49.0	51.0	-	-	1	2
39.1	60.9	-	-	1	3
31.2	68.8	1	1	-	3
22.8	77.2	-	1	-	3
13.6	86.4	1	-	-	3

function of the titanium "buffer" washer was to minimize the formation of the intermetallic phase Ti_2Ni as will be described later.

As has already been pointed out, the first liquid to form in a titanium-nickel shim seal has the composition of the lowest melting eutectic 71.5 w/o Ti, 28.5 w/o Ni. Under equilibrium conditions, the composition of the liquid remains constant until one of the components is consumed. If alloying is continued, at a temperature higher than that of the eutectic (942°C), the melt will continue to dissolve the remaining component and become "titanium-rich" or "nickel-rich" with respect to the eutectic composition. These terms are used extensively throughout this report and are intended to have this meaning.

B. Ceramic-to-Ceramic Seals with Titanium-Rich Alloys

Figure 6 shows the microstructure of a seal made with an alloy having the composition 71.8 w/o Ti, 28.2 w/o Ni. This is but slightly higher in titanium content than the eutectic 71.5 w/o Ti, 28.5 w/o Ni. The phase layer adjacent to the ceramic is only 2-1/2 microns wide, while the thickness of the entire braze joint is only 33 microns.

The thinness of the various layers coupled with their inaccessability to analysis by x-ray diffraction, often made positive identification of the many phases which were encountered quite difficult. Such positive identification, however, was not considered necessary for successful attainment of the objectives set forth in PROGRAM OF EVALUATION AND INVESTIGATION. Consideration of known phase equilibria for the titanium-nickel system (and other pertinent systems) augmented by polarized light microscopy, microhardness, and a few microprobe analyses permitted identification of the more important phases which existed in the various seals to be discussed.

In the seal shown in Figure 6, the globular phase which occurs near the center of the braze joint is the brittle intermetallic compound Ti_2Ni. It was found to have a Knoop hardness of 1145 (in this particular seal) and occasional splitting of a grain under the diamond indenter attests to its brittleness. Immediately surrounding and between the Ti_2Ni grains are dark colored regions of alpha (transformed beta) titanium. Two layers are found adjacent to the ceramic, neither of which has been positively identified. Both layers are, however, optically anisotropic and are believed to be alpha titanium solid solutions.

The layer immediately in contact with the ceramic surface appears to contain dispersed particles of another phase. This braze joint was analyzed for Ti, Ni, and Aℓ, by the microemission x-ray spectrometer technique, and the results obtained are discussed in another section of this report.

It is helpful to our understanding of the origin and relative quantities of the observed phases to trace the path of solidification of a melt having this near-eutectic composition. At the sealing temperature of about 1040°C, this 71.8 w/o titanium, 28.2 w/o nickel alloy would be all liquid. Reaction[6,7] with the ceramic occurs rapidly and probably involves the formation of TiO_x at the interface and diffusion of aluminum and oxygen into the alloy. Aluminum is extensively soluble in both beta and alpha titanium, and is an effective alpha stabilizer.[8,9] The $\alpha/\alpha + \beta$ phase boundary rises rapidly with increasing aluminum content, from the 882°C transformation temperature of pure titanium to 1240°C at 31 w/o aluminum. A binary titanium alloy containing about 11 w/o aluminum would be all alpha up to a temperature of 1040°C. Although no information could be found on the effect of aluminum additions to titanium-nickel alloys, alpha-stabilizing element additions to beta-eutectoid systems are generally known to extend the $\alpha + \beta$ field to higher temperatures. For example, 6 w/o aluminum in a Ti-4 w/o Cr alloy has a beta transus temperature of 980°C as compared with 820°C for the aluminum-free alloy.

Oxygen is an even more effective alpha stabilizing element; about 4 w/o of oxygen being as effective as 31 w/o of aluminum in raising the $\alpha/\alpha + \beta$ transformation temperature. A binary titanium alloy containing only about 2-1/2 w/o oxygen would be all alpha at the sealing temperature of 1040°C.

The two layers adjacent to the ceramic surface have already been mentioned. Initially, upon examining the polished section and noting the large grains which make up the second layer from the ceramic, it was thought that this light etching layer might be a nickel-rich beta titanium solid solution since about 9 w/o nickel is known to permit retention of beta on quenching. Examination of the TTT curves, Figure 3, for a titanium-6 w/o nickel alloy, in light of the cooling rate which occurs after the making of a seal, indicates that retention of beta would be virtually impossible. Furthermore, the grains of this layer are definitely optically anisotropic.

Upon cooling the binary titanium-nickel alloy to the eutectic temperature (942°C for the binary titanium-nickel system), Ti_2Ni would make its appearance simultaneously with the disappearance of the liquid. At this temperature, the alloy should consist of 65 w/o Ti_2Ni and 35 w/o titanium. Cooling to room temperature may cause decomposition of the eutectoid with a resulting slight increase in Ti_2Ni at the expense of the titanium solid solution. At room temperature, the equilibrium alloy should consist of 76 w/o Ti_2Ni, 24 w/o alpha titanium. These phases, in approximately these proportions (considering the higher density of Ti_2Ni), can be seen to exist in the seal shown in Figure 6.

After the eutectic liquid has formed and reaction with the ceramic has occurred, we are, however, no longer dealing with a simple binary alloy. It is probable that the layer adjacent to the ceramic is an oxygen and aluminum-rich titanium solid solution with dispersed particles of other phases. The layer adjacent to this, containing primary alpha titanium grains (also containing aluminum and oxygen), probably solidified from the melt at the sealing temperature. The large Ti_2Ni grains and small patches of transformed beta found in the center of the braze joint solidified at the eutectic temperature.

If the seal is heated for a somewhat longer period of time at the sealing temperature, diffusion of oxygen and aluminum into the alloy occurs to the extent that no transformed beta is found in the joint at room temperature, as shown in Figures 7, 8, and 9 to be discussed later.

The rapid rate of diffusion of nickel in titanium is partially responsible for the large and well defined nickel containing phases seen in these photomicrographs and was demonstrated by placing a washer of titanium and one of nickel in intimate contact and heating to a temperature of about 880°C for five minutes. This is approximately the same time and temperature at which a seal assembly is "soaked" to thermal equilibrium before increasing the temperature to form the eutectic liquid. Figure 10 is a photomicrograph of this titanium-nickel couple. Equiaxed primary alpha with transformed beta in the grain boundaries would be obtained after heating commercially pure alpha titanium to this temperature; the central portion of the titanium washer can be seen to have such a structure. Adjacent to the nickel, however, the titanium has the basket-weave structure formed by transformation of beta to alpha during cooling, indicating that sufficient nickel must

have diffused into the titanium to shift the composition of the alloy into the beta field (see Figure 5). A similar effect is seen on the side of the titanium washer which was in contact with a Kovar washer during the heat treatment.

Figure 11 portrays a section of a seal made with an alloy which was somewhat richer in titanium (76.8 w/o Ti, 23.2 w/o Ni) than the eutectic seal shown in Figure 6. As would be predicted from the phase diagram, less Ti_2Ni exist in the alloy at room temperature.

Figure 12 shows a section of a seal made with an alloy which was still richer in titanium. It was so rich, in fact (83.2 w/o Ti, 16.8 w/o Ni), that calculations show that the joint should contain, at the sealing temperature, approximately 40 w/o liquid and 60 w/o beta solid solution. Although the use of brazing alloys having broad melting ranges is generally considered undesirable due to possible liquation, no such trouble was encountered with the "titanium-rich" series of alloys. The advantages of using a very titanium-rich alloy considerably outweigh the theoretical disadvantage of not possessing a sharp melting point, as explained in the following paragraphs.

The photomicrograph (Figure 12) shows the usual alpha titanium layers adjacent to the ceramic. Between these layers, however, one sees a region containing but a very small amount of Ti_2Ni, the balance being transformed beta, as predicted by the phase diagram and in conformity with the solidification process previously discussed. It will be noted that no cracks exist in this seal or the seal shown in Figure 11. In general, it can be said that under the same sealing conditions (time and temperature), the tendency toward the formation of cracks in the alloy decreases as the titanium content of the alloy increases. The reason for this is the reduction of the amount of Ti_2Ni which forms in the joint and a consequent reduction in the stresses which are introduced as a result of the thermal expansion mismatch between the several phases and the ceramic. With a large proportion of the relatively ductile titanium present, destructive stresses cannot be set up.

Microhardness measurements were made on the several phases contained in this alloy and illustrate the effect just discussed. The Ti_2Ni in the center of the alloy had a hardness of 925 KHN. The transformed beta titanium surrounding this Ti_2Ni, and comprising the bulk of the entire alloy layer, had a hardness of only 302 KHN. The light colored, alpha titanium layer was extremely hard at 988 KHN. The re-

action layer in contact with the ceramic surface was so thin that its hardness could not be measured but it certainly would not be expected to be soft.

The aforementioned ceramic-to-ceramic seals made with alloys having titanium contents the same as or greater than that of the lowest melting eutectic in the titanium-nickel system (71.5 w/o Ti, 28.5 w/o Ni) were all prepared using a heating schedule similar to that shown in Figure 2, Curve A. The power to the oven was cut off about one minute after initial melt formation was observed. Shorter sealing times can be and generally are used. Sealing times of from 10 to 30 seconds after initial melt formation are typical for sealing of practical devices.

Prolonged heating after the melt is formed is quite damaging to the quality of the resulting seal. Figures 7, 8, and 9 show seals having compositions identical to those of Figures 6, 11, and 12, respectively, but were held at temperature for 10 minutes after the melt was formed. Although such a prolonged heating is not practical, it clearly shows the embrittling effect of excessive reaction with the ceramic. All seals which received prolonged heating at the sealing temperature can be seen to contain many cracks. The large grains of Ti_2Ni in the central region, as well as the alpha titanium layers adjacent to the ceramic make the seal shown in Figure 7 appear similar to that of the seal of the same composition which received a normal heat treatment (Figure 6). The major difference lies in the hardness of the titanium phase of the "overbrazed" seal and the excessive cracking which results from the inability of the titanium to yield plastically or elastically. Hardening of the titanium results from contaminants introduced by reaction with the alumina ceramic.

Whereas titanium-rich alloys have been shown to be definitely advantageous when sealing is accomplished using a normal sealing schedule, they do not prevent cracking if prolonged heating at sealing temperature is permitted, as shown in Figures 8 and 9. The alloy in these two titanium-rich alloy seals was so brittle and cracked that fragments were picked out during polishing. The alloy shown in Figure 9 contains a very large Ti_2Ni area in the center with the usual alpha titanium layers on either side.

C. Ceramic-to-Titanium Seals

A seal between 0.010-inch thick titanium and ceramic, using a 0.0003-inch nickel washer to form the sealing liquid, results in the structure shown in Figures 13 and 14. The seal shown in Figure 13 received a normal time-temperature sealing treatment. A thin layer of Ti_2Ni can be seen lying parallel to but about 0.001 inch from the ceramic-metal interface. Such joints appear to be very strong and reliable in spite of the presence of a small quantity of Ti_2Ni.

Hardness measurements were made at seven points between the center and the outside of the alloy layer, five measurements between the center and the layer of Ti_2Ni and two more measurements between this layer and the surface of the ceramic. The hardness readings varied somewhat but, in general, can be said to have increased from 284 KHN at the center of the alloy layer to 542 KHN near the ceramic.

Another seal of the same type, i.e., ceramic-to-titanium, but which had reached a slightly higher temperature during sealing did not contain the Ti_2Ni layer and showed a smoothly increasing microhardness from the center to the edge. The readings were 239 (center), 255, 342, 394, 470 and 726 KHN very close to the reaction layer which is formed in contact with the ceramic.

If a seal of this type is sealed according to Schedule A but is given a prolonged hold, for example five minutes, at the peak temperature attained, the seal appears as in Figure 14. No Ti_2Ni grains are visible due to complete diffusion of the nickel through the titanium washer. Some Ti_2Ni should, however, occur in equilibrium with alpha titanium at room temperature if eutectoid decomposition occurs during cooling (the eutectoid reaction is very rapid in the titanium-nickel system, see Figure 3). Even if the two 0.0003-inch nickel shims and the 0.010-inch titanium washer were reacted to form a homogeneous alloy with a resultant composition of 90 w/o Ti and 10 w/o Ni, the alloy should contain, under room temperature equilibrium conditions, approximately 74 w/o alpha titanium and 26 w/o Ti_2Ni. Large grains of Ti_2Ni are formed during high-temperature life testing, as will be discussed later.

Microhardness measurements on the seal of Figure 14, from the center to the edge, gave readings of 925, 842, 770, 988, 896 and 988, showing the effect of contaminants introduced through reaction with the alumina.

In contrast with the ceramic-to-ceramic seals previously discussed, this long time-temperature sealing treatment of a ceramic-to-titanium seal did not affect its vacuum tightness or cause failure of the bond during metallographic mounting. Although the alloy is undesirably hardened, multiple layers of different phases do not exist, with their differing thermal expansions, to set up severe stresses leading to cracking. Furthermore, the larger volume of metal can hold more oxygen before damaging embrittlement is encountered.

Sealing to a thick titanium washer satisfies our desire (as discussed in Section B. Ceramic-to-Ceramic Seals with Titanium-Rich Alloys) to use an alloy so rich in titanium that little Ti_2Ni can exist. Also, by using the thick titanium washer, the eutectic liquid which forms at the sealing temperature exists for a very short time, disappearing as the eutectic forming element, nickel, diffuses into the titanium.

That hardening of the titanium washer is not due merely to nickel in solid solution in titanium or present as finely dispersed Ti_2Ni was shown by melting a nickel shim onto the surface of a titanium washer for six minutes at temperatures of 1000°C and 1100°C. Hardness measurements across the titanium washer gave readings ranging from 240 to a maximum of only 270 Knoop. This experiment was performed using several methods of supporting the titanium washer in the oven, none of which permitted contact with a ceramic.

D. Reaction of Titanium with Various Metal Oxides

A brief experiment was conducted to ascertain whether gross differences in the hardening of titanium would result if sealed to metal oxides other than alumina, particularly the "fluxing oxides" contained in a 97 percent alumina ceramic.

Specimens were prepared by sealing 0.010-inch titanium washers to thin slices cut from a boule of sapphire (Al_2O_3), a crystal of periclase (MgO), and a rod of fused silica (SiO_2). A 0.0005-inch nickel washer was used to effect the seal between the titanium and the oxide slice. All three specimens were sealed simultaneously with tantalum washers separating the specimens in the stack.

The specimens were mounted, polished, and microhardness measurements were made at intervals across the 0.010-inch titanium washer as well as a short distance into the supporting tantalum

washer which, during sealing, became bonded to the titanium. The hardness data obtained are plotted in Figure 15.

From these few data, one would say that the hardening of titanium, at the titanium-ceramic interface, is relatively little affected by the oxide to which it is sealed.

It appears, however, that the hardness of the titanium at considerable distances from the interface is dependent upon the type of oxide. Although quite inconclusive, these data do support the observation, made in connection with life testing of seals at a temperature of 700°C, that the rate of hardening of titanium is related to the composition of the ceramic to which it is sealed.

E. Ceramic-to-Metal Seals (Tantalum, Kovar, Stainless Steels)

Titanium and nickel foil washers, in the proper thickness to yield the near-eutectic composition (71.8 w/o Ti, 28.2 w/o Ni) or the titanium-rich composition (76.8 w/o Ti, 23.2 w/o Ni) were used for butt sealing cylindrical ceramic specimens to either side of 0.010-inch thick washers of tantalum, Kovar, Type 304 and Type 430 stainless steel. The ceramic specimens were made from body A-976.

Figures 16, 17, 18, and 19 show polished sections of seals to these four metals. The seal between tantalum and ceramic, Figure 16, appears somewhat similar to that obtained between two ceramics. Although reaction with the tantalum has occurred, it does not embrittle the sealing alloy. Seals to tantalum are no more difficult to make than ceramic-to-ceramic seals. It is preferable, however, to use a titanium-rich sealing alloy in order to minimize Ti_2Ni formation or, preferably, a titanium "buffer" washer, as will be discussed in a subsequent section.

The sealing alloy in the Kovar (Figure 17) and Type 304 stainless steel (Figure 18) seals has been altered appreciably in composition due to enrichment by nickel from the metal washer. The resulting alloy is extremely hard and brittle and shows many cracks. Although it is possible to make vacuum-tight seals to these two metals, it requires extremely close control over the time-temperature sealing schedule. Even the use of the titanium-rich titanium-nickel sealing alloy which has been found advantageous in ceramic-to-ceramic sealing does not assure consistently vacuum tight seals.

Using a single shim of titanium and relying on alloying with the nickel in the Kovar appeared to be the most satisfactory method of effecting ceramic-to-Kovar seals, but even this procedure did not eliminate the need for a critically precise sealing schedule.

Reaction of the titanium-nickel sealing alloy with Type 430 stainless steel is considerably less vigorous than with Type 304 stainless steel, probably due to the absence of nickel and the resultant low melting titanium-nickel eutectic. Figure 19 shows that little erosion of the Type 430 washer occurred. Although sealing to Type 430 is somewhat less difficult, the preparation of seals to both types of stainless steel requires considerably closer temperature control than is required for ceramic-to-ceramic or ceramic-to-titanium sealing.

The four seals shown in Figures 16, 17, 18, and 19 were made simultaneously, and thus received identical time-temperature treatments. Although all seals except the one to Type 304 stainless steel were vacuum tight, the sealing schedule which was used was not necessarily the optimum one for each type.

F. Ceramic-to-Metal Seals Using Titanium "Buffer" Washers

In order to minimize Ti_2Ni formation, by keeping the titanium-nickel sealing alloy as rich in titanium as possible, seals were prepared using a titanium "buffer" washer between the ceramic and the desired structural metal. The titanium buffer washers as well as the structural seal metal washers (tantalum, Kovar, Type 304 and Type 430 stainless steel) were 0.010-inch thick. Nickel foil washers (0.0003-inch thick), placed on either side of the titanium buffer washers formed a liquid phase at the 942°C eutectic temperature which simultaneously effected a bond to the ceramic and to the structural metal washer.

Figures 20, 21, 22 and 23 show photomicrographs of polished sections of portions of these seals. The central region is the titanium buffer washer, the ceramic-to-titanium interface appearing at one side of the photomicrograph and the titanium-to-structural metal interface appearing at the other side.

The seal to tantalum, Figure 20, shows relatively little erosion of the tantalum at the titanium-tantalum interface. Hardness measurements show a gradual increase in hardness from 172 KHN

at the center of the tantalum washer to 323 KHN at the center of the titanium buffer washer. Such seals are very easily and reliably made.

Figure 21 shows the seal to Kovar. The titanium buffer washer has been partially melted, throughout its thickness, due to reaction with the Kovar supplying nickel (and cobalt) to the melt. In this case, the use of a titanium buffer washer is totally unsatisfactory.

The polished section of the seal to Type 304 stainless steel is shown in Figure 22 while the seal to Type 430 stainless steel is shown in Figure 23. In both of these seals, extensive reaction at the titanium-structural metal interface has occurred, resulting in the formation of one or more new phase layers at this interface.

G. Ceramic-to-Ceramic Seals with Nickel-Rich Titanium-Nickel Alloys

A limited amount of effort was applied to the preparation of ceramic-to-ceramic seals by forming, in situ, nickel-rich titanium-nickel alloys of specific compositions, using titanium and nickel foil washers in the proportions to yield the desired weight percent compositions. The reader is reminded that the term "nickel-rich," as it is used here, refers to compositions containing nickel in amounts greater than the lowest melting eutectic, i.e., greater than 28.5 w/o Ni.

The seal shown in Figure 24 was made with an alloy having the composition 65.8 w/o Ti, 34.2 w/o Ni. As would be predicted from the phase diagram, the structure is predominately Ti_2Ni.

Figure 25 shows a seal made with the composition 49.0 w/o Ti, 51.0 w/o Ni. Under equilibrium conditions such an alloy should contain, at room temperature, approximately 77 w/o TiNi and 23 w/o of the very brittle Ti_2Ni. The phase adjacent to the ceramic, on both sides of the seal, is Ti_2Ni and can be seen to contain many cracks. The bulk of the alloy layer is composed of TiNi and was found to have a hardness of 677 KHN. "Overbrazing" did not change the structure of such seals.

The seal of Figure 26 contains an alloy having the composition 39.1 w/o Ti, 60.9 w/o Ni and should contain, under equilibrium conditions, two phases: a large proportion of TiNi and a lesser

amount of $TiNi_3$. However, three phases appear to be present in this seal, one of which comprises the layer adjacent to the ceramic on each side of the seal, is optically isotropic, displays a few cracks, and is believed to be Ti_2Ni. The matrix is TiNi, is isotropic, and has a hardness of 677 KHN. The third phase occurs as particles dispersed in the TiNi and sometimes as a layer adjacent to the Ti_2Ni. This phase is anisotropic and believed to be $TiNi_3$. "Overbrazing" of such seals reduced the amount of non-equilibrium Ti_2Ni.

Although vacuum tight, high strength, seals were obtained with many compositions, the sealing alloys which were formed did not always have the phase composition which would be predicted from the equilibrium diagram nor were reproducible results always obtained with a given composition. The problem is believed to stem largely from the use of foil washers which, during alloying, permitted liquation.

Since homogeneous melts of each of the desired titanium-nickel sealing alloy compositions would be required to overcome this difficulty, additional effort was shelved until the testing of ceramic-to-nickel seals had been completed and the high-temperature potentialities of high nickel content phases could be better assessed.

H. Ceramic-to-Nickel Seals

Figures 27 and 28 show polished sections of seals which were made to 0.010-inch thick, Grade 499, nickel washers using thin (0.0005-inch) titanium foil to form a liquid sealing alloy.

The phase diagram indicates that the first liquid to form would have the composition of the lowest melting eutectic. As the temperature is raised, the melt disolves more nickel and the composition drifts toward the composition of the brittle intermetallic compound Ti_2Ni.

If the foregoing process were terminated after the melt had dissolved approximately 8 w/o nickel, the alloy would contain, upon cooling to room temperature, predominately Ti_2Ni.

This is essentially what happens when a seal is made to a thick nickel washer at a low temperature. Figure 27 shows the structure of a seal which received the same time-temperature treatment

as is normally given to titanium-rich alloy seals or seals to titanium metal. The alloy region next to the ceramic is predominately Ti_2Ni and can be seen to contain numerous cracks. Equilibrium conditions are not, however, attained in such a seal because of the "infinite" supply of nickel in contact with the melt. This results in a zone of TiNi, approximately seven microns wide, adjacent to the Ti_2Ni layer. Termination of the cracks at the surface of this zone suggests that the layer is ductile as does the microhardness of 434 KHN. A third layer exists in this seal but is not readily visible in the photograph. This layer of $TiNi_3$, approximately three microns wide and lying adjacent to the TiNi layer, is optically anisotropic, and is readily visible under polarized light or by etching with a nitric-acetic acid nickel etch.

Heating a similar seal to a maximum temperature of approximately 1280°C results in the structure shown in Figure 28. The light colored zone between the nickel and the ceramic is $TiNi_3$. A few unidentified orange-colored particles appear in this layer. A reaction zone between the $TiNi_3$ layer and the nickel is evidenced by loss of the nickel grain boundaries in this region. Such seals are very strong, easily prepared, and reliably vacuum-tight.

Sealing to nickel in such a manner as to form only the "ductile" phase TiNi was not achieved. During the latter part of the study, after more precise temperature control was introduced and more pure nickel was being used, it was found possible (by holding several minutes at 1100°C) to make seals wherein the bulk of the alloy layer was TiNi and only a very small amount of a third phase, probably Ti_2Ni, could be seen at the alloy-ceramic interface. A narrow band of $TiNi_3$ occurred, as would be expected, at the TiNi-Ni interface. Such seals, however, were not always vacuum tight. In light of the probably reaction (for which evidence will be presented later) of any intermediate phases with the "infinite" supply of nickel during life testing at high temperature (particularly at 900°C), as well as the instability[1] of TiNi, the value of attaining such a seal is questionable.

Figure 29 is a photomicrograph of a seal which was effected at a temperature of 1315°C, slightly above the $TiNi_3$-Ni eutectic. The seal consists of a nickel solid solution at the nickel-ceramic interface. Such seals are very sensitive to time-temperature sealing conditions---no soak at the peak temperature is required or has been found desirable. Although seals of this type can be prepared to be vacuum tight and may offer advantages for high-temperature applications, their

mechanical strength appears to be reduced, as will be described in a later section.

Figure 30 shows a seal which was heated for four minutes at 1090°C using thermocouple temperature control. The structure is similar to that of Figure 27, that is, Ti_2Ni adjacent to the ceramic, next a region of TiNi, then a narrow reaction zone of $TiNi_3$, and finally the nickel washer. The interesting thing here is that the aforementioned orange-colored particles are concentrated in the $TiNi_3$ phase layer and a crack can be seen to be propagating (starting at the edge of the fillet) right through the center of this layer.

When the seal is made at a temperature just below the 1304°C eutectic, these orange-colored particles will be found in the $TiNi_3$ layer as was mentioned in connection with the discussion of Figure 28. If the seal is made at a temperature above the 1304°C eutectic, these particles will then be found lying adjacent to the ceramic. (See Figure 29.) They are believed to be formed from impurities in the nickel, and seals very recently made using ultra-high purity nickel washers do not show any of these particles.

II. High-Temperature Life Testing

A. General

The test specimens consisted of two 0.690-inch diameter, 0.095-inch wall, 0.200-inch long ceramic rings sealed to each other or to either side of a metal washer having the same inside and outside diameters. In most instances, the test specimens had been sealed three or four at a time in the vacuum bell jar shown in Figure 1.

Life testing was performed at two temperatures, 700°C and 900°C, and a variety of seal types were used in order to study the effect of sealing alloy composition, seal stress (as influenced by the type of seal metal used and/or the use of "buffer" washers), ceramic purity (pure sintered alumina and 97 percent alumina), etc. The seals were thermally cycled to room temperature at the end of each 240-hour interval. They were not, however, always leak checked at the end of each 240-hour interval.

Several types of seal specimens were life tested. Two of the specimen types were of ceramic-to-ceramic construction, one

sealed with the near-eutectic composition (71.8 w/o Ti, 28.2 w/o Ni), and the other with the titanium-rich composition (76.8 w/o Ti, 23.2 w/o Ni). Another type of specimen which was used was of ceramic-to-titanium construction wherein the seal was effected through the use of a 0.0003-inch thick nickel foil washer on either side of the 0.010-inch thick titanium washer. (When a ceramic-to-metal seal is referred to, it is to be understood that the structural metal washer was sandwiched between and sealed to two ceramic specimens, i.e., a "compensated" butt seal.) Other seal systems which were tested included specimens of ceramic-to-tantalum seals made with the titanium-rich titanium nickel alloy, ceramic-to-tantalum seals made with thick (0.010-inch titanium "buffer" washers located on either side of the tantalum washer, as well as ceramic-to-Kovar, ceramic-to-Type 304 stainless steel and ceramic-to-Type 430 stainless steel made with titanium "buffer" washers. Still other specimens included ceramic-to-ceramic seals made with high nickel content titanium-nickel alloys and ceramic-to-nickel seals.

At the end of the first 240-hour life test at a temperature of 900°C, it was clear that failure of titanium phase-containing seals was due to hardening and embrittlement of the seal alloy. It was not known, however, whether the embrittling element, probably oxygen, was being introduced through continued reaction with the ceramic at the test temperature or gettering of residual gas in the test chamber. In order to help answer this question, pieces of 0.010-inch thick titanium, tantalum and columbium washers ("coupons") were exposed, along with the seal test specimens, with hardness measurements being made on each coupon before and after exposure. Since the data indicated (Table V, Test No. 2) that the titanium coupons were being hardened significantly by such exposure, additional life tests were conducted wherein the test specimens as well as the titanium washers for hardness determination were enclosed in an optically opaque wrapping of titanium foil before being placed on the molybdenum boat for insertion into the test chamber. It was assumed that the titanium would, through its gettering ability for oxygen, nitrogen, and carbonaceous materials, provide a significantly improved atmospheric environment within the enclosure. That this was the case is shown by the data of Table V, Tests No. 3 and No. 4 to be discussed later.

Although life testing under conditions to be encountered in outer space could be better simulated through the use of a well-trapped or vac-ion pumped system, it may be difficult to provide such a good environment for a thermionic converter during testing on the ground. It

may be even more difficult to provide a suitably pure protective atmosphere for converters in non-space applications. If the quality of a seal would be rapidly degraded in a vacuum of 10^{-4} to 10^{-5} Torr, it might place severe restrictions on the applicability of seals of this type.

In the tables and discussion to follow, the samples which were enclosed within the titanium foil wrapper before being placed in the vacuum test chamber are designated "wrapped" while those which were life tested, unwrapped, in the same or another test chamber are designated "exposed."

B. Hardness Testing of Exposed and Wrapped Titanium, Tantalum, and Columbium Coupons

Microhardness measurements were made across the thickness of the 0.010-inch thick washers of titanium, tantalum, and columbium, which had been included with the ceramic-to-metal seal test specimens during life testing at 700°C and 900°C. Although less accurate than other hardness measurements, Knoop hardness at a 10-gram load was chosen in order to permit direct comparison with the hardness measurements to be made on the various phases contained in the sealing alloys.

Table V presents the Knoop hardness values which were obtained on wrapped and exposed specimens, and the values are repeated in other tables where their availability would make data comparison more convenient. The maximum and minimum hardness is indicated in those cases where the washer varied significantly in hardness across its thickness. Five different tests were conducted. In Test No. 3, wrapped and exposed metal specimens were contained within the same ceramic chamber of the dual-chamber life test equipment. The data indicate that the titanium foil wrapping material improved the atmosphere sufficiently to give some protection even to the exposed specimens. In Test No. 6, the exposed samples were tested during the same 720 hours as the wrapped samples, but the two groups were in different test chambers attached to the same vacuum manifold.

The minor amount of hardening experienced by the exposed specimens of titanium, as compared with those of Test No. 5, suggest that the presence of a large amount of titanium foil in one chamber was effective in improving the atmosphere in the other test chamber.

Table V - Knoop Hardness of Titanium, Tantalum, and Columbium Coupons

Test No.	Test Conditions	Knoop Hardness Number		
		Titanium	Tantalum	Columbium
1	Before testing	189	215	138
2	240 hours at 900°C, exposed	956-769	260-210	174-144
3	240 hours at 900°C, wrapped	269	137	100
	240 hours at 900°C, exposed but in same test chamber	329	179	125
4	240 hours at 700°C, exposed	220	150	10[illegible]
5	720 hours at 700°C, exposed	500-400	160-130	-
6	720 hours at 700°C, wrapped	207	137	110
	720 hours at 700°C, exposed in different test chamber	230	156	-

The hardnesses of the three metals "before testing" was determined on the metals "as received," and the decrease in hardness which occurred during certain tests was due to annealing.

The data indicate the relative sensitivity of the three metals - titanium, tantalum, and columbium - to the residuals in an oil diffusion pumped vacuum system operating at a pressure in the range of 1 to 5 x 10^{-5} Torr.

C. 900°C Life Tests

1. General

The first life test was conducted at a temperature of 900°C for 240 hours and included specimens as shown in Table VI. None of the ceramic-to-ceramic or ceramic-to-titanium seal specimens were leak tight at the end of 240 hours of exposure. Most of the ceramic-to-nickel seals were vacuum tight at the end of 240 hours, and remained so during an additional 670 hours of exposure, as will be discussed in a later section.

Changes in hardness of titanium, tantalum, and columbium coupons exposed for 240 hours at 900°C indicated that the atmosphere could have been a significant source of embrittling elements. These figures, shown in Table V, are repeated in Table VI.

The second life test conducted at 900°C also continued for a period of 240 hours and included specimens similar to those of the first test. In this test, however, one group of specimens was wrapped in titanium foil while another group, contained within the same test chamber, was exposed to the test atmosphere. Included in each of these groups were several flexural strength test specimens as well as 0.010-inch thick coupons of titanium, tantalum, and columbium for hardness measurements. Test results are given in Tables V and VII.

As in the first test, only the ceramic-to-nickel specimens were still vacuum tight at the end of 240 hours of exposure. Most of the flexural strength test specimens were so weak that they fell apart during leak testing.

Hardness measurements made on the wrapped and exposed coupons of titanium, tantalum, and columbium contained within the chamber during the second life test indicate that the atmosphere

Table VI - First 900°C Life Test

Seal Type	Vacuum Tight Specimens After Indicated Hours				
	Initially	240	480	670	710
Ceramic-to-Ceramic (71.8 w/o Ti, 28.2 w/o Ni)					
a. A-923 ceramic	5	0			
b. A-976 ceramic	5	0			
Ceramic-to-Ceramic (76.8 w/o Ti, 23.2 w/o Ni)					
a. A-923 ceramic	5	0			
b. A-976 ceramic	5	0			
Ceramic-to-Titanium					
a. A-976 ceramic	5	0			
Ceramic-to-Nickel					
a. A-923 ceramic	9	7	7	6*	6
Titanium Coupon**	189 KHN	956-769 KHN			
Tantalum Coupon**	215 KHN	260-210 KHN			
Columbium Coupon**	138 KHN	174-144 KHN			

*One vacuum tight specimen removed for analysis at 480 hours.

**The titanium, tantalum, and columbium coupons for hardness measurement were exposed under the same conditions as the seal specimens, i.e., 240 hours at 900°C, but in a separate experiment.

Table VII - Second 900°C Life Test

Seal Type	Vacuum Tight Specimens After Indicated Hours: Initially	240	480
Ceramic-to-Ceramic (76.8 w/o Ti, 23.2 w/o Ni)			
a. A-923 ceramic, exposed	3	0	
b. A-923 ceramic, wrapped*	3	0	
c. A-976 ceramic, wrapped*	3	0	
Ceramic-to-Ceramic Flexural Strength Test Specimens (76.8 w/o Ti, 23.2 w/o Ni)			
a. A-923 ceramic, exposed	4	0	
b. A-923 ceramic, wrapped*	4	0	
Ceramic-to-Titanium			
a. A-923 ceramic, exposed	3	0	
b. A-923 ceramic, wrapped*	3	0	
c. A-976 ceramic, wrapped*	3	0	
Ceramic-to-Titanium Flexural Strength Test Specimens			
a. A-923 ceramic, wrapped*	4	0	
b. A-923 ceramic, exposed	4	0	
Ceramic-to-Tantalum (76.8 w/o Ti, 23.2 w/o Ni)			
a. A-923 ceramic, wrapped*	2	0	
b. A-976 ceramic, wrapped*	4	0	
Ceramic-to-Nickel			
a. A-923 ceramic, wrapped*	3	3	3
Titanium Coupon	189 KHN		
a. Wrapped	-	269 KHN	
b. Exposed	-	329 KHN	
Tantalum Coupon	215 KHN		
a. Wrapped	-	137 KHN	
b. Exposed	-	179 KHN	
Columbium Coupon	138 KHN		
a. Wrapped	-	100 KHN	
b. Exposed	-	125 KHN	

*A-976 and A-923 specimens were in separate titanium wrappings.

must have been quite low in embrittling elements. This is shown in Table V, Test No. 3, as well as in Table VII.

A few comments about each type of specimen tested, the results obtained, and pertinent observations concerning the microstructure and hardness of the sealing alloy and seal metals after testing are contained in the following sections. The discussions will be devoted primarily to specimens of the second life test since this test was conducted under the more favorable vacuum conditions.

2. Ceramic-to-Titanium Seals

Nine specimens were included in the second life test, six wrapped and three exposed. All samples were, however, in the same test chamber, and all nine were leakers at the end of the test. Figure 31 is a photomicrograph of a polished section of one of the seals which had been wrapped in titanium. The microhardness of the alpha titanium region near the center of the alloy layer was 988 KHN. By comparison, the hardness of the central alpha titanium region of one seal (exposed) from the first life test at 900°C was 1057 KHN. Large regions of Ti_2Ni formed near the center of the washer during life testing and specimens from both life tests appeared similar.

Coupons of titanium, tantalum, and columbium, both wrapped and exposed, had hardnesses as shown in Table V, Test No. 3 and repeated in Table VII. These data show that the tantalum and columbium had lower hardnesses after 240 hours at 900°C than they did before life testing. This decrease is primarily due to annealing since the materials were initially measured in the "as roll" condition. It should also be noticed that the metal samples which were exposed to the test atmosphere, but were contained within the same test chamber as the wrapped samples, had the same hardnesses, indicating that the environment throughout the test chamber was quite good. By comparison, coupons which had been exposed to the test atmosphere during the first life test increased substantially in hardness, as shown by Test No. 2 of Table V. Titanium, with its greater gettering ability was hardened to 956 KHN, while the tantalum and columbium had maximum hardnesses of 260 and 174, respectively. Thus, it is obvious that wrapping the ceramic seal specimens in titanium foil for the second life test provided protection from er brittling contaminants in the test atmosphere. Therefore, the severe hardening which occurred in those seal samples (of the second life test) containing a titanium phase was due primarily to continued

reaction of the sealing alloy with the ceramic. The four wrapped and four exposed flexural strength test specimens of the second life test had been so severely damaged by continued reaction that they fell apart upon removal from the test chamber or during lead checking.

3. Ceramic-Titanium "Reaction" Specimens

In a separate experiment, a 0.010-inch thick washer of titanium was merely "sandwiched" (without bonding) between two ceramic rings; this sandwich being wrapped in titanium foil to provide additional protection in the vacuum life test chamber. Two such sandwiches were prepared, one using rings of the pure sintered alumina body A-976, and the other using the 97 percent alumina body A-923. These wrapped sandwich specimens were then heated for 240 hours at 900°C.

Upon unwrapping the specimens at the end of the test, it was found that the inner titanium foil wrapping was quite ductile except where it had been in contact with the ceramic, as had been previously observed with other wrapped specimens from the second life test.

Figure 32 is a photomicrograph of a polished section of the titanium-ceramic (A-976) sandwich at the end of 240 hours at 900°C. Extensive reaction can be seen to have occurred at the titanium-ceramic interface resulting in a phase layer approximately 25 microns wide located adjacent to the ceramic. This layer is fine grained, anisotropic, and contains particles of one or more additional phases. Extensive grain growth occurred throughout the remainder of the titanium washer, and the alpha titanium grains, in many places, occupy the entire width of the washer. The hardness of these grains averaged 806 Knoop. The bond between the titanium and ceramic appeared to be quite strong and did not separate even during preparation of the metallographic section.

A virtually identical result was obtained with the titanium-97 percent alumina ceramic sandwich specimen except, in this case, failure occurred at the titanium-ceramic interface during mounting of the specimen. The microstructure and hardness of the several phases were, however, the same. Hardness of the central alpha titanium region was 846 KHN.

Thus, this experiment indicates that extensive reaction will occur between titanium and aluminum oxide when merely

placed in intimate contact at a temperature of 900°C, leading to severe hardening and embrittlement of the titanium. Similar hardening of any sealing alloy which contains a titanium phase (α or β solid solution) in contact with the ceramic would be expected.

4. Formation of Conducting Films on Ceramic Surfaces

It was noted that the seal specimens, as well as the just discussed "reaction" specimens, which had been wrapped in titanium foil and heated for 240 hours at 900°C were covered with a golden-brown, conducting metallic deposit suggestive of TiO. Where the ceramic had contacted the titanium foil, reaction had occurred to such an extent that an intimate bond to the foil had been effected, and when the ceramic was removed, a ring of foil came with it. The remaining foil was, however, still ductile.

Thinking that the deposit may have been one of the products of the reaction which had occurred at the specimen-foil interface, an experiment was conducted wherein ceramic specimens were placed in small boats made of molybdenum foil and merely covered with a titanium foil cover (not in contact with the ceramic). Both the A-923 and A-976 types of ceramics were used. The specimens were heated for 240 hours at 900°C. At the end of the test, both types of ceramic were found to be covered with the same type of deposit. The molybdenum foil directly underneath each specimen was, however, clean. Another test cell covered with a piece of titanium foil which had been previously vacuum fired showed the same type of deposit.

Spectrographic analysis of the deposit on both the ceramic surface and molybdenum boat showed the deposit to be predominately titanium. X-ray diffraction analysis of the deposit on the molybdenum boat was quite inconclusive but several lines matching those of Ti_2O were indexed.

The data indicate that,although extensive reaction occurs between an alumina ceramic and titanium when placed in contact for 240 hours at 900°C, contact is not necessary to cause the observed metallic deposit. That the deposit is not due merely to sublimation of volatile impurities from the titanium is indicated by the finding that the deposit consisted only of titanium as well as the fact that prior vacuum firing of the titanium did not prevent the deposit. Life tests which were

conducted with wrapped specimens of A-923 and A-976 ceramics for 720 hours at 700°C showed the same, although somewhat thinner, golden colored deposits. In light of the extremely low vapor pressure of titanium at 700°C, it seems improbable that the observed deposit could result from mere sublimation of titanium.

Although an explanation for this phenomenon cannot be offered, it has been suggested to the writer that gases evolved from the ceramic may enter into a type of reaction similar to the "water cycle" which is observed with tungsten.

5. Ceramic-to-Tantalum Seals

Six specimens of ceramic-to-tantalum seals made with the titanium-rich titanium-nickel sealing alloy (76.8 w/o Ti, 23.2 w/o Ni) were tested, wrapped, and all six were leakers at the end of the test.

6. Ceramic-to-Ceramic Seals

Nine specimens of ceramic-to-ceramic seals made with the 76.8 w/o Ti, 23.2 w/o Ni alloy were tested in the second life test. Six were wrapped and three were exposed, but all were contained within the same test chamber. All nine were leakers at the end of the test. Wrapped specimens of seals to both types of ceramics (A-976 and A-923) had structures and hardnesses similar to seals from the first life test. Photomicrographs of one of these seals are shown before testing in Figure 33 and after testing in Figure 34.

7. Ceramic-to-Nickel Seals

A group of nine ceramic-to-nickel specimens was included in the first life test at 900°C. At the end of 480 hours of testing, exposed, at a temperature of 900°C, seven of these specimens were still vacuum tight. One of the vacuum tight specimens was removed for sectioning and the others were returned to the chamber for additional testing. During an additional 190 hours, no additional failures occurred.

Failure of one of the specimens was not unexpected since it had been sealed at too low a temperature to properly form the desired phase, $TiNi_3$, at the interface. The cause of failure of the other specimen is unknown.

A photomicrograph of the interface in the vacuum tight specimen removed from test at 480 hours is shown in Figure 35. It is significant that the $TiNi_3$ phase layer at the ceramic-nickel interface has been reduced in thickness and, in many places along the length of the seal, has disappeared completely. Apparently the $TiNi_3$ phase continues to react with the virtually infinite supply of nickel forming a nickel solid solution. A layer of the aforementioned unidentified orange-colored particles can be seen. In some regions these particles are contained within the $TiNi_3$ phase layer while in other areas, solutioning of the $TiNi_3$ phase has left the orange particles in the nickel solid solution. In a ceramic-to-nickel seal before heat treatment, these particles are always contained within the $TiNi_3$ layer (as shown in Figure 27).

Hardness increased slightly from 132 KHN in the center of the nickel washer to 214 KHN near the $TiNi_3$ phase. Several measurements in the $TiNi_3$ phase gave readings ranging from 600 to 769 Knoop.

Curvature of the advancing phase boundary of the nickel solid solution can be seen; the boundary being "pinned" in places by the orange-colored particles.

D. 700°C Life Tests

1. General

The first life test at 700°C, conducted with various types of seals exposed to a vacuum of 1×10^{-5} Torr, was terminated at the end of 2830 hours with all seals being leakers. Failure of the several types of seals occurred at various times and will be discussed in the sections to follow.

Although this test, the results for which are given in Table VIII, included a variety of different types of seals, five seal types are most important. They include ceramic-to-ceramic seals effected through the use of the titanium-nickel alloy of near-eutectic composition (71.8 w/o Ti, 28.2 w/o Ni), ceramic-to-ceramic seals made with a titanium-rich titanium-nickel alloy (76.8 w/o Ti, 23.2 w/o Ni), ceramic-to-tantalum seals made with the titanium-rich titanium-nickel alloy (76.8 w/o Ti, 23.2 w/o Ni), ceramic-to-titanium seals, and ceramic-to-nickel seals. Twelve ceramic-to-ceramic seal specimens were made using the pure, sintered alumina ceramic (A-976) of nearly

Table VIII - First 700°C Life Test

Seal Type*	Vacuum Tight Specimens After Indicated Hours									
	Initially	240	480	960	1200	1630	1680	1920	2350	2830
Ceramic-to-Ceramic (71.8 w/o Ti, 28.2 w/o Ni)										
a. A-923 ceramic	6	6	2	0						
b. A-976 ceramic	6	6	4	0						
Ceramic-to-Ceramic (76.8 w/o Ti, 23.2 w/o Ni)										
a. A-923 ceramic	6	4	3	3	-	-	0			
b. A-976 ceramic	6	6	6	4	-	-	0			
Ceramic-to-Titanium										
a. A-976 ceramic	6	6	6	6	-	-	6	6	-	0
Ceramic-to-Tantalum (76.8 w/o Ti, 23.2 w/o Ni)	10	-	10	-	6	6	-	-	0	
Ceramic-to-Tantalum with Titanium Buffer Washers	4	-	4	-	4	4	-	-	0	
Ceramic-to-304 Stainless Steel with Titanium Buffer Washers	3	-	3	-	0					
Ceramic-to-430 Stainless Steel with Titanium Buffer Washers	4	-	4	-	4	3	-	-	0	
Ceramic-to-Kovar with Titanium Buffer Washers	4	-	4	-	1					
Ceramic-to-Nickel	9	-	9	-	0					

*Unless otherwise indicated, the seal specimens were prepared using A-923 alumina ceramic.

theoretical density while the other 12 ceramic-to-ceramic seals were made using the 97 percent alumina ceramic (A-923). All of the seals to titanium were made using the A-976 ceramic, while the seals to tantalum and nickel used the A-923 ceramic. Most of these 49 seals were still leak tight at the end of 240 hours of exposure.

After 480 hours, only 15 of the original 24 ceramic-to-ceramic seals were still leak tight, although all of the other types were still intact. At the end of 1680 hours, none of the ceramic-to-ceramic types were leak tight. The ceramic-to-titanium seals were still all leak tight after 1920 hours of exposure but were all leakers when tested again at the end of 2830 hours of exposure.

Data on four other types of seals which were life tested along with the aforementioned seals are presented in Table VIII. All were of the titanium "buffer" washer type, that is, they consisted of ceramic-to-titanium-to-metal-to-titanium-to-ceramic wherein the seal metal was either tantalum, Kovar, Type 304 or Type 430 stainless steel. The data show that the "buffered" seals to Type 304 stainless steel were the first to fail at only 480 hours of exposure. The seals to Kovar were the next to fail. The buffered seals to tantalum and Type 430 stainless steel were leak tight when tested at 1630 hours, but had all failed when tested again after 2350 hours.

Included with the test specimens were coupons of titanium, tantalum, and columbium for hardness measurements. Microhardness testing at the end of 240 hours of exposure showed a very slight increase in the hardness of the titanium but a decrease in the hardness of the tantalum and columbium (Table V). Additional samples which were exposed for 720 hours still showed a decrease in the hardness of the tantalum (from 215 to 147 KHN) but the hardness of the titanium had increased from 189 KHN to more than 400 KHN. It appears that although the atmosphere is good enough to prevent hardening of tantalum and columbium at this temperature, it is not adequate for titanium over long periods of time. Thus, it is possible that a portion of the embrittlement of the test seals was due to gettering of residuals in the test chamber by the titanium-nickel sealing alloy or the titanium seal metal.

The second life test at 700°C was conducted using seal specimens wrapped in titanium foil in an attempt to determine to what extent gettering of residuals in the test chamber had contributed to the embrittlement and consequent failure of the seals in the first test.

This test was of 720 hours duration and, as with all other tests, included cycling to room temperature at 240-hour intervals. Specimens of titanium, tantalum, and columbium for hardness measurements were wrapped with the seal specimens. The test results are presented in Tables V and IX.

The microhardness data included in Tables V and IX show that the test environment could not have contributed to any observed hardening of the seal metals or sealing alloys of the specimens in the second life test.

2. Ceramic-to-Ceramic Seals

The ceramic-to-ceramic specimens sealed with either eutectic or titanium-rich titanium-nickel alloys were the first to fail in both the first and second life tests. The slightly better performance of the flexural strength specimens was probably due to their smaller diameter and greater wall thickness, resulting in a more favorable stress situation and longer leak path.

Figure 33 is a photomicrograph of an A-976 ceramic-to-ceramic seal before life testing. A photomicrograph of a portion of the same seal after 1680 hours of exposure at 700°C in the first life test is shown in Figure 36. The hardness of the alpha titanium layer adjacent to the ceramic was 1022 KHN. Both the A-976 and the A-923 ceramic-to-ceramic seals of the second life test showed similar changes in structure occurring after only 720 hours of testing.

3. Ceramic-to-Titanium Seals

Figure 37 shows a polished section of one of the A-976 seals from the first 700°C life test after 1920 hours of exposure. The hardness of the titanium adjacent to the ceramic is 726 KHN while near the center of the 0.010-inch thick washer it is 632 KHN. Before heat treatment, these points had hardnesses of approximately 540 and 280 KHN, respectively, and the structure shown in Figure 13.

Figure 38 shows a section from a similar seal (A-976 ceramic) after 720 hours at 700°C in the second life test, i.e., wrapped in titanium foil. The appearance of this seal before testing is shown in Figure 39. It can be seen that a reaction zone has formed in the titanium at the titanium-ceramic interface during life testing. This

Table IX - Second 700°C Life Test

Seal Type	Vacuum Tight Specimens Initially	Vacuum Tight Specimens After 720 Hours
Ceramic-to-Ceramic (76.8 w/o Ti, 23.2 w/o Ni)		
a. A-923 ceramic	2	0
b. A-976 ceramic	2	0
Ceramic-to-Ceramic Flexural Strength Test Specimens (76.8 w/o Ti, 23.2 w/o Ni)		
a. A-923 ceramic	4	3
Ceramic-to-Titanium		
a. A-923 ceramic	2	0
b. A-976 ceramic	2	1
Ceramic-to-Titanium Flexural Strength Test Specimens		
a. A-923 ceramic	4	3
Ceramic-to-Tantalum (76.8 w/o Ti, 23.2 w/o Ni)		
a. A-923 ceramic	1	1
b. A-976 ceramic	3	1
Ceramic-to-Nickel		
a. A-923 ceramic	2	2
b. A-976 ceramic	3	3
Titanium Coupon	189 KHN	207 KHN
Tantalum Coupon	215 KHN	137 KHN
Columbium Coupon	138 KHN	110 KHN

new phase layer develops in seals to A-923 as well as A-976 ceramic and in exposed as well as wrapped specimens. The thickness of the layer appears to be related to the length of time at temperature, i.e., to the amount of reaction which has occurred with the ceramic.

Figure 40 presents a section of a seal to the A-923 ceramic which was tested, wrapped, along with the seal shown in Figure 38. The only difference between these two seals is the type of ceramic which was used. The only significant difference in the structure after 720 hours of testing at 700°C is a very slightly wider "new phase layer" at the interface of the seal to A-923 and slightly greater hardening of the titanium washer. Whether either of these observations is significant is questionable since the seals before testing looked identical (Figure 39), but the titanium in the seal to the A-923 ceramic was slightly harder indicating that it may have received a slightly more severe time-temperature treatment during sealing. The Knoop hardness values of several points across the washer of both the A-923 and A-976 seals are indicated on the photomicrograph of the A-976 seal, Figure 39.

4. Ceramic-to-Nickel Seals

Figure 41 is a photomicrograph of one of the ceramic-to-nickel seals which was a leaker after being exposed for 1200 hours at 700°C in the first life test. In contrast with the "solutioning" of the $TiNi_3$ phase layer which occurs when life tested at 900°C, no change in structure or thickness of this layer occurred. A few small cracks through the $TiNi_3$ layer were observed, however, as shown in the photomicrograph. It is believed that these cracks constitute the leak path through such seals and are probably the result of the thermal expansion mismatch between the 0.010-inch thick nickel washer, the 0.0008-inch thick $TiNi_3$ phase layer, and the alumina ceramic.

Table IX shows that the ceramic-to-nickel seals from the second life test were all still vacuum tight after 720 hours of testing. It should be noted that the group includes seals to both types of ceramic, bodies A-923 and A-976. Only additional life testing will show whether these seals will develop leaks as did the seals from the first life test after 1200 hours.

The observed cracks in the $TiNi_3$ layer, as well as its hardness, suggest that the thickness of this layer should be held to a minimum or even eliminated. Some seals have been made under conditions

of time and temperature which preclude $TiNi_3$ formation in favor of the nickel solid solution. Although the sealing schedule for such seals is somewhat more critical and the strength appears lower, as will be discussed in a later section, such seals warrant further study and life testing.

5. Ceramic-to-Tantalum Seals

The ceramic-to-tantalum seals of the first life test had surprisingly long lives as compared with the ceramic-to-ceramic specimens sealed with the same alloy, the titanium-rich titanium-nickel composition. Figure 42 shows the structure of one of these seals before life testing, while Figure 43 shows the microstructure after 2350 hours at 700°C.

Prior to sectioning of the life tested seal, it was thought that the improved life might be due to the capability of tantalum to getter oxygen and to act as a "sink" for the products of reaction of the sealing alloy with the ceramic. That this is not the case is shown by microhardness measurements at seven places across the thickness of the washer, yielding Knoop values ranging from 105 to 117. Although the reason for the improved life is still obscure and may be related to factors such as location of the Ti_2Ni layer with respect to the interface, the thermal expansions and ductilities of the several phases, etc., one thing is obvious---there is only one sealing alloy-ceramic interface from which hardening elements can be derived!

Seals of this type have been used in cesium vapor thermionic converters operating with a seal temperature of about 600°C for several thousand hours without failure. However, very few cycles to room temperature were performed. Although such seals do not show, during life testing, any changes occurring in the sealing alloy near the interface, a few small cracks have been observed. It is believed that use of thin titanium "buffer" washers would provide a margin of safety to such seals operating at this temperature, particularly if repeated thermal cycling is planned.

6. Ceramic-to-Metal Seals Using Titanium "Buffer" Washers

Figures 44, 45, and 46 show ceramic-to-metal seals employing titanium "buffer" washers which were exposed for 1200

hours at 700°C in the first 700°C life test. The same seals, before life testing, are shown in Figures 21, 22, and 23. These photomicrographs are presented merely to show the extreme brittleness of the alloys or intermetallic compounds which are formed in such seals at the titanium-metal interface. Failure at this interface is apparent in the seals shown in Figures 45 and 46.

E. Discussion of Life Tests Results

The accumulated data make it clear that any sealing alloys which contain a titanium phase (α or β solid solution) are not suitable for sealing to alumina ceramics when the intended operating temperature of the resulting seal approaches 900°C. Failure occurs through loss of hermeticity or, in more severe cases, physical separation of the component parts. The reason for failure stems from continued reaction of the sealing alloy with the ceramic, resulting in severe hardening and embrittlement of the titanium phase and/or the formation of new phases at the interface. Severe embrittlement alone would not necessarily lead to failure---it is the stresses which are developed in the alloy or at the interface, due to thermal expansion mismatch, which actually initiate the failure cracks. Other factors, such as phase changes and thermal expansion anisotropy, can contribute to these stresses.

Sealing alloys and procedures which minimize the formation of the hard and brittle intermetallic compounds, such as Ti_2Ni, are generally desirable. This does not, however, enable a seal to endure 900°C exposure, since it is the titanium phase in such seals which suffers the embrittlement caused by oxygen contamination.

At a temperature of 900°C, reaction with the ceramic is so rapid and the resulting embrittlement so severe that, at the end of 240 hours of exposure of a titanium phase-containing seal, any effect of ceramic composition and/or gettering of residuals in the test chamber is completely masked. In the experiment wherein a ceramic ring was merely placed in contact with a titanium washer at a temperature of 900°C, embrittlement of the washer was equally as severe with the pure sintered alumina (A-976) as with the 97 percent alumina body (A-923) at the end of the 240-hour test.

At a test temperature of 700°C, the life of the various types of seals is related to the rate of hardening of the sealing alloy.

Hardening results from both continued reaction of the active alloy with the ceramic as well as gettering of residuals in the test atmosphere. The fact that the tantalum washer in the ceramic-to-tantalum seal discussed in the previous section was not hardened after 2350 hours of exposure to a temperature of 700°C, while a tantalum coupon exposed for 720 hours at the same temperature showed slight hardening, suggests that gettering may not be as significant a source of embrittlement as would be indicated by the hardness coupons. This may be due largely to the difference in geometry of the specimens, i.e., the difference in area of the solid-gas interface at which "gettering" can occur and from which hardening elements must diffuse. The rate of reaction of the alloy with the ceramic is considerably reduced from that which occurs at 900°C, and one might speculate that it would virtually cease at a temperature of from about 550°C to 580°C, a temperature range below which titanium does not dissolve its surface oxide.

Although the data are quite inconclusive, it appears that the rate of hardening of titanium sealed to a pure sintered alumina (body A-976) is somewhat less than that of titanium sealed to a 97 percent alumina ceramic. This may be caused by the greater ease of reduction of several of the fluxing oxides, notably SiO_2, in the 97 percent alumina ceramic. The rate of hardening also appears to be related to the volume of material into which hardening elements can diffuse as well as the number of ceramic-alloy interfaces from which embrittling elements can be released.

For short time exposure to a temperature of 700°C, suitable sealing systems include alumina-to-titanium and alumina-to-tantalum. Alumina-to-columbium should also prove satisfactory. Prudent seal design is, of course, assumed.

For seal temperatures to 900°C, the only seals examined so far which show promise are those made with high nickel content titanium-nickel alloys or titanium shim seals to nickel. In the latter case, attainment of a vacuum tight seal necessitates a time-temperature sealing schedule which promotes the formation of the single phase $TiNi_3$ or a nickel solid solution at the interface. Uncompleted test results indicate that if $TiNi_3$ is allowed to form, its thickness must be held to a minimum if it is to withstand thermal cycling. Elimination of $TiNi_3$ in favor of a nickel solid solution, by sealing above the 1304°C eutectic, may prove advantageous for high-temperature compatibility. This, however, has yet to be demonstrated.

III. Microprobe Analyses

Although extensive use of microemission x-ray spectrometry would have been desirable, this service was not readily available. Consequently, only a few analyses were made to confirm the identity of certain phases which appeared in several typical seals.

The electron spot diameter was estimated to be 0.5 micron while excited x-rays were emitted from approximately a two-micron diameter area. Pure titanium, nickel, and aluminum were used as standards. Mutual enhancement and absorption of x-ray emission from the several elements in the alloys under investigation were such that integrated relative x-ray intensities were found to be nearly equivalent to percentage composition.

The seal specimen shown in Figure 6 was one of the specimens examined. Analysis of eight areas (grains) in the central Ti_2Ni region gave average weight percentages as follows:

Nickel	33.5 w/o
Titanium	64.6 w/o
Aluminum	0.14 w/o

Analysis of the dark etching, transformed beta areas showed:

Nickel	8.2 w/o
Titanium	86.1 w/o
Aluminum	1.03 w/o

These analyses confirm the tentative phase identification made metallographically.

A similar (but not the same) sample, exposed for 1680 hours at 700°C in the first life test, was analyzed for aluminum content. The Ti_2Ni phase in the center of the alloy layer was found to have an aluminum content of 0.05 w/o. The area which had previously shown the structure of transformed beta, but now contained large, light-etching grains, had an aluminum content of 1.17 w/o.

The interest in aluminum content, before and after heat treatment, stemmed from the thought that it might serve as an indictor of the amount of reaction which had taken place with the ceramic. Although

the second sample analyzed did not show an appreciable increase in aluminum content of the central titanium phase region after 1680 hours at 700°C, other data certainly indicate that reaction with the ceramic has occurred. It is possible that the oxygen derived from the reduction of Al_2O_3 diffuses throughout the alloy layer while the aluminum remains near the interface, possibly as a titanium-aluminum intermetallic compound. P. H. Brace et al[10] postulated a similar mechanism to account for observations made in connection with the melting of titanium alloys in alumina crucibles.

Although there can be little doubt that continued reaction of titanium with an alumina ceramic occurs during a 900°C life test, the one microprobe analysis which was attempted did not provide the proof which was being sought for a similar reaction occurring at a temperature of 700°C.

Analysis of the phase layers adjacent to the ceramic in the seal of Figure 6 was attempted. Since the spectrographer encountered difficulty trying to position the beam accurately on these thin phase layers, the instrument was started in the central Ti_2Ni or titanium phase region and stepped automatically in one-micron steps toward and through the outer layers. At each step, the integrated intensities of titanium, nickel, and aluminum were recorded for that step before moving to the next position. The consecutive steps for the three elements were then connected with a smooth curve yielding the plot shown in Figure 47. Both the titanium and nickel spectrometers were set at 100 percent full scale, while the aluminum spectrometer was set at 10 percent full scale. The start and finish of each designated layer is oriented as closely as was possible. A number of traverses were made and each appeared similar.

Errors associated with location of the ceramic-alloy interface coupled with the "averaging" effect of emission from a two-micron diameter area prohibits the making of any conclusions concerning the aluminum content of the several phase layers near the interface. The small hump (about three percent) in the nickel curve coinciding with the ceramic-alloy interface was observed in all of the traverses which were made. No explanation will be attempted.

Another microprobe analysis was made of the phase region at the termination of the cracks in the sealing alloy of Figure 26. That

this phase is TiNi is shown by the following analysis:

Nickel	55.5 w/o
Titanium	46.3 w/o
Aluminum	0.05 w/o

IV. Flexural Strength Tests

A limited number of flexural strength tests were made using four-point loading of a test specimen having dimensions as shown in Figure 48. These tests were conducted to determine the sensitivity of mechanical strength to the time-temperature sealing schedule. Only gross changes in strength were being sought. The specimens were brazed in the same manner as those which were prepared for life testing.

The principal difficulty which was encountered in the use of this specimen stemmed from the method of brazing. The specimens were brazed in a vertical position with pressure applied axially by means of a spring. No fixturing was used to keep the two ceramic cylinders in axial alignment. As a result, they slipped off-center to varying degrees when the eutectic liquid was formed. In almost every case, the lowest flexural strengths could be associated with the most eccentric specimens while the highest strengths were obtained with the specimens showing the best axial alignment.

Since eccentricity of the test specimen caused such a large spread in strength values, the actual values obtained are listed in Table X and no attempt has been made to calculate average values. It is believed that comparison of the highest values obtained would be the most meaningful manner of using the data.

All ceramic-to-ceramic and ceramic-to-titanium specimens were sealed using the same heating schedule (Figure 2, Schedule A). They differed in the length of time that they were held above the 942° eutectic temperature. All specimens were vacuum tight.

The data show that the strength of these types of seals is not particularly sensitive to soak time at temperature. Most of the failures occurred at the ceramic-to-sealing alloy interface. In a few of the ceramic-to-titanium seals, failure occurred partially through the ceramic.

Table X - Flexural Strength of Ceramic-to-Metal Seals

A. Ceramic-to-ceramic seals brazed with the titanium-rich titanium-nickel alloy

Specimens	Flexural Strength (psi) for Various Lengths of Time above the Eutectic		
	30 Seconds	90 Seconds	300 Seconds
1	17,800	31,000	26,400
2	18,600	17,800	20,900
3	31,000	25,600	30,200
4	-	21,300	27,900

B. Ceramic-to-titanium seals

Specimens	Flexural Strength (psi) for Various Lengths of Time above the Eutectic		
	30 Seconds	90 Seconds	300 Seconds
1	17,900	24,400	25,600
2	20,900	25,600	24,800
3	14,300	23,600	22,500
4	-	31,000	-

C. Ceramic-to-nickel seals

Specimens	Flexural Strength (psi) for Two Sealing Temperatures	
	1280°C	1315°C
1	24,000	5,000
2	16,700	3,100
3	24,800	5,000
4	-	3,100

Microhardness measurements across the titanium washer of several of the ceramic-to-titanium seals yielded the following data. Hardness measurements on a seal held 90 seconds above the eutectic showed the hardness to decrease with distance from the interface. At the center of the titanium washer the hardness was 380 KHN. On the other hand, the hardness of the titanium washer of a seal held five minutes above the eutectic temperature was essentially the same throughout, and averaged 726 KHN. Even though the titanium washer is severely hardened as oxygen contamination is introduced through continued reaction at the sealing temperature, the weakest link is always at the interface and, when stressed in flexure, the seal will fail at the interface.

The ceramic-to-nickel seals, on the other hand, show an entirely different effect of the time-temperature sealing schedule, particularly temperature, on strength. The specimens were prepared using 0.0005-inch thick washers of titanium foil on either side of a 0.010-inch thick Grade 499 nickel washer. The sealing time at peak temperature was held constant, about one minute---it was the peak temperature attained which differentiates these two tests. In one case, the maximum temperature was approximately 1280°C, while in the other it was about 1315°C. The former is just below the $TiNi_3$-Ni eutectic (1304°C) while the latter is just above this temperature.

The flexural strength data show distinct differences in flexural strength resulting from these two different sealing schedules. Heating to a temperature just below the highest eutectic permits the formation of a layer of $TiNi_3$ at the interface and results in the highest strength. If the eutectic temperature is exceeded, the $TiNi_3$ is replaced by a nickel solid solution and the strength of the seal drops off markedly. Failure occurred through the ceramic a short (a few to 10 mils) distance from the interface - none of the seals failed at the interface or through the intermetallic or solid solution layer. Photomicrographs of these seals are shown in Figures 28 and 29. Hardness measurements were made at several points across each of these seal types. The hardness averaged 800 KHN near the center of the 0.0006-inch thick $TiNi_3$ layer of the seal of Figure 28. At a distance of 0.0008 inch into the nickel washer from the nickel-$TiNi_3$ interface, the hardness was down to 136 KHN and it remained about the same as measurements were made across the nickel washers. For the seal made at the higher temperature, Figure 29, the hardness of the nickel solid solution at a distance of about 0.0004 inch from the alloy-ceramic interface was 250 KHN. At 0.001 inch from

the interface, the hardness was 146 while at the center of the 0.010-inch thick nickel washer it was 135 KHN.

All of the specimens were prepared using ceramic cylinders made from body A-923, a 97 percent alumina body containing SiO_2, MgO, and CaO. The flexural strength of unground, sharp edged, solid rectangular test bars of this ceramic, measuring 3/16 inch x 3/16 inch x 1-1/2 inch long broken under three-point loading on a 1.2-inch span, averages 55,000 psi.

CONCLUSIONS AND RECOMMENDATIONS

Seals or sealing alloys containing a titanium phase (alpha or beta solid solution) in contact with alumina are unsuitable for long-time exposure to a temperature of 700°C or for even short-time application at temperatures approaching 900°C. Failure of such seals results from continuing reaction of the "active" sealing alloy with the ceramic at the operating temperature, resulting in embrittlement and ultimate failure of the alloy or the alloy-ceramic bond.

If alumina-to-metal sealing, through the use of molten alloys capable of reacting chemically with the ceramic surface, is to be used for fabricating high-temperature seals for thermionic converters, then means must be found for inhibiting further reaction at the operating temperature of the seal.

This study pointed out several approaches which warrant further study and evaluation, including: (a) the forming, during sealing, of a titanium-containing metal phase or phases which are more stable thermodynamically at the desired operating temperature than aluminum oxide (e.g., the $TiNi_3$ or nickel solid solution prepared in the ceramic-to-nickel seals of this study), (b) by minimizing the quantity of active element to that which is necessary to achieve a bond (such as by the titanium hydride technique), or (c) by using sealing alloys which are insensitive to oxygen contamination. In addition, an evaluation should be made of the high-temperature capabilities of seals prepared using alloys of other "active" metals such as zirconium, columbium, and hafnium.

Further work, aimed at a seal with 900°C capability, should not be restricted to active sealing techniques but should include an evaluation of electron beam welding, the development of cesium-resistant metallizing techniques for pure alumina, and the use of cermets.

REFERENCES

1. W. J. Buehler and R. C. Wiley, "The Properties of TiNi and Associated Phases," U. S. Naval Ordnance Laboratory Report NOLTR 61-75 (August 1961).

2. E. R. Stover and J. Wulff, "The Nickel-Titanium-Carbon System," Trans. AIME, 215, pp. 127-136 (1959).

3. F. C. Kelley, "Metallizing and Bonding Non-Metallic Bodies," U.S. Patent No. 2, 570, 248.

4. R. J. Bondley, "Metal-Ceramic Brazed Seals," Electronics (July 1947).

5. "Sealing Metal and Ceramic Parts by Forming Reactive Alloys," IRE Transaction Component Parts, 4, pp. 28-31 (March 1957). J. E. Beggs, U.S. Patent No. 2, 857, 663.

6. C. R. Kurkjian and W. D. Kingery, "Surface Tension at Elevated Temperatures. III, Effect of Cr, In, Sn, and Ti on Liquid Nickel Surface Tension and Interfacial Energy with Al_2O_3," Journal Phy. Chem., 60, pp. 961-963 (July 1956).

7. W. M. Armstrong, A. C. D. Chaklader, and J. F. Clarke, "Interface Reactions between Metals and Ceramics: I, Sapphire-Nickel Alloys," Journal Amer. Ceramic Soc., 45 (3), pp. 115-118 (1962).

8. H. R. Ogden, D. J. Maykuth, W. L. Finlay, and R. I. Jaffee, "Constitution of Titanium-Aluminum Alloys," Trans. AIME, 191, pp. 1150-1155 (1951).

9. E. S. Bumps, H. D. Kessler, and M. Hansen, "Titanium-Aluminum System," Trans. AIME, 194, pp. 609-614 (1952).

10. P. H. Brace, W. J. Hurford, and T. H. Gray, "Preparation and Properties of Titanium-Base Alloys," Industrial and Engineering Chemistry, 42 (2), pp. 227-236 (1950).

11. D. J. Maykuth, H. R. Ogden, and R. I. Jaffee, "The Effects of Alloying Elements in Titanium. Volume A: Constitution," DMIC Report 136A (September 1960).

BIBLIOGRAPHY

D. H. Polonis and J. Gordon Parr, "Phase Transformation in Titanium-Rich Alloys of Nickel and Titanium," Trans. AIME, 206, pp. 531-536 (1956).

A. E. Jenkins and H. W. Werner, "The Structure and Some Properties of Titanium-Oxygen Alloys Containing 0-5 a/o Oxygen," Jour. Inst. of Metals, 80, pp. 157-166 (1951-1952).

W. Rostoker, "Selected Isothermal Sections in the Titanium Rich Corners of the Systems Ti-Fe-O, Ti-Cr-O, and Ti-Ni-O," Trans. AIME, 203, pp. 113-116 (1955).

H. R. Ogden, R. I. Jaffee and F. C. Holden, "Structure and Properties of Ti-C Alloys," Trans. AIME, 203, pp. 73-80 (1955).

A. D. McQuillan, J. Inst. Metals, 80, 363 (1951-1952).

D. H. Polonis and J. Gordon Parr, "Martensite Formation in Powders and Lump Specimens of Ti-Fe Alloys," Trans. AIME, 203, pp. 64 (1955).

A. Joukainen, N. Grant, and C. Floe, "Titanium-Copper Binary Phase Diagram," Trans. AIME, 194, p. 776 (1952).

A. Taylor and R. W. Floyd, "The Constitution of Nickel-Rich Alloys of the Nickel-Chromium-Titanium System," Jour. Inst. Metals, 80, pp. 577-588 (1951-1952).

F. B. Cuff, N. J. Grant, and C. F. Floe, "Titanium-Chromium Phase Diagram," Trans. AIME, 194, pp. 848-852 (1952).

D. J. Maykuth, H. R. Ogden, and R. I. Jaffee, "Titanium-m-Manganese System," Trans. AIME, 197, pp. 225-230 (1953).

R. J. VanThyne, H. D. Kessler, and M. Hansen, "System Titanium-Chromium-Iron," Trans. AIME, 197, pp. 1209-1216 (1953).

R. W. Fountain and W. D. Forgeng, "Phase Relations and Precipitation in Cobalt-Titanium Alloys," Trans. AIME, 215, pp. 998-1008 (1959).

A.Taylor and R. W. Floyd, "The Constitution of Nickel-Rich Alloys of the Nickel-Titanium-Aluminum System," Jour. of the Inst. of Metals, 81, pp. 25-32 (1952-1953).

L. Stone and H. Margolin, "Titanium-Rich Regions of the Ti-C-N, Ti-C-O, and Ti-N-O Phase Diagrams," Trans. AIME, 197, pp. 1499-1502 (November 1953).

D. J. Maykuth, H. R. Ogden and R. I. Jaffee, "Titanium-Tungsten and Titanium-Tantalum Systems," Trans. AIME, 197, pp. 231-237 (February 1953).

W. Rostoker, "Observations on the Occurrence of Ti_2X Phases," Trans. AIME, 194, pp. 209-210 (February 1952).

J. McMullin and J. T. Norton, "The Ternary System Ti-Ta-C," Trans. AIME, 197, pp. 1205-1208 (September 1953).

J. Taylor and P. Duwez, "Constitution of Titanium-Rich Ti-Cr-Al Alloys at 1800 and 1400°F," Trans. AIME, 197, pp. 253-256 (February 1953).

I. Cadoff and J. Nielson, "Titanium-Carbon Phase Diagram," Trans. AIME, 197, pp. 249-252 (February 1953).

P. Duwez and J. L. Taylor, "The Structure of Intermediate Phases in Alloys of Titanium with Iron, Cobalt, and Nickel," Trans. AIME, 188, p. 1173 (1950).

R. I. Jaffee, H. R. Ogden, and D. J. Maykuth, "Alloys of Titanium with Carbon, Oxygen and Nitrogen," Trans. AIME, 188, pp. 1261-1266 (1950).

B. R. Coles and W. Hume-Rothery, "The Equilibrium Diagram of the System Nickel-Manganese," Jour. Inst. Metals, 80, pp. 85-92 (1951-1952).

D. J. Maykuth, F. C. Holden, D. N. Williams, H. R. Ogden, and R. I. Jaffee, "The Effects of Alloying Elements in Titanium. Volume B: Physical and Chemical Properties, Deformation and Transformation Characteristics," DMIC Report 136B (May 1961).

H. R. Ogden and F C. Holden, "Metallography of Titanium Alloys," TML Report No. 103 (May 1958).

F. R. Brotzen, E. L. Harmon, and A. R. Troiano, "Decomposition of Beta Titanium," Trans. AIME, 203, pp. 413-419 (1955).

E. Ence and H. Margolin, "Re-examination of Ti-Fe and Ti-Fe-O Phase Relations," Trans. AIME, 206, pp. 576-579 (1956).

H. R. Ogden, D. J. Maykuth, W. L. Finlay and R. I. Jaffee, "Mechanical Properties of High Purity Ti-Al Alloys," Trans. AIME, 197, pp. 267-273 (1953).

W. L. Fink, K. R. VanHorn, and R. M. Budge, "Constitution of High Purity Aluminum Titanium Alloys," Trans. AIME, 98, pp. 421-436 (1931).

Max Hansen, D. J. McPherson, and W. Rostoker, "Constitution of Titanium Alloys Systems," WADC Technical Report 53-41 (February 1953).

C. S. Pearsall and P. K. Zingesser, "Metal to Non-metallic Brazing," MIT Research Lab of Electronics, Technical Report No. 104 (April 5, 1949).

H. L. Meredith, "Brazing and Soldering Titanium," Automotive Industries, p. 34 (August 15, 1953).

D. Canonico and H. Schwartzbart, "Titanium-Clad Steel by the Vacuum-Brazing Process," Welding Journal, p. 71 (February 1959).

"Brazing and Soldering of Titanium and its Alloys," Armour Research Foundation, Final Technical Report, Contract No. DA-11-022-ORD-288 (January 1953).

W. J. Lewis, P. S. Rieppel, and C. B. Voldrich, "Brazing Titanium to Titanium and to Mild and Stainless Steels," WADC Technical Report 52-313, Part I (1952) and Part II (1953).

L. A. Yerkovich, "Final Report on Titanium Brazing," Cornell Aeronautical Laboratory, Inc., Contract No. NOa(s)51-294-c (October 1952).

R. A. Long, "Development of New Nickel-Base Brazing Alloys Having Ductility," Welding Journal, pp. 259-264 (June 1961).

APPENDIX

ILLUSTRATIONS

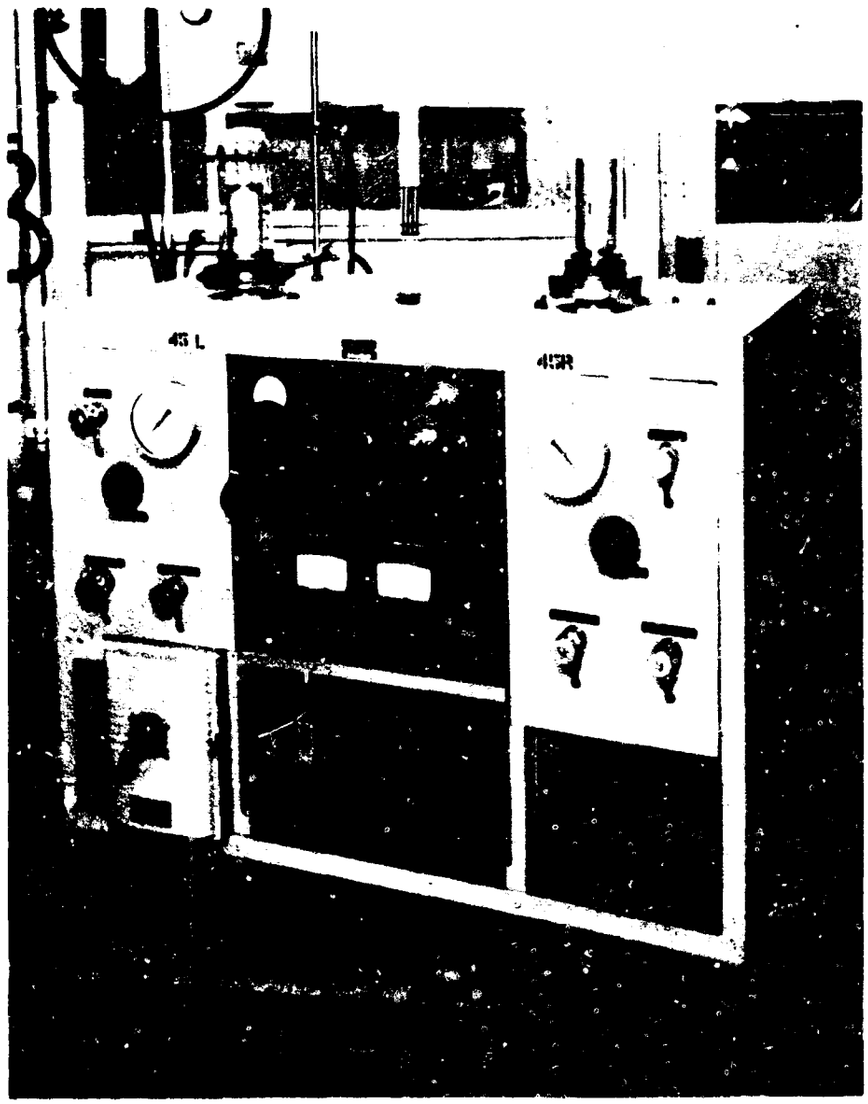

Figure 1 - Vacuum bell jar containing resistance-heated tantalum oven

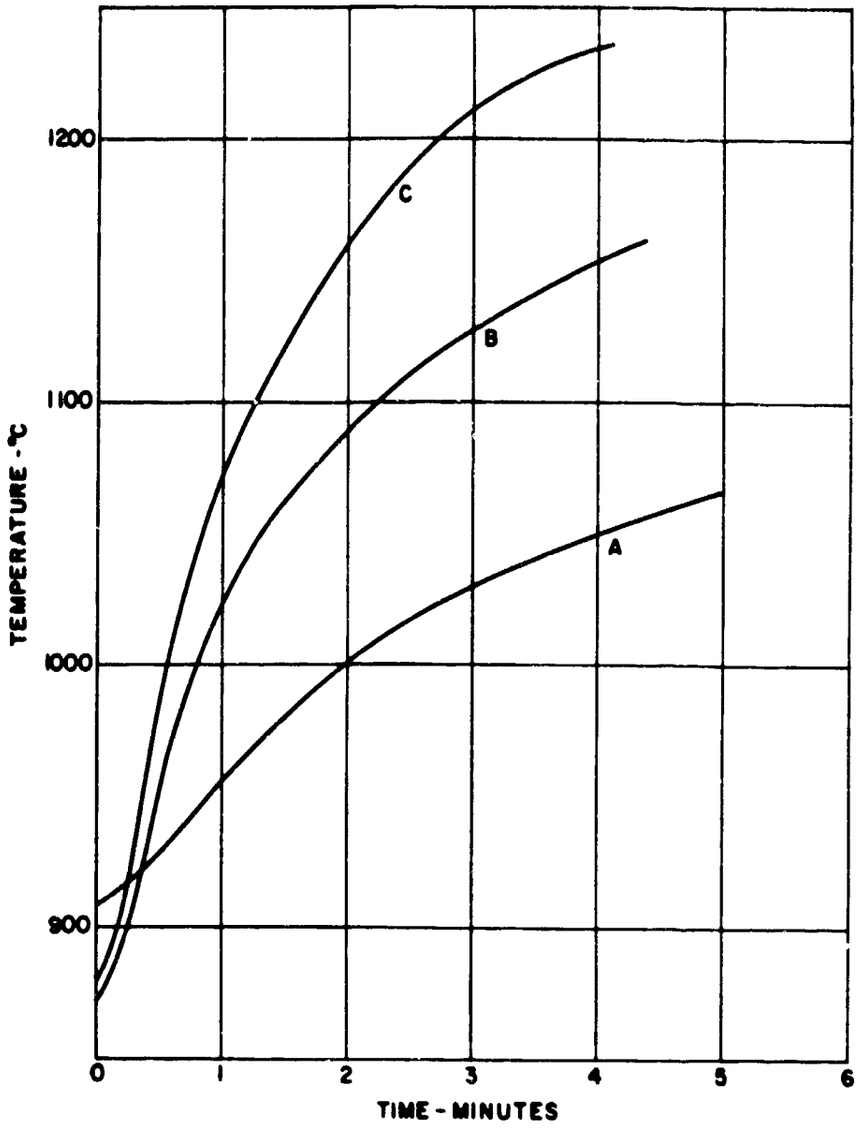

Figure 2 - Time-temperature heating schedules

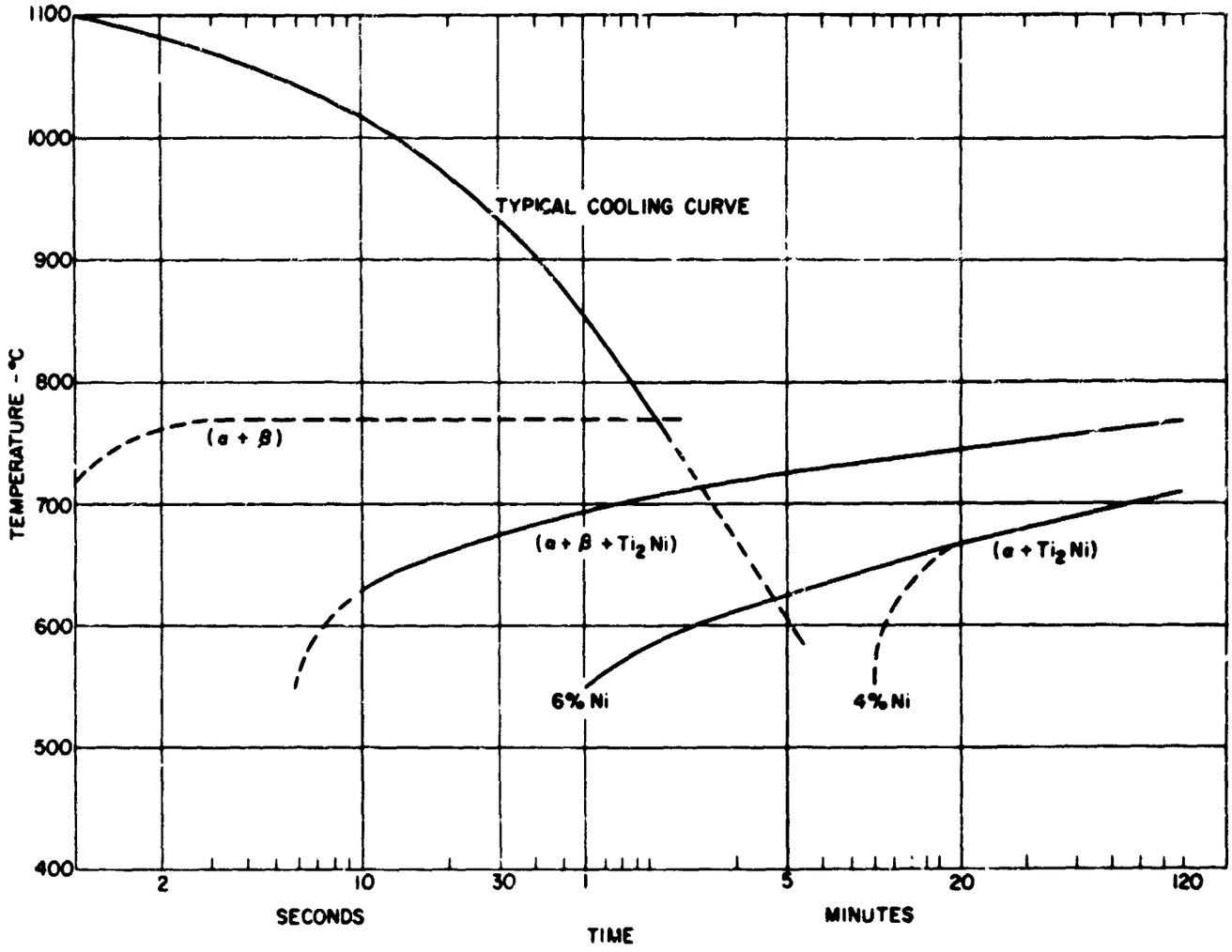

Figure 3 - TTT curve for a titanium-6 w/o nickel alloy

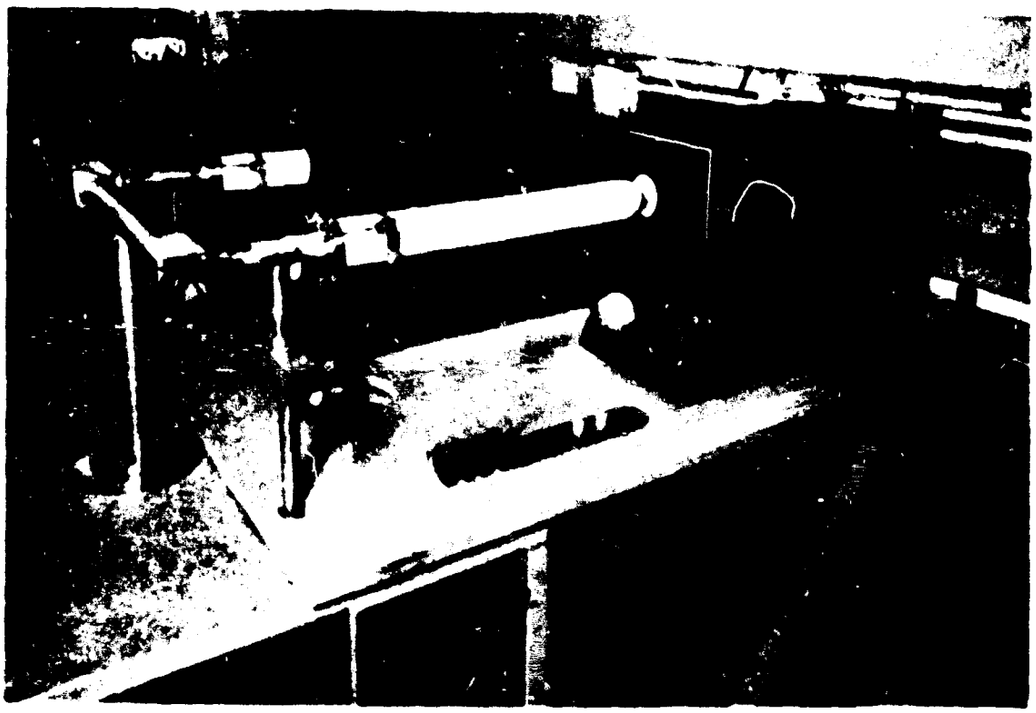

Figure 4 - High-temperature vacuum life test station

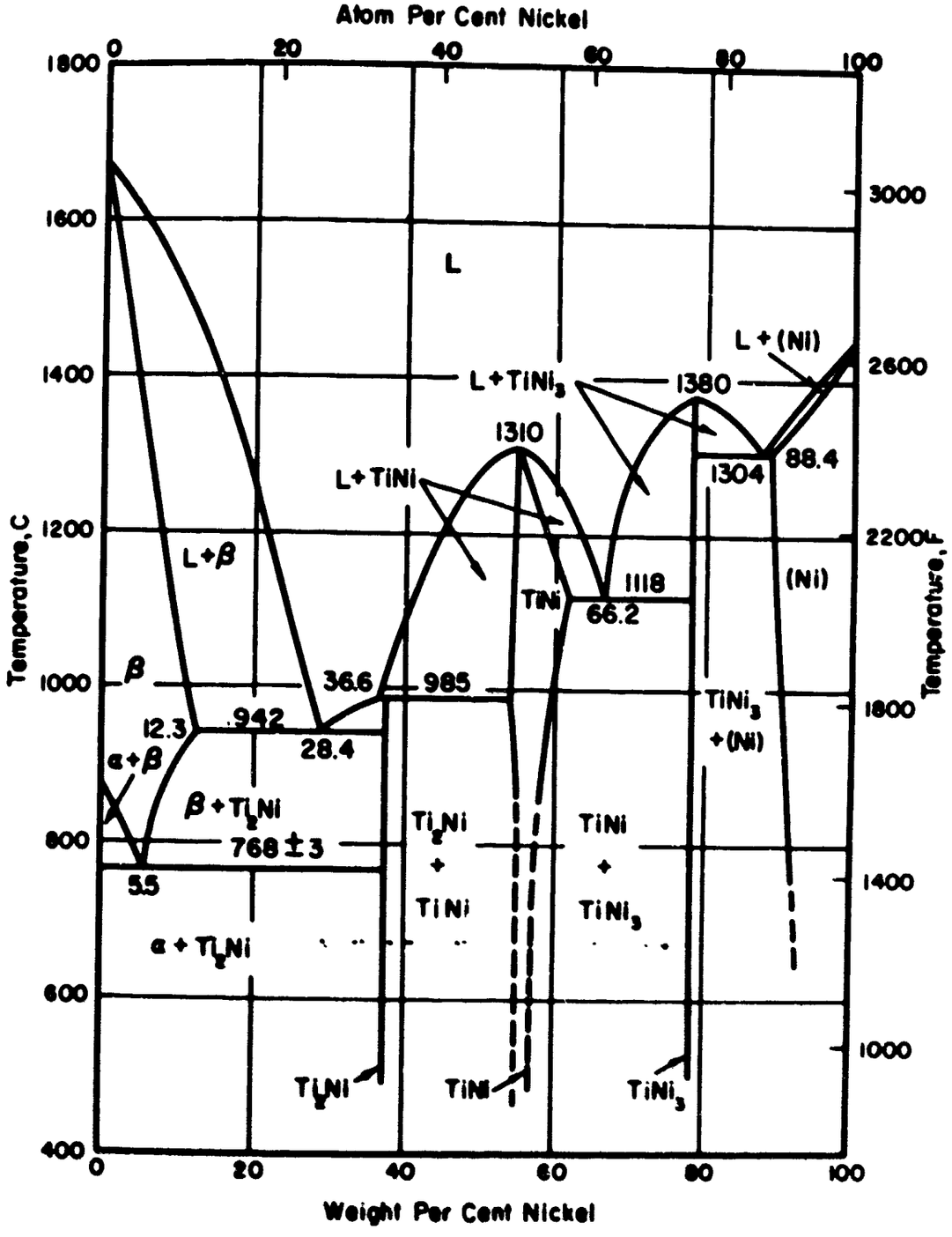

Figure 5 - Titanium-nickel phase diagram[11]

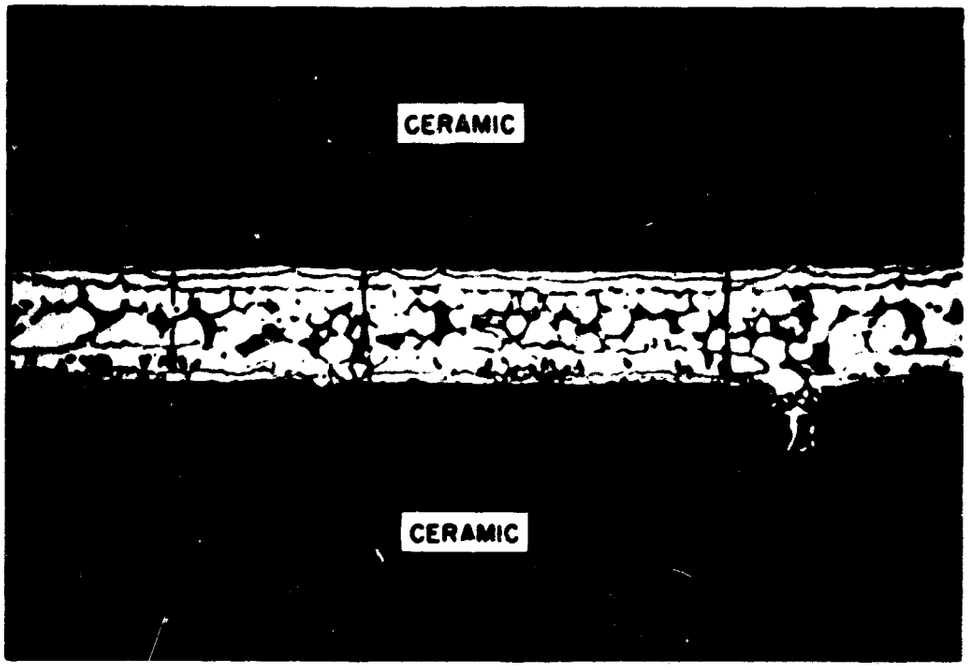

Figure 6 - Photomicrograph of ceramic-to-ceramic seal brazed with 71.8 w/o titanium, 28.2 w/o nickel alloy, 500 X

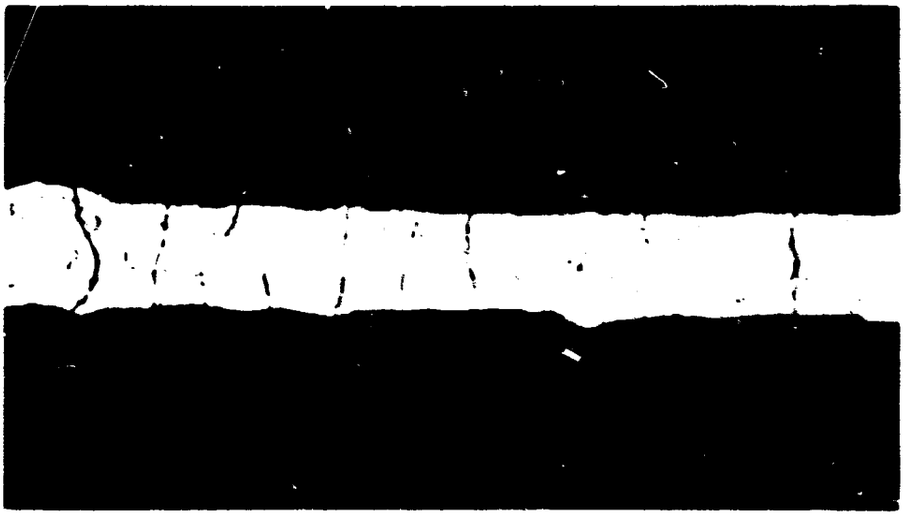

Figure 7 - Photomicrograph of effect of "overbrazing" on the seal shown in Figure 6, 500 X

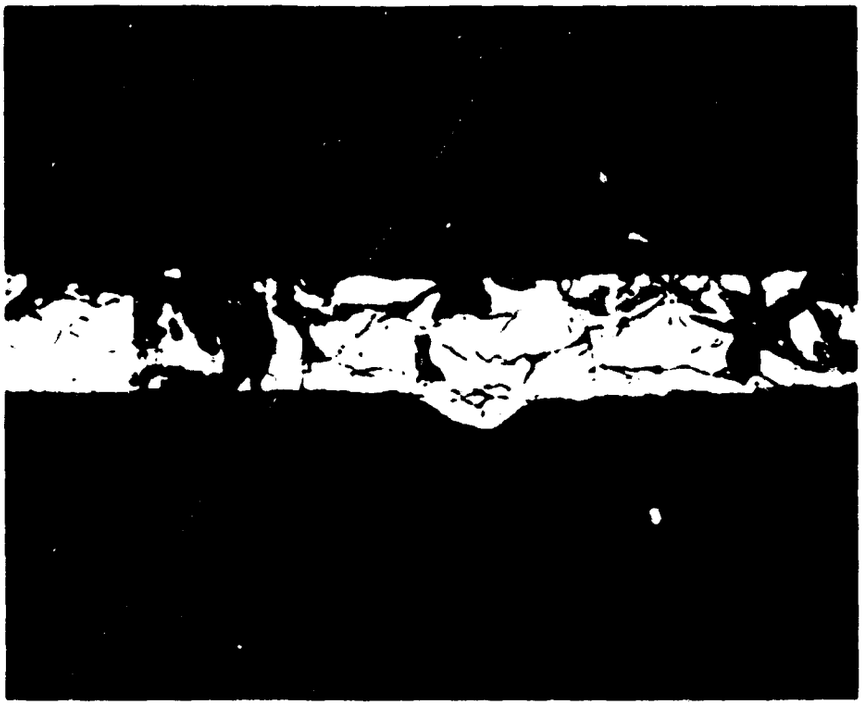

Figure 8 - Photomicrograph of effect of "overbrazing" on the seal shown in Figure 11, 500 X

Figure 9 - Photomicrograph of effect of "overbrazing" on the seal shown in Figure 12, 500 X

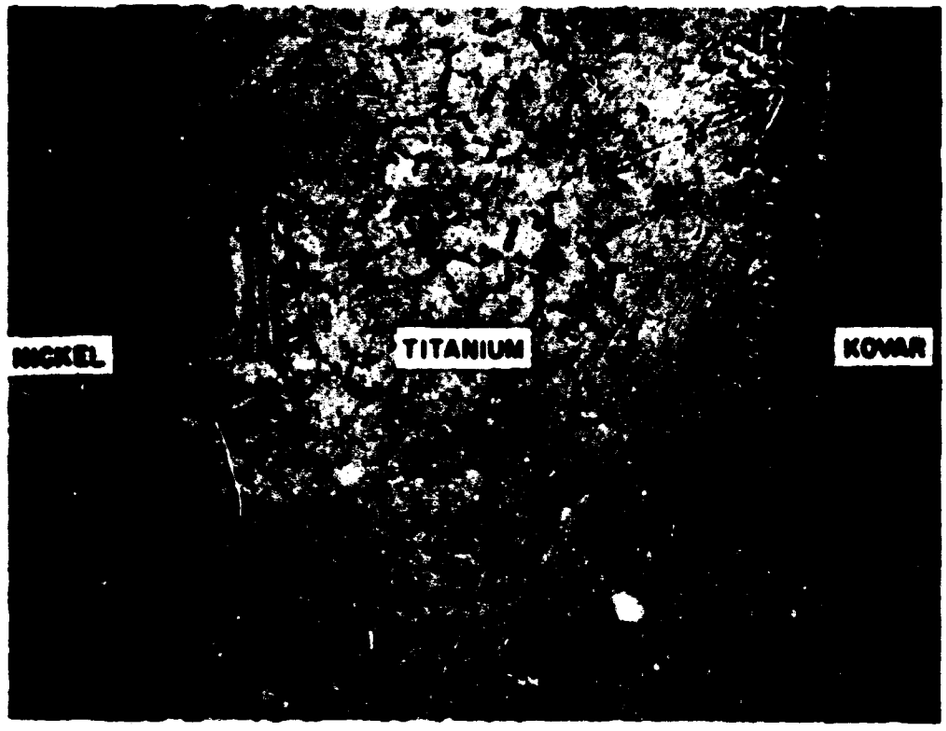

Figure 10 - Photomicrograph of titanium-nickel diffusion couple, 500 X

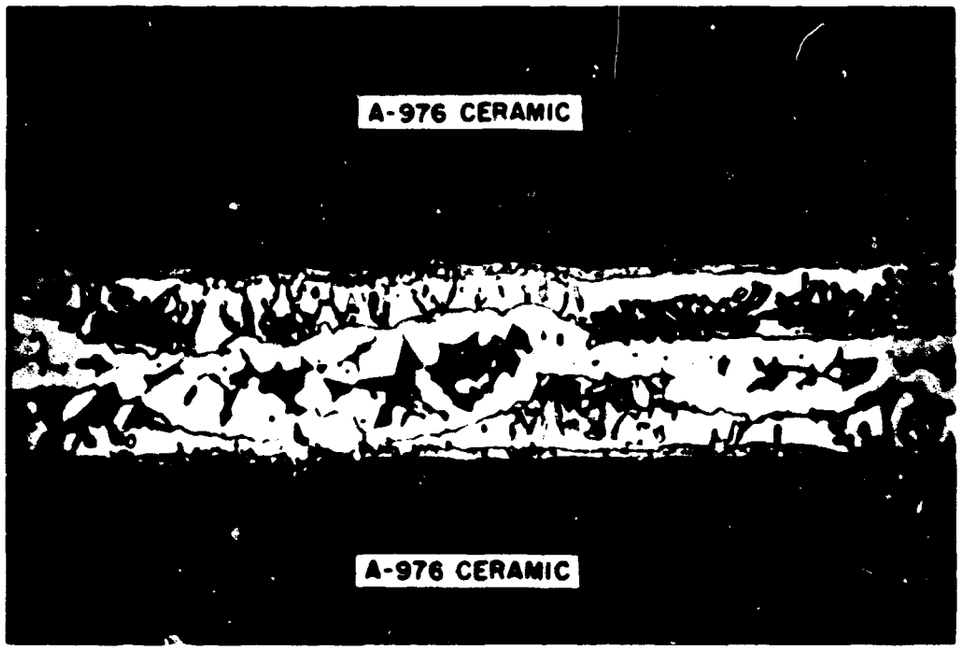

Figure 11 - Photomicrograph of ceramic-to-ceramic seal brazed with 76.8 w/o titanium, 23.2 w/o nickel alloy, 500 X

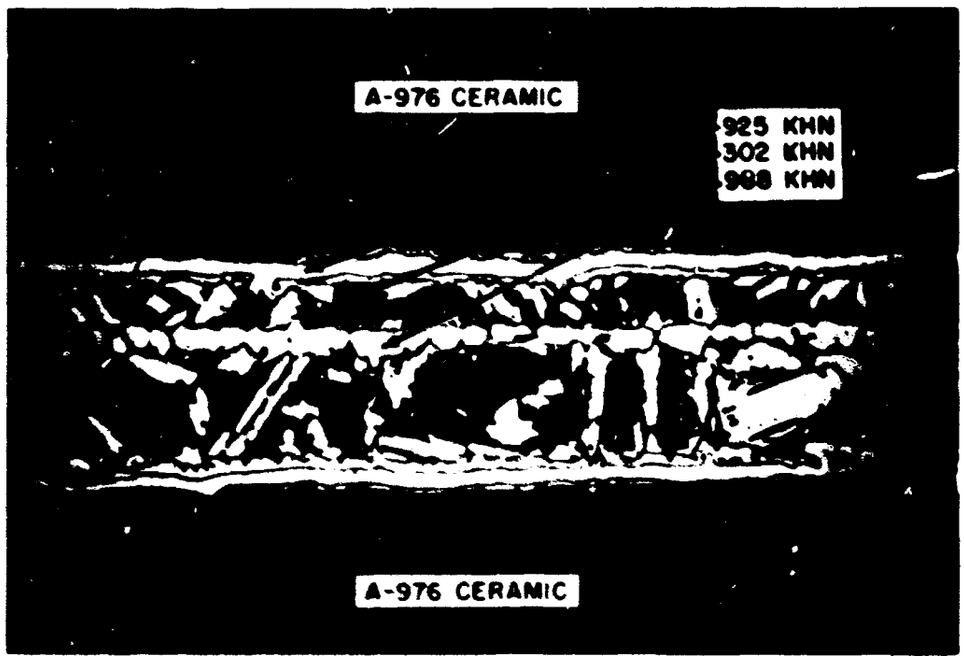

Figure 12 - Photomicrograph of ceramic-to-ceramic seal brazed with 83.2 w/o titanium, 16.8 w/o nickel alloy, 500 X

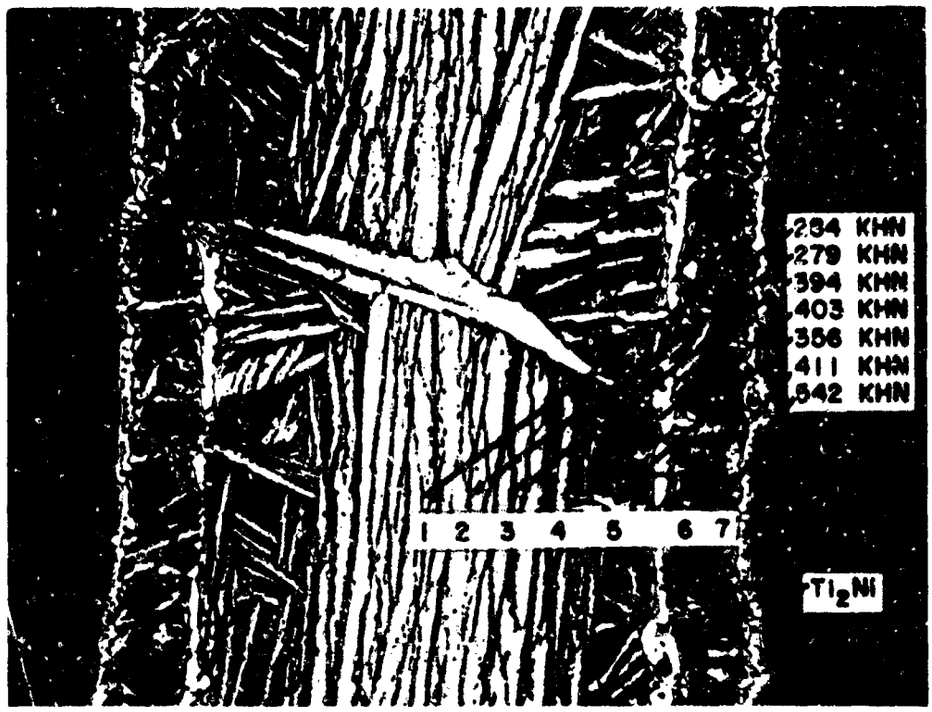

Figure 13 - Photomicrograph of ceramic-to-titanium seal, 500 X

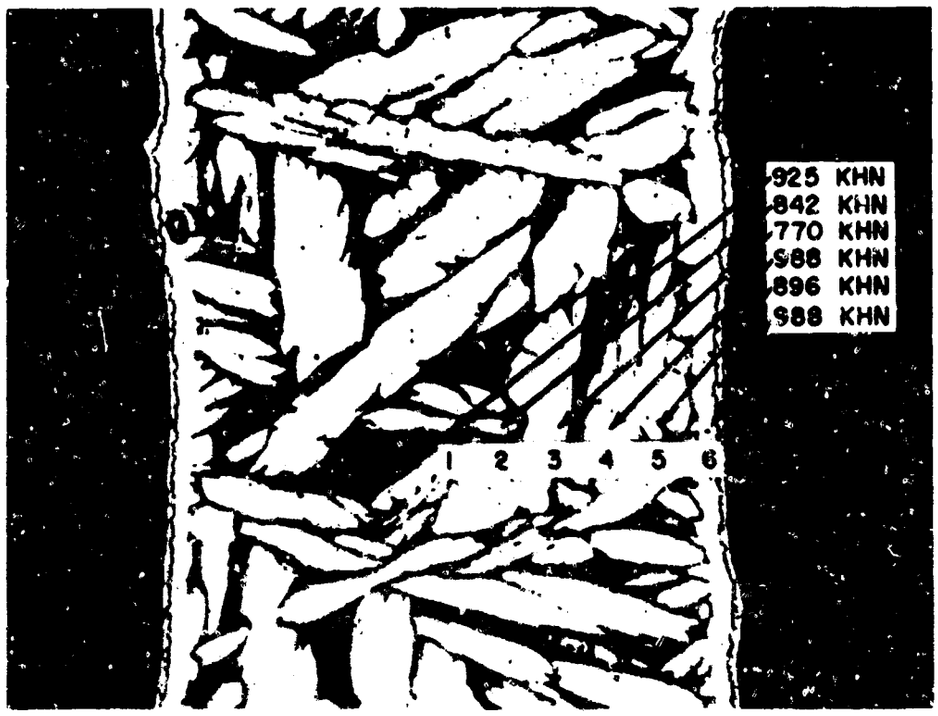

Figure 14 - Photomicrograph of effect of prolonged heating at sealing temperature on the seal shown in Figure 13, 500 X

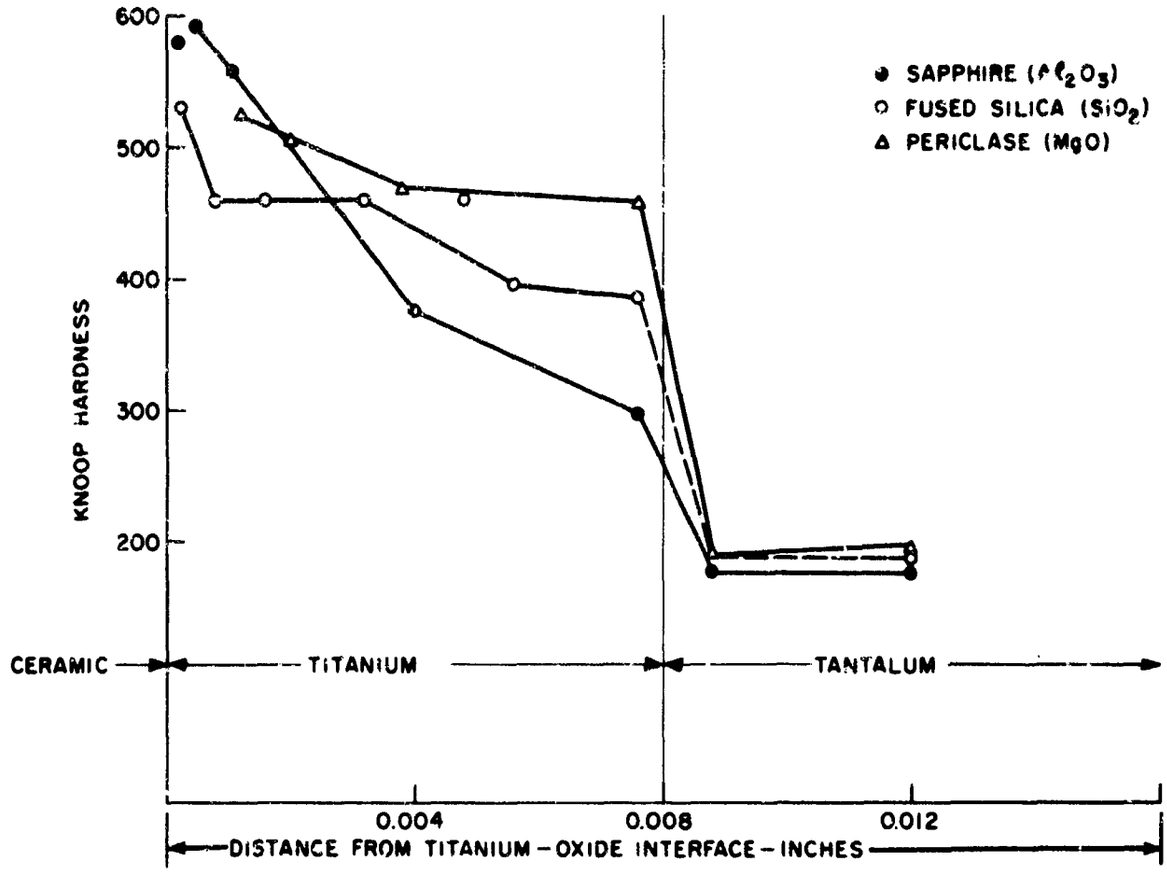

Figure 15 - Knoop hardness transverses across selected titanium-metal oxide seals

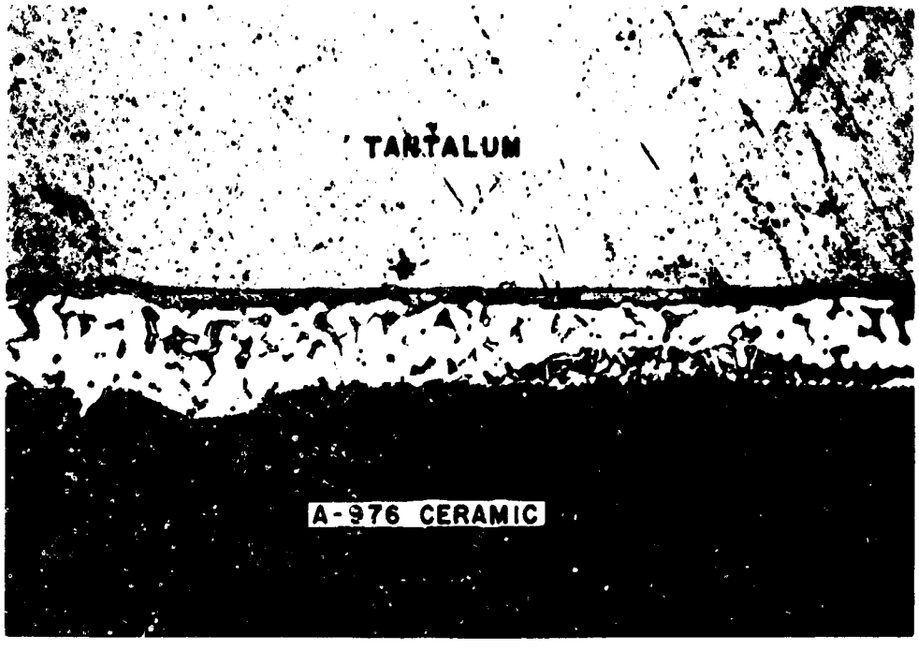

Figure 16 - Photomicrograph of ceramic-to-tantalum seal, 500 X

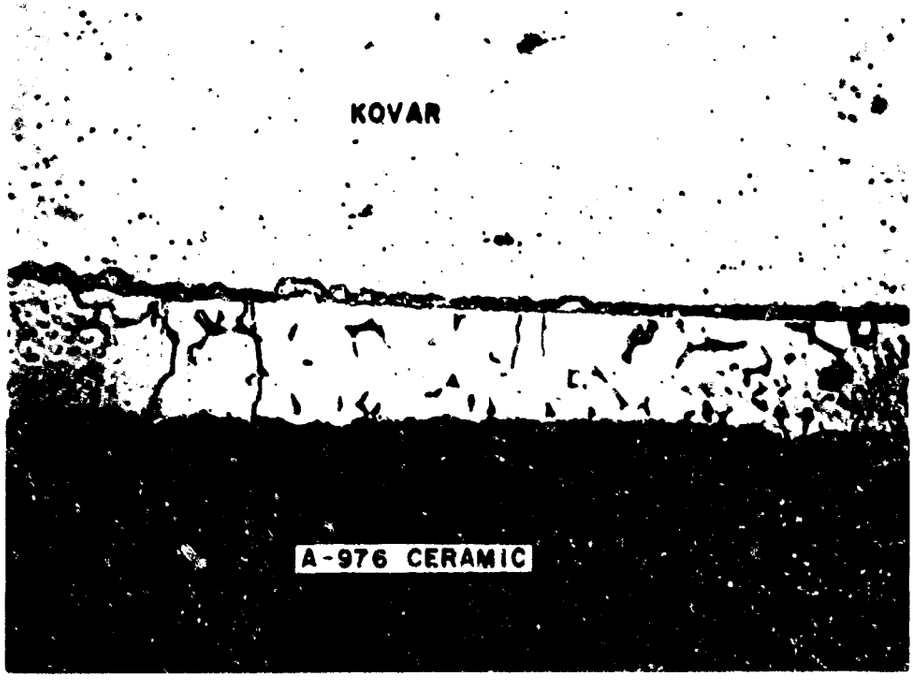

Figure 17 - Photomicrograph of ceramic-to-Kovar seal, 500 X

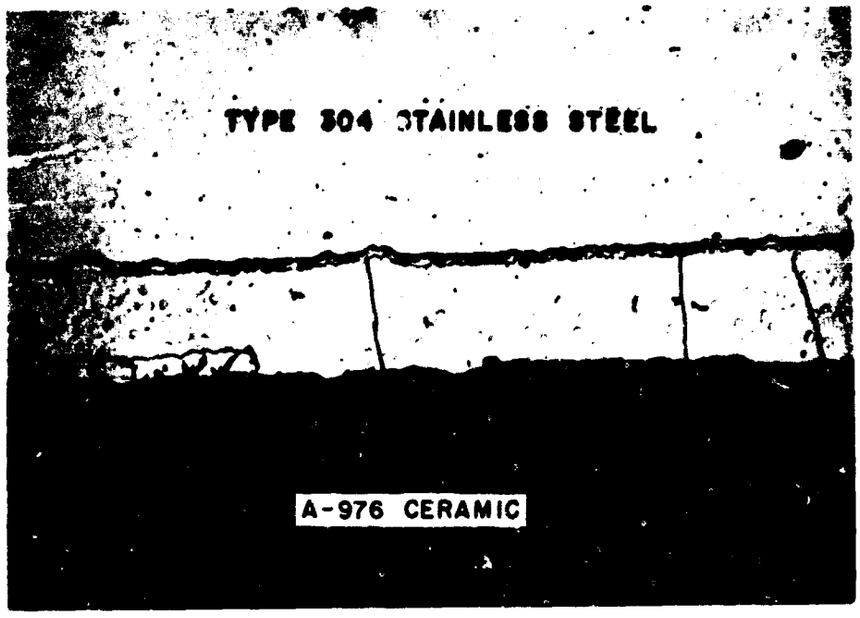

Figure 18 - Photomicrograph of ceramic-to-Type 304 stainless-steel seal, 500 X

Figure 19 - Photomicrograph of ceramic-to-Type 430 stainless-steel seal, 500 X

Figure 20 - Photomicrograph of ceramic-to-tantalum seal using titanium "buffer" washers, 500 X

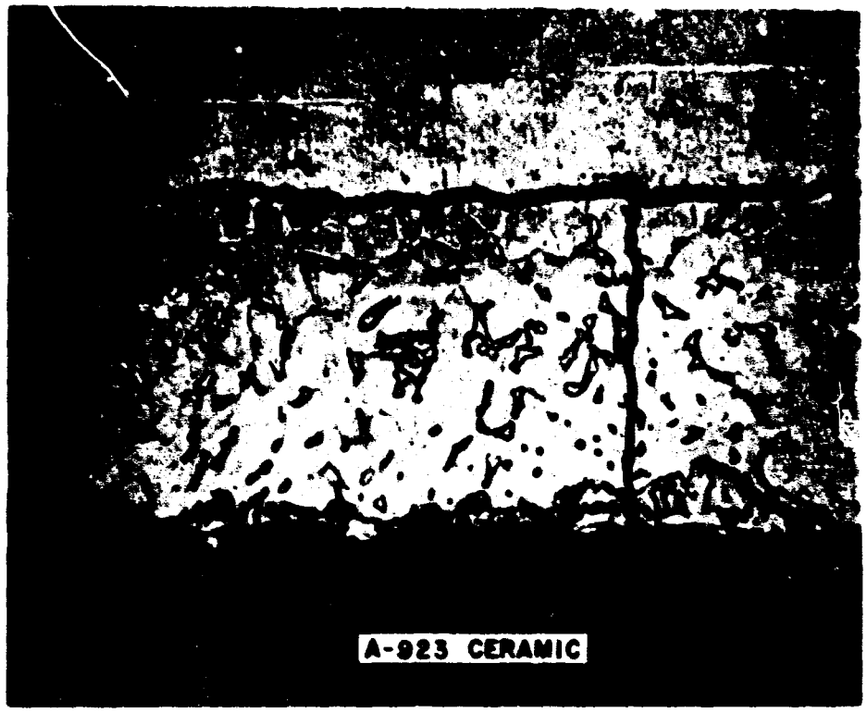

Figure 21 - Photomicrograph of ceramic-to-Kovar seal using titanium "buffer" washers, 500 X

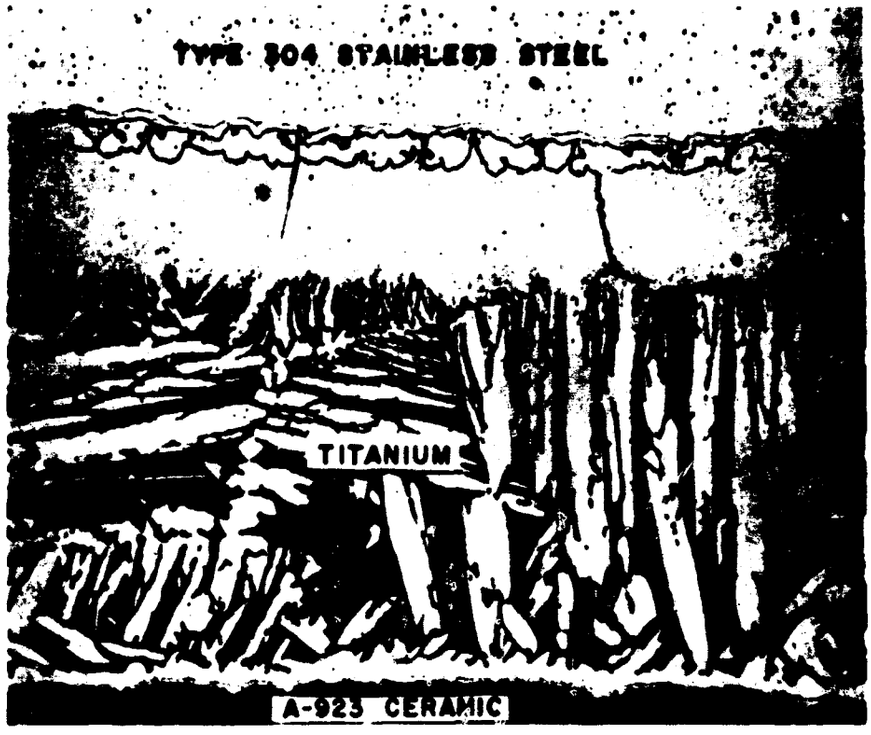

Figure 22 - Photomicrograph of ceramic-to-Type 304 stainless-steel seal using titanium "buffer" washers, 500 X

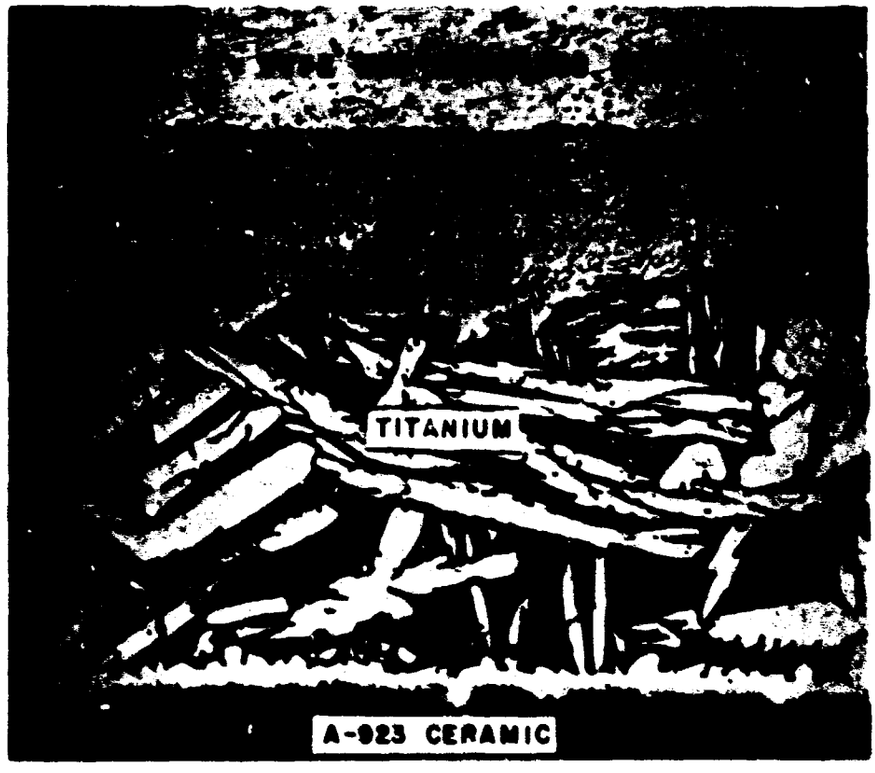

Figure 23 - Photomicrograph of ceramic-to-Type 430 stainless-steel seal using titanium "buffer" washers, 500 X

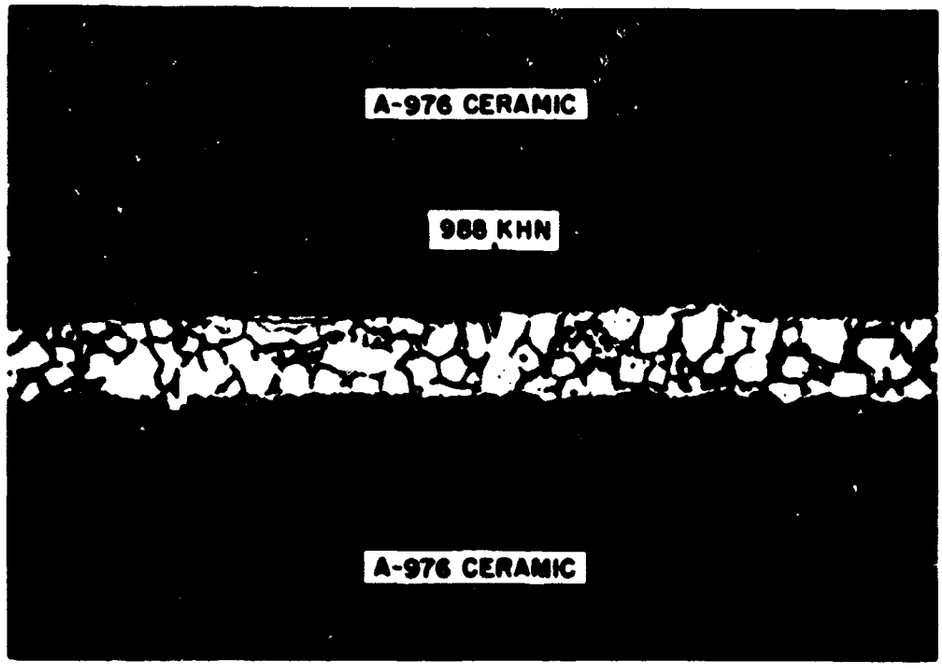

Figure 24 - Photomicrograph of ceramic-to-ceramic seal brazed with 65.8 w/o titanium, 34.2 w/o nickel alloy, 500 X

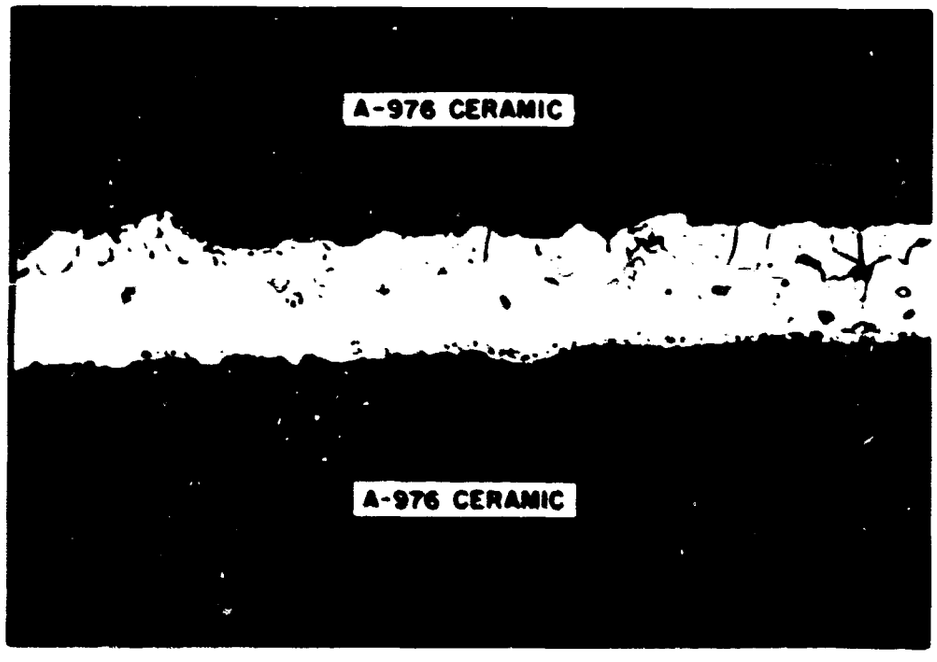

Figure 25 - Photomicrograph of ceramic-to-ceramic seal brazed with 49.0 w/o titanium, 51.0 w/o nickel alloy, 500 X

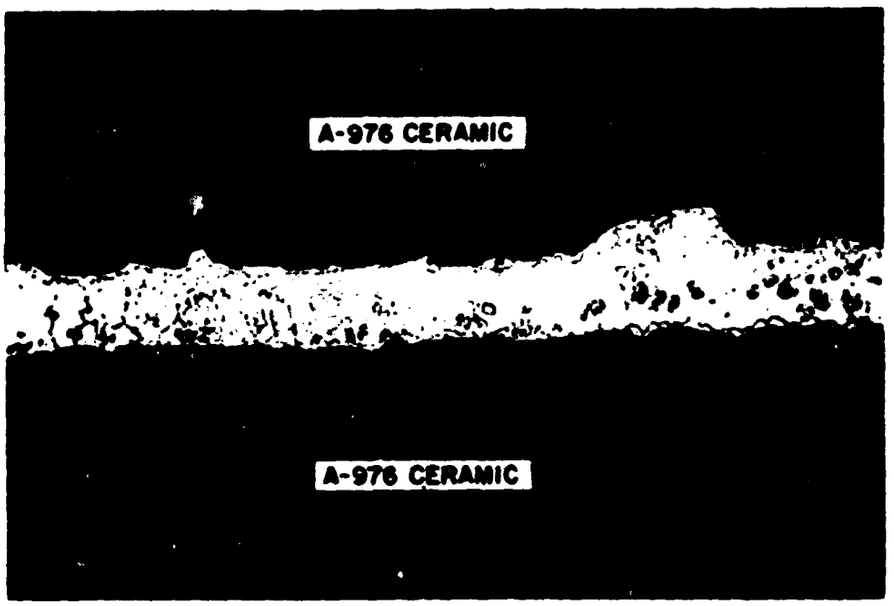

Figure 26 - Photomicrograph of ceramic-to-ceramic seal brazed with 39.1 w/o titanium, 60.9 w/o nickel alloy, 500 X

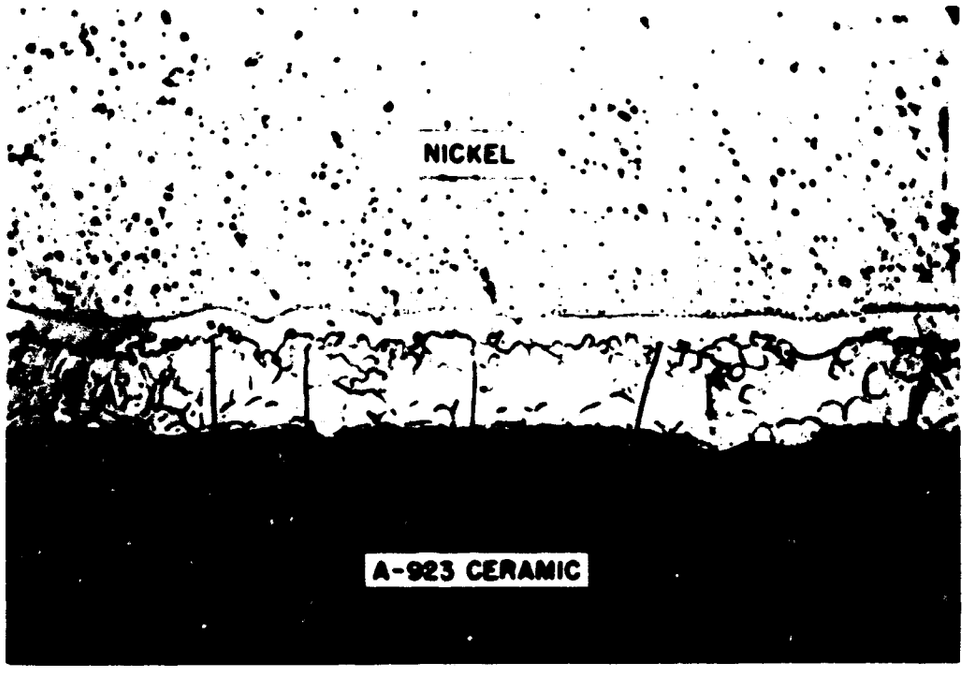

Figure 27 - Photomicrograph of ceramic-to-nickel seal made at a low sealing temperature, 500 X

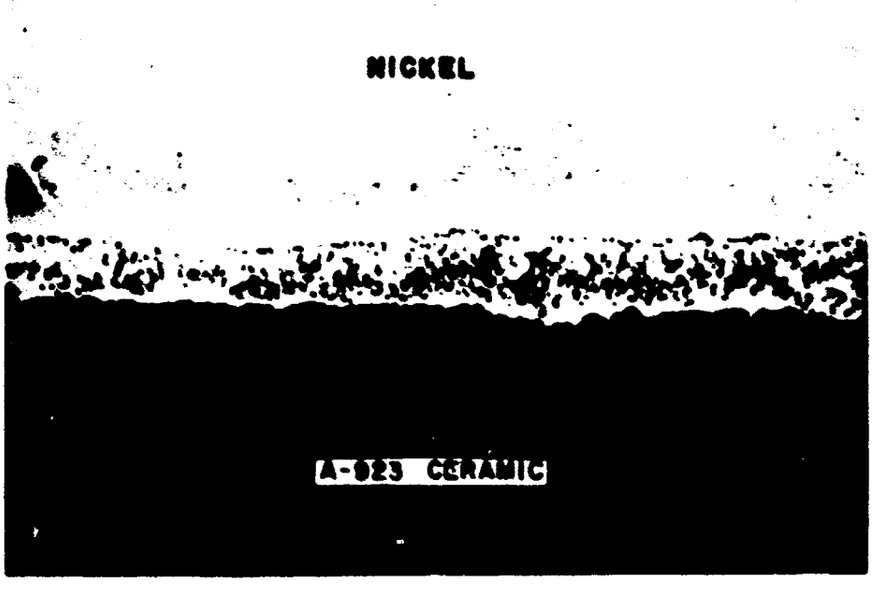

Figure 28 - Photomicrograph of ceramic-to-nickel seal made at a temperature of approximately 1280°C, 500 X

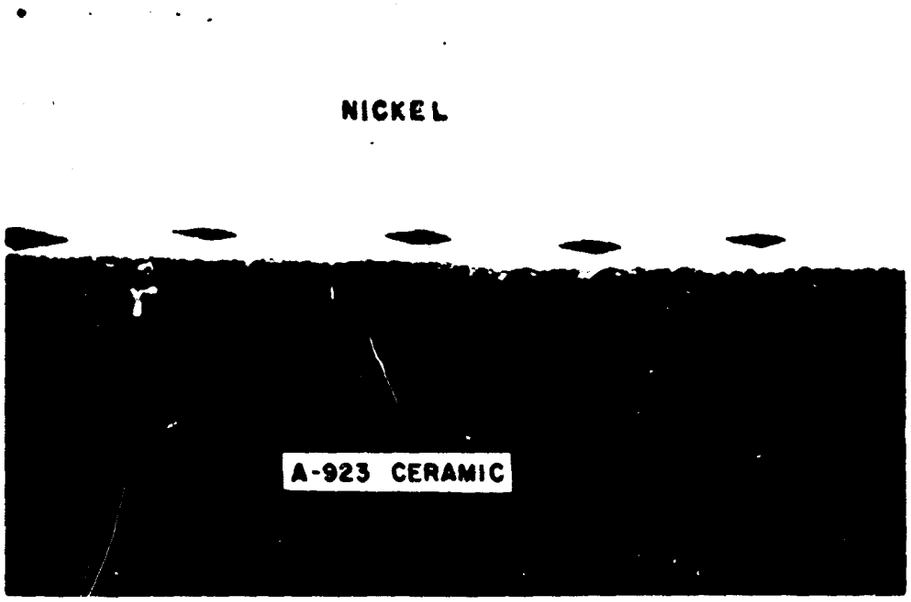

Figure 29 - Photomicrograph of ceramic-to-nickel seal made at a temperature of 1315°C, 500 X

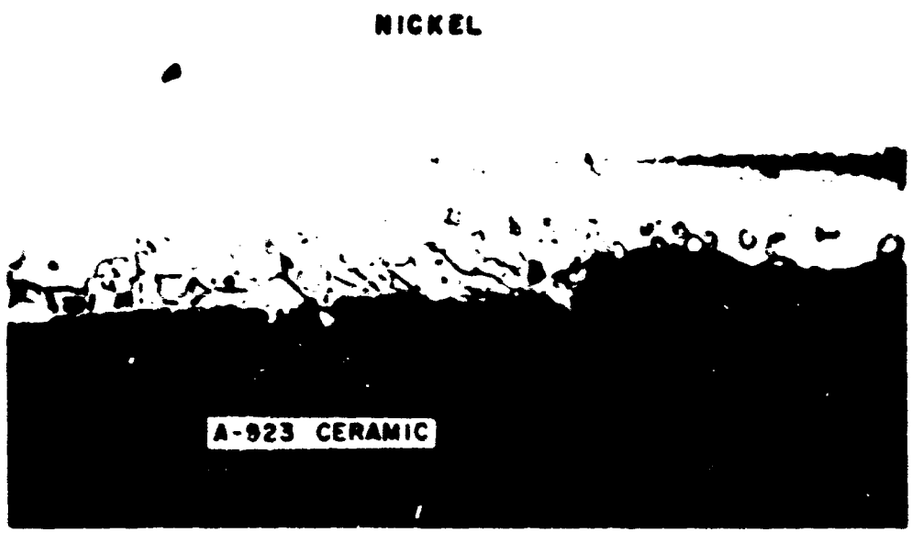

Figure 30 - Photomicrograph of ceramic-to-nickel seal heated for four minutes at a temperature of 1090°C showing crack through $TiNi_3$ zone, 500 X

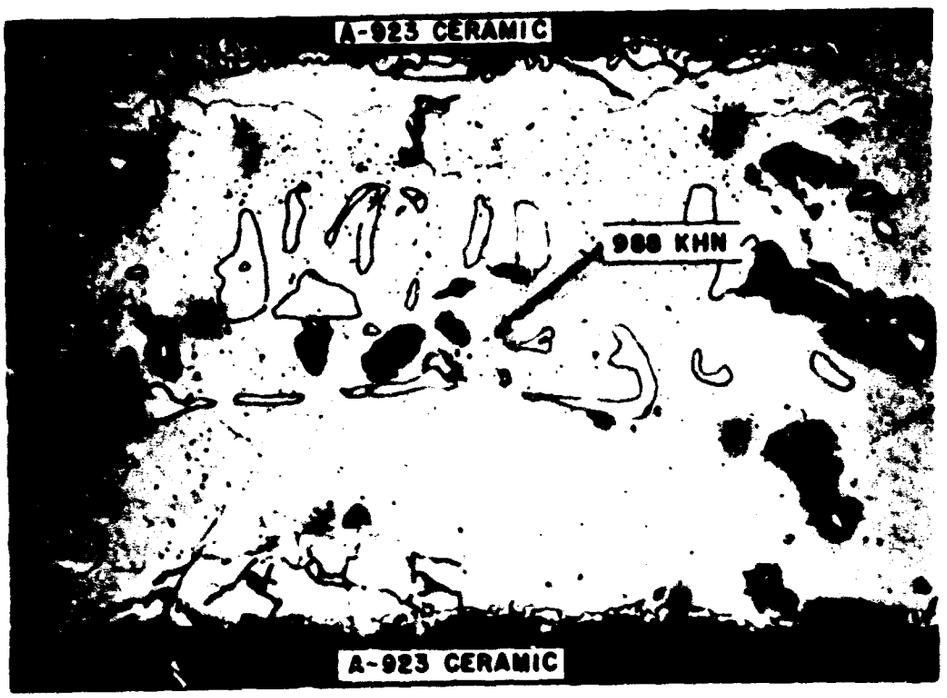

Figure 31 - Photomicrograph of wrapped ceramic-to-titanium seal after 240 hours at a temperature of 900°C, 500 X

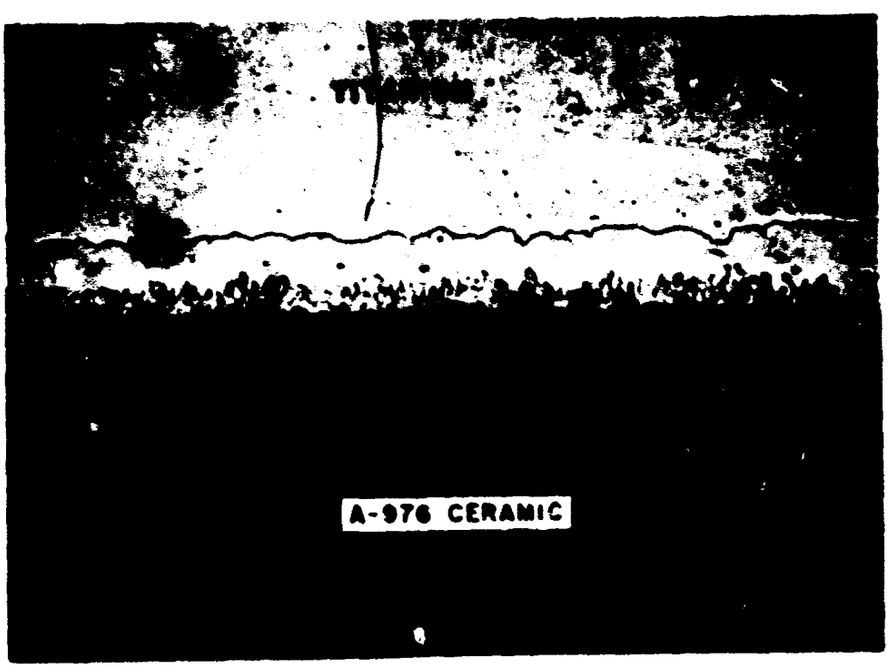

Figure 32 - Photomicrograph of ceramic-titanium "reaction" specimen after 240 hours at a temperature of 900°C, 500 X

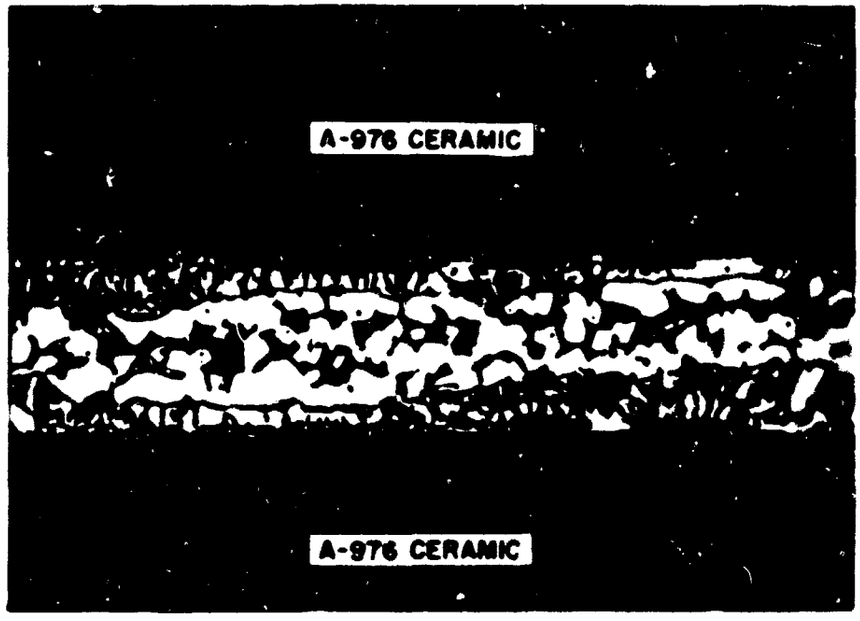

Figure 33 - Photomicrograph of ceramic-to-ceramic seal brazed with 76.8 w/o titanium, 23.2 w/o nickel alloy, 500 X

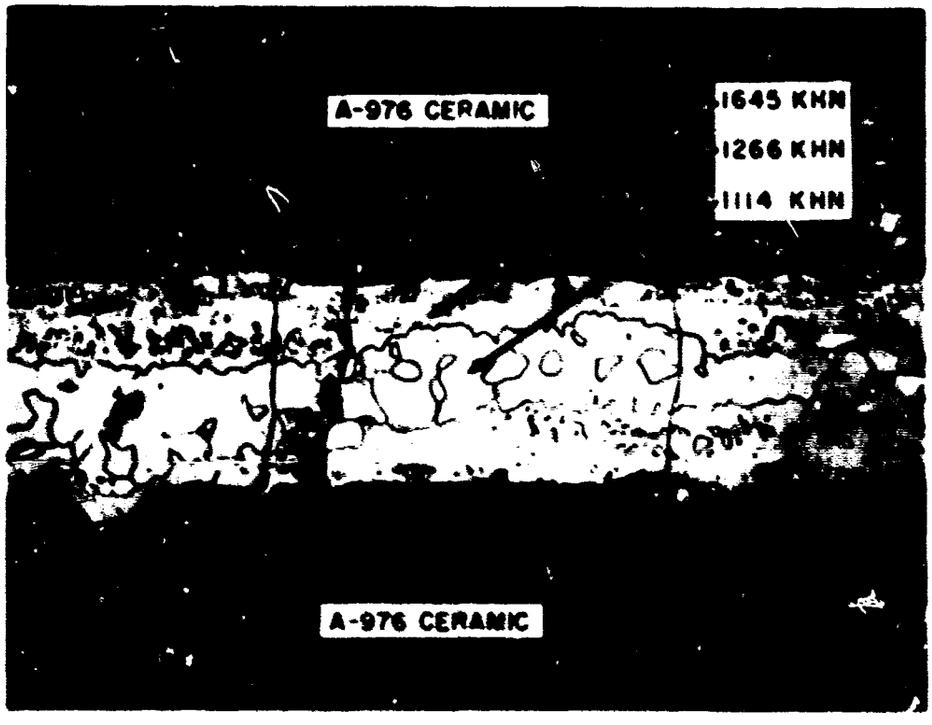

Figure 34 - Photomicrograph of seal shown in Figure 33 after 240 hours at a temperature of 900°C, 500 X

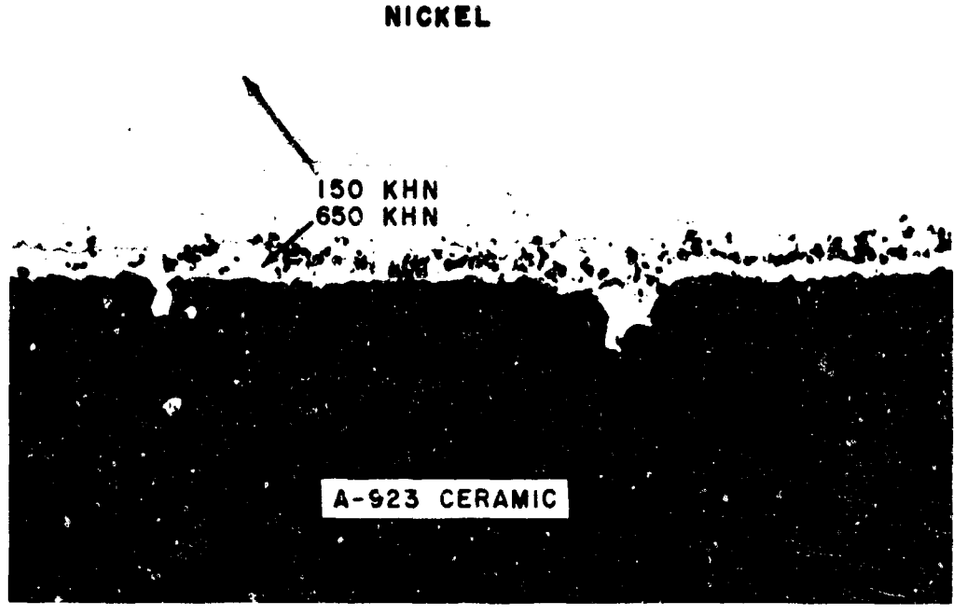

Figure 35 - Photomicrograph of ceramic-to-nickel seal after 480 hours at a temperature of 900°C, 750 X

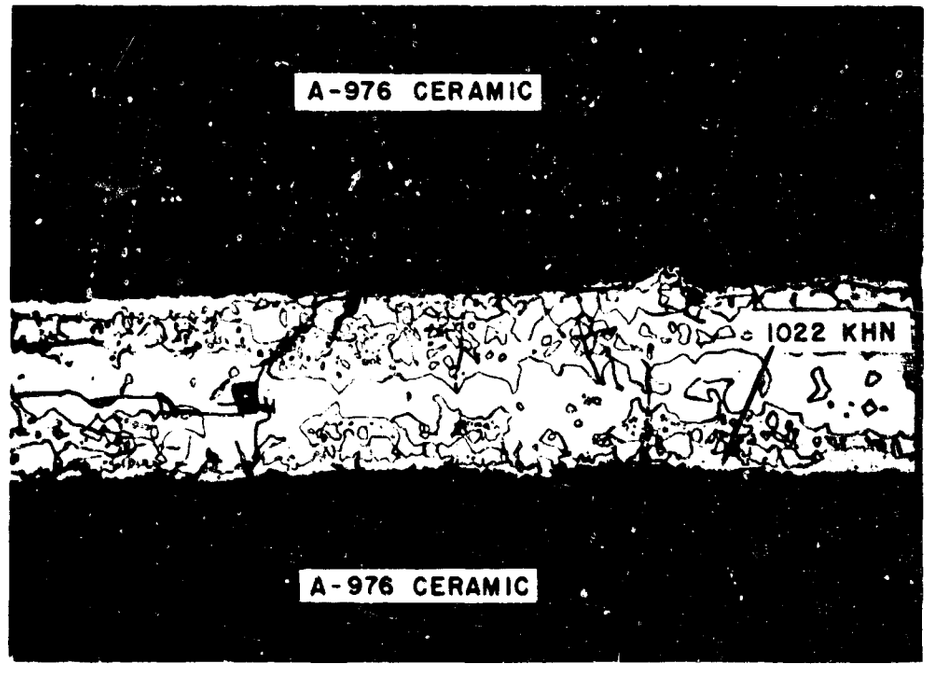

Figure 36 - Photomicrograph of seal shown in Figure 33 after 1680 hours at a temperature of 700°C, 500 X

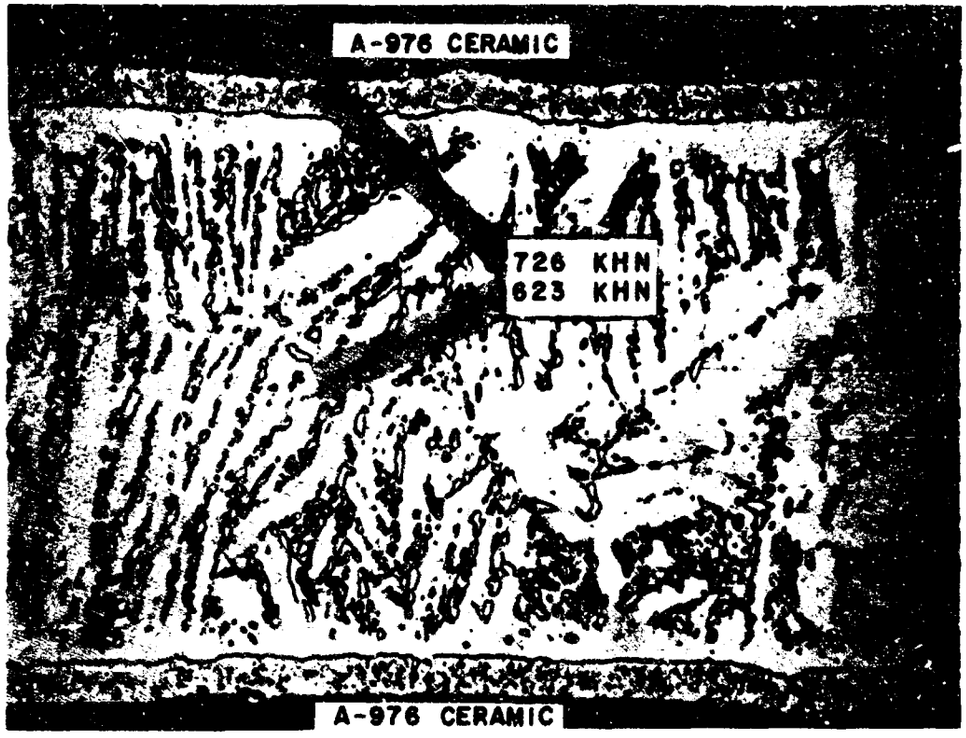

Figure 37 - Photomicrograph of ceramic-to-titanium seal after 1920 hours at a temperature of 700°C, 500 X

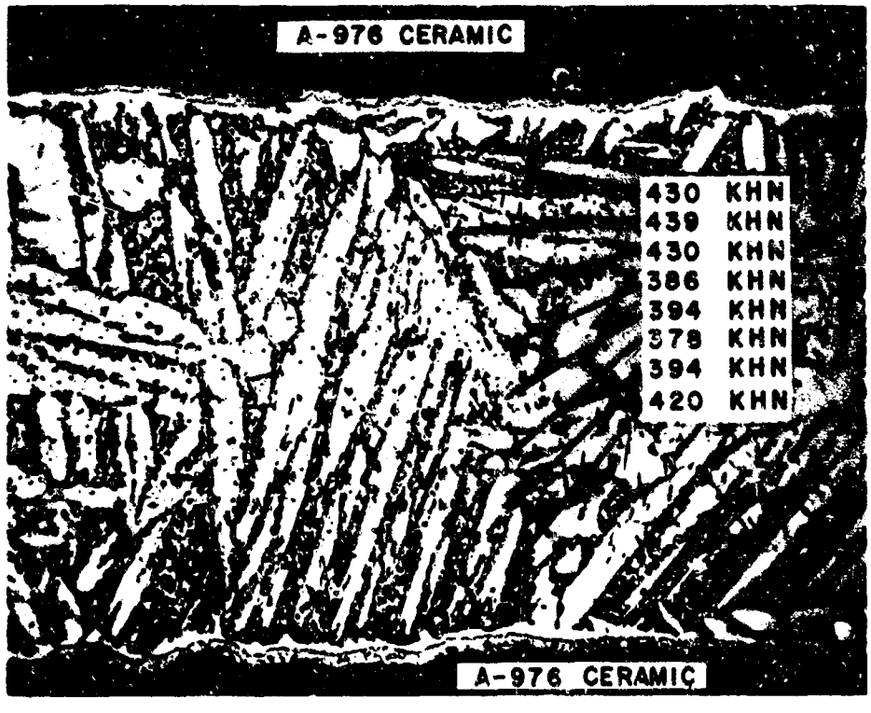

Figure 38 - Photomicrograph of wrapped ceramic-to-titanium seal (A-976 ceramic) after 720 hours at a temperature of 700°C, 500 X

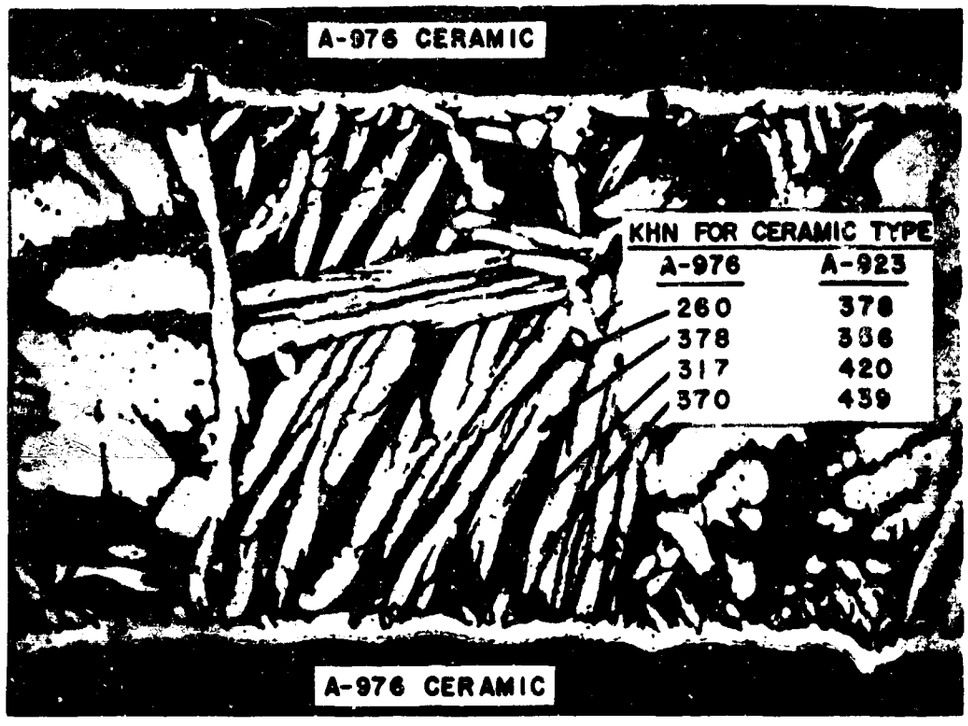

Figure 39 - Photomicrograph of seal shown in Figure 38 before life testing

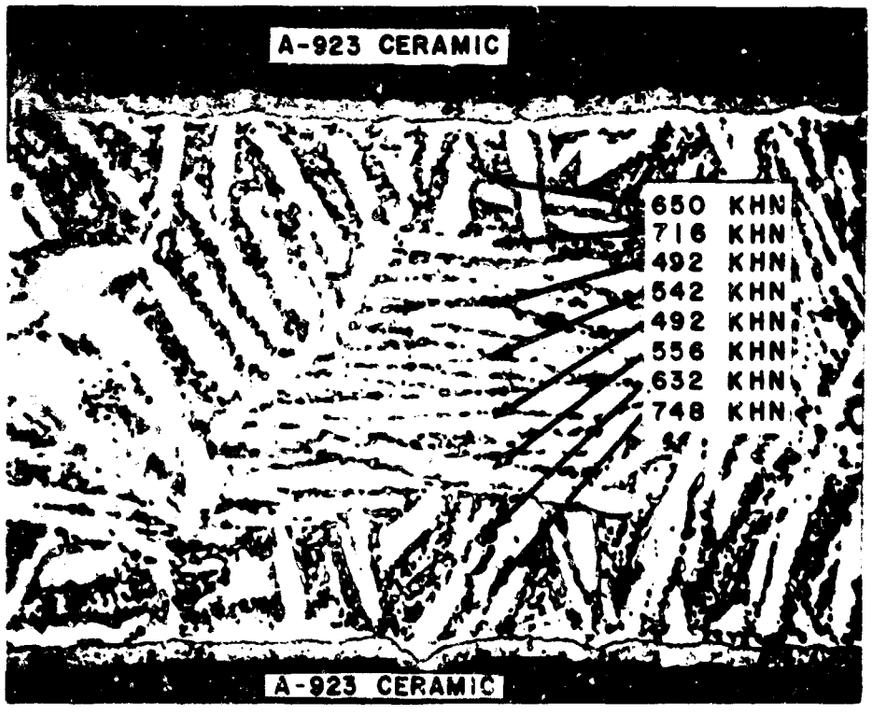

Figure 40 - Photomicrograph of wrapped ceramic-to-titanium seal (A-923 ceramic) after 720 hours at a temperature of 700°C, 500 X

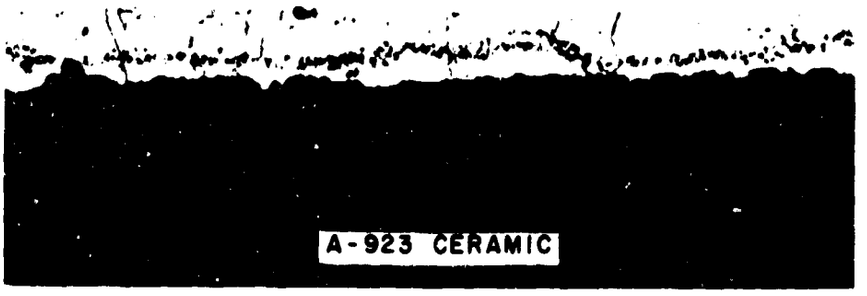

Figure 41 - Photomicrograph of ceramic-to-nickel seal after 1200 hours at a temperature of 700°C, 500 X

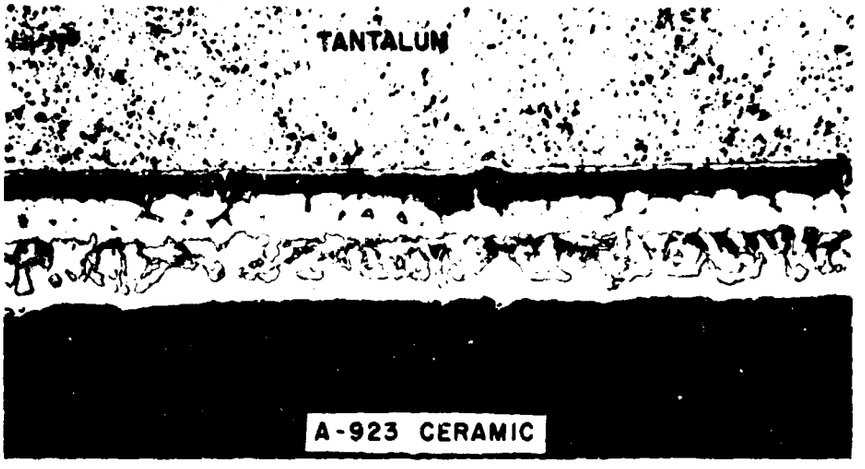

Figure 42 - Photomicrograph of ceramic-to-tantalum seal before life testing, 500 X

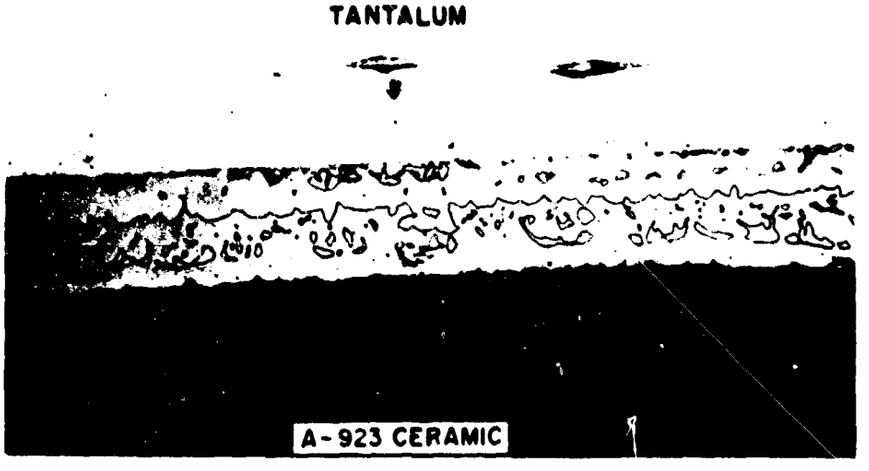

Figure 43 - Photomicrograph of seal shown in Figure 42 after 2350 hours at a temperature of 700°C, 500 X

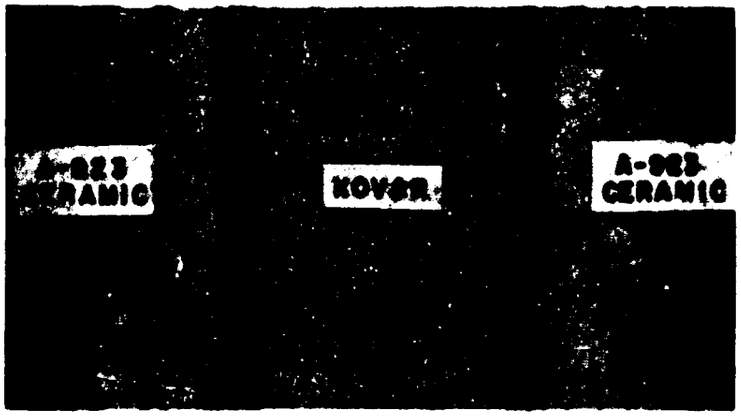

Figure 44 - Photomicrograph of seal shown in Figure 21 after 1200 hours at a temperature of 700°C, 250 X

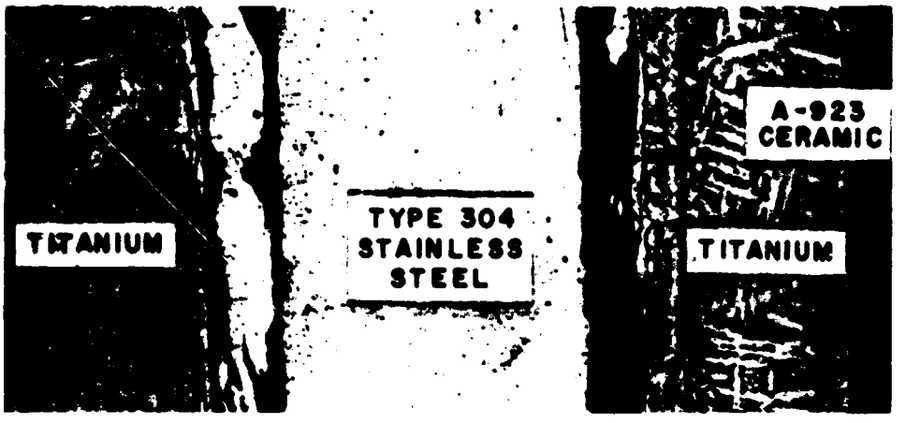

Figure 45 - Photomicrograph of seal shown in Figure 22 after 1200 hours at a temperature of 700°C, 250 X

Figure 46 - Photomicrograph of seal shown in Figure 23 after 1200 hours at a temperature of 700°C, 250 X

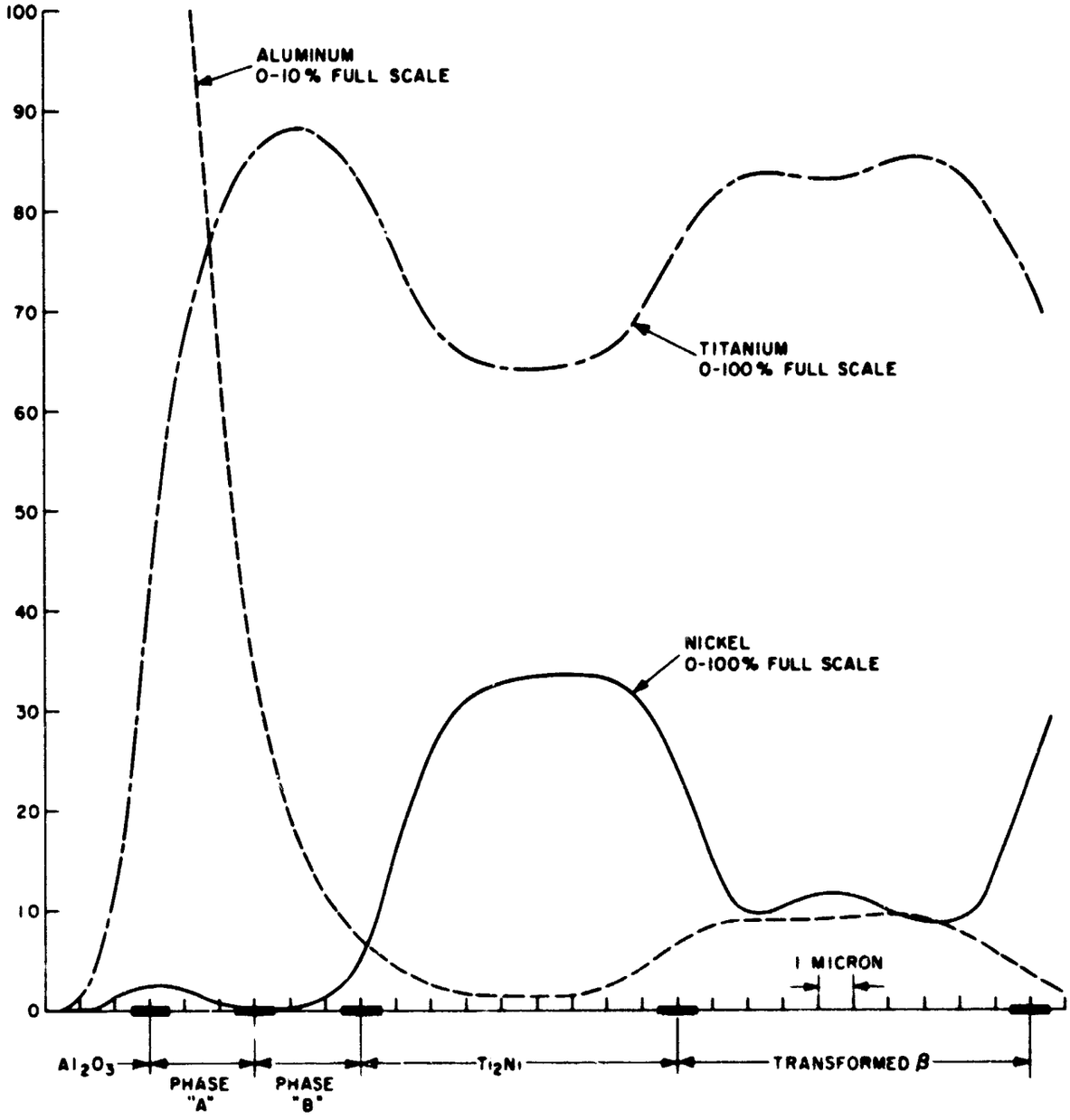

Figure 47 - Microprobe traverse across the brazing alloy of the seal shown in Figure 6

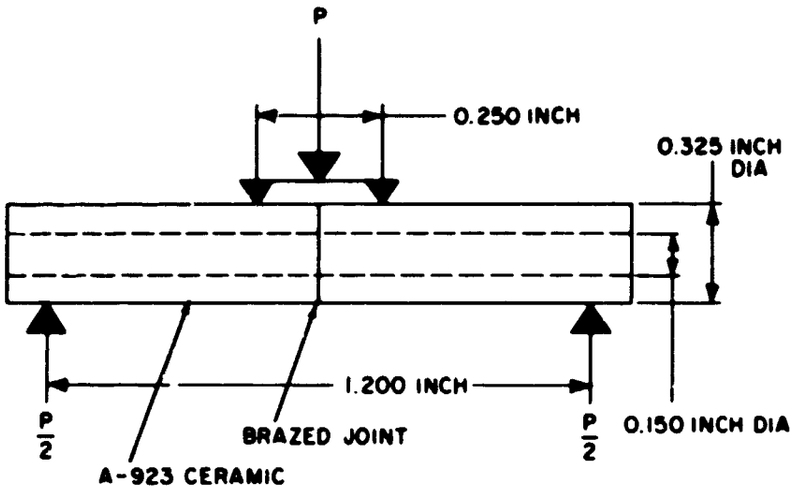

Figure 48 - Flexural strength test specimen

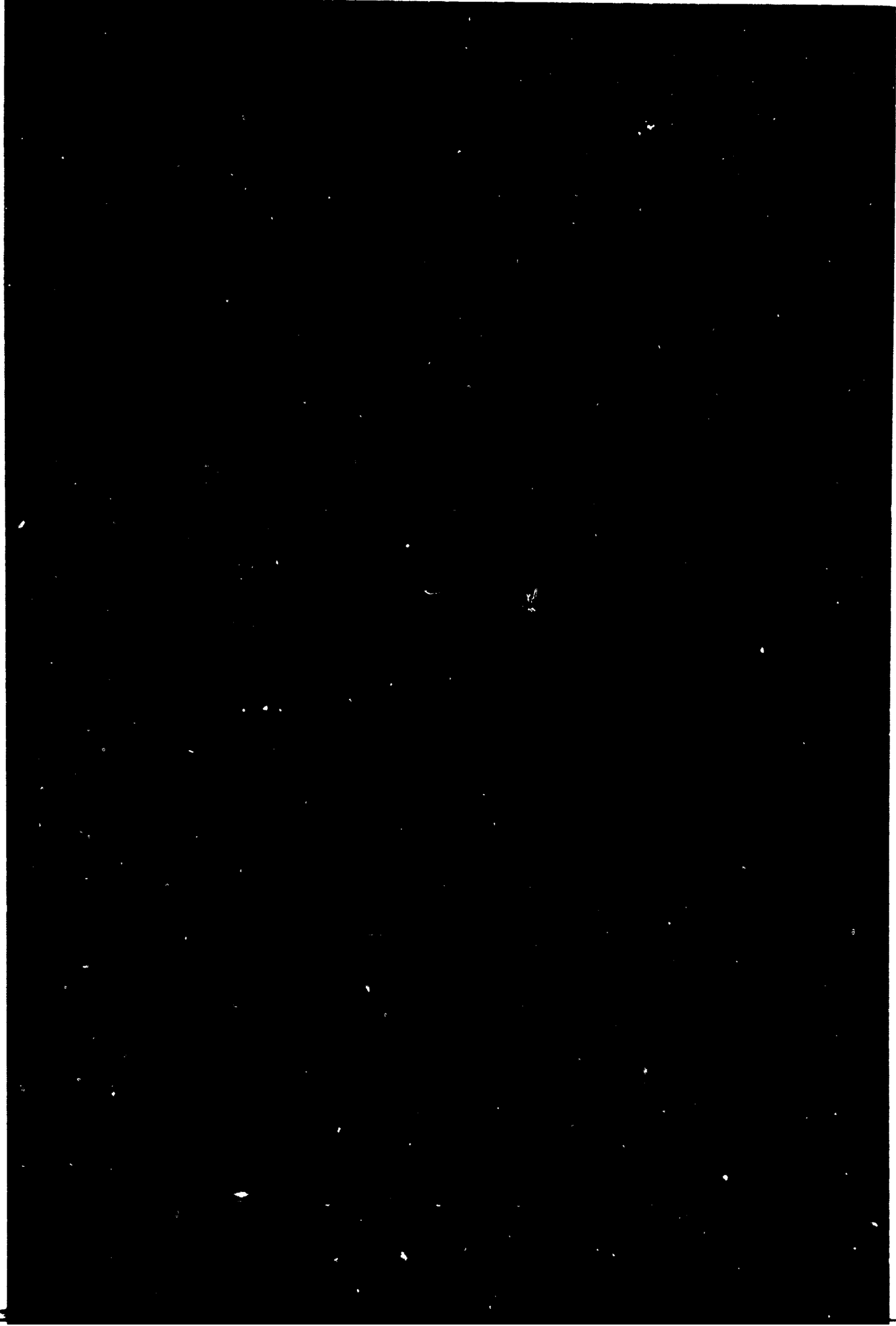

SECTION III

Experimental Studies of the Emission and Discharge Characteristics of the Ta-Cs System

by

M. D. Gibbons
Power Tube Department
General Electric Company

TABLE OF CONTENTS

LIST OF ILLUSTRATIONS

EXPERIMENTAL STUDIES OF THE EMISSION AND DISCHARGE CHARACTERISTICS OF THE Ta-Cs SYSTEM

by
M. D. Gibbons

INTRODUCTION

The performance of the cesium thermionic converter depends critically on the work functions of the electrodes and the mode of current transfer between the electrodes. These two considerations are dependent. The work functions establish the boundary potentials of the converter gap, and control the current capabilities of the emitter. The electron current transfer is governed by the production of ions. Ions are produced by surface ionization and by the low voltage, hot cathode discharge. The former is understood, the latter is not.

The two objectives for this study were: (1) to determine the parameters of the hot cathode, arc discharge, and thereby possibly gain an understanding of the discharge mechanism, and (2) to measure the emission properties of refractory materials in cesium vapor, especially in the presence of a discharge. These objectives were pursued simultaneously since they are related. For example, the breakdown voltage of the discharge depends on the fields produced by the difference of the work functions of the electrodes. Likewise, the emission capability of the emitter seems to depend on the emitter sheath, and possibly the arrival at the emitter of ionized and excited cesium from the discharge. This report will present experimental results obtained on the emission and discharge characteristics on the Cs-Ta system as well as discharge measurements taken of the Cs-W system.

EXPERIMENTAL APPROACH

One experimental tube used for this study is shown in Figure 1.* The emitter base surface is the closed end of a tantalum cylinder; the emitter-collector gap can be adjusted by means of a bellows. Because of the difficulty in aligning the double-ended tube, the emitter surface is not perfectly parallel with the collector and guard ring surface. Therefore, the spacings reported herein are measured from the point of contact

*See APPENDIX for illustrations

between the emitter and collector. A W-Re thermocouple, used to measure the emitter temperature, was calibrated with an optical pyrometer for temperatures above 700°C. This calibration curve was then extended to lower temperatures using the published data as a guide for the extrapolation. Cesium pressure was determined by the temperature of a silicone fluid bath into which the whole tube was immersed.

In a similar tube containing a tungsten emitter, the W-Re thermocouple was unreliable because the junction detached from the emitter. Temperature measurements in this tube were taken with an optical pyrometer. All optical pyrometer readings were corrected for the emissivity of tungsten and the transmission through glass and silicone fluid.

EXPERIMENTAL EMISSION RESULTS

For low pressures, mainly those corresponding to cesium reservoir temperatures of 39°C, 67°C, and 99°C, retarding and Schottky plots were made to obtain the zero-field saturated emission data. The results obtained from these two methods were in agreement. Some of these curves are shown in Figure 2 which presents the emission current versus voltage for different spacings near the emission peak for the 99°C cesium curve. The variation with S (the emitter-collector spacing in mils) shows space charge limitations for large spacing. During these measurements, light emitted because of the existence of various excitation levels was observed originating just in front of the collector. For example, at 2.7 volts, the second resonance levels were observed. As the voltage increased, this blue excitation would move toward the emitter, while light from higher excitation levels was observed in front of the collector. No discontinuities were observed in the tube current for voltages even in excess of the cesium ionization potential, except for the two large spacing curves. For these two curves, abrupt increases in current were observed (see Figure 2) due to a discharge occurring outside the emitter-collector gap.

For higher cesium pressures, a discharge occurred at voltages for which the electron emission was still space charge limited. In this case, the discharge itself overcame the effect of space charge. This technique works fairly well for the 190°C cesium curve, and partially for the 255°C cesium curve. However, for a Cs reservoir temperature of 315°C, the current fails to show any sign of saturating, as illustrated in Figure 3. These data were taken by switching the applied voltage on momentarily, causing an intense discharge in the guard ring-to-shield

region. Care was taken to keep the guard ring and collector at the same potential at the point where the current was measured, using an adjustable resistor in the anode circuit. The steep slope and the square root dependence on voltage suggest an anomalous Schottky region.[1] This is not unreasonable if one assumes that the emitter surface is made up of patches having various crystal orientations. However, the anomalous Schottky mechanism does not explain the high current densities of hundreds of amp/cm^2 that were observed in this region. The anomalous Schottky effect can be looked upon as a mechanism that limits the emission. The normal Schottky effect cannot account for the several hundredfold increase in the current density.

Another objection to this interpretation is the fact that a similar curve was obtained when the emitter was at a temperature of 2475°K. At this temperature the surface should be almost free of cesium. However, if one postulates that the discharge along with the normal positive ion sheath causes a return of positive ions to the emitter surface, this increased flux of positive ions due to both the discharge current and the retarding effect of the positive sheath on surface ionized cesium can be viewed as an increase in cesium adsorption, which effectively lowers the work function. This lower work function at the higher emitter temperatures seems to be the cause of the increase of emission above that normally expected.

This reasoning can easily be applied to the region where copious surface ionization occurs. Effects like this have been observed by the author near the emission minimum for lower cesium pressures when larger applied fields were used. Its direct applicability to higher coverages seems doubtful unless there are very large ion currents, that is, in the order of the neutral cesium arrival rate. However, in a discharge, many excited neutrals impinge on the emitter surface. An excited atom may be ionized by surface ionization when the difference between the ionization potential and the excited level is less than the work function. The excited atoms may effectively act as a species with a lower ionization potential. This would then shift the $J_+ = 492\ J_-$ line toward the emission peak of the S curve. If the field at the emitter retards these ions, the effective coverage can increase, giving abnormally high emission density. Although surface ionization of excited atoms is energetically possible at lower work functions, it is not known whether the process occurs.

One experiment was tried to detect ionization of excited atoms at a lower work function. Radiation from a CsI lamp was let into the converter gap and it was hoped that this radiation would produce excited atoms. Since the incident Cs lines were quite broad, it was hoped that the hot Cs in the neighborhood of the emitter could absorb the wings of the resonance lines. No effect was observed. The experiment is inconclusive because it is not known if any excited atoms were produced. During the experiment, the Cs in the CsI lamp was used up, and it is not known if any appreciable Cs resonance radiation was available.

As the coverage increases, the possiblity of secondary processes at the emitter surface increases. Beside photo effects, potential ejection of electrons due to cesium ion neutralization can occur when the work function is less than one-half the ionization potential.[2] However, this too requires very high ion current to cause the large increase of electron emission that was observed. De-excitation of an excited cesium atom could result in potential ejection of an electron if the difference between the ionization potential and the excited level is greater than the work function and if the excitation energy is greater than the work function. Even the adsorption of a neutral cesium atom could cause potential ejection of electrons, if the work function is less than the adsorption energy. In fact, the perturbing effect of the field of an incoming cesium ion in the presence of a field of the positive sheath might cause the emission of one or more electrons before the ion is finally neutralized at the surface. Although all these processes are energetically possible, the basic probabilities are unknown, and require experimental study.

A simplified calculation of this returned ion effect is as follows. Consider a surface with the following particle currents:

μ_a = the neutral arrival rate
ν_a = the neutral evaporating rate
μ'_+ = the ion arrival rate from the plasma region
ν_+ = the ion emission rate
μ_+ = the total ion arrival rate.

Assume that the ion particle current entering the plasma region (ν'_+) is related to the ion emission rate at the surface.

$$\nu'_+ = \nu_+ \exp\left(-\frac{eV}{kT}\right) \qquad (1)$$

where V is the sheath potential. The total ion arrival rate is

$$\mu_+ = \mu'_+ + \nu_+ - \nu'_+ \qquad (2)$$

Assuming that surface ionization is independent of whether the Cs arrives as an atom or an ion, one finds that:

$$\nu_+ = (\mu_a + \mu_+)\beta \qquad (3)$$

where β is the surface ionization probability and is given by

$$\beta = \left[1 + \frac{\omega_a}{\omega_+} \exp\left(\frac{e(I - \phi)}{kT}\right)\right]^{-1} \qquad (4)$$

where I = the first ionization potential of cesium

ω_a / ω_+ = the ratio of the statistical weights, and has a value of "2" for Cs

ϕ = the work function.

Combining Equations 1, 2, 3,

$$\mu_+ = \frac{\mu'_+ + \mu_a \beta \left[1 - \exp\left(-\frac{eV}{kT}\right)\right]}{1 - \beta\left[1 - \exp\left(-\frac{eV}{kT}\right)\right]} \qquad (5)$$

The total arrival rate of Cs is given by,

$$\mu_t = \mu_+ + \mu_a = \frac{\mu'_+ + \mu_a}{1 - \beta\left[1 - \exp\left(-\frac{eV}{kT}\right)\right]} \qquad (6)$$

Thus, if β approaches unity, μ_t can be much larger than the neutral Cs arrival rate.

The sheath potential can be evaluated, by assuming that the electron and ion densities are equal just outside of the sheath, and that both electrons

and ions are emitted with thermal velocities characteristic of the emitter temperature. In the ion-rich case,

$$V = \frac{kT}{e} \ln \left(\frac{492\, J_+}{J_-} \right) \tag{7}$$

This now gives

$$\mu_+ = \frac{\mu'_+ + \mu_a \beta \left(1 - \frac{J_-}{492\, J_+} \right)}{1 - \beta \left(1 - \frac{J_-}{492\, J_+} \right)} \tag{8}$$

and

$$\mu_t = \frac{\mu'_+ + \mu_a}{1 - \beta \left(1 - \frac{J_-}{492\, J_+} \right)} \tag{9}$$

The total arrival rate can easily be reduced to

$$\mu_t = \frac{\mu'_+ + \mu_a - \frac{J_-}{492\, e}}{1 - \beta} \tag{10}$$

In previous work by the author on the Ta-Cs system, a set of emission curves (Figure 4) were measured which show considerable distortion near the emission minimums. This distortion is believed due to the return ion effect. These data were taken by going from high to low temperatures. When the emission is measured in the other direction, the distortion is much less. In general, the emission in this region depends on the applied voltage (not in the usual way) and also on time effects. In going from lower to higher temperatures, the emission in this region tends to increase with time when the emitter is held at a constant temperature. The connection between the Langmuir-Taylor two-phase region and the return ion effect is not certain, and more precise measurements of these effects are needed before anything more definite can be stated.

Figure 5 shows resulting curves of emission versus reciprocal temperature for this particular tantalum emitter used during this study program. The solid lines indicated in Figure 5 are an

extrapolation of the Langmuir-Taylor results for tungsten.[3] The Ta-Cs system has greater emission at the lower pressures and the peaks are shifted to lower temperatures. These results are in disagreement with data taken with Ta wires.[4] The Ta surface used in this study was found to have developed a preferred orientation of the 100 surface, which Webster[5] has shown to be one of the higher emission surfaces in Cs vapor. This is presumably the main reason for the disagreement. If the process proposed above involving the increased flux of Cs due to the retarding field for ions at the emitter is considered, then another possible reason for this disagreement is that the collection efficiencies of thin wires and plane surfaces could be different for the returning positive ions. Measured ion emission data show that the Cs arrival rate is consistent with that predicted from the Cs reservoir temperatures. The emission peak observed on cooling from emitter temperature of 2500°K indicates that the emission is not due to contamination by materials such as oxygen. The vacuum emission taken before and once during these measurements agree with the published values for Ta. The distortion of the high pressure curves is probably due to the experimental technique of using the discharge to neutralize space charge and obtain the saturated current.

These results indicate a Ta surface similar to that used in this study would also be a fairly good collector material; for example, the 314°C Cs curve indicates an effective work function of 1.33 ev at 1000°K.

DISCHARGE STUDIES

The discharge studies involve measurements of the breakdown voltage (V_B) and maintenance voltage (V_M) for various cesium pressures, emitter temperatures, and emitter-collector spacings. These measurements were taken by observing the current-voltage relations using a low-impedance 60-cycle sweep. The values of V_B and V_M were determined by observing the current discontinuities in the current-voltage characteristics caused by the onset and cessation of the discharge. At high pressures and emitter temperatures, the transition into the arc mode is indefinite; that is, there is a smooth transition between the modes. Most of the data in this report refers to the conditions before these potentials become indistinguishable.

Figure 6a shows the electron potential diagram which represents the gross features of the potential distributions just before breakdown. It is assumed that breakdown is due to the electrons which are accelerated

after passing over the electron space charge barrier. These electrons produce ions or excited atoms by impact with cesium neutrals, some of which can be in an excited state. The maximum potential that these electrons can acquire (neglecting collisions) is termed the collector sheath potential. Its value just prior to breakdown will be called V'_c, and is given by

$$V'_c = V_B + \phi_e - \phi_c + V_e \tag{11}$$

In the case of the maintenance potentials, it is assumed that the electron space charge barrier is negligible, and that a positive sheath forms as shown in Figure 6b. This neglects the double sheath which exists where the electron emission is more than 492 times the ion emission. The maximum potential acquired in this case is assumed to be the emitter sheath potential. Its value just prior to the extinction of the discharge is called V'_e, and is given by

$$V'_e = V_M + \phi_e - \phi_c + V_c - V_p \tag{12}$$

The applied voltages, V_B and V_M, are the quantities that are actually measured. What should be known for an understanding of the mechanism of this discharge is V'_c and V'_e, as given in the preceding equations. With the aid of the emission data described in the first part of this report, the effective ϕ_e can be found. In all this work, the collector was assumed to have a work function of 1.9 electron volts; that is, it was assumed that the collector was covered by many monolayers of cesium. With the aid of the measured emission before and after breakdown, an estimate of V_e can be made by means of the Boltsmann relation. As the temperature of the emitter approaches that at which $J_+ = 492\, J_-$, the sheath potential approaches zero and then goes positive. The V_e correction is cut off artifically and rapidly as this point is approached. This is justified because the ion emission has a very strong dependence on the emitter temperature.

In considering the maintenance potentials, a knowledge of $V_c - V_p$ is required. The collector sheath, V_c, depends on the random current density arriving at the collector. It is assumed that all other currents are negligible. The random current density is a function of the unknown electron density and temperature. The plasma loss, V_p, depends also on the electron temperature. From a simplified calculation based on Agnew's spectrographically determined electron density and temperature as a

function of cesium pressure, an estimate of V_c can be obtained.[6] V_p can be determined from the resistivity work of Mohler[7] and from Agnew's electron temperature. However, before much confidence can be placed in these corrections for V_c and V_p, the electron densities and temperatures should be measured under the same conditions as are the discharge parameters.

The discharge results which will be reported are peculiar to this particular emitter surface and geometric arrangement of the electrodes. The effect of electrode geometry was manifested by disconnecting the guard ring. In this case, all parameters are shifted upward in potential, indicating that the field at the edge of the collector and possibly the emitter influences the discharge parameters.

Figure 7a* shows the breakdown and maintenance potentials versus spacing for different emitter temperatures at a pressure corresponding to a reservoir temperature of 190°C. In general, there is little dependence on spacing for both the breakdown and maintenance potentials, except for the maintenance curves at the lower temperatures. If the correction for the contact potential is made, the curves shown in Figure 7b are obtained. At small spacings, most of the values of $V_B + \phi_e - \phi_c$ intercept zero spacing at approximately 3.25 volts, while the $V_M + \phi_e - \phi_c$ values are grouped around 0.75 volt. The deviations of the two lower emitter-temperature curves for both the breakdown and maintenance potential, and the 1317°K curve for the maintenance potential are due to the fact that the emission density is decreasing rapidly as the emitter temperature moves away in either direction from the temperature of the emission peak.

Figure 8a shows the breakdown and maintenance potentials for three spacings at a cesium reservoir temperature of 190°C. The maintenance potentials show the effect of limited current as one proceeds to the higher and lower temperatures from the emission peak. The breakdown curves seem to be decreasing linearly with emitter temperature. However, if the contact potential correction is inserted, the curves shown in Figure 8b are obtained. Note that the values of $V_B + \phi_e - \phi_c$ go through a broad

*In this illustration and in those following, the term relative spacing means the spacing as read on the micrometer. The point of contact of the emitter and collector is usually one to two mils less that the closest spacing experimental point given in the illustrations.

minimum at about 3.1 volts. If the correction for the space charge sheath, V_{ss}, is added, this curve has a maximum value near 3.65 volts. Next by adding the voltage equivalent to the two kT thermal energy term, the resulting potential is within one-tenth of a volt of the ionization potential of cesium. Thus, it appears that the breakdown for this hot cathode discharge at these emitter temperatures and a Cs pressure corresponding to 190°C is due to ionization by electron impact from the ground state of cesium. If all the corrections to the maintenance potential are added, the minimum of the maintenance potential curve occurs near the peak emission. By adding the voltage equivalent of the two kT energy term to the minimum maintenance potential, the resultant potential is very close to the second resonance level for cesium. Data for higher emitter temperatures could not be taken because the pressure-distance characteristics for these conditions were such that the discharge tended to leave the emitter-collector gap when an attempt was made to go to higher temperatures.

The breakdown and maintenance potentials versus spacing data at 255°C cesium reservoir temperature are presented in Figure 9a. The breakdown potential appears to depend linearly on spacing, while the maintenance potential appears to be independent of spacing. If these data are corrected for the contact potential difference, the results are as shown in Figure 9b. The correction for the contact potential tends to bunch the breakdown curves at small spacings near 2.2 volts. The maintenance potentials are bunched about 0.4 volt. The 1200°K breakdown curve has also been corrected for the space charge sheath and its dependence on spacing. The linear dependence of the breakdown voltage on spacing is the result of the increase in the number of collisions at these higher pressures.

The breakdown and maintenance potentials versus the emitter temperature for different spacings at a 255°C cesium reservoir temperature are shown in Figure 10a. Again the high breakdown and maintenance potentials at low emitter temperatures are due to the lack of sufficient current density to support the discharge. As the emitter temperature increases, the maintenance potential becomes independent of spacing and varies more slowly with temperature. Both the breakdown and maintenance curves cross zero potential at high emitter temperatures and enter the discharge region familiar in converter work. Figure 10b shows the same data with the various corrections. The breakdown data, when corrected for the contact potential, tends to exhibit a flat region, especially for very close spacings. For example, the breakdown potential

is fairly constant at 2.2 volts for the 10-mil spacing curve. This flat region, when corrected for the space charge sheath, is raised to about 2.6 volts. If the voltage equivalent is added to the 2 kT term, this value is about one-tenth of a volt above the second resonance level. As the temperature is increased, the corrected breakdown potential drops to a level very near the first resonant level. The curves for the smaller spacing enter this discharge mode first. Note that at this pressure, the transition into the discharge mode, is considerably above the emitter temperature where the positive ion sheath is expected to form. This possibly indicates that excited states created by the thermal energy of the emitter are necessary for the discharge in this pressure range. The maintenance potentials (shown grouped together in one curve), when corrected for contact potential, are independent of the emitter temperatures and are constant at a potential of one-half a volt. However, at high emitter temperatures, the $V_M + \phi_e - \phi_c$ curve rises to meet the breakdown curve. The correction for $V_c - V_p$ on the maintenance potential shows that the maintenance potential increases gradually with emitter temperature. This increase in the emitter sheath potential is probably due to the need to overcome the decrease in electron emission as the emitter temperature approaches that of the emission minimum. When the emitter temperature is raised above the temperature where $J_+ = .92J_-$, the breakdown data should be corrected in the same way as the maintenance data. This correction is shown as the $V_B + \phi_e - \phi_c + V_c - V_p$ curve. These corrections now place the sheath potentials at 3.5 and 3.25 volts for the breakdown and maintenance processes, respectively, when the converter is operating in the discharge mode.

The discharge studies at higher Cs pressures are incomplete, because the tube failed during this series. In Figure 11, the breakdown and maintenance potentials are shown versus spacing at an emitter temperature of 1815°K and a cesium temperature of 312°C. The corrected breakdown curve is steeper than those corresponding to 255°C, but starts out at a lower voltage. Again, the increased slope compared to the 255°C Cs curve is due to the increase in the number of collisons resulting because of the higher pressure. The maintenance potentials show a small dependence on spacing, and are slightly higher in value than the 255°C Cs temperature.

Figure 12 shows the breakdown and maintenance potentials versus emitter temperature for a spacing of approximately 10 mils and a cesium reservoir temperature of 315°C. It is interesting to note that at the high temperatures where arc mode occurs, the $V_B + \phi_e - \phi_c$ curve levels off

under 0.3 volts. When the emitter temperature is higher than the $J_+ = 492\,J_-$ temperature, the potential diagram of Figure 6b should apply to the breakdown conditions. The effective breakdown potential is then $V'_e = V_B + \phi_e - \phi_c + V_c - V_p$. At high emitter temperatures, the corrected curves for both the breakdown and maintenance potentials level off very close to the first resonance level of Cs (1.38 and 1.45 ev). This strongly suggests a multi-step process as the cause for the arc mode. Again, it must be emphasized that the correction $V_c - V_p$ is based on electron density and temperature measurements taken at much higher emitter temperatures (2470°K) than those used here. Therefore, the reliance that can be placed on curves with the $V_c - V_p$ correction is small.

In order to obtain a precise knowledge of the various sheaths in the discharge mode, it is necessary to make three types of measurements - the emission from both the emitter and collector, the discharge parameters, and finally the electron densities and temperatures in the converter gap. In the Ta experimental tube described thus far, the first two types of measurements were made, while the third measurement was calculated. An experimental tube, attempted during the latter half of the program, would have permitted making the three type of measurements. However, this tube was never successfully operated because of several mishaps. The tube had the following features.

(1) Both emitter and collector could be heated, thus enabling a more precise evaluation of the emission characteristics. Also the contact potential correction in the shield calculations would be eliminated if both electrodes were maintained at the same temperature during the discharge measurements.

(2) Adjustable emitter-collector gap.

(3) Sapphire windows, permitting more sensitive spectrographic measurements of the plasma properties.

(4) Shielded probe in the surface of one guard ring permitting a check on the spectrographically determined densities and temperatures.

(5) A tungsten filament for a more precise calibration of the spectrometer and temperature measurements.

(6) Two identical tantalum electrodes plus a guard ring for each electrode.

A molybdenum-electrode tube with adjustable spacing and sapphire windows was built during this contract. It too was not tested successfully, this time because of a leak in one of the press leads.

However, measurements were taken on a tungsten-emitter tube. The emitter surface was a tungsten cap which was diffusion bonded to the closed end of a Ta cylinder. The measurements made on the W-tube included the discharge parameter and some spectrographically determined ion density. Emission measurements were not made due to a failure of the W-Re thermocouple. The temperatures reported in the following paragraphs were taken with an optical pyrometer and were corrected for the emissivity and transmission of the experimental apparatus. The emission data of Taylor-Langmuir were used to make the various corrections for the sheath calculations since it was felt that these emission data are not strictly applicable to this particular W emitter because of the various phenomena mentioned in the emission portion of this report. However, the Taylor-Langmuir data are used to give a rough idea of the sheath potentials.

In Figure 13, the breakdown potential, V_B, and the maintenance potential, V_M, are presented for a pressure corresponding to 267°C for the Cs bath temperature and for two emitter collector spacings. These data are very similar to those taken with the Ta tube. Figure 14 shows the V_B and V_M taken at a bath temperature of 314°C for the same two spacings.

During these measurements, the ion or electron densities were determined by a technique first used for Cs by L. Agnew and P. M. Stone of Los Alamos. This method consists of measurements of certain cesium line widths which have been broadened by what is known as plasma broadening. Plasma broadening is essential because of the spreading of atomic energy levels due to a perturbation caused by ions and electrons of the dense plasma while the atom is in the process of radiating. Plasma broadening is far greater than broadening due to other causes, and is easily measured since the half width is in the order of several Angstroms. In general, plasma broadening depends on both the ion density and temperature. However Agnew and Stone discovered that the broadening of the fundamental series of Cs is nearly proportional to the ion density and nearly independent of temperature.

In this study, the line broadening was measured by a Jarrell-Ash 500-mm Ebert scanning monochromator with a resolution of 32Å/mm. The monochromator was equipped with adjustable slits. An ion density of 6.5×10^{13} per cm^3 was found for the discharge mode at a pressure corresponding to a bath temperature of 267°C. Figure 15 shows the measured ion density versus emitter temperature along with V_B and V_M for an emitter collector spacing of 0.050 inch and a cesium bath temperature of 314°C. Ion densities were obtained from the half width of the 6870 Angstrom line. By assuming Langmuir-Taylor emission data, and using the Saha equation to find the electron temperatures corresponding to the measured arc ion density, the various corrections were made for the collector sheath in the breakdown case, and for the emitter sheath in the maintenance case.

Figure 16 shows the calculated emitter sheath potential and the measured ion densities versus emitter temperatures for an emitter-collector spacing of 0.050 inches and a bath temperature of 314°C. These data are for the case when the tube is operating as a converter in the discharge mode.

These tungsten data are in general agreement with the tantalum data, but before more precise conclusions can be drawn, the emission, the discharge parameters, and the plasma properties must be measured simultaneously in a single experimental tube.

It was observed that discharges can be started and maintained between sections of the same electrode when there is a temperature gradient along the electrode. For example, at a temperature of 255°C for the Cs equilibrium, a visible discharge occurs between the hot thin sections of the Ta emitter cylinder and the emitter heat shielding. This discharge can be started by either going to high emitter temperatures or by striking a discharge in the emitter-collector gap. The usual hysteresis is observed, and the discharge disappears at approximately 1440°K.

SUMMARY

The emission results indicate that this particular Cs-Ta surface has an emission capability greater than that reported by Langmuir and Taylor for Cs-W, with the emission maxima shifted to lower emitter temperatures. The large enhancement of the emission during the discharge is believed due to the lowering of the work function by the effective increase in adsorption due to the retarding effect for ions of the field at the emitter surface. The discharge parameter study indicates that at a

pressure of the order of 1 mm and high emitter temperature, the discharge mode is the result of a multi-step process. The emitter sheath potentials available appear close to the first resonance level.

Ion densities determined by line broadening and the discharge parameters were measured on a tungsten-emitter tube. These tungsten data are similar to the tantalum data. However, these results manifest the need for having the emission, discharge parameters, and plasma properties measured simultaneously in the same experimental vehicle.

REFERENCES

1. C. Herring and M. H. Nichols, Rev. Mod. Phys., 21, p. 185 (1949).

2. H. D. Hagstrum, Phys. Rev., 96, p. 336 (1954).

3. J. B. Taylor and I. Langmuir, Phys. Rev., 44, p. 423 (1933).

4. J. M. Houston, Third Proceedings of the Round Table Discussion of Thermionic Converters, June 1961.

5. H. F. Webster, J.A.P., 32, p. 1802 (1961).

6. L. Agnew, Bull. Am. Phys. Soc. II, 6, p. 343 (1961).

7. F. L. Mohler, J. Research NBS, 21, p. 873 (1938).

ACKNOWLEDGEMENTS

The author gratefully acknowledges the many helpful discussions with members of the Physical Electronics Section staff of the General Electric Research Laboratory.

APPENDIX

ILLUSTRATIONS

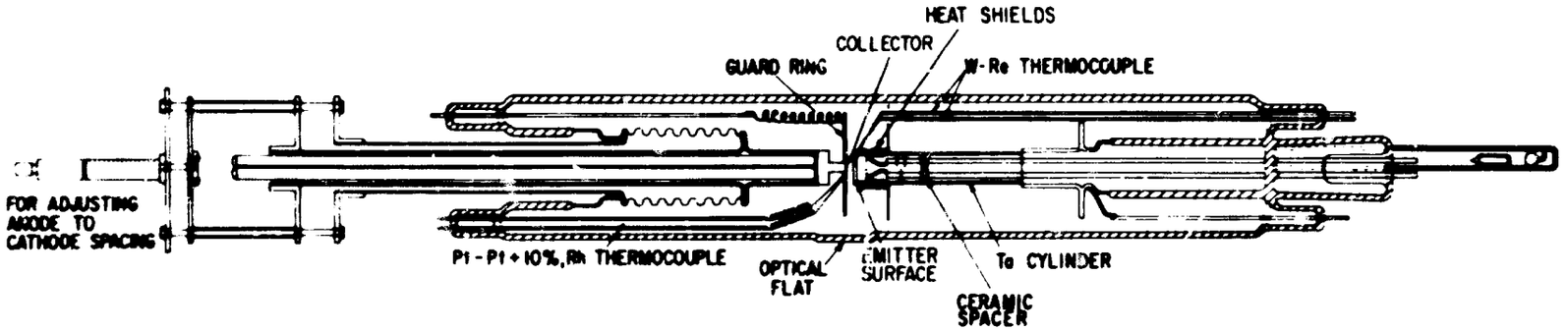

Figure 1 - Schematic drawing of the experimental tube

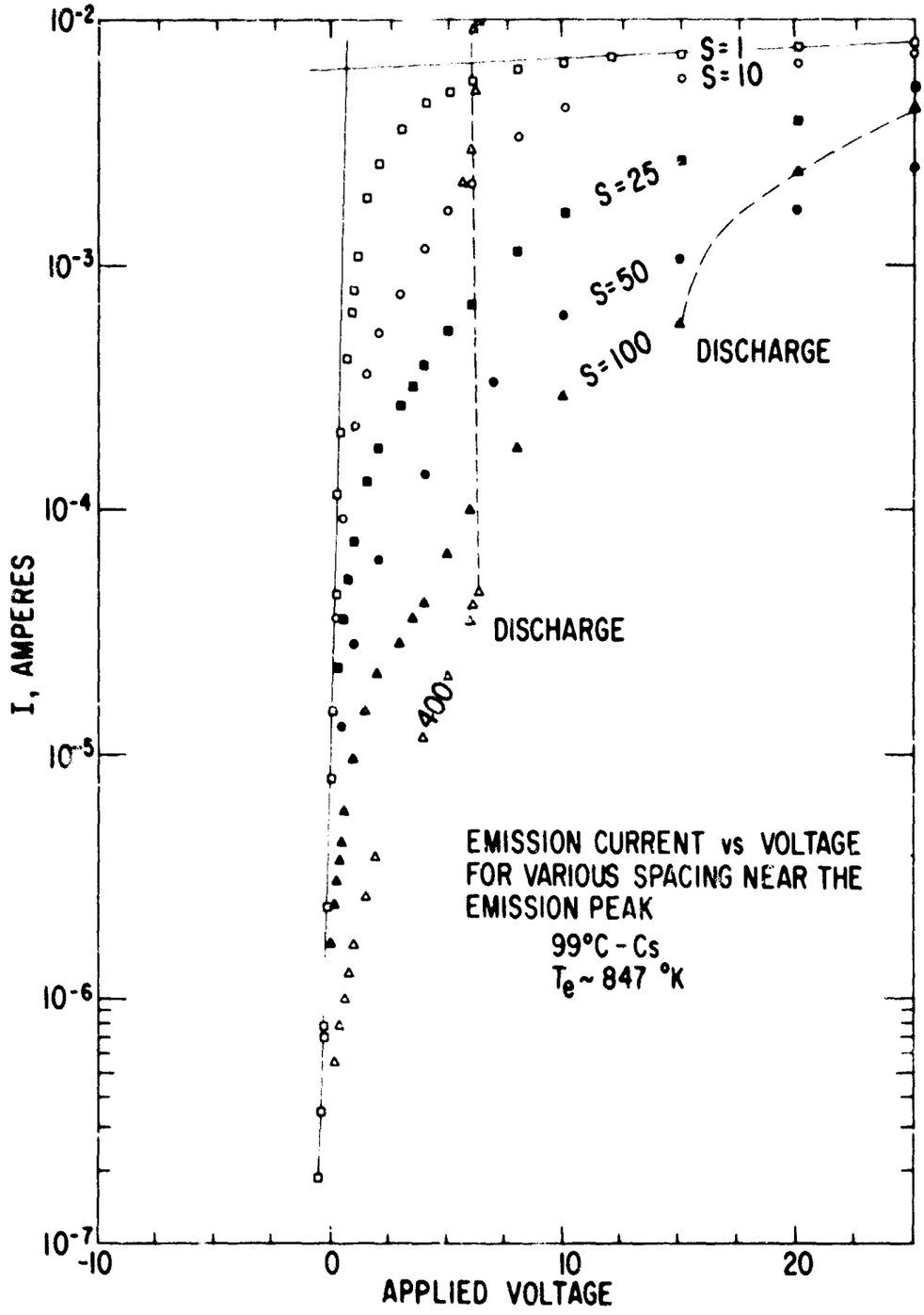

Figure 2 - Retarding plot for various emitter collector spacings, S. The spacing, S, is given in thousands of an inch (mils)

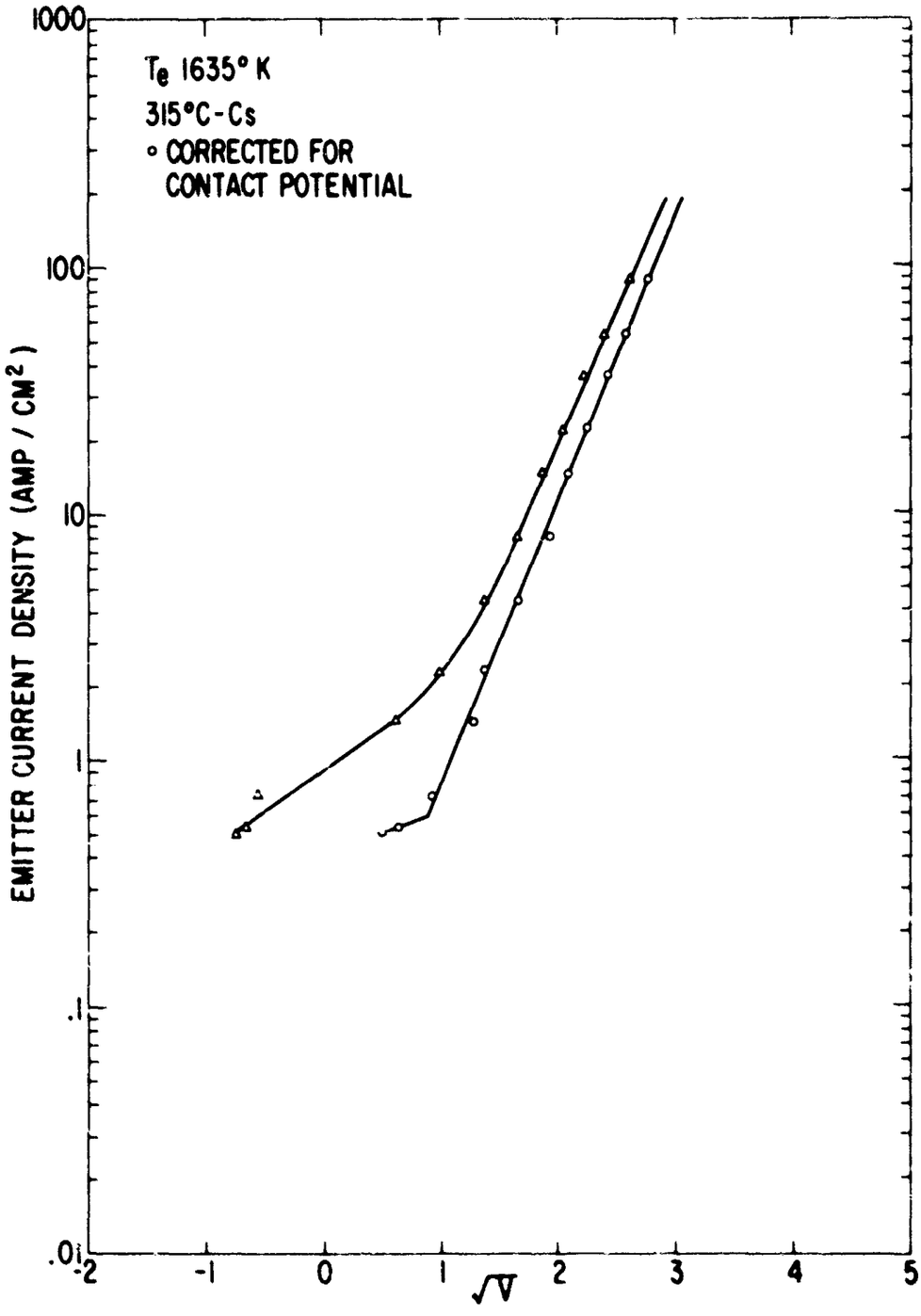

Figure 3 - Schottky plot illustrating the anomalous Schottky region. The triangles are the original data while the circles are the same data corrected for the contact potential difference

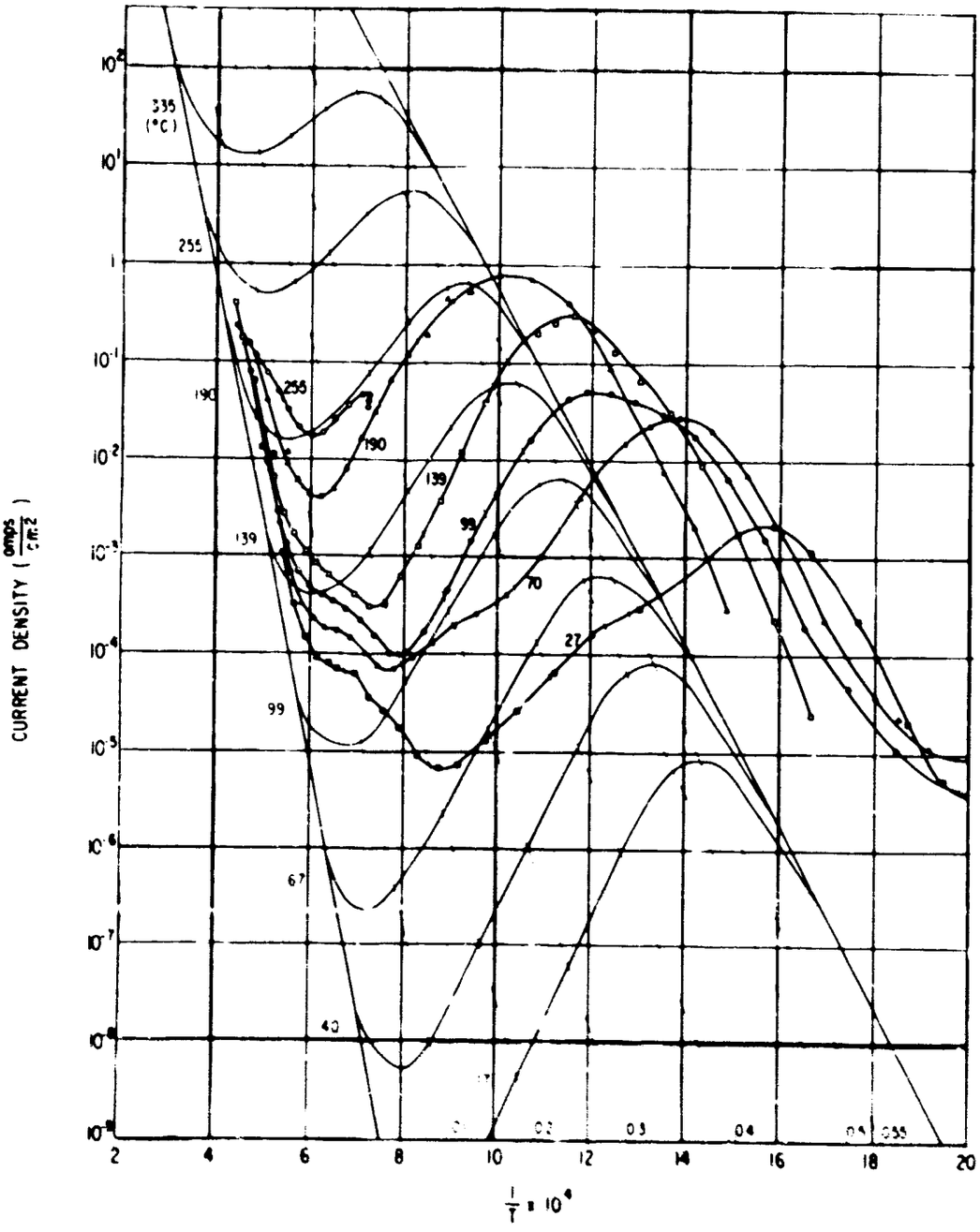

Figure 4 - Emission curves for the Ta-Cs system showing distortion near the emission minimums

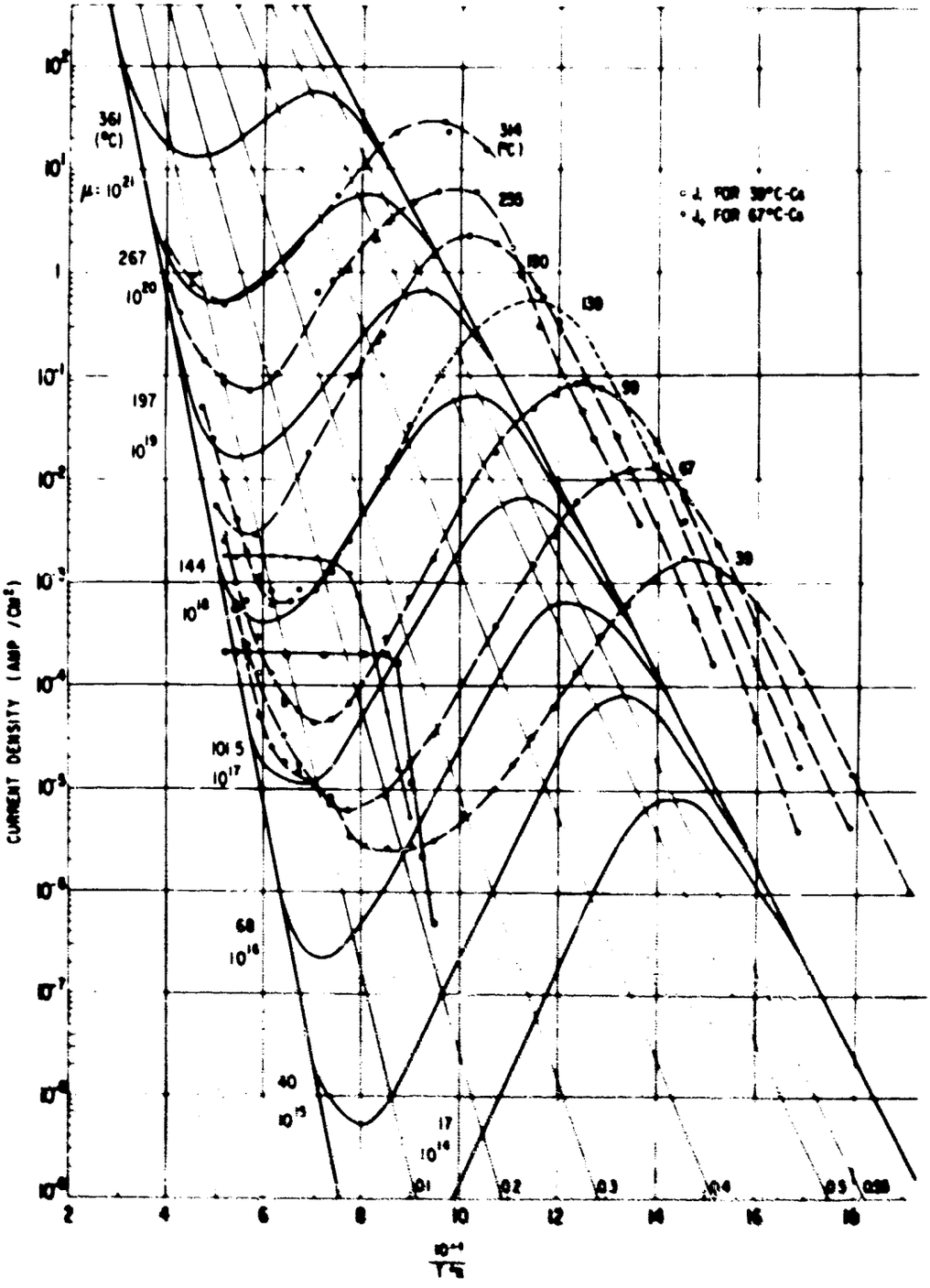

Figure 5 - Emission density versus reciprocal emitter temperature for the Ta-Cs system (dash curves) as compared with the Taylor-Langmuir data (solid curves)

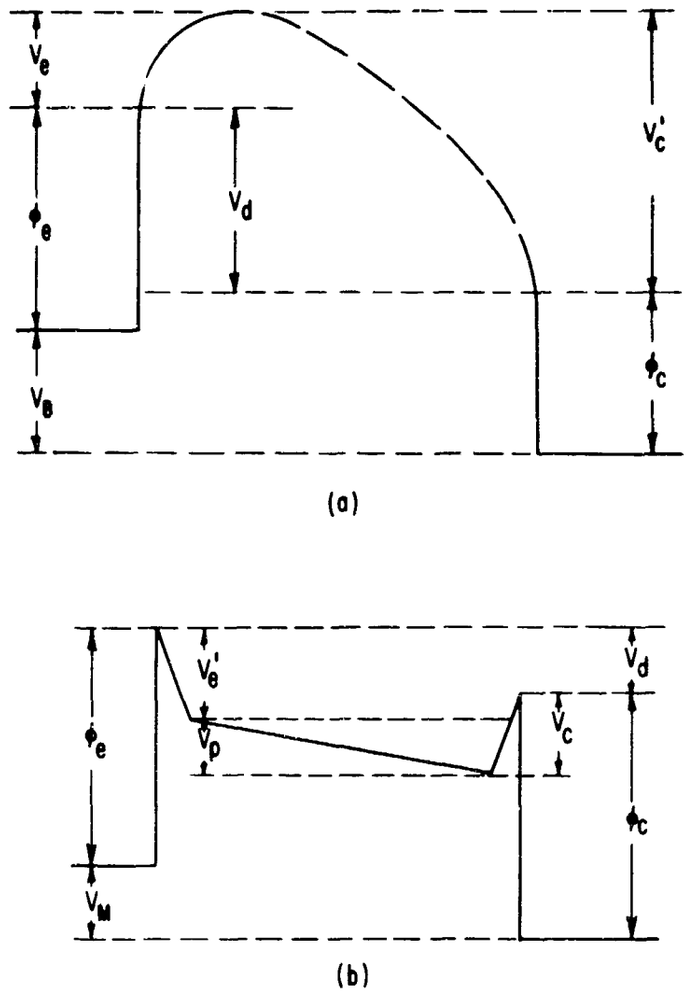

Figure 6 - Electron potential diagrams illustrating the simiplified model used for the breakdown (a) and the maintenance (b) processes

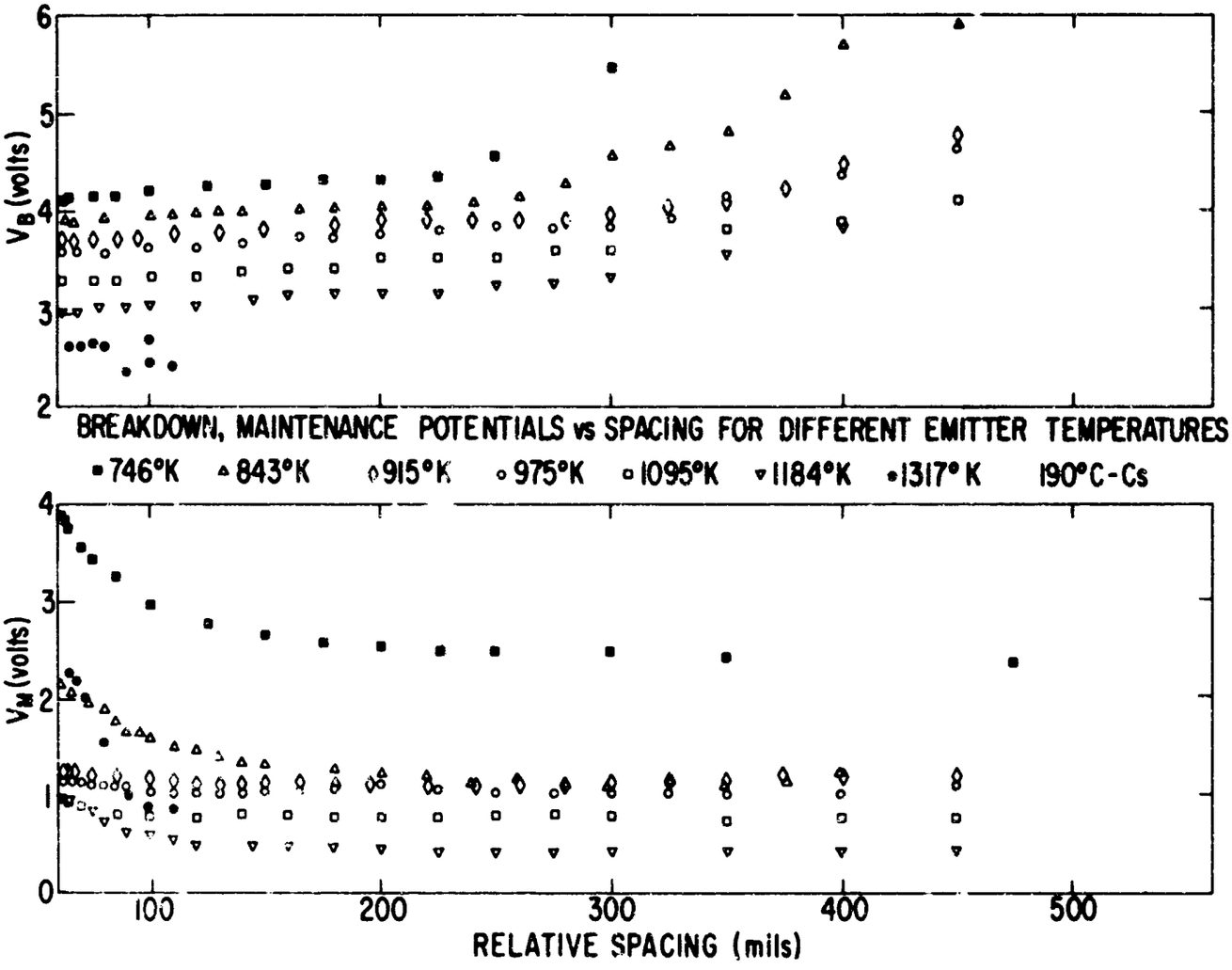

Figure 7a - Spacing dependence of the breakdown and maintenance potentials for various emitter temperatures at 190°C for cesium

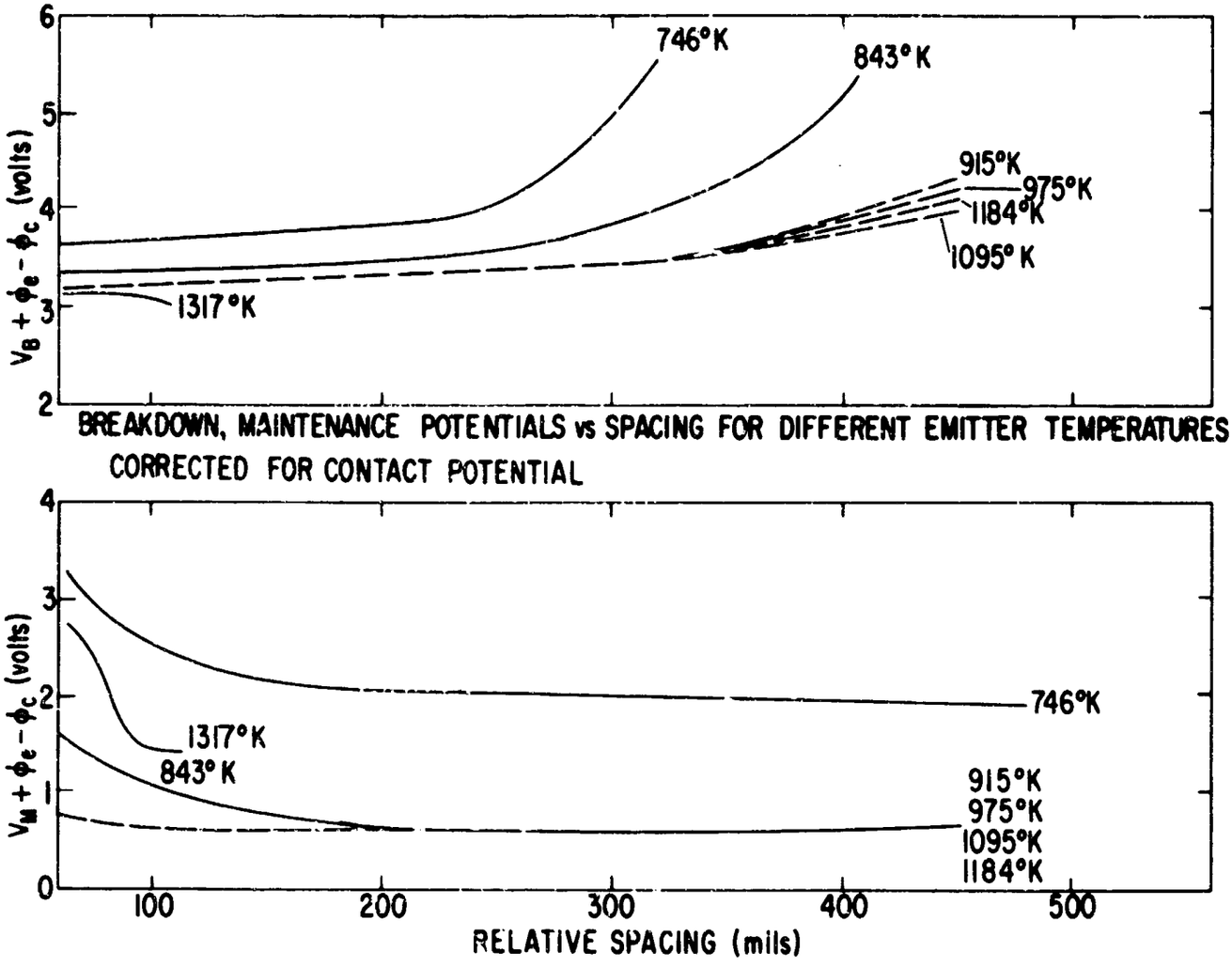

Figure 7b - Data of Figure 7a corrected for contact potential

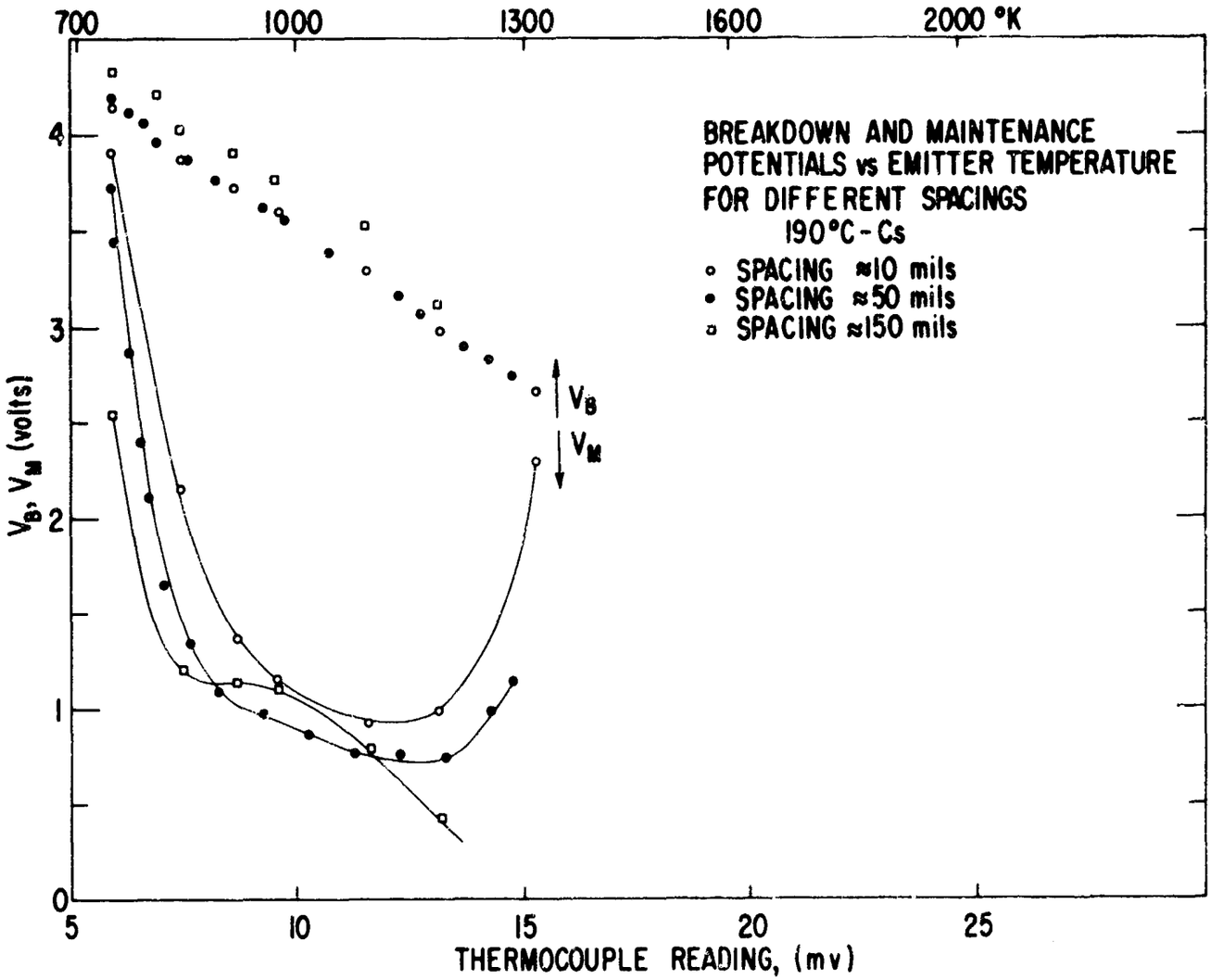

Figure 8a - Breakdown and maintenance potential dependence on emitter temperature (thermocouple reading)

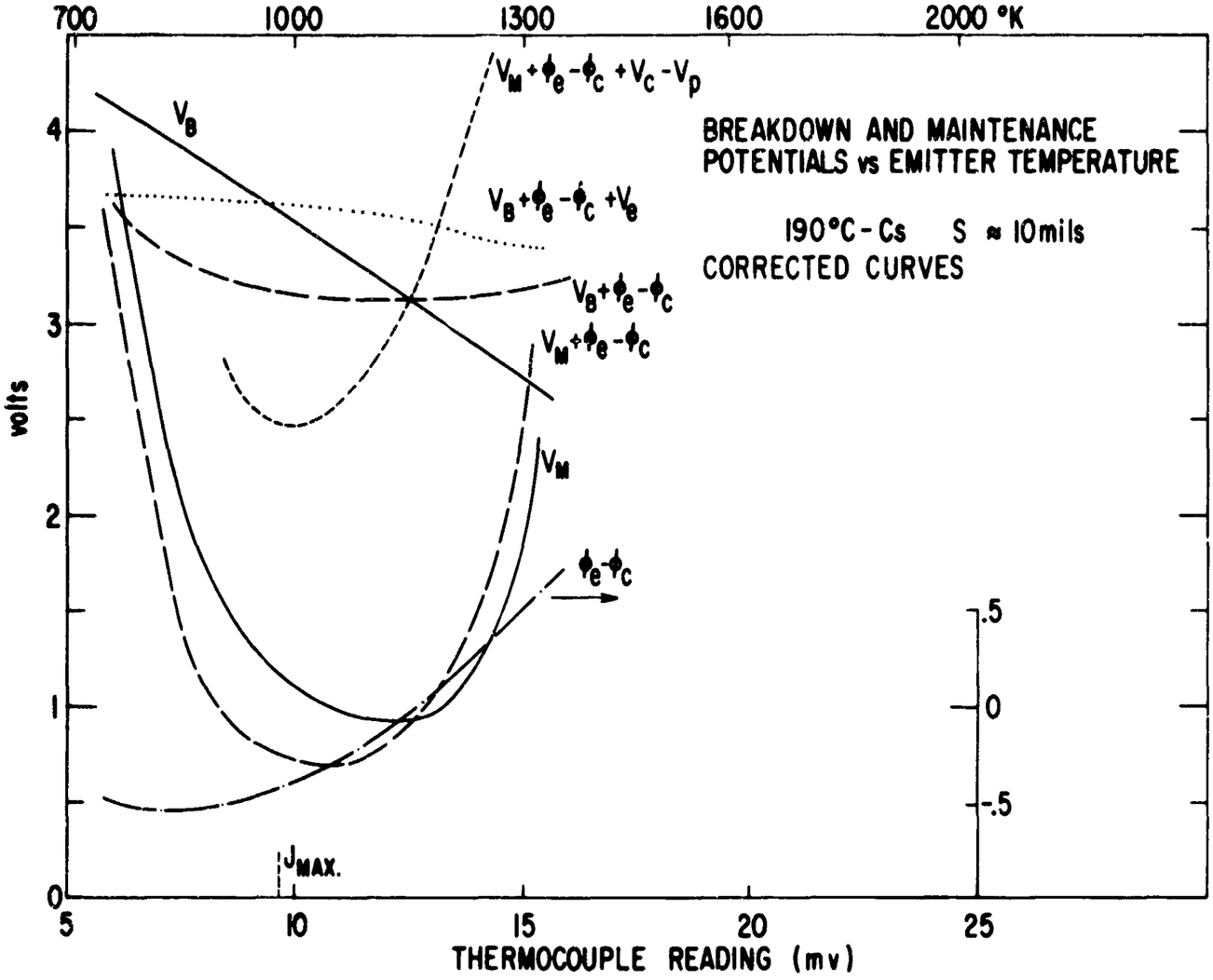

Figure 8b - Data of the 10-mil spacing curve of Figure 8a with the appropriate corrections for the contact potential, $\phi_e - \phi_c$, the emitter sheath, V_e, the collector sheath, V_c, and the plasma drop, V_p

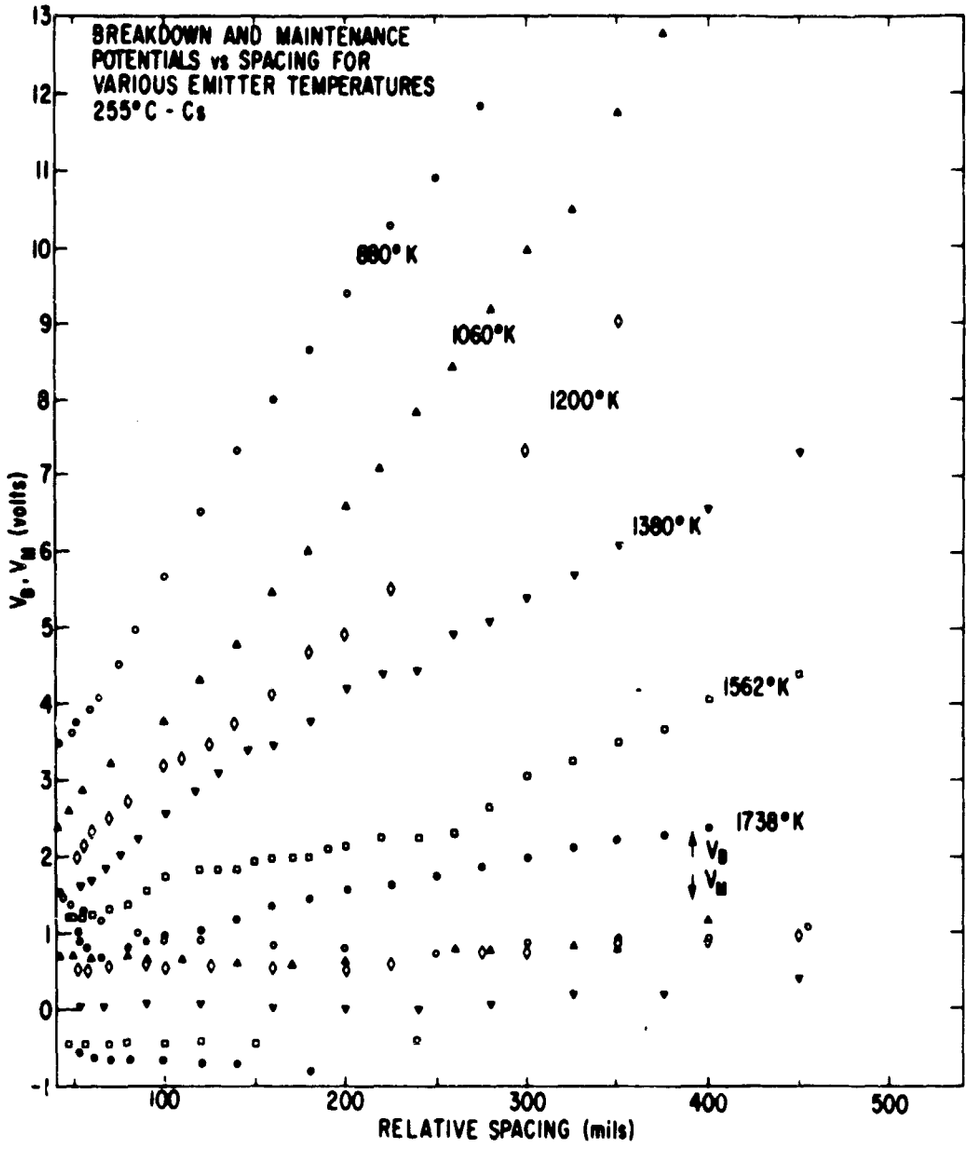

Figure 9a - Spacing dependence of the breakdown and maintenance potentials for different emitter temperatures for a cesium temperature of 255°C

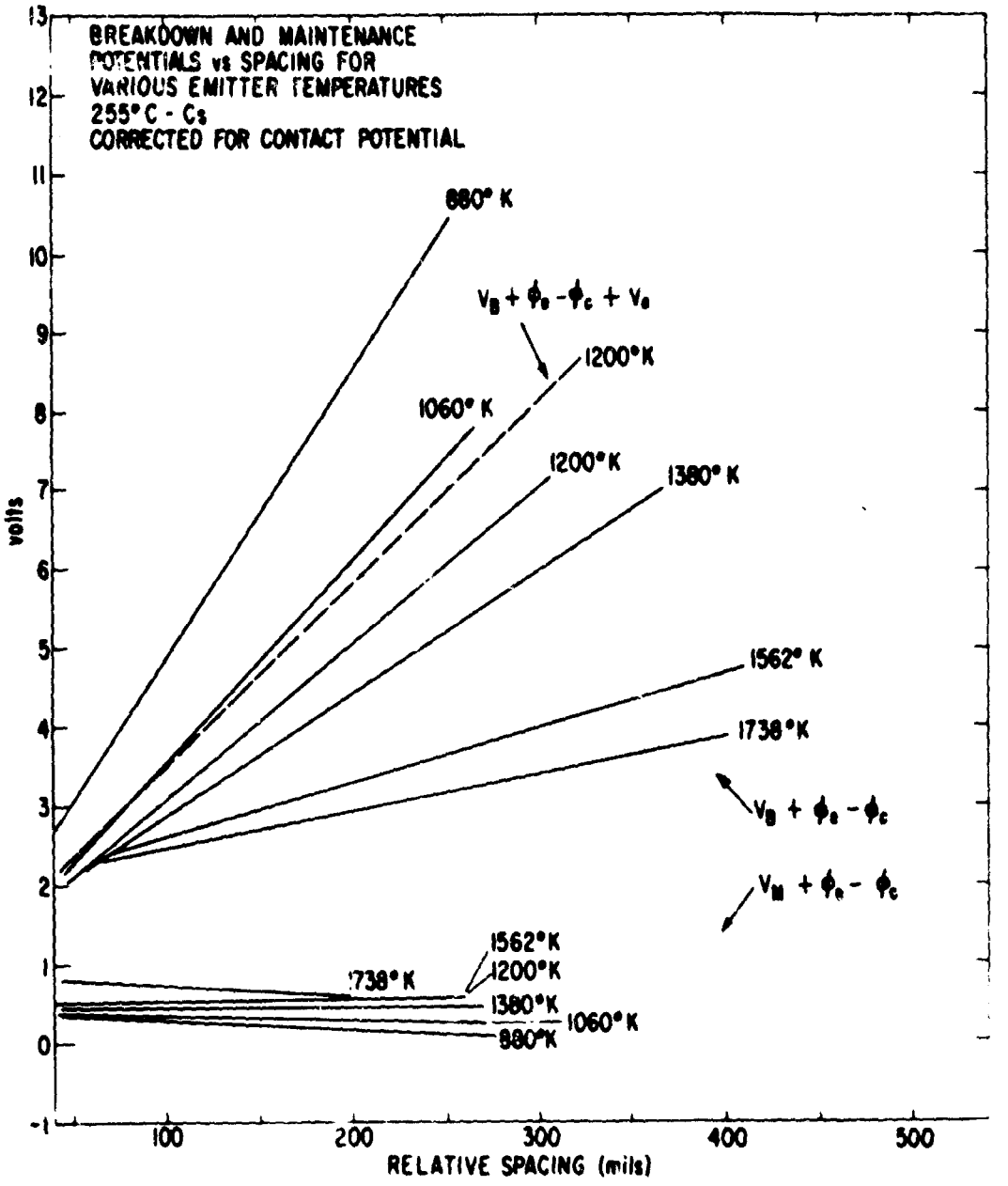

Figure 9b - Data for Figure 9a corrected for contact potential

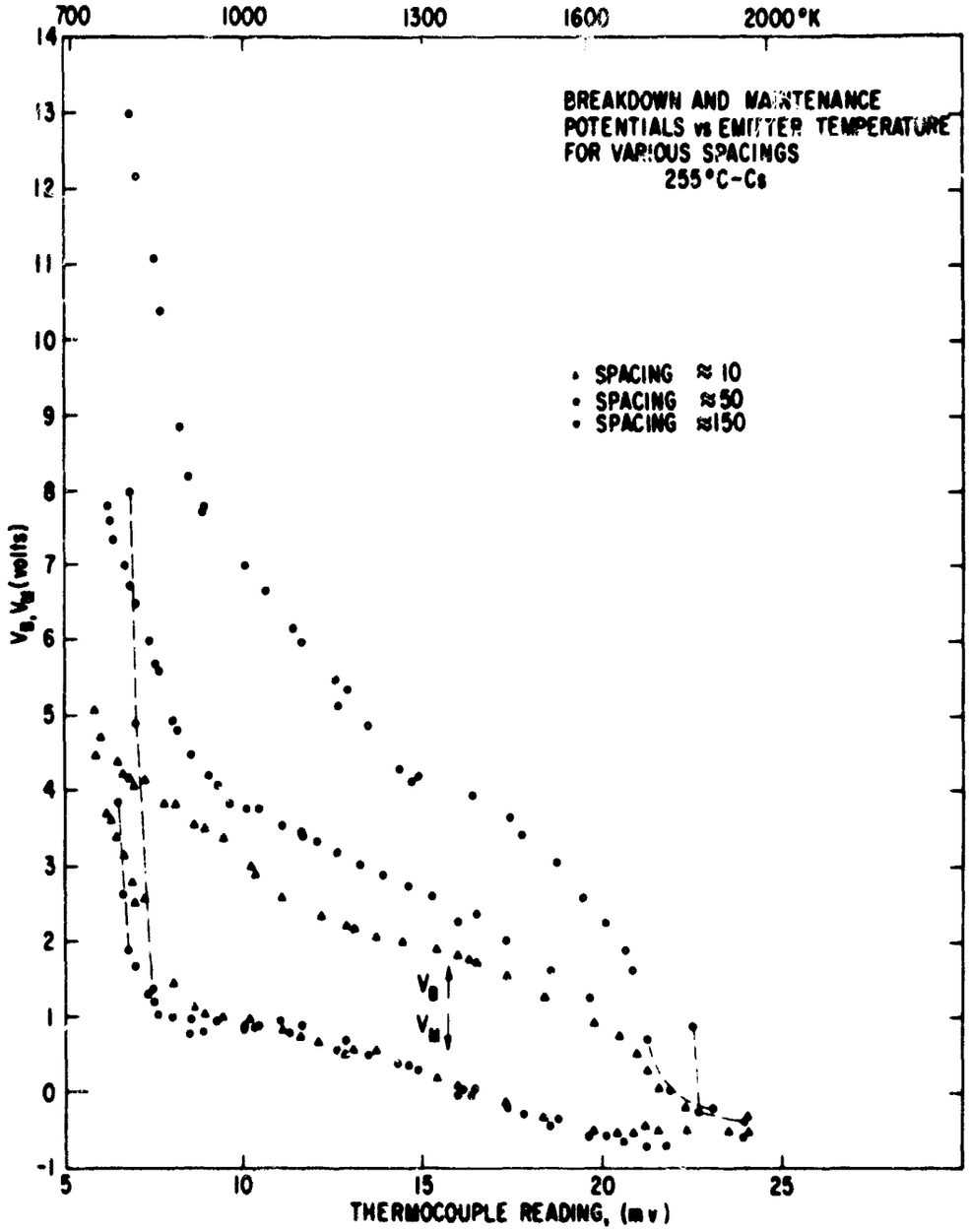

Figure 10a - Breakdown and maintenance potenitals versus emitter temperature for various spacings for a cesium temperature of 255°C

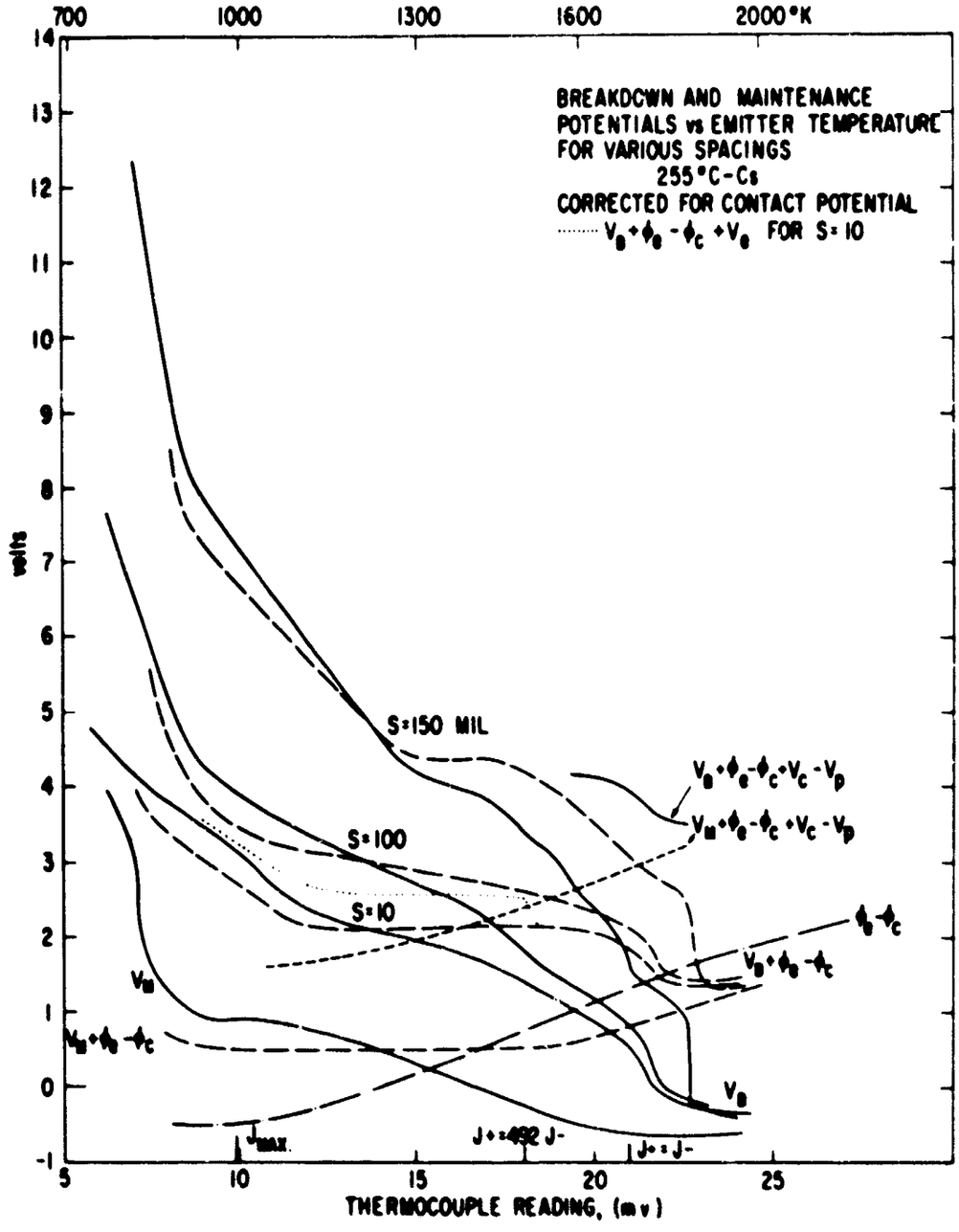

Figure 10b - Data of Figure 10a with the various corrections

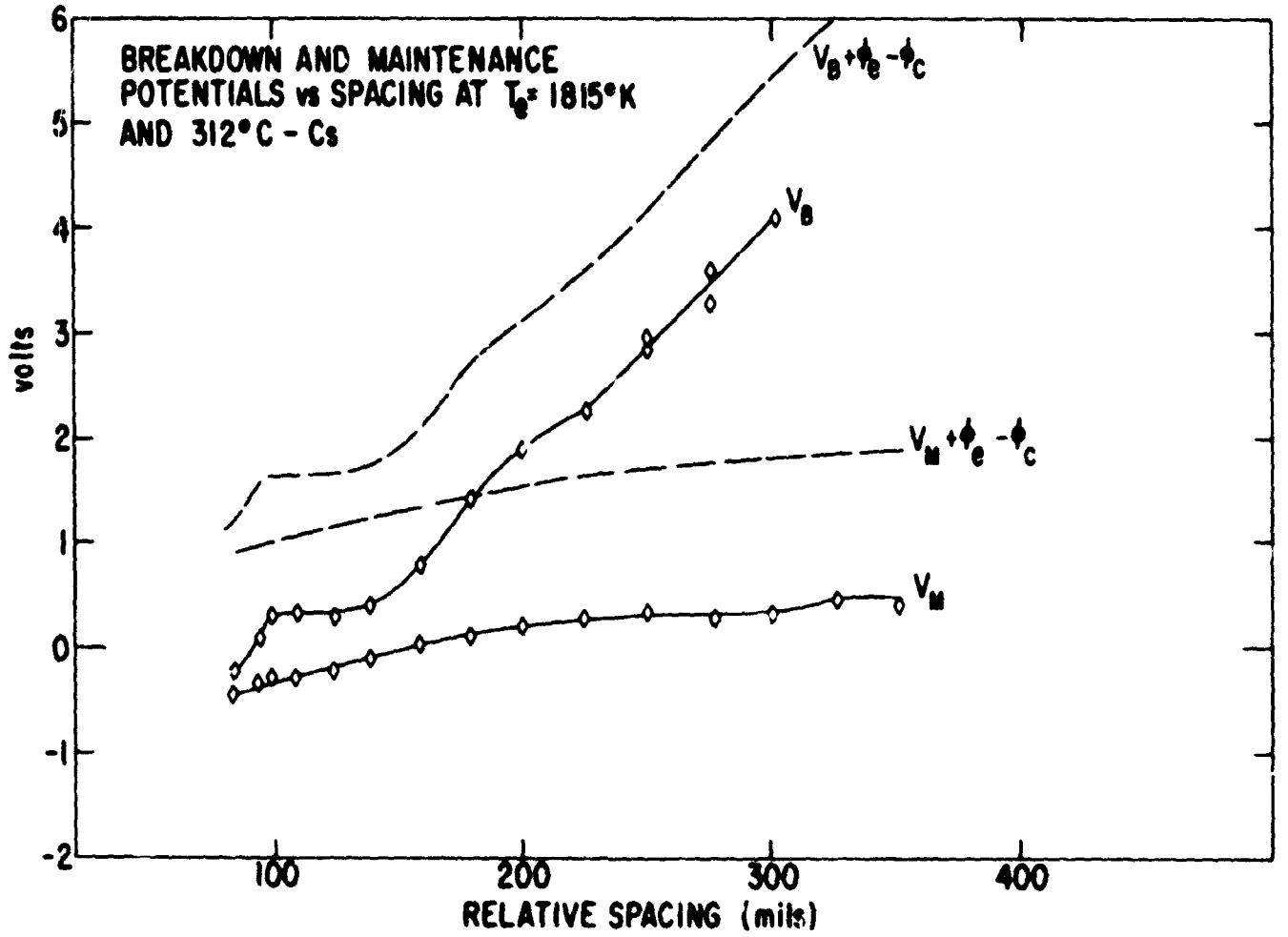

Figure 11 - Spacing dependence of the breakdown and maintenance potentials for a cesium temperature of 312°C

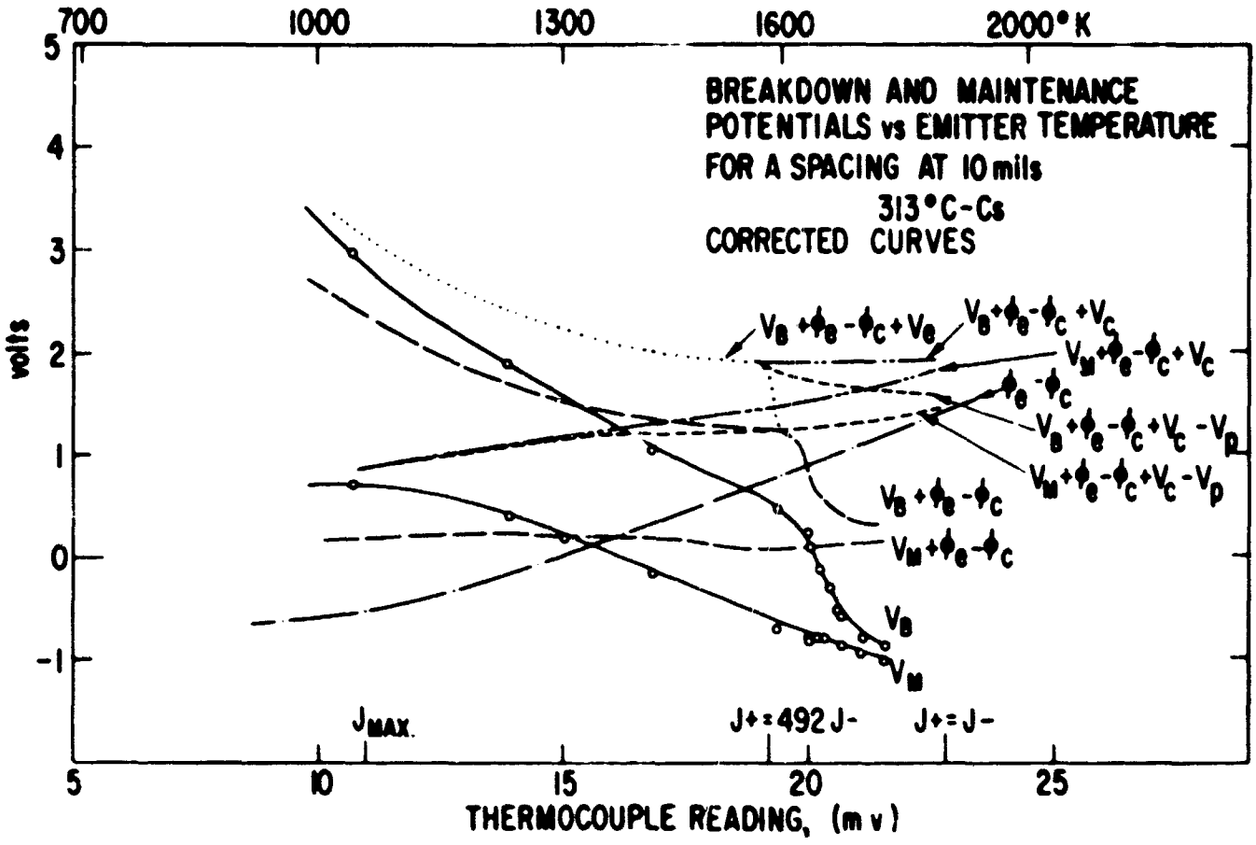

Figure 12 - Breakdown and maintenance potentials versus emitter temperature for a cesium reservoir temperature of 315°C, along with the corrected curves

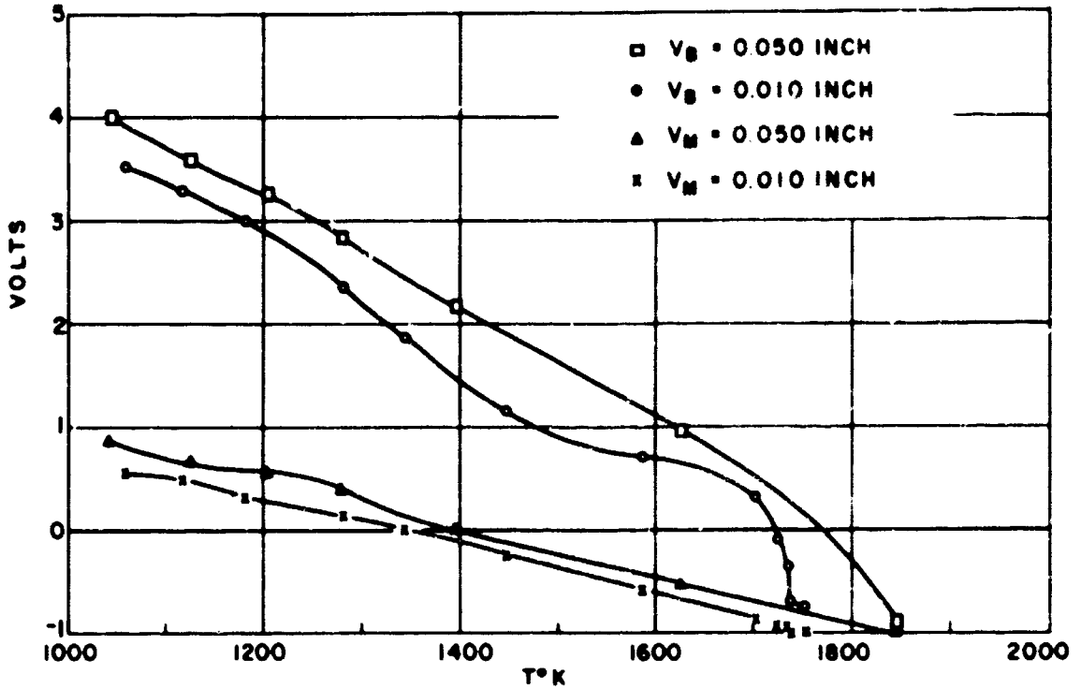

Figure 13 - Breakdown and maintenance potentials versus emitter temperature for the tungsten emitter, for a cesium bath temperature of 267°C and emitter collector spacing indicated

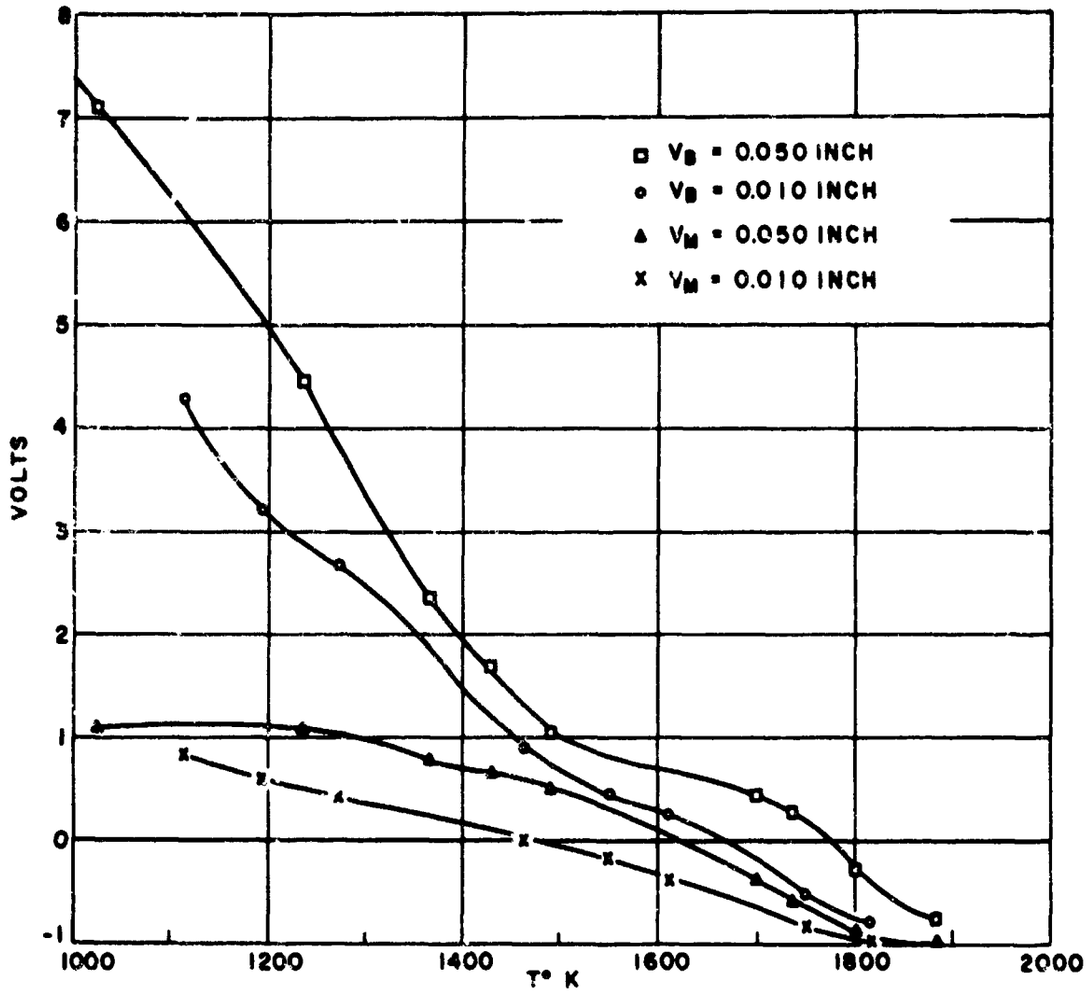

Figure 14 - Breakdown, V_B, and maintenance potentials versus emitter temperature for the tungsten emitter, for a cesium bath temperature of 314°C and spacings indicated

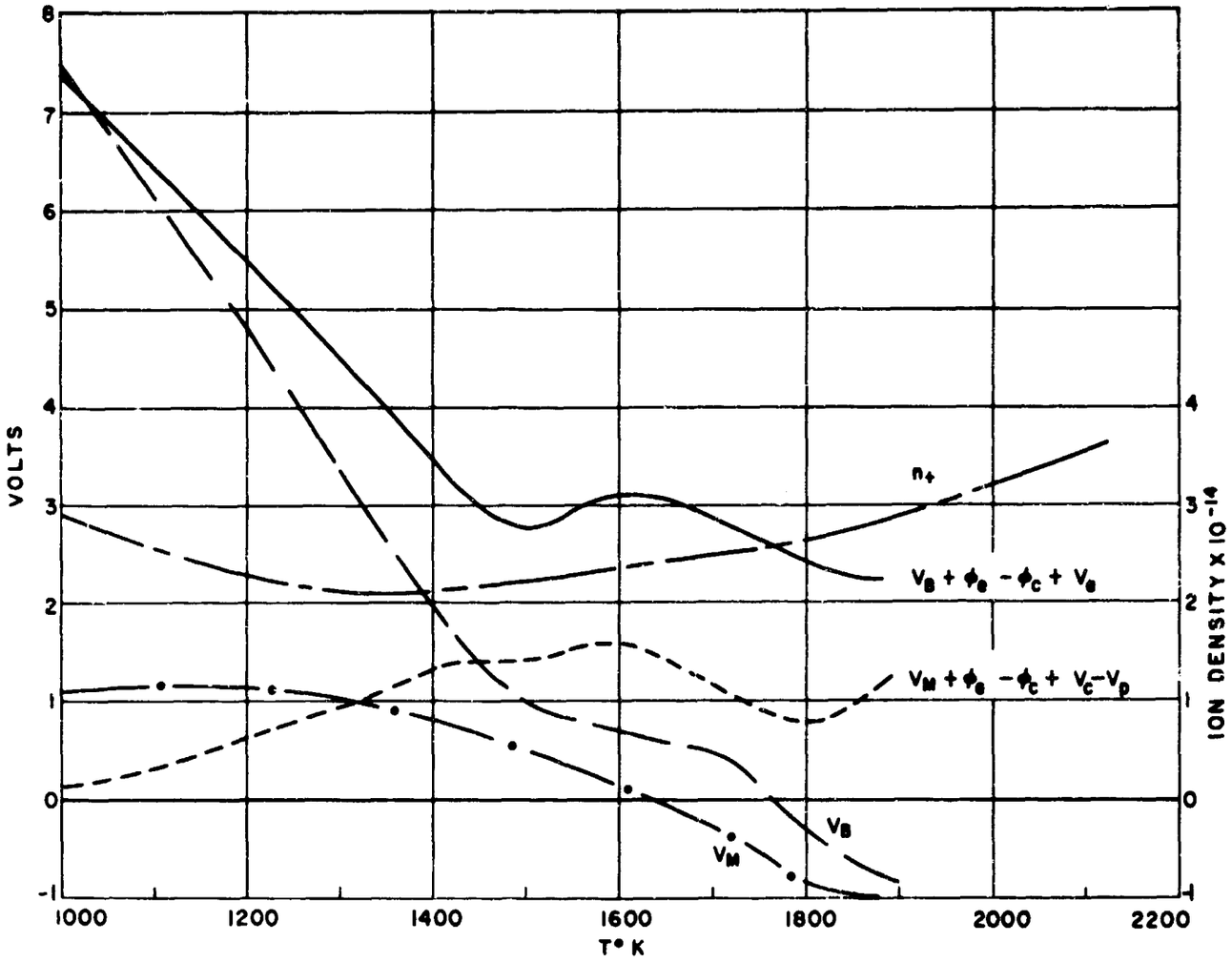

Figure 15 - Breakdown and maintenance data along with ion density measurements for a cesium bath temperature of 314°C and a spacing of 0.050 inch. Results of the sheath calculations versus emitter temperature are indicated

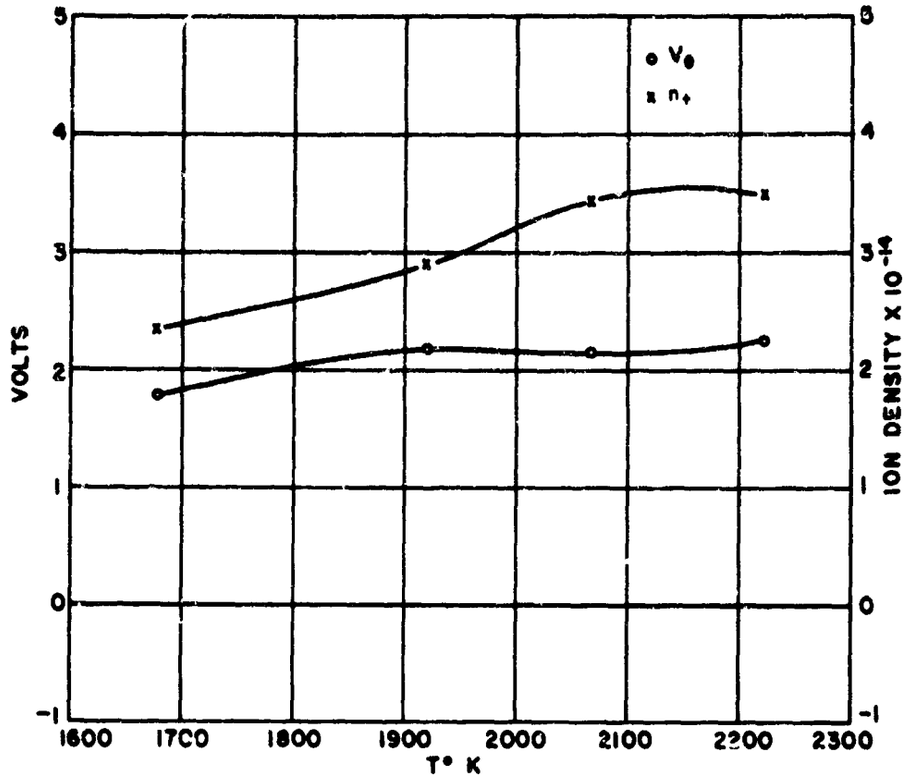

Figure 16 - Calculated emitter sheath potential and measured ion density versus emitter temperatures for a cesium bath temperature of 314°C and a spacing of 0.050 inch